

**Physicochemical studies on the mutants of the
VC0395_0300 protein of *Vibrio cholerae***

THESIS

Submitted in partial fulfillment
of the requirements for the degree of
DOCTOR OF PHILOSOPHY

by

Om Prakash Chouhan
ID. No: 2012PHXF0405G

Under the Supervision of
Dr. Sumit Biswas



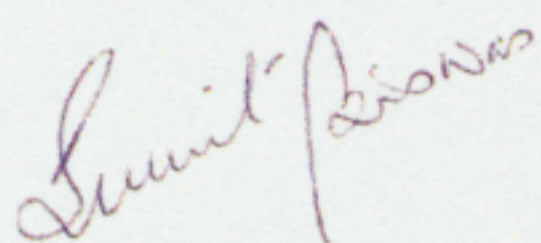
BITS Pilani
Pilani | Dubai | Goa | Hyderabad

**BIRLA INSTITUTE OF TECHNOLOGY AND SCIENCE
PILANI (RAJASTHAN) INDIA
2019**

BIRLA INSTITUTE OF TECHNOLOGY AND SCIENCE, PILANI

CERTIFICATE

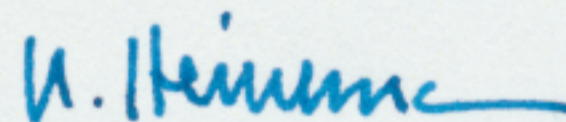
This is to certify that the thesis entitled "**Physicochemical studies on the mutants of the VC0395_0300 protein of *Vibrio cholerae***" submitted by Om Prakash Chouhan, ID No. 2012PHXF0405G for award of Ph.D. degree of the Institute embodies original work done by him under our supervision.



Signature of the Supervisor

Dr. Sumit Biswas
Assistant Professor,
Department of Biological Sciences

Date:



Signature of the Co-Supervisor

Prof. Dr. Udo Heinemann
Max Delbrück Center for Molecular
Medicine, Berlin, Germany

Date: 11 July 2018

Abstract

Vibrio cholerae, the cause of seven noted pandemics, leads a dual lifecycle, which switches between its virulent form in the human host, and the sessile, non-virulent form in aquatic bodies in surface biofilms. Surface biofilms have been known to be associated with a ubiquitous protein present in all branches of bacteria, known as the GGD(/E)EF domain protein. The diguanylate cyclase activities of these proteins are universally established. Cyclic-di-GMP (c-di-GMP) synthesized by diguanylate cyclases serve as an important and ubiquitous secondary messenger in almost all bacterial systems. c-di-GMP regulates diverse cellular functions in bacteria at the transcriptional, translational and posttranslational levels. The cellular functions regulated by c-di-GMP include cell motility, cell cycle progression, virulence, biofilm formation, antibiotic productions and other unknown functions. The VC0395_0300 protein from chromosome 1 of the *V. cholerae* classical strain O395, serotype O1 has been established in our ViStA lab to be a diguanylate cyclase with a necessary role in biofilm formation. This thesis work reports the mutations in the central positions of the GGEEF active site of the VC0395_0300 protein by site-directed mutagenesis. The conditions for maximum production of mutated protein have been optimized. All the mutated proteins were biophysically characterized to analyze their structural and biochemical features. For instance, the mutant proteins have been studied using spectrofluorimetry and circular dichroism spectroscopy. Diguanylate cyclase activities for all mutated proteins were determined by HPLC assay method. While there is a significant loss-of-biofilm-forming activity in the mutants, the basis for the same needed an investigation at the structural level. The wild type and mutated proteins have been crystallized to reveal the GGEEF domain structure, understanding the reaction mechanism for c-di-GMP synthesis and steric inhibition for the diguanylate cyclase activity. The overall structure of the protein does not show significant changes due to the mutagenesis, despite the loss of biofilm formation in the mutants.

In conclusion, the major aspects of the thesis are as follows:

- Functional and biophysical characterization of the mutant proteins of VC0395_0300, compared with the wild type protein.
- Structure elucidation of the GGEEF domain in VC0395_0300.
- Role of mutations and the importance of amino acids in the GGEEF active site.

ACKNOWLEDGEMENT

Undertaking this Ph.D has been a truly life-changing experience for me. During this period of time, I have met many people who have helped me in the scientific or non-scientific way and making my time very pleasant and interesting during my research. I am always grateful to them and would like to thank all of them from bottom of my heart.

Foremost, I would like to thank the biggest contributor to my thesis, my Supervisor Dr. Sumit Biswas for his guidance and mentorship during the entire period of my Ph.D. Without his guidance, this work would never have been achievable. He has taught me the methodology to carry out research and to present the research works as clearly as possible. Thanks a lot Sir, for all your help and constant support.

I would like to express my deep and sincere gratitude to my co-supervisor Prof. Udo Heinemann (MDC, Berlin). I am extremely grateful to him for allowing me to utilize his laboratory facilities wholeheartedly. His observations, intellectual freedom about my work and comments helped me a lot to establish the overall direction of the research and to move forward with the investigation in depth.

I would also like to acknowledge my Doctoral Advisory Committee (DAC) members, Dr. Malabika Biswas and Dr. Kundan Kumar for their constant advice and support during my entire research tenure.

I express my gratitude to the Vice-Chancellor BITS-Pilani, Director of BITS, Pilani – KK Birla Goa Campus, Academic Research Division (ARD)BITS, Pilani – KK Birla Goa Campus and Head of Department of Biological Sciences for giving me the opportunity to serve in this prestigious institute while pursuing my research and providing me all necessary facilities.

My special thanks to Dr. Yvette Roske and Dr. Ankur Garg for their supportive and productive discussions on my research work at Heinemann's lab. Thanks to Birgit Cloos and Andreas Knespel to make all necessary arrangement for me in lab at MDC, Berlin or for my accommodation during that time, I am also thankful to Dr. Martin, Saša Petrović, Qianqian Ming, Nancy and other member of Heinemann's lab for being nice to me and their excellent support in lab work.

I thank past and current members of our research group - Dr. Ram Kothandan, Dr. Divya Bandekar, Mr. Subhasish Sahoo and Ms. Malvika Sudhakar for their constant support and friendship. My special thanks to all the past and current research scholars from Dept of biological sciences and Dept of chemistry for their timely help in all aspect. My research was made easy with the help of Biological Sciences Supporting Staff Mrs Kamna Upadhay, Mr Mahadev Shetkar and Mr Mahaling Lamani for the timely help throughout my research work at BITS Goa.

As we all know, friends makes the world beautiful. My research period was made so by all my friends from Berlin and BITS Goa campus, especially my closest group we called as “The Originals” and “Teen Uchkee” for being funny, critical and always supporting. I had a wonderful time with them and thanks for making my time wonderful.

I am also grateful to the funding received throughout my Ph.D. tenure from BITS Pilani Institutional fund to undertake my Ph.D. I am gratefully to MDC Berlin and the German Academic Exchange Service or DAAD for funding my research work.

I will always be indebted to my parents, for helping and going beyond their capability to help me out during this challenging period and encouraging me at every stage of my personal and academic life. Their blessings always granted me wisdom, health and inner strength to undertake the research task and enabling me to its completion. The word THANKS are not enough to show my gratitude for them.

Om Prakash Chouhan

BRIEF CONTENTS

Chapter	Title	Page
1	Introduction and Review of Literature	1
2	Site-directed mutagenesis of <i>VC0395_0300</i> gene and cloning in <i>E. coli</i>	44
3	Expression and purification of mutant proteins	59
4	Biophysical characterization of <i>VC0395_0300</i> mutant proteins	80
5	Structure elucidation of <i>VC0395_0300</i> and its mutant proteins	111
6	Summary of the results	137

TABLE OF CONTENTS

	PAGE
Thesis title page (Annexure I)	
Certificate from Supervisor & Co-supervisor (Annexure II)	
Abstract	1
Acknowledgements	II
Table of contents	V
List of figures	IX
List of tables	XIII
List of abbreviations	XV
Chapter 1: Introduction and Review of Literature	
1.1 <i>Vibrio cholerae</i> : An Introduction	1
1.2 Cholera: History and background	3
1.3 <i>Vibrio cholerae</i> Life-cycle	5
1.3.1. Control of cholera through vaccination	8
1.3.2. <i>V. cholerae</i> : Biofilm formation	9
1.3.2.1. Surface attachment	10
1.3.2.2. Colony formation	11
1.3.2.3. Dispersal	12
1.4 Regulation of biofilm formation	13
1.5 c-di-GMP and Biofilm in <i>V. cholerae</i>	16
1.5.1 Receptors for c-di-GMP	22
1.5.1.1 c-di-GMP and microbial physiology	23
1.5.1.2 Regulation of flagellar gene	24
1.5.1.3 Control of motility to sessility transition	24
1.5.1.4 Regulation of extracellular matrix component	24
1.5.1.5 Pili and c-di-GMP	25
1.5.1.6 Adhesins and c-di-GMP	25
1.5.1.7 Cyclic di-GMP and Virulence	26

1.6 Genome analysis of <i>V. cholerae</i>	28
1.7 GGDEF protein in <i>V. cholerae</i>	30
1.8 Gaps in Existing Research	34
1.9 Objectives of the Proposed Research	35
1.10 References	36

Chapter 2: Site-directed mutagenesis of VC0395_0300 gene and cloning in *E. coli*.

2.1 Introduction	44
2.2 Materials and Methods	45
2.2.1 Genomic DNA isolation	45
2.2.2 Site-Directed Mutagenesis	45
2.2.3 Agarose gel electrophoresis	47
2.2.4 Restriction digestion	48
2.2.5 Vector DNA preparation	48
2.2.6 Ligation	49
2.2.7 Preparation of competent <i>E. coli</i> cells	49
2.2.8 Transformation	50
2.2.9 Plasmid isolation	50
2.3 Results and Discussions	51
2.3.1 Site-Directed Mutagenesis	51
2.3.2 Cloning of recombinant plasmid DNA	54
2.4 Conclusions	56
2.5 References	57

Chapter 3: Expression and purification of mutant proteins

3.1 Introduction	59
3.2 Materials and Methods	60
3.2.1 Culture condition	60
3.2.2 Protein over expression and solubility test	60
3.2.3 SDS-PAGE	60
3.2.4 Protein Constructs preparations	61

3.2.5 Large scale protein purification	62
3.2.6 Cell Lysis	63
3.2.7 GST affinity chromatography and Tag cleavage	63
3.2.8 Cation exchange chromatography	65
3.2.9 Size-exclusion chromatography (SEC)	65
3.2.10 Concentration of protein and protein storage	66
3.2.11 Protein concentration determination	66
3.3 Results and discussions	67
3.3.1 Pilot scale protein expression	67
3.3.2 Bulk protein production	68
3.3.3 Protein Constructs	70
3.4 Conclusions	76
3.5 References	77
Chapter 4: Biophysical characterization of VC0395_0300 mutant proteins	
4.1 Introduction	80
3.2 Materials and Methods	81
4.2.1 Diguanilate cyclase activity	81
4.2.2 Scanning Electron Microscopy	82
4.2.3 Quantification of microbial biofilm	83
4.2.4 Bacterial Motility assays	83
4.2.4.1 TTC Assay	84
4.2.4.2 Soft agar plate method	84
4.2.5 Circular dichroism (CD) spectroscopy	84
4.2.6 Fluorescence spectroscopy	85
4.2.6.1 Thermal Denaturation	85
4.2.6.2 Chemical Denaturation	85
4.2.6.3 Fluorescence quenching	86
4.3 Results and discussions	87
4.3.1. Diguanilate cyclise activity of mutants	87
4.3.2 Structures of biofilms	90

4.3.3 Quantification of Biofilm and bacterial motility	93
4.3.4 Effect of mutation on secondary structure of protein	96
4.3.4.1 Fluorescence spectroscopy	96
4.3.4.2 Analysis of secondary structural composition of protein by CD	103
4.4 Conclusions	106
4.5 References	108
Chapter 5: Structure elucidation of VC0395_0300 and its mutant proteins	
5.1 Introduction	111
5.2 Materials and Methods	112
5.2.1 Protein production in bulk scale	112
5.2.2 Crystallization	112
5.2.3 Crystallization of mutant proteins	113
5.2.4 Data collection and processing	114
5.3 Results and discussions	115
5.3.1 Protein productions for crystallization setup	114
5.3.2 Structure of VC0395_0300 ₍₁₆₁₋₃₂₁₎	118
5.3.3 Structure of mutants of VC0395_0300	124
5.4 Conclusions	131
5.5 References	133
Summary of Results	137
Future Scope of Work	140
Appendices	
A Reagents used	141
B List of Licences	146
C List of Publications	147
D List of Conferences and Workshops	149
E Brief Biography of the Candidate	150
F Brief Biography of the Supervisor	151

LIST OF FIGURES

Figure No	Figure legend	Page
Chapter 1		
Figure 1.1	Cholera outbreak in time duration 2010 to 2015 Cholera disease outbreak in the recent year of 2017 in Yemen	5
Figure 1.2	Life cycle of <i>V. cholerae</i> in aquatic environment and transmission into host	6
Figure 1.3	Mechanism of cholera toxin in human host intestine	7
Figure 1.4	Representation of different stages for biofilm formation in <i>V. cholerae</i>	11
Figure 1.5	Structure of VpsR from <i>S.cerevisiae</i> . C-terminal DNA binding domain (Helix-Turn-Helix HTH).	14
Figure 1.6	Regulatory network in <i>V. cholerae</i> . Interaction of c-di-GMP with various transcriptional activators	15
Figure 1.7	Crystal Structure of the <i>Vibrio cholerae</i> Quorum-Sensing Regulatory Protein HapR	16
Figure 1.8	Chemical structure of c-di-GMP molecule and Chemical reaction for c-di GMP formation and hydrolyzation catalyze by GGDEF protein and EAL protein	17
Figure 1.9	Crystal structure of a catalytically active GG(D/E)EF domain containing protein from <i>Marinobacter aquaeolei</i>	21
Figure 1.10	Diversity of c-di-GMP binding receptor, transcription factor and protein that's shows affinity to c-di-GMP and affect microbial physiology at different level	22
Figure 1.11	Graphical representation of <i>V. cholerae</i> chromosome	30
Figure 1.12	Showing no of GGDEF and EAL domain-containing protein in five major bacterial phyla	31

Chapter 2

Figure 2.1	Structure of VC0395_0300 protein with the position of amino acid in the polypeptide chain.	51
Figure 2.2	Site-Directed Mutagenesis in <i>VC0395_0300</i> gene.	53
Figure 2.3	All mutated protein structure along with Wild type VC0395_0300 protein structure	53
Figure 2.4	Representation of recombinant plasmid of gene <i>VC0395_0300</i> with PGEX-6P1 vector DNA.	54
Figure 2.5	Agarose gel for all mutated cloned plasmid and vector	54
Figure 2.6	Agarose gel for restriction digested mutated constructed plasmid and vector DNA.	55

Chapter 3

Figure 3.1	Protein purification steps used for all proteins.	64
Figure 3.2	SDS-PAGE gel pictures showing over expression of all mutant proteins at best-optimized conditions	68
Figure 3.3	Overall protein purification steps for full length VC0395_0300 (G237R) protein.	69
Figure 3.4	Secondary structure prediction of VC0395_0300 by Psipred, used for protein truncation.	70
Figure 3.5	Overall protein purification steps for VC0395_0300(G237R) ₁₆₀₋₃₂₁ .	71
Figure 3.6	Protein purification steps VC0395_0300(E238K) ₁₆₀₋₃₂₁ .	72
Figure 3.7	Protein purification steps VC0395_0300 (E239K) ₁₆₀₋₃₂₁ and VC0395_0300 (F240I) ₁₆₀₋₃₂₁ .	73
Figure 3.8	15% SDS - PAGE gel showing full-length protein and N-terminal truncates of VC0395_0300 protein which were used for various experiments.	75

Chapter 4

Figure 4.1	HPLC assay for diguanylate cyclase activity of mutant proteins at best-optimized conditions.	89
Figure 4.2	Scanning Electron microscopy images for biofilm of VC0395_0300(G237R) under high vacuum conditions at 10000, 15000 and 30000X zoom.	91
Figure 4.3	Scanning Electron microscopy images for all mutant strains with the wild-type strain	92
Figure 4.4	Quantification of biofilm formation using crystal violet method	94
Figure 4.5	Bacterial motility test at best-optimized conditions	96
Figure 4.6	Fluorescence emission signal after excitation of Trp residue at 295 nm	98
Figure 4.7	Fluorescence emission signal of Gdn denatured protein after excitation of Trp residue at 295 nm	100
Figure 4.8	Stern – Volmer curves for fluorescence signal after quenching of Trp residues in protein.	103
Figure 4.9	Circular dichroism spectroscopy analysis of VC0395_0300 and all mutated protein samples.	105

Chapter 5

Figure 5.1	Various protein constructs used for protein crystallization experiments.	116
Figure 5.2	Crystallizations drop pictures showing initial positive crystals formation in various conditions in primary screening.	117
Figure 5.3	Best protein crystal for VC0395_0300 ₍₁₆₁₋₃₂₁₎ protein after fine screen and all conditions optimized.	118
Figure 5.4	VC0395_0300 ₍₁₆₁₋₃₂₁₎ protein structure alignment with PleD, WspR and 3IGN.	120

Figure 5.5	VC0395_0300 protein sequence alignment with DGC protein in PleD from <i>Caulobacter crescentus</i> , 3IGN from <i>Marinobacter aquaeolei</i> and WspR from <i>Pseudomonas aeruginosa</i> by ClustalW.	121
Figure 5.6	Protein Structure of VC0395_0300 ₍₁₆₁₋₃₂₁₎	123
Figure 5.7	Best protein crystal after all conditions optimized for (A) Protein constructs VC0395_0300 _(G237R) (B) Protein constructs VC0395_0300 _(E238K) .	124
Figure 5.8	Crystal structure for protein constructs of VC0395_0300 _(G237R) protein	127
Figure 5.9	Crystal structure for protein constructs of VC0395_0300 _(E238K) protein	128
Figure 5.10	Alignment of mutant protein constructs with wild type VC0395_0300 ₍₁₆₁₋₃₂₁₎ protein.	129

LIST OF TABLES

Table	Table Heading	Page
Chapter 1		
Table 1.1	Scientific Classification of bacteria	1
Table 1.2	The ancient history of c-di-GMP	18
Table 1.3	Virulence phenotypes affected by c-di-GMP	26
Table 1.4	Characteristic of <i>V. cholerae</i> chromosome	28
Table 1.5	GGDEF domain-containing proteins in <i>V. cholerae</i>	31
Chapter 2		
Table 2.1	Components for PCR reactions	46
Table 2.2	PCR program for amplification	46
Table 2.3	List of primers used for amplification of <i>vc0395_0300</i> gene	47
Table 2.4	Components for restriction digestion reaction mixture	48
Table 2.5	Components for ligation reaction mixture	49
Chapter 3		
Table 3.1	List of primers used to make for different protein constructs of VC0395_0300 gene	61
Table 3.2	List of plasmids used to produce different protein constructs of VC0395_0300 gene.	62
Table 3.3	Different protein constructs for VC0395_0300 and their protein expressions properties	74
Chapter 4		
Table 4.1	Fluorescence properties of aromatic amino acids	97
Table 4.2	Stern - Volmer constant (K_w) values for all mutated protein	102
Chapter 5		
Table 5.1	Method of crystallization set up for VC0395_0300(161-321) protein.	113
Table 5.2	Method of crystallization set up for mutant protein constructs	114

Table 5.3	Deign of VC0395_0300 protein constructs and trial for crystallization.	115
Table 5.4	X-ray diffraction Crystallographic data and Refinement Statistics for VC0395_0300(161-321) protein.	119
Table 5.5	X-ray diffraction Crystallographic data and Refinement Statistics for mutant proteins.	125

LIST OF ABBREVIATIONS

A ₅₉₅	Absorbance at 595 nm
A ₆₀₀	Absorbance at 600 nm
AI	Auto inducer
Amp	Ampicilin
Amp ^R	Ampicilin resistance gene
APS	Ammonium per sulphate
bp	Base pair
BSA	Bovine serum albumin
CBB G250	Coomassie brilliant blue G-250
CBB R250	Coomassie brilliant blue R-250
CT	Cholera toxin
CD	Circular dichroism
DNA	Deoxyribonucleic acid
DNase	Deoxyribonuclease
DTT	Dithiothreitol
EDTA	Ethylenediamine tetra acetic acid
EPS	Extracellular polysaccharides
EtOH	Ethanol
EtBr	Ethidium bromide
GTP	Guanosine-5'-triphosphate
GMP	Guanosine mono phosphate
GST	Glutathione S transferase
GdnHCl	Guanidine hydrochloride
HPLC	High pressure liquid chromatography
IPTG	Isopropyl thio-β-D-galactoside
Kan	Kanamycin
Kan ^R	Kanamycin resistance gene
Kb	Kilo base pairs
kD	Kilodalton
LA	Luria bertani Agar
LB	Luria bertani broth
M	Molar

Mb	Mega base pairs
ml	Millilitre
mM	Millimolar
µg	Microgram
µl	Microlitre
ng	Nanogram
nm	Nanometer
ORF	Open reading frame
OD	Optical density
OD ₆₀₀	Optical density at 600nm
OD ₅₉₅	Optical density at 595nm
PEG	Polyethylene glycol
pGpG	5'-phosphoguananylyl (3'-5') guanosine
PCR	Polymerase chain reaction
pmol	Picomol
rpm	Revolution per minute
REC	Receiver domain
RNase	Ribonuclease
SDS	Sodium dodecyl sulphate
TEMED	N,N,N',N'-Tetramethylethylenediamine
Tris	Tris (hydroxymethyl) amino methane
TTC	Triphenyl tetrazolium chloride
Trp	Tryptophan
Tyr	Tyrosine
UV	Ultra violet
WHO	World Health Organisation

1.1. *Vibrio cholerae*

Vibrio cholerae is the causative agent of a severe diarrhoeal disease known as cholera that occurs most repeatedly all over the world. The microorganism *V. cholerae* was described for the first time by Robert Koch in 1883. The microorganism is a Gram-negative, rod or comma-shaped, heterotrophic, highly motile bacterium with single flagella on one end (Polar/Monotrichous) which helps the bacterium to swim in the aquatic environment (**Hdelberg 2000**).

The organism contains two chromosomes as its genome (**Trucksis et al 1998**). Its primary larger chromosome contains all the genes which are required for its cellular function and some genes for regulation of virulence. The second chromosome was initially considered as a plasmid but later on, discovered to contain some housekeeping genes, genes for heat shock proteins and genes which are essential for metabolic pathways (**Colwell and Huq 1994**). This bacterium *V. cholerae* has different types of strains, some of which are pathogenic while others are non-pathogenic. Strains differ in their virulence gene content, antibiotic resistance, and surface antigens (such as the 0139 lipopolysaccharides and O-antigen capsule). Some recent evidence shows that nonpathogenic or nontoxicogenic *V. cholerae* can be converted into a pathogenic or toxigenic strain in the environment by phage transduction (transfer of cholera toxin CT encoding gene) (**Colwell and Huq 1994, Watnick 1999, Camilli 2008**).

Table 1.1 Scientific classification of *V. cholerae*.

Microbial	Taxonomy	Characterizations
Domain	Bacteria	A Large group which consists of microscopic, single cell prokaryotic organism that lacks a membrane-bound nucleus, mitochondria or another membrane-bound organelle.
Phylum	Proteobacteria	Mostly group of Gram-negative bacteria but some of Gram-positive; their outer membrane mainly

composed of lipopolysaccharides

Class	Gammaproteobacteria	class of several medically, ecologically, and scientifically important groups of bacteria	
Order	Vibrionales	Motile bacteria which move using their flagella.	
Family	Vibrionaceae	Gram-negative facultative anaerobes which are capable of fermentation and have polar flagella.	
Genus	Vibrio	Curved-rod shaped facultative anaerobes which are oxidase positive and do not form spores. Typically possess two chromosomes which are unusual in other bacteria.	
Species	<i>V. cholerae</i>	Includes pathogenic and nonpathogenic both strains which differ in their toxicity, virulence power, and their gene content.	
Species	Serogroup (Group of microorganisms which differ only in by their composition of antigens)	Biotypes (Group of microorganisms having same specific genetic constitute)	Serotypes (Group of microorganisms which characterized by a specific set of cell surface antigens)
<i>V. cholerae</i>	O1	Classical	Inaba
		El Tor	Ogawa
	O139		

V. cholerae as a species includes both pathogenic and nonpathogenic strains that vary in their virulence and gene content. At present, more than 200 different serogroups of *V. cholerae* are recognized, and out of them only 2 major serogroups are associated with epidemic cholera, viz., O1 and O139. Serogroup O1 is further classified into two major serotypes, Inaba and Ogawa and two biotypes, classical and El Tor. This subgroup are determined by their physiological properties, most importantly, the presence and absence of polymyxin B resistance, number of cholera toxin-encoding genes, hemolysin activity and presence of

mannose-sensitive hemagglutinin. Strain O395 is a classical serotype O1 serotype strain of the Ogawa biotype. O1 strains may exhibit serotype conversion or switch between Inaba and Ogawa serotypes. O395 has been extensively used for scientific study or molecular analysis of virulence factors (**Colwell and Huq 1994, Hdelberg 2000**).

1.2 Cholera: History and background

There is some evidence which shows cholera or a similar type of disease was present as early as the time of Hippocrates, and perhaps even earlier, but modern history of cholera started in the year 1817. In 1817, an epidemic outbreak was first reported in India. It subsequently spread across the continent and became a pandemic outbreak of cholera disease in the whole south Asian region. In early nineteenth century, it was believed that cholera disease was caused by “miasma”, which means through bad air. The bacterium for this disease was first reported by Italian scientist Filippo Pacini in Italy in 1854. He gave a germ theory and identified a comma-shaped microorganism responsible for the disease but its accurate nature and his results were not widely recognized. The word **cholera** comes from Greek term “Kholera” = Khole means “Bile”. Later on, John Snow a doctor-scientist in London, (father of epidemiology) found that this disease was not air borne, but spread through contaminated water. Thirty years later in 1884, Robert Koch discovered that *V. cholerae* is the causative agent of disease cholera. He claimed the successful isolation of pure culture of the causative agent of this disease from patients' stool sample (**Hdelberg 2000**).

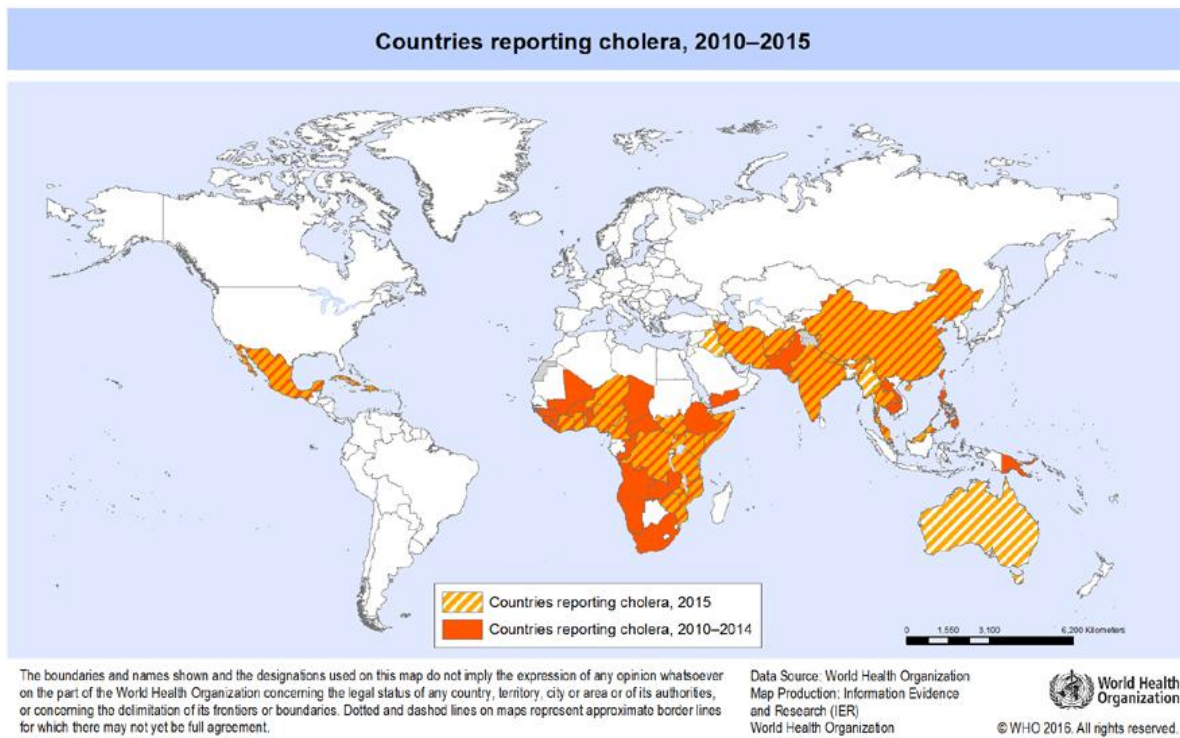
Cholera had its origin in the Indian subcontinent. The disease spread by trade routes to Russia and Europe in 1817, and later on from Europe to America and after that spread all over the world. In ancient history, there have been seven cholera pandemics in the last 200 year (**Charles and Ryan 2011**). In brief, the seven pandemics are:

- First - South Asia and the Middle East (1817 to 1823).
- Second - India, Russia, England and America (1829 to 1849).
- Third - Asia, Europe, North America, Brazil and Africa (1852 to 1849).
- Fourth - India, Mecca, Europe and North America (1863 to 1879).
- Fifth - India, Russia, Japan and Europe (1881 to 1896).
- Sixth - Asia and Africa (1923).

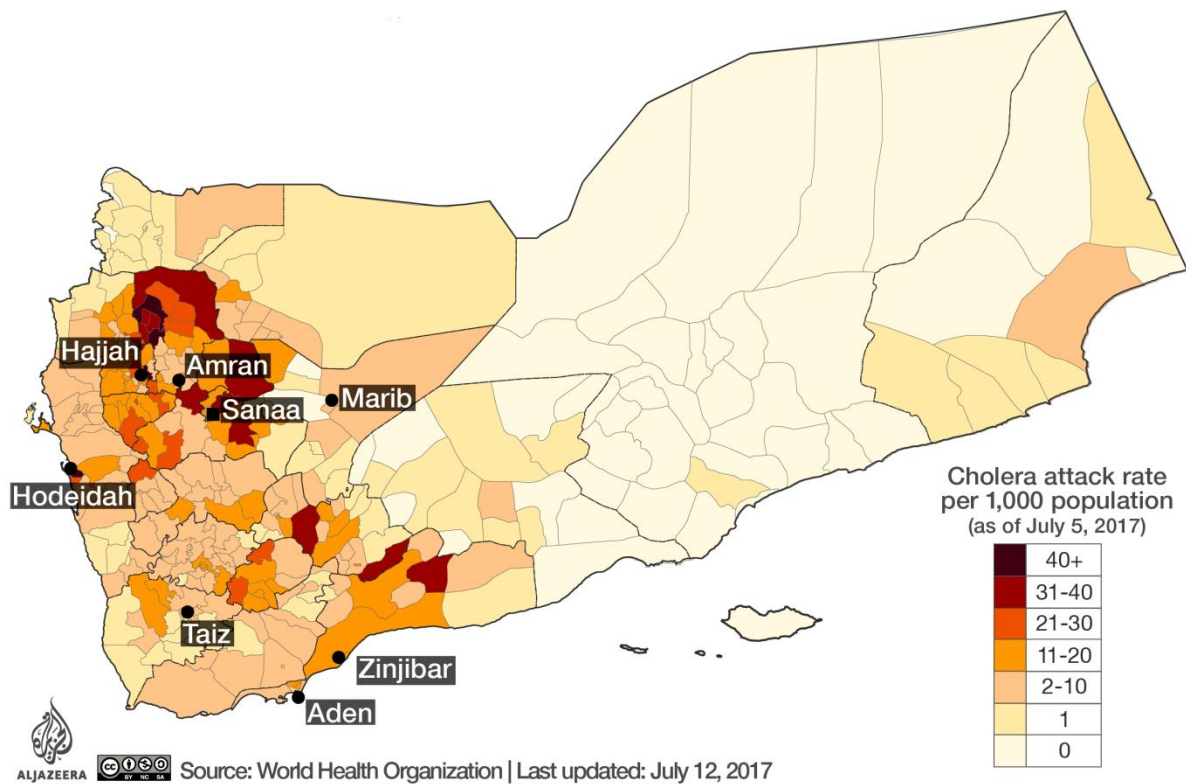
- Seventh - Originated in Indonesia and even today persists in underdeveloped countries (1961 to continue on and off).

More than tens of millions of people died in the 19th century due to this disease. In India alone, eight million people died because of cholera in between 1900 and 1920. In America and Europe cholera was not considered as a health threat due to better water sanitation such as filtering, chlorination, RO treatment and best hygienic conditions, however in developing countries including India it still heavily affects the human population. At present, around 100,000 deaths occur over the world in each year. Approx 4-5 million cases are observed in the entire globe and 8-10% of them suffer severe disease characterized by vomiting, loose motion, diarrhea, stomach cramps, dehydration, and severe shock. Death can occur within some days if there is no treatment.

In this recent era, when we have advanced medical facilities, cholera still remains extremely virulent disease. This disease is still affecting both children as well as adults. In a very recent study in the year 2017, explosive outbreaks of this disease have been reported from Yemen (figure 1B). According to WHO reports it was the worst cholera outbreak in the world which claimed more than 2000 lives in just six months (April 2017 to August 2017).



(A)



(B)

Figure 1.1: (A) Cholera outbreak in time duration of 2010 to 2015. (B) Showing cholera disease outbreak in the recent year of 2017 in Yemen

1.3. *V. cholerae*: Life-cycle

In the year 1854, Filippo Pacini isolated and described the Gram-negative mono flagellate *V. cholerae* bacterium and a year later John Snow revealed that the bacteria is spreading through the water supply. After a while, scientists discovered that the causative agent of diarrhoeal disease actually possesses a dual mode of survival. *V. cholerae* has two distinct types of life cycle in aquatic environment, the bacteria can be either in free-living single motile planktonic form with polar flagellum or it can be in a stable sessile biofilm form. This dual nature of *V. cholerae* gives them extra protection from adverse environmental conditions and makes the bacteria survive in nutrient limitation, low oxygen, radiation, and predation by eukaryotes such as protozoa (Colwell and Huq 1994, Heithoff and Mahan 2004, Camilli et al 2009, Carla et al 2013,).

V. cholerae can form its biofilm on any type of solid surface, including biotic or abiotic surfaces. When the bacteria exist in the mobile form, they swim and can attach to

zooplankton or phytoplankton and later, develop a biofilm. Most of the zooplankton and other aquatic organisms are covered with chitinous exoskeletons, which can be used as a carbon source for *V. cholerae*. So, aquatic organisms with chitinous exoskeletons and other zooplanktons serve as a reservoir for *V. cholerae*. In a biofilm, *V. cholerae* can be present in various forms, like typical rod-shaped cells, quiescent cells (bacteria with coccoid shape rather than normal curved rod-shaped, that cannot be cultured in the laboratory). Quiescent cells can become normal, curved rod-shaped active cells (due to environmental signal), and hyperinfective cells (hyperinfective states refer to highly active cells, lower number of these type of cells are required to infect a host or cause disease). Bacterial biofilms containing various types of cells have important biological significance for survival (**Colwell and Huq 1994, Karatan and Watnick 2009**). Bacteria can adjust their growth according to environmental clue. For example, quiescent cells can reduce their metabolic need in stress conditions and continue with reduced growth until conditions will improve or they can act like as infective bacterial seeds for cholera and can spread through the water supply (**Camilli 2009, Rodney 2002, Tischler et al 2015**).

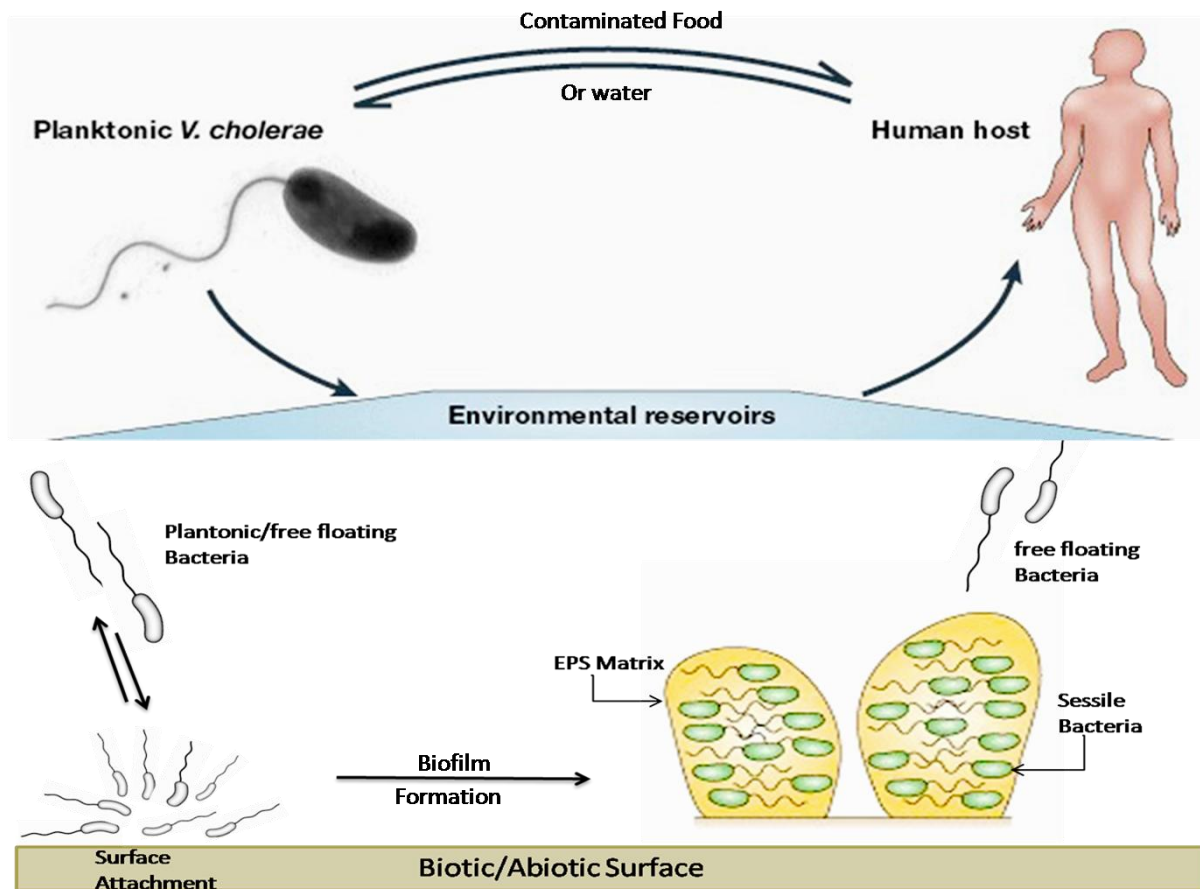


Figure 1.2: Life cycle of *V. cholerae* in aquatic environment and transmission into host.

When *V. cholerae* (free-living mobile bacteria or in form of biofilm) enter into the human host, through contaminated food or water, they can also colonize into the host's gastrointestinal tract (**Hammer and Bassler 2003, 2009**). In the intestinal tract, bacteria stop the synthesis of flagellin protein to save energy and don't need flagella for movement. They start producing a mucinase enzyme that enables the bacterium to enter the mucus layer that protects the gastrointestinal epithelium from foreign infectious bacteria.

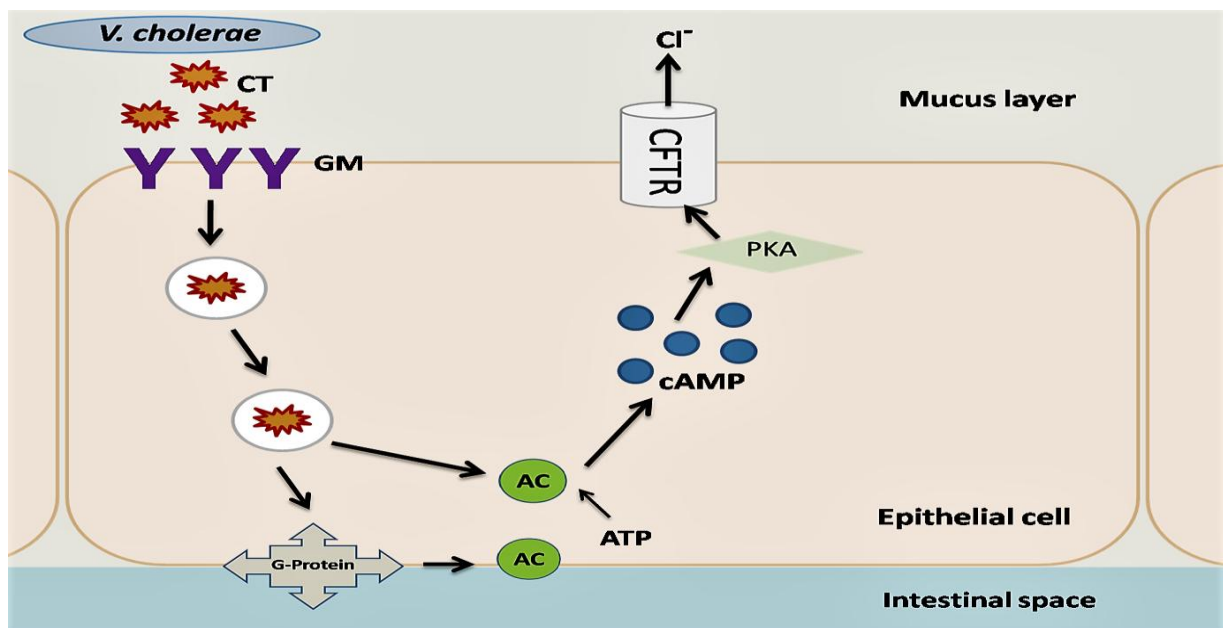


Figure 1.3: Mechanism of cholera toxin in human host intestine. CT = Cholera toxin, AC = Adenylate cyclase, PKA = Protein kinase, CFTR = Cystic fibrosis transmembrane conductance regulator (a membrane protein), GM = Ganglioside.

After entering the intestinal wall, *V. cholerae* multiply faster than aquatic environment and start producing various toxic proteins (known as cholera toxin, CT), which ultimately results in severe watery diarrhea to host. Andrew Camilli suggested that in the human intestine the bacterium becomes 700 times more infectious than control strain due to activation of several genes in the intestinal environment (**Colwell and Huq 1994**).

The cholera toxin is actually a complex of six different protein subunits (a single A subunit and 5 other B subunits), which are interconnected by a disulfide bond (**Joachim 2002**). When cholera toxin binds to the epithelial cell surface, the complex will enter the cell via endocytosis. The disulfide bonds of the complex are reduced and A subunit bind to human host protein Arf6 (ADP-ribosylation factor 6). Binding to Arf6 cause conformational changes

that induce constitutive cAMP production. Reduced cholera toxin subunit activates membrane G-protein and stabilizes ADP-ribosylation reaction. Activated G-protein induces adenylyl cyclase activity and affects intracellular cAMP level, which leads to activation of membrane-bound CFTR protein. Activation of CFTR and high level of cAMP cause secretions of sodium, potassium, and bicarbonate along with water into gastrointestinal tract finally resulting in loss of body fluid and dehydration leads to a severe problem to host (**Lim et al 2006, 2007**). Under these conditions, the bacteria are also shed in the stool and again enter to aquatic environment to infect a new host through contaminated food or water. The complete cycle of *V. cholerae* in the aquatic environment and to the human host is shown in figure 1.2.

1.3.1 Control of cholera through vaccination

Transmission of cholera can be controlled by maintaining good hygienic and sanitary conditions. For the last few decades, scientists are continuously trying to develop a strong vaccine against cholera disease. Acquired immunity from exposure to the infectious bacteria (probably as a result of interaction with various antigenic components) has been reported in some cases (**Joachim and Karl 2002**). The immunity may last for three years, but the immunity varies from individual to individual, or from biotype to biotype. For example, classical biotype show higher protection against all classical serotype while El Tor induced immunity is present against El Tor isolates only. In the former, vaccination included inactivated cholera toxin or phenol activated whole cell that provides short time protection and sometimes it causes disease symptoms. In the last decades, various forms of vaccine that have been devised included inactivated bacterial cells or killed toxin subunits in different ratio (**Glass et al 1982, Joachim and Karl 2002**).

A few approaches addressed in modern vaccine developments for cholera can be listed as below:

1. *V. cholerae* is usually colonized at the mucosal membrane of an epithelial cell of the small intestine, and bacteria is noninvasive which grow only in M cells. After cholera infection, when antibody production is induced due to lymph node activity, antibody secretions ensure immune responses against invading bacteria in the intestinal lumen. To provide strong immune responses oral vaccine with live attenuated strains is an important strategy to induce intestinal immunity.

2. In disease conditions, all primary symptoms of the disease are caused by cholera toxin. For this reason, initial vaccine development was focused to make bacterial strains which were deficient for the toxin-producing gene. However, later studies suggested that such strains can also develop significant disease symptoms in human due to the presence of various other virulent factors. Therefore the combination of various virulence factors in vaccine development is now underway.
3. In *V. cholerae*, toxin-coregulated pili (TCP) play important role in colonization in the small intestine and are also available for cholera toxin receptor. The use of cholera toxin as a vaccine for treatment of disease may lead to conversion from nontoxigenic to toxigenic form by ctx induction.
4. The use of attenuated cholera toxin producing strains as a vaccine in cholera treatment reported not safe because some cases results shows its conversion to toxigenic form make a doubt on vaccine safety issue.
5. The evolution through horizontal gene transfer in bacteria makes it likely to develop new epidemic strains makes more complicated for stable vaccine productions against cholera infection.
6. Some bacterial biofilm nonculturable strains (VNC) are also present, which play important role in cholera infection through contaminated water sources. Our understanding for bacterial biofilm and VNC states are still limited. A complete knowledge about bacterial biofilm formation and various pathogen states will be helpful to make strategies for prevention of cholera outbreak.

Environmental persistence for the interepidemic mode of *V. cholerae* is also an important obstacle for vaccine productions (**Ogunniyi 2008**). The number of difficulties experienced in past attempts leaves a question mark in the process of vaccine development of *V. cholerae*.

1.3.2 *V. cholerae*: Biofilm formation

V. cholerae is an interesting microorganism which has two distinct lifestyles which can be interchanged according to situations. Infective bacterial strains are mostly found in the aquatic environment from where they can transfer to host. In the aquatic environment, bacteria shed by cholera patients (primarily due to lack of proper sanitation) are present and it is this stage which is much more infectious as compared to laboratory cultured bacteria

(Heithoff and Mahan 2004, Urs and Jacob 2006, Camilli et al 2009). If the bacteria are transmitted to fresh hosts, the bacterial transmission cycle continues.

At other times, when *V. cholerae* transfer from the host gastrointestinal tract to the aquatic environment, there may be a sudden change in surrounding environmental conditions. In this external environment, the bacteria face very harsh conditions such as nutrient limitations, lower temperature, level of oxygen and massive change in osmolarity. *V. cholerae* evolve in such a way that organism can survive against all dramatic drastic changes in its surrounding. As response to environmental stress the bacterium can prepare itself by making changes in its own proteome by inducing favourable genes or suppressing other unfavourable genes to adapt in stress conditions. In such harsh conditions, bacteria live together as a bacterial biofilm, and this mode of life gradually became very favorable for survival of bacteria (Rodney 2002, Tischler and Camilli 2004, Waters et al 2006, Gjermansen 2006). Biofilm gives extra level of protection to fight against all possible detrimental conditions such as osmolarity, protozoan predation, and nutrient availability. *V. cholerae* biofilm formation is a cyclic process which involves three main steps:

1. Surface attachment,
2. Colony formation and
3. Dispersal.

1.3.2.1 Surface attachment

In the initial step for biofilm formation, motile *V. cholerae* scan solid surfaces for attachment, though the preference is always for chitinous exoskeleton of zooplankton or phytoplankton. The chitin from these surfaces can be used as a carbon source. *V. cholerae* has single polar flagellum at one end which works by a Na⁺ motor. This flagellum rotates fast and generates torque forces in the bacterial cell body and as a result of this force, bacteria can move in one direction in clockwise paths. Many studies have suggested that *V. cholerae* have strategies which make the bacterium assay a surface prior to starting biofilm formation (Wong 2016). MSHA-pili also play very important role for scanning and attachment to the surfaces and allow the bacteria to fix to start colonization (Rodney 2002, Römling et al 2013, Gerard 2016). The fate of active flagellum after attachment is still not completely

known. Current research indicates that it might be degraded after initial attachment or it can play a role to hold another cell together and become a structural element in the biofilm. According to Watnick (2001) and Lauriano (2004), the absence or mutation in a flagellar gene (*FlaA*) triggers exopolysaccharide production which in turn, induces biofilm formation. After successful attachment, bacteria start to adjust and start multiplication or colonization.

1.3.2.2 Colony formation

After initial attachment on the surface, bacterial cell starts multiplication and produce extracellular matrix made of polysaccharide and protein. In a mature *V. cholerae* biofilm, distinct morphological and phenotypic cell would be present (Wong 2016). At the onset of colony formation, the size of an average cell is bigger, which continuously decreases with later growth of biofilm. Drescher et al. (2016) observed that at the beginning of biofilm formation (when cells are fewer than 100 in number) the cell reaches an average size of about 2.4 μM , which goes down to 1.8 μM for cellular communities with 1000 in number. With the increase in cellular concentration and number, interbacterial distances also decrease in biofilm matrix.

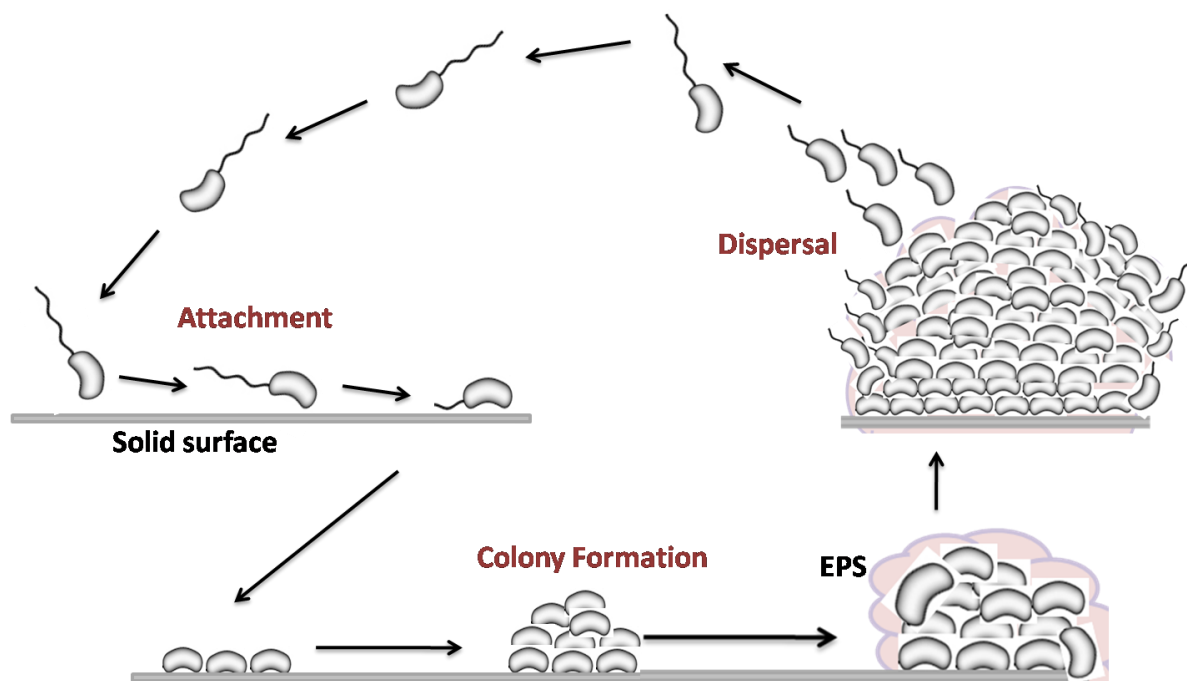


Figure 1.4: Representation of different stages for biofilm formation in *V. cholerae*

Apart from cell morphology and cellular concentration, the pattern for biofilm formation also varies with growth stage. For example, initially when cells are 2-6 in number, growth occurs

by elongation in only one direction (1D); for 40-100 cells, growth will be two directional (2D); this later goes on into three directions (3D) for cell number more than 200-1000 cells. When cells are growing in 3D, they start producing extracellular matrix made of polysaccharides, protein, and a small amount of nucleic acids (**Joachim and Karl 2002, Gerard 2016**). The extracellular matrix in *V. cholerae* biofilm is rich in sugar, and the total polysaccharides content cover up to 50% of the matrix which is produced by cells shortly after attachment. Vibrio polysaccharides (VPS) are essential for holding all cells together and making the 3D structure. Protein is the second important part of the extracellular matrix. *V. cholerae* produces three distinct proteins in the biofilm - RbmA, RbmC, and Bap1 which have different functions in the biofilm. RbmA protein takes part in cell adhesion, architecture and biofilm stability process, while RbmC is secreted on cell outer surface to create flexible envelopes for cells where they can grow or multiply. Bap1 protein maintains pellicle strength and contributes mostly to pellicle hydrophobicity that allows the biofilm to spread with the controlled air-water interface (**Römling et al 2013, Hay and Zhu 2015**). Few studies also suggest that Bap1 may be also involved in antibacterial resistance (**Hammer and Bassler 2009**). A detailed study is still required to find out the contribution of matrix proteins in biofilm formation and their interaction with an outer membrane protein.

1.3.2.3 Dispersal

After the maturation of biofilm, when conditions are favourable, bacteria start to detach from extracellular matrix. This is a last and important step for *V. cholerae* biofilm formation. After getting environmental and internal signal, bacterial cells try to disperse and colonize a new surface. Environmental conditions such as high/low oxygen level, the concentration of phosphate etc, has negative regulation on biofilm formation. Ca^{2+} concentration in the extracellular environment can also inhibit *vps* gene transcription and induce the dispersal of *V. cholerae* biofilm. Nitric oxide (NO) which is naturally produced in the aquatic environment by many lower eukaryotes or prokaryotes has also been reported to have an effect on dispersal of a microbial biofilm (**Colwell and Huq 1994, Hay and Zhu 2015**). There are atleast two deoxyribonucleases and the Xds protein which have also been reported to play a part in biofilm dispersal (**Sisti et al 2013, Römling et al 2013**). Mutations in these deoxyribonucleases and Xds induced biofilm formation and altered detachment of bacteria from the matrix. After detachment from matrix, bacteria can swim freely in water as their flagellum become active and then they search for a new solid surface (zooplankton or phytoplankton) for biofilm formation. The degradation of biofilm and extracellular matrix is

induced by various environmental signal and other proteins which are directly or indirectly involved in this process. However, these systems are still not well illustrated.

1.4. Regulation of biofilm formation

Biofilm formation is one of the most important environmental adaptations used as a tactic by various microorganisms, whereby, they undergo phenotypic variations favourable to survive in stress conditions. There are two things which are included in microbial biofilm formation: increase in cellular concentration and production of extracellular matrix. Formation of biofilm is a biologically expensive process for the microorganism, but the formation is a must to survive in stress conditions. To save the energy, this process is highly regulated with the interplay of various factors. In *V. cholerae*, cellular multiplication is regulated by transcriptional activators (such as VpsR and VpsT), transcriptional repressor protein and sigma factors RpoS and RpoE (**Ryan et al 2010**). The second part of microbial biofilm viz., the production of extracellular matrix is controlled by quorum sensing and signaling regulatory pathways mediated by secondary messenger molecule (**Watnick and Kolter 2000, Tischler and Camilli 2005, Hengge et al 2006**).

In *V. cholerae* the structural genes for extracellular polysaccharide synthesis (VPS) are located on *vps-1* (*vpsA* to *vpsK*) and *vps-2* (*vpsL* to *vpsQ*) operons. Both the operons *vps-1* and *vps-2* are reported for the involvement of their genes in biofilm formation. The expression of these operons is regulated by various factors including *VpsR*, *VpsT* and *HapR*. *VpsR*, a member of response regulator family positively regulates biofilm formation in *V. cholerae*. From a structural aspect, *VpsR* has response regulatory domain (REC) in its N-terminal, an ATPase and Helix-Turn-Helix (HTH – a DNA binding domain) in C-terminal region (Figure 1.5). *VpsR* takes part in biofilm formation process and controls gene expression level; it directly binds to the *vps* promoter regions which are involved in polysaccharide synthesis. The upregulation of extracellular matrix protein-coding genes is also reported by Beyhan et al (2007). These findings suggest that *VpsR* play its role in pathogenesis for *V. cholerae*. A very recent study shows that it can bind to cyclic-di-GMP (secondary messenger molecule), which is known as a master regulator of lifestyle switch in *V. cholerae* (**Hengge et al 2006, Hay and Zhu 2015**).

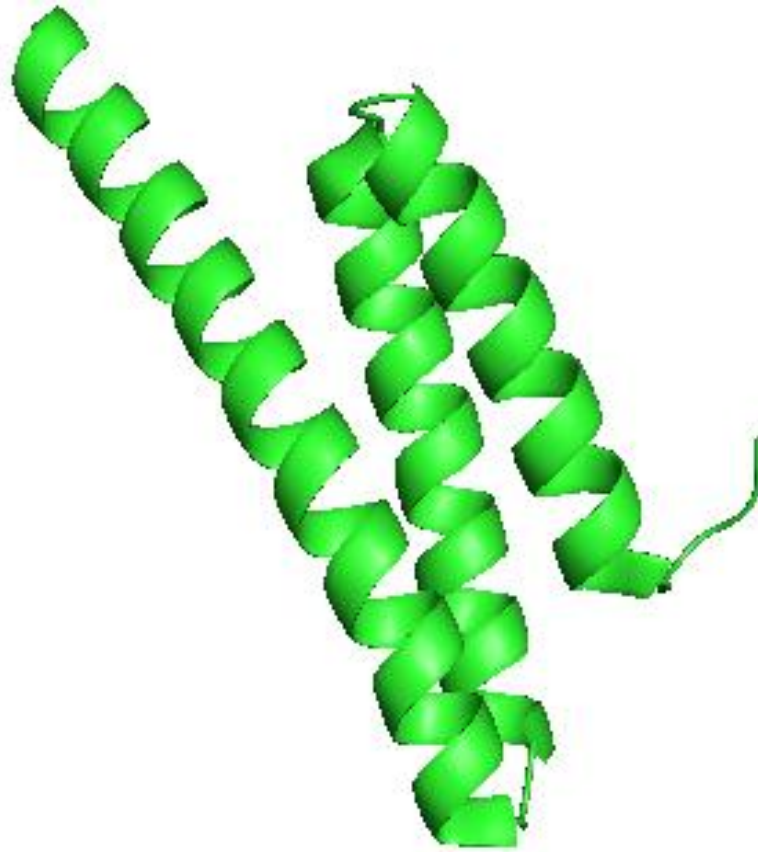


Figure 1.5: Structure of VpsR from *S. cerevisiae*. C-terminal DNA binding domain (Helix-Turn-Helix HTH).

VpsT is another response regulatory protein which positively regulates biofilm formation in *V. cholerae*. It can also bind *vps* promoter region and directly control gene expression. Similar to *vpsR*, a mutation in *vpsT* gene reduces the expression of extracellular polysaccharide and matrix protein synthesis – the main components for biofilm formation. VpsT and VpsR have also been reported for regulation of other genes such as c-di-GMP metabolism and genes encoding for various hypothetical protein whose functions are still unknown. So based on these studies, we can say that both *VpsR* and *VpsT* are interconnected and regulate many other genes which take part in biofilm formation in *V. cholerae*. Yildiz (2004) suggested that VpsR and VpsT both have recognition sites in *vps-1*, *vps-2* and *vps-L* operon which acts as regulatory sequences. Recent findings revealed that VpsT can act as a regulatory protein and has recognition sequences for RbmA (protein that takes part in cell adhesion), whereas RbmC and Bap1 (*rbmC* and *bap1*: involved in biofilm elasticity and pellicle strength) promoters also contain recognitions sites for VpsR protein (**Boyd and O'Toole 2012, Zhao-Xun 2015**). All these findings revealed that both of these proteins

act as strong regulators by targeting various other regulatory regions which directly or indirectly take part in biofilm formation in *V. cholerae* (Figure 1.6).

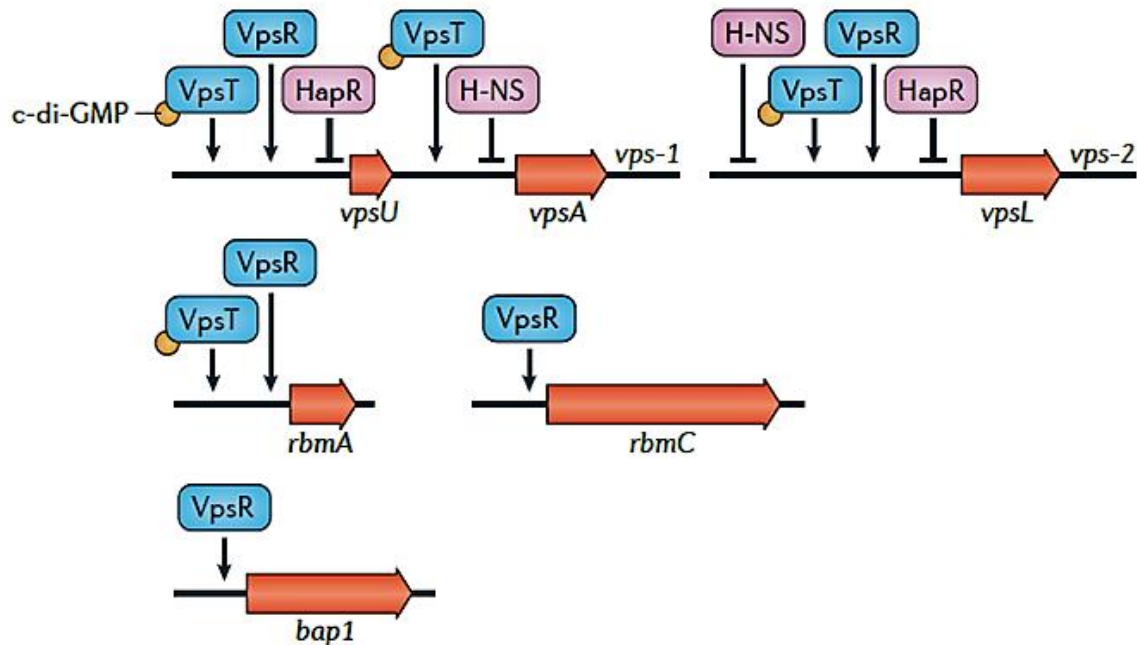


Figure 1.6: Regulatory network in *V. cholerae*. Interaction of c-di-GMP with various transcriptional activators.

Other than these positive regulators, there are many negative regulators also present in *V. cholerae* which repress biofilm formation pathways. HapR is one such example for the negative regulator in *V. cholerae*, which directly binds to the *vps-2* operon at its first gene of *vpsL* and *vpsT* (Jonas et al 2008, Sudarsan et al 2008). HapR has HTH domain at its N terminal region and a dimerization domain at C terminal region (Figure 1.6). Dimerization domain is reported for binding of an amphipathic ligand (Barends 2009). The activation of HapR for biofilm regulation (biofilm dispersal) is controlled by a small molecule which involves in the quorum sensing pathway. At lower concentration of quorum sensing molecule AI-2 and CAI-1 (at lower cell density in biofilm), RpoN and LuxO will be phosphorylated, this phosphorylation activates the transcription of sRNAs (quorum sensing regulatory RNA). The activated sRNAs work with sRNA chaperone Hfq and prevent the translation of the *hapR* gene, which leads to upregulation of biofilm formation (Figure 1.6). In contrast, at higher concentration of CAI-1 and AI-2 for higher cell density in biofilm, the receptors on the cell surface (CqsS and LuxQ) dephosphorylate LuxO protein thereby triggering repression of

sRNA. This whole activity activates HapR expression which ultimately leads to dispersal of biofilm (**Tchigvintsev et al 2010**).

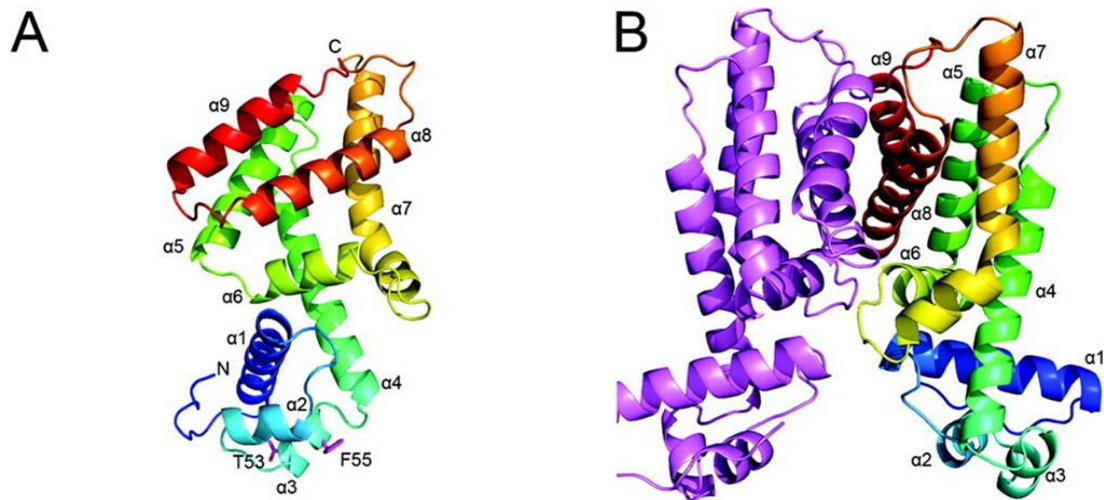


Figure 1.7: Crystal Structure of the *Vibrio cholerae* Quorum-Sensing Regulatory Protein HapR. (A) HapR monomer. The DNA binding surface is at the bottom in this orientation. (B) Two chain of HapR molecule as a dimer. (Rukman S. De Silva et al. 2007)

A histone-like protein H-NS is also reported to function as a transcriptional regulator. Due to its preferences for AT-rich regions, it is thought of as a modulator which has an important role in nucleoid topology (**Kulshina et al 2009**). It is reported that strains lacking mutation in *hns* or *hns* have increased biofilm formation, and results reveal that H-NS control directly binding to *vpsL*, *vpsA* and *vpsT* as a negative regulator. It is also reported that binding of VpsT to the *vpsL* prevents H-NS mediated silencing (**Christen et al 2007**).

1.5. c-di-GMP and biofilm in *V. cholerae*

Cyclic diguanosine monophosphate (c-di-GMP) was discovered first by Benziman et al. at the Hebrew University of Jerusalem (**Ross et al 1987**). Benziman suggested that this was an allosteric factor which involved in the process for cellulose biosynthesis in *Gluconacetobacter xylinus*. Over time, in the last 30 years, c-di-GMP became a hot topic for research in bacterial signaling pathways. Scientists discovered the various roles of this molecule in many other pathways (Table 1.2).

c-di-GMP or cyclic diguanylate is a nucleotide-based ubiquitous secondary messenger molecule in bacteria, also reported in some of archaea and eukaryotes (**Ryjenkov 2005**,

Srivastava et al 2013). Many scientific studies revealed that c-di-GMP regulates diverse cellular functions in bacteria at the transcriptional, translational and posttranslational levels. The cellular functions regulated by c-di-GMP include cell motility, cell cycle progression, virulence, biofilm formation, antibiotic productions and other unknown functions (**Ryan et al 2010, Römling 2013**). During the last 20 years, several researchers have discovered that it has a key role in transition in bacterial lifestyle (from mobile to sessile states or planktonic to biofilm transition). It is reported that c-di-GMP promotes the production of extracellular matrix or component for biofilm extracellular polysaccharides, as well as induces expression of adhesions which help to establish biofilm formation in many bacteria. Results also found inhibition of bacterial motility by suppressing the expression of flagellar genes and flagella activity by c-di-GMP.

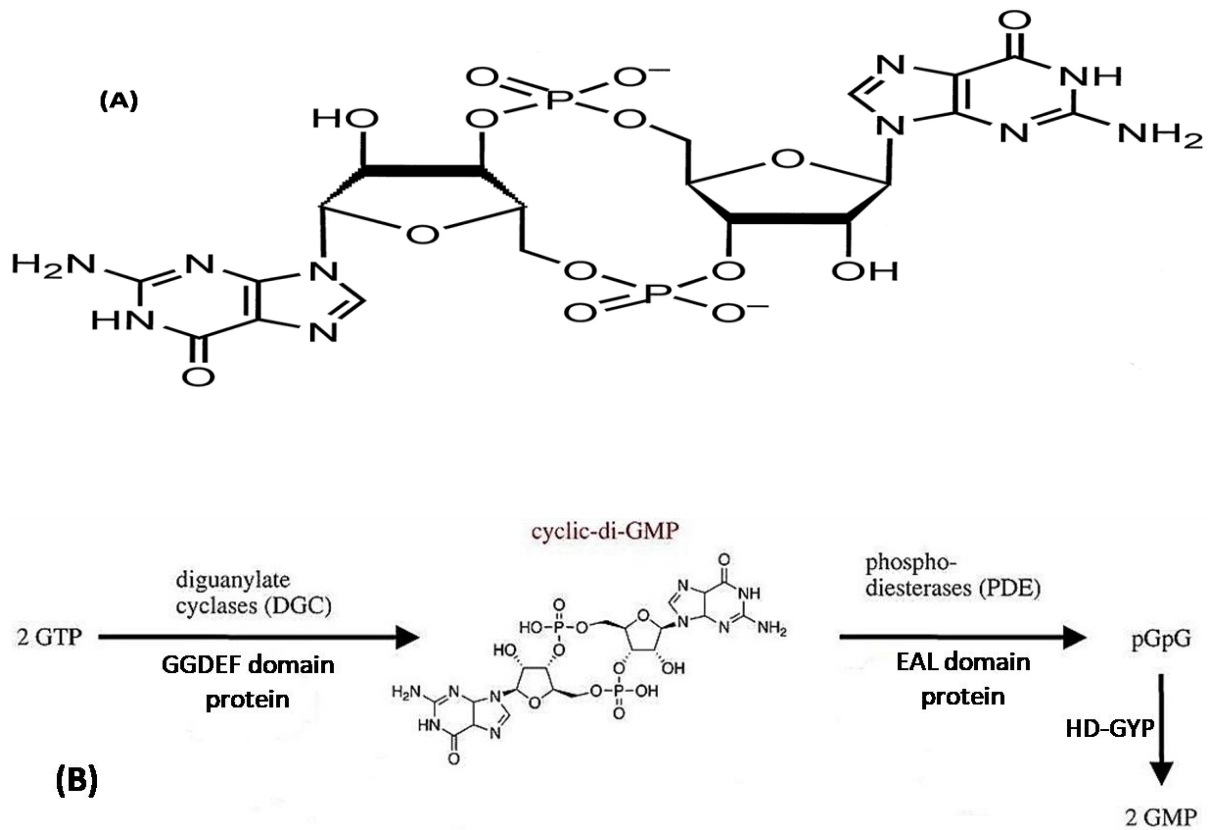


Figure 1.8: (A) Chemical structure of c-di-GMP molecule. (B) Chemical reaction for c-di-GMP formation and hydrolyzation catalyze by GGDEF protein and EAL protein.

TABLE 1.2 The ancient history of c-di-GMP. (Source Romling et al 2013)

Time	Events	References
220 BC	Qin dynasty in China Reportedly the first use of the Kombucha “tea mushroom,” a symbiotic culture of yeast and acetobacteria which produces a thick cellulose pellicle	
1946	First studies of bacterial cellulose synthesis at The Hebrew University	Hestrin S. (1947)
1987	Discovery of c-di-GMP, its chemical synthesis, proof that c-di-GMP is the true activator of cellulose synthase	Ross P. (1987)
1995	Discovery that c-di-GMP suppresses replication of cancer cells	Amikam D. (1995)
1995	Characterization of GGDEF domain in the <i>C. crescentus</i> response regulator PleD	Hecht GB (1995)
1998	Characterization of DGC and c-di-GMP PDE genes	Tal R. (1998)
1998	Characterization of the EAL domain protein BvgR in <i>Bordetella pertussis</i> , alignment of the EAL domains	Merkel TJ (1998)
1999	Description of the HD-GYP domain, proposal of a c-di-GMP-related novel signal transduction system	Galperin MY (1999)
1999	Characterization of the GGDEF-containing response regulators PleD and CelR	Aldridge P. (1999)
2000	Involvement of AdrA, a transmembrane protein with a C-terminal GGDEF domain, in intercellular adhesion	Slater H. (2000)
2000	Involvement of the HD-GYP domain protein RpfG in regulation of pathogenicity in <i>Xanthomonas campestris</i>	Tatusov RL (2000)
2000	The COG database identifies GGDEF, EAL, and HD-GYP domain genes in most bacteria but not in archaea	Ausmees N. (2001)
2001	Genetic proof that the GGDEF domain has DGC activity	Ausmees N. (2001)
2001	Detailed description of the GGDEF, EAL, and HD-GYP domains as components of bacterial signal transduction	Galperin MY (2001)
2001	Binding of oxygen to its PAS domain regulates activity of the c-di-GMP PDE from <i>G. xylinus</i>	Chang AL (2001)

2004	Crystal structure of the GGDEF domain, experimental proof of its DGC activity, identification of the allosteric I site for feedback inhibition	Chan C. (2004) Paul R. (2004)
2004	Proposal that c-di-GMP is a universal second messenger	Jenal U. (2004)
2004	c-di-GMP involvement in pathogenesis of <i>Yersinia pestis</i> and <i>Vibrio cholerae</i>	Kirillina O. (2004) Tischler AD (2004)
2004	c-di-GMP and transition from sessility to motility	Simm R. (2004)
2005	GGDEF-catalyzed c-di-GMP biosynthesis in various bacterial phyla	Ryjenkov DA (2005)
2005	Experimental proof of the PDE activity of the EAL domain	Bobrov AG (2005)
2005	Biofilm dispersal by c-di-GMP	Christen M. (2005)
2006	Description of the c-di-GMP-binding PilZ domain	Amikam D. (2006)
2006	Description of global c-di-GMP network regulation by the stress sigma factor RpoS in <i>E. coli</i>	Karaolis DK (2006)
2006	Experimental proof that the PilZ domain binds c-di-GMP	Ryjenkov DA (2006)
2007	Characterization of GGDEF-EAL domain proteins in which both domains are enzymatically active	Kim YK (2007)
2007	Description of immunostimulating activity of c-di-GMP	Ebensen T. (2007)
2008	Discovery of a c-di-GMP-sensing riboswitch	Sudarsan N. (2008)
2008	Description of global c-di-GMP network regulation by the RNA-binding protein CsrA and the quorum sensing system	Jonas K. (2008) Waters CM (2008)
2009	Crystal structure of the EAL domain	Barends TR (2009)

2010	Discovery of the second c-di-GMP-sensing riboswitch	Lee ER (2010)
2011	Molecular mechanism of regulation of LapG proteolytic activity through the c-di-GMP receptor LapD	Navarro MV (2011)
2011	Identification and structural characterization of the first eukaryotic c-di-GMP receptor	Burdette DL (2011)
2012	Discovery of a c-di-GMP signaling system in the eukaryote <i>Dictyostelium</i> , a social amoeba	Chen ZH (2012)

In bacteria, the c-di-GMP molecule is synthesized by a class of enzymes known as diguanylate cyclases (DGCs) which always possess a GGDEF domain in it. GGDEF domain in DGC contains a conserved sequence motif of five amino acids (GGD(/E)EF = Gly-Gly-Asp (/Glu)-Glu-Phe) and known as A-site or active site. A-site in DGC serves as a binding site for substrate molecule and takes part in c-di-GMP synthesis (**Figure 1.7**). Most of the DGCs, but not all have a secondary binding site for c-di-GMP known as I-site or inhibitory site, which allosterically regulate c-di-GMP synthesis process in bacteria.

Breakdown of this secondary messenger molecule is catalyzed by another specific class of enzymes known as phosphodiesterase (PDEase), which contain either EAL or HD-GYP domains in it (Figure 1.8B). The intracellular level of this messenger molecule is thus regulated by opposing actions of DGC and PDE enzymes. GGDEF domain-containing DGC enzyme utilizes two molecules of guanosine-5'-triphosphate (GTP) and synthesizes one molecule of c-di-GMP, which can be further degraded by PDE (EAL or HD-GYP domain-containing enzyme) activity. Phosphodiesterase break c-di-GMP into 5-phosphoguanylyl-(3-5)-guanosine, which further hydrolyzed into two molecules of GTP (Figure 1.8B). Several DGC or PDE proteins contain both GGDEF and EAL domains in same polypeptide chain along with environmental sensory domain which indicates that these proteins are interrelated and function in a complex signal integration systems. There are possibilities that when both DGC and PDE domains are present in the same polypeptide chain, only one of the two domains would be enzymatically active and the other domain would just serve as the binding site for the substrate or take part in regulation. The very first protein identified in *G. Xylinus* contained both GGDEF and EAL domains, but the protein had either DGC or PDE activity at a single time (**Tal et al 1998, Chang et al 2001**). Similar results were found for BifA protein from *Pseudomonas aeruginosa* (**Chou et al 2016**).

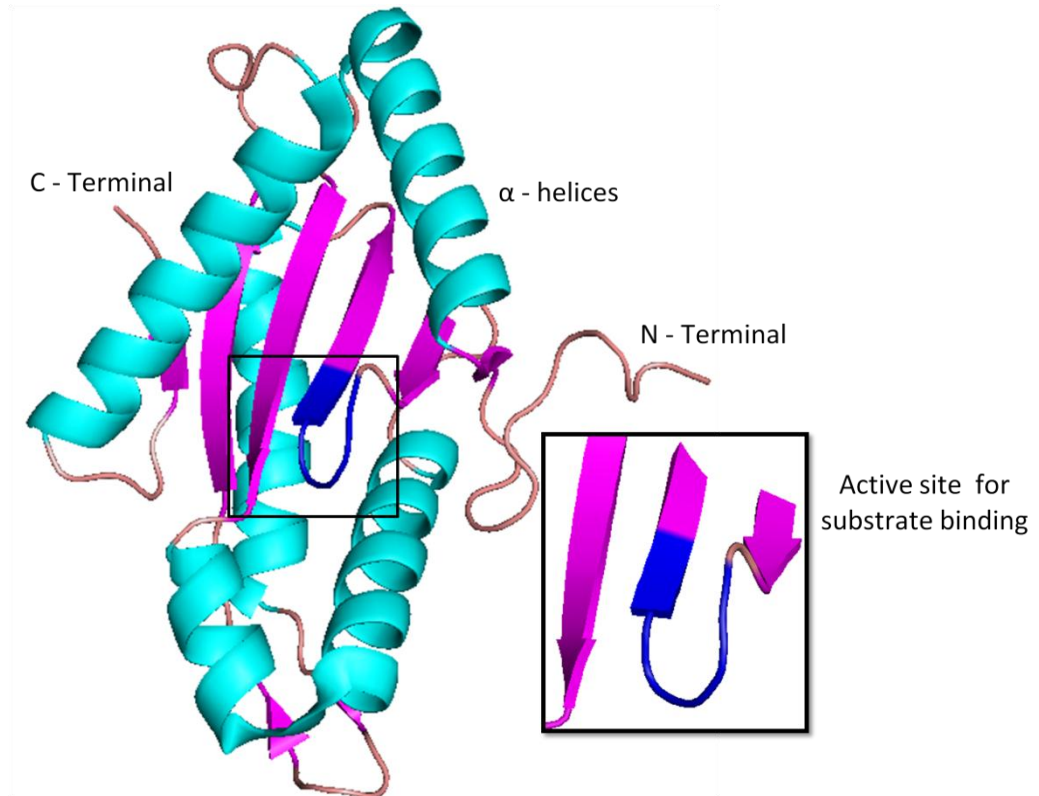


Figure 1.9: Crystal structure of a catalytically active GG(D/E)EF domain containing protein (DGC=diguanylate cyclase) from *Marinobacter aquaeolei*. Active site of protein with signature GGDEF amino acids is showing in the box. (Vorobiev et al 2012).

In recent studies, researchers have discovered few proteins with bifunctionally active DGC and PDE (**Zhao 2015**). In such case, results indicate that when enzymatically active GGDEF and EAL domains are present in same polypeptide chain, the domains will be differentially regulated by external or internal signals in bacteria so at a single time, only one enzyme activity will be prevalent. *Vibrio parahaemolyticus* has a gene *scrC* which belongs to a *scrABC* operon, and takes part in the switch between motile to sessile form and extracellular polysaccharide production. This protein ScrC has both GGDEF and EAL domains and it shows both DGC and PDE activity in bacteria depending on quorum sensing signals. When cell density is high in biofilm, an autoinducer will bind to a periplasmic domain of ScrB. Binding to ScrB leads to stimulation of a switch from DGC to PDE activity for ScrC in *V. parahaemolyticus* (**Boles and McCarter 2002, Ferreira et al 2008, Trimble and McCarter 2011**). MSDGC-1 is another example of this type of protein from

Mycobacterium smegmatis which has GGDEF and EAL along with GAF domain, showing activity both for synthesizing and degradation of c-di-GMP (**Bharati et al 2012**).

1.5.1 Receptors for c-di-GMP

Now it is very well known that c-di-GMP is ubiquitously present in all bacterial group and several bacteria contains dozen of protein or RNAs which involve in c-di-GMP related signaling pathways (**Slater et al 2000, Galperin 2005**). The enzymes involved in these pathways can be easily identified through their signature domain such as GGDEF, EAL, and HD-GYP. According to several results, researchers found there are multiple number of proteins in bacteria which can be a target for c-di-GMP binding, and it's not essential to have sequence or structural similarity. Based on primary sequence or known binding site for c-di-GMP, several classes of receptors are identified including PilZ domain receptors, I-site receptors in GGDEF domain, degenerated DGC or PDE domain receptors, and HD-GYP domain receptors (Figure 1.10).

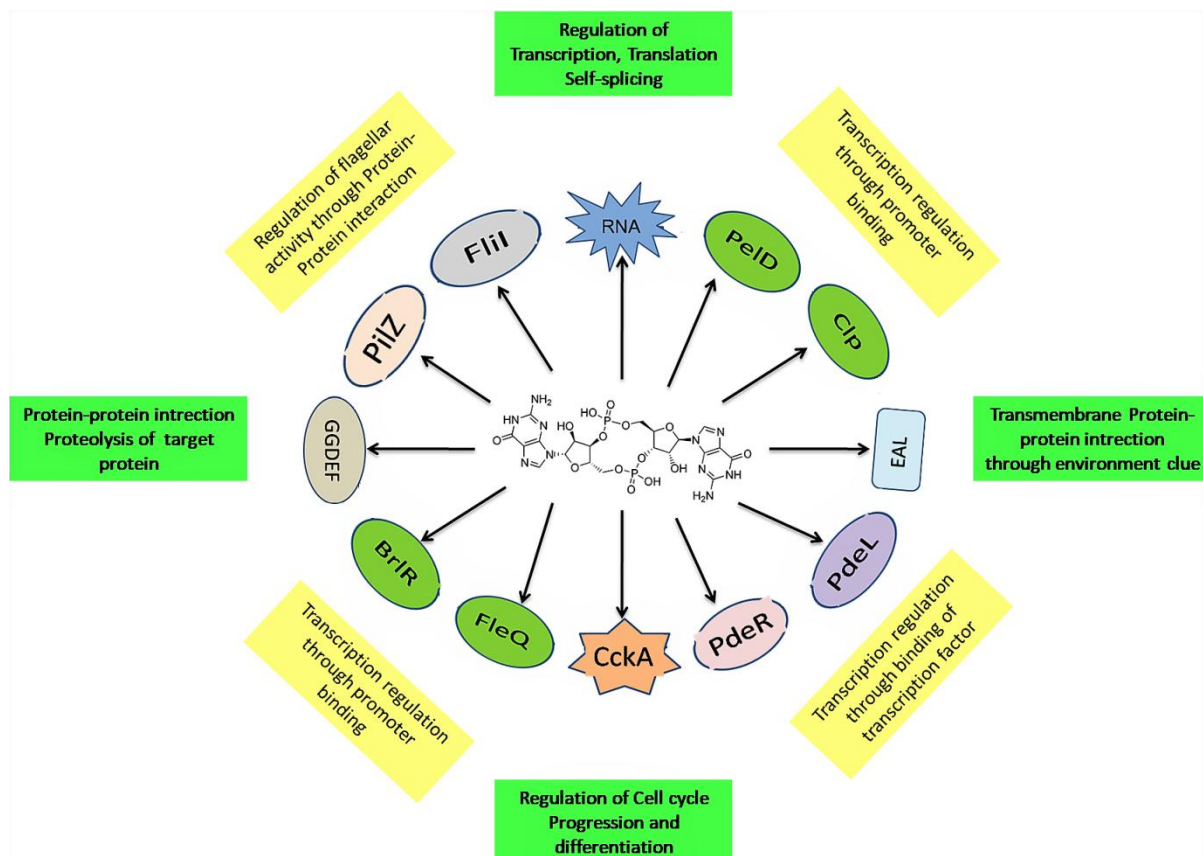


Figure 1.10: Diversity of c-di-GMP binding receptor, transcription factor and protein that shows affinity to c-di-GMP and affect microbial physiology at different level.

The most common protein receptor for c-di-GMP is GGDEF and EAL domain-containing protein. In DGCs, the protein has I-site for c-di-GMP binding to regulate product formation. Catalytically inactive GGDEF domains can also sometimes serve as the binding site for c-di-GMP (**Chan et al 2004, Christen et al 2006, Opoku-Temeng et al 2016**). The degenerated or catalytically inactive EAL domains can also serve as c-di-GMP receptors. FimX is a well-known example of this type of protein which was reported in *P. aeruginosa*, involved in pilus based motility. There are several results available now for c-di-GMP binding to PilZ domain, for example, BcsA from *G. Xylinus*, YcgR from *E. coli*, DgrA from *C. crescentus* and PlzC, PlzD from *V. cholerae*. X-ray and NMR structure revealed that binding of c-di-GMP to PilZ domain is not always the same and it can vary from protein to protein. To bind with c-di-GMP, a protein can adopt different oligomeric states, which can be important to relay different regulatory signals (**Ryjenkov et al 2006, Krasteva et al 2012, Kuchma et al 2015**).

Proteins with PilZ domains are widely spread among bacteria, but not all DGC or PDE serve as PilZ domain. For example, in *E. coli* only two proteins, BcsA and YcgR are considered to functions as PilZ domain, while the others are not. In *B. bacteriovorus* there are 15 PilZ domain proteins present while it has only 12 GGDEF, EAL, and HD-GYP proteins (**Chan et al 2004, Ryjenkov et al 2006**). Other than these protein receptors, it is also revealed that c-di-GMP can bind two different type of riboswitches. The c-di-GMP molecule can also bind regulatory segments of mRNA, to cause change in secondary structure or stability which ultimately affect the translation of encoded protein (a phenomena known as riboswitch) (**Tamayo et al 2007, Lee et al 2010**).

1.5.1.1 c-di-GMP and microbial physiology

When c-di-GMP was first discovered, it was known as a novel secondary messenger molecule involved in signaling pathways for bacterial biofilm formation in *G. xylinus*, *Salmonella enterica*, *V. cholerae*, and *P. aeruginosa* and cell differentiation in *C. crescentus* (**D'Argenio and Miller 2004, Jenal et al 2004, 2006, Paul et al 2004, Simm et al 2004**). Over the period of time, the list of the phenotypic characters affected by c-di-GMP has grown. The important key role played by c-di-GMP is in the switch between motile to sessile lifestyles and this has already been reported for a range of bacteria. In the aquatic environment, regulation of the transmission from motile to sessile forms involves c-di-GMP in all possible ways. These include motility (swimming, swarming, twitching, and gliding

movement), surface attachment (through fimbriae and pili), extracellular matrix component (polysaccharide, matrix protein, and another structural filament), biofilm dispersal etc (**Tamayo et al 2005**).

1.5.1.2 Regulation of flagellar gene

Free-living planktonic bacteria use flagellar movement for swimming. Other than swimming, the bacterial flagella can also be used as an organelle which helps for initial temporary attachment to the surface. Several results show that c-di-GMP regulate the flagellar motility in numerous bacteria. YcgR is a protein in *S. enterica* involved in flagellar motility, and it has been identified as a c-di-GMP receptor. YcgR protein takes part in control of flagellar rotation which leads to direction for movement. It binds to two other subunits of flagellar proteins, FliG and FliM and makes complex FliGMN. When c-di-GMP binds to YcgR, it causes a conformational change in YcgR which ultimately affects the flagellar movement (**Fang and Gomelsky 2010, Paul et al 2010**). c-di-GMP also regulates the expression of the *ycgR* gene. The c-di-GMP dependent YcgR regulation is reported in *E. coli*, *S. enterica* and member of Gamma and Betaproteobacteria which have YcgR homologs (**Fang and Gomelsky 2010**).

1.5.1.3 Control of motility to sessility transition

There are some reports that show a high level of intracellular c-di-GMP in bacteria leads to sessility and low-level induces surface swarming motion (**Benach et al 2007**). The O'Toole group (2015) reported that c-di-GMP signaling involves in *P. aeruginosa* is responsible for swarming motion through the DGC protein SadC and PDE activity by BifA. McCarter also revealed a molecular mechanism for c-di-GMP based regulation of swarming motion in *V. parahaemolyticus*. According to their results, a higher level of intracellular c-di-GMP suppresses the *laf* gene expression which encodes for lateral flagella involved in surface swarming motion in *V. parahaemolyticus* (**Beyhan et al 2007, Boehm et al 2010**).

1.5.1.4 Regulation of extracellular matrix component

Numerous studies show that c-di-GMP regulation is important for several extracellular matrix components involved in biofilm formation. These matrix components can be regulated on the transcriptional, posttranscriptional, and posttranslational levels by c-di-GMP. Here we highlight a few examples of c-di-GMP regulation of matrix components for biofilm formation

in microorganisms. Cellulose is known as a key component of biofilm and the enzymes which involve in cellulose synthesis *viz.*, cellulose synthases have a binding site for c-di-GMP (**Ryjenkov et al 2006**). The poly β -1,6-N-acetylglucosamine (PAG) is an exopolysaccharide (component for biofilm matrix) involved in intercellular adhesion in several bacteria. The activation of biosynthesis of PAG by c-di-GMP is reported in *Y. pestis*, *E. coli* and *Pectinobacterium atrosepticum* (**Kirillina et al 2004, Opoku-Temeng et al 2016**). In *P. aeruginosa* Pel and Psl polysaccharides components present in the extracellular matrix are both synthesized due to activation by c-di-GMP.

1.5.1.5 Pili and c-di-GMP

Non-flagellar filamentous proteinous appendages present on bacterial surfaces are known as pili or fimbriae. These pili or fimbriae are always associated with a surface attachment on biotic or abiotic solid surfaces. Expression of pili or fimbriae associated gene is tightly regulated by c-di-GMP signaling. The activation of type 3 fimbrial cluster in *K. pneumonia* by c-di-GMP has been reported at the transcriptional level (**Johnson et al 2011**). The DGC (with GGDEF domain) protein YfiN induces type 3 fimbriae gene expression, while PDE protein MrkJ suppresses type 3 fimbriae gene expression. In *P. aeruginosa* cup fimbriae (fimbrial gene cluster for five different genes *cup A, B, C, D* and *cupE*; chaperon/user pathway = Cup) are identified for their adhesive properties and contribution to biofilm formation. The expression of four cup fimbriae genes *cup A, B, C, D* is negatively regulated by c-di-GMP on the transcriptional level. Curli fimbriae structural component for extracellular matrix, present in *E. coli*, *S. enterica*, and several other bacteria have been reported to be directly regulated by c-di-GMP (**Bobrov et al 2005**).

1.5.1.6 Adhesins and c-di-GMP

Apart from fimbriae or pili adhesions, there are other structural components for biofilm formation which allow or contribute to surface adherence and stabilizing the extracellular matrix on solid surfaces. The adhesive protein LapA found in *P. putida* and *P. fluorescens* is required for irreversible surface attachment. LapA proteins exist on the bacterial cell surface and promote bacterial adhesion to solid surfaces (**Karatan and Watnick 2009**). These proteins are also involved in cell to cell interconnection and provide stability to biofilms and manage their dispersal (**Gjermansen et al 2006, Liu et al 2010**). Scientists suggest that at a low intracellular level of c-di-GMP, LapA protein is proteolyzed by a transmembrane protein known as LapD. LapD protein has a binding site for c-di-GMP; c-di-GMP binding

causes conformational changes in the periplasmic domain that leads LapD to sequester another protein LapG and inhibit its proteolytic activity, thus ultimately preventing LapA activity (**Hengge 2009, 2016**). The two-component secretion system in *P. aeruginosa*, the CdrAB which includes helical adhesin protein was also noted to be positively regulated by c-di-GMP at the transcriptional level.

1.5.1.7 Cyclic di-GMP and virulence

The virulence resulting from c-di-GMP signaling pathways has been highlighted in numerous pathogens. In *V. cholerae*, it was reported that c-di-GMP plays an important role in expression of cholera toxin which is a major virulence factor. It is well-established that low intracellular levels or absence of c-di-GMP in *V. cholerae* induce expression of various virulence factors (**Camilli et al 2008**). Studies also reveal that deletion of all phosphodiesterase suppresses virulence while deletion of all DGC induces virulence in various ways in *Brucella melitensis* infection (**Petersen et al 2011**). The inhibition of acute infection in *Y. pestis* and *B. burgdorferi* by the higher intracellular level of c-di-GMP was also reported. There are numerous reports which suggest that almost all secretion systems are subjected to c-di-GMP mediated regulation in microorganisms.

TABLE 1.3 Virulence phenotypes affected by c-di-GMP. (Source Romling et al 2013)

Phenotype	Species	c-di-GMP level	enzymes involved	References
<i>In vivo</i> virulence	<i>X. campestris</i>	Variable	PDE RpfG and 12 additional PDEs/DGCs	Ryan RP (2007)
	<i>P. aeruginosa</i>	Variable	5 DGCs/PDEs	Kulesekara H. (2006)
	<i>S. typhimurium</i>	Variable	PDE STM3615, DGC STM2672, DGC STM4551	Ahmad I. (2011)
	<i>A. phagocytophilum</i>	High	DGC PleD	Lai TH (2008)
	<i>B. melitensis</i>	Low	PDEs BpdA and BpdB, DGC CgsB	Petersen E. (2011)
	<i>F. novicida</i>	Low	Overexpression of DGC	Choy WK (2004)
Adherence	Adherent-invasive	Low	PDE YhjH, DGC	Claret L.

to host cells	<i>E. coli</i>		AdrA	(2007)
	Uropathogenic <i>E. coli</i> CFT073	High	DGC YdeH, PDE C1610, and 10 additional DGCs/PDEs	Caiazza NC (2007)
Host cell invasion	<i>B. pseudomallei</i>	Low	PDE CdpA	Lee HS (2010)
	Adherent-invasive <i>E. coli</i>	Low	PDE YhjH	Claret L. (2007)
	<i>E. chaffeensis</i>	Elevated	PDE PleD	Kumagai Y. (2010)
	<i>S. typhimurium</i>	Variable	DGCs STM1987 and STM4551, PDE STM3611 and STM4264	Ahmad I. (2011)
Cytotoxicity to host cells	<i>B. pseudomallei</i>	Low	PDE CdpA	Lai TH (2008)
	<i>L. pneumophila</i>	Low	Overexpression of DGC	Kumagai Y. (2011)
	<i>P. aeruginosa</i>	Variable	DGCs, PDEs	Kulesekara H (2006)
Intracellular infection	<i>A. phagocytophilum</i>	Elevated	DGC PleD	Caiazza NC (2007)
	<i>E. chaffeensis</i>	Elevated	DGC PleD	Kumagai Y. (2011)
	<i>L. pneumophila</i>	Low	DGC	Levi A. (2011)
	<i>F. novicida</i>	Low	Overexpression of DGCs	Zogaj X. (2012)
Modulation of immune response	<i>S. typhimurium</i>	Low	DGC STM1283, PDEs STM4264 and STM2503	Ahmad I. (2011)

In *V. cholerae*, the cholera toxin substrate for type II secretion system, in *Xanthomonas campestris* endoglucanases, in *Dickeya dadantii* the pectate lyase production are notably inhibited by c-di-GMP signaling pathways (**Tischler and Camilli 2005, Ryan RP et al 2007, Römling et al 2010, 2013**). The expression of transcriptional factor *toxF* (related to a transcriptional activator of cholera toxin) requires phosphodiesterase activity of VieA to maintain a low level of c-di-GMP in *V. cholerae*. The expression of VirB6 and other surface-exposed proteins (a component of type IV secretion system), which are involve in

pathogenicity for *E. chaffeensis* is regulated by c-di-GMP dependent proteolysis (**Kumagai et al 2010**). The c-di-GMP signaling pathways for biofilm regulation play an important role in chronic infection. Results reveal that after one-year persistence in cystic fibrosis lungs *P. aeruginosa* can develop bacterial colony after intracellular level of c-di-GMP goes up (**Schmidt et al 2005, Tamayo et al 2007, Minasov et al 2009**).

1.6. Genome analysis of *V. cholerae*

V. cholerae notably contains two closed circular chromosomes in it. Chromosome I (29,61,146 base pairs with G+C content 46.9%) is twice in size as compared to chromosome II (10,72,314 base pairs with G+C content 47.7%). The majority of the essential genes which are required for normal cellular functions such as growth and viability are located on the larger chromosome, but some of the essential genes are also located on chromosome II. Genes such as *dsdA*, *thrS* and other genes which code for important intermediaries of metabolic pathways and ribosomal protein-encoding gene (L20 and L35) are found on chromosome II (**Heidelberg et al 2000**).

Table 1.4 Characteristic of *V. cholerae* chromosome

	Chromosome I	Chromosome II
Size (base pair)	29,61,146	10,72,314
Total number of sequences	36,797	14,367
G + C percentage	47.7	46.9
Total Number of ORFs	2770	1115
ORFs size	952	918
percentage of the coding region	88.6	86.3
Number of rRNA operons	8	0
Number of tRNA	94	4
Number of conserved hypothetical proteins	478	165
Number of hypothetical proteins	515	419
Number of Rho-independent terminators	599	193

All essential genes required for cellular growth and virulence for *V. cholerae* are asymmetrically distributed in both chromosomes. Most of the genes encoded for DNA repair and replication, transcription, translation process, important cellular enzyme required for metabolic pathways, cell-wall synthesis, and genes essential for bacterial pathogenicity (lipopolysaccharide synthesis, cholera toxin) are located on the larger chromosome I. All the ribosomal RNA operons and one set of all tRNA coding genes are present on chromosome I, four tRNA coding genes are also located on smaller chromosome, but their duplicates copies are found on chromosome I. Smaller chromosome II mostly contains hypothetical genes (59%) and other genes with unknown functions. Chromosome II sequence revealed that large part (125 kbp) of this genomes localized as Integron Island and also carries the *3-hydroxy-3-methylglutaryl CoA reductase*, a gene actually evolved from archaea (**Heidelberg et al 2000**). Chromosome II is not considered as a plasmid or megaplasmid because it contains some of the housekeeping and other essential genes in it which are necessary for metabolism, it also carries heat shock protein, and 16S rRNA genes that are used for tracking evolutionary relationships between bacteria.

Earlier studies proposed that chromosome II is actually a megaplasmid which was engulfed by ancestral vibrio species from other organisms (**Heidelberg et al 2000**). One extra copy of genome becomes very advantageous for *V. cholerae* in many different ways. For instance, in adverse environmental conditions one chromosome can migrate into daughter cell without second chromosome (aberrant segregation). The daughter cell containing only one chromosome is known as drone cell. These types of cells maintain their metabolic activity but they will be replication defective. The drone cells would be a potential source of viability but they remain nonculturable (VBNC). Drone cells are often found in biofilms and they play a very important role in maintaining viability or enhancing survival of the cell. Under these adverse environmental conditions, two set of chromosomes give an extra advantage to the cell, due to differences in copy number so another chromosome may have accumulated genes that can express better at higher or lower copy number.

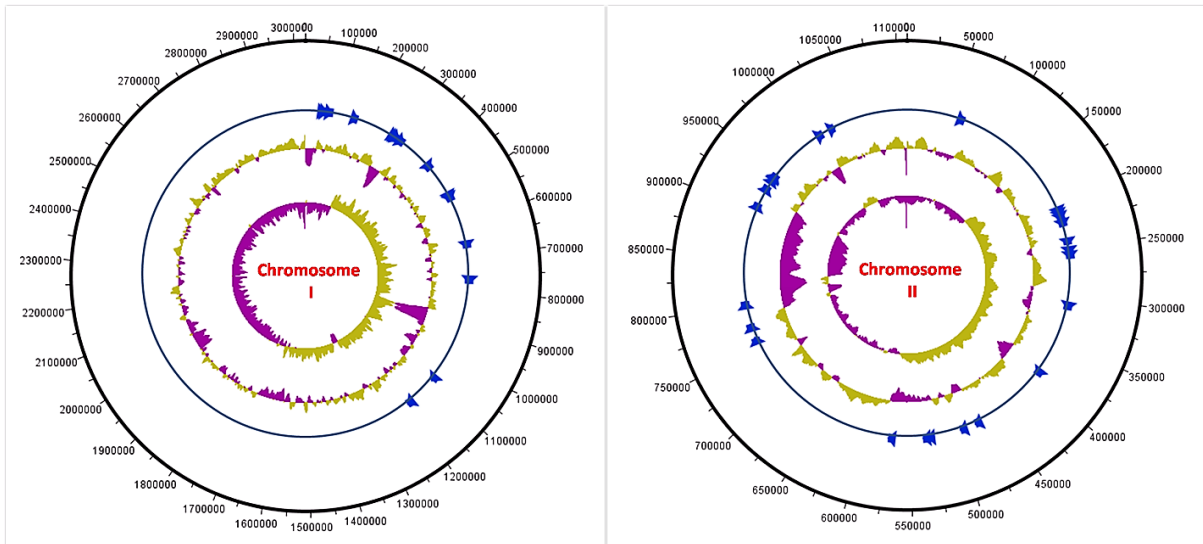


Figure 1.11: Graphical representation of *V. cholerae* chromosome. This map was generated by software DNA plotter using whole genome sequence for both chromosomes. Outer most line represent genomic sequence, second line represent the position of GGDEF domain containing protein in chromosome. Inner most two line shows mean G+C percentage and GC skew respectively.

1.7. GGDEF protein in *V. cholerae*

The GGDEF family proteins are responsible for c-di-GMP synthesis in bacteria, which can be further hydrolyzed by EAL domain-containing protein. Various scientific reports suggest that GGDEF and EAL domains are tandemly arranged in the same polypeptide chain. (**Ryjenkov et al 2005, Gjermansen et al 2006, Römling et al 2013**). All GGDEF family proteins necessarily contain the GGDEF domain, with conserved five amino acids (GGD(/E)EF = Gly-Gly-Asp(/Glu)-Glu-Phe) which serve as a signature motif. In last two decades, it has been confirmed that GGDEF family proteins are found in a wide range of organisms (Figure 1.12). Pei and Grishin (**2001**) suggested that DGC activity of GGDEF proteins is distantly similar to adenylate cyclases. Though the classes have low sequence similarity, but the globular structure of GGDEF protein has a remarkable similarity to adenylate cyclases (**Pei and Grishin 2001, Linder 2006**). All DGC enzymes have a loop like structure with conserved GGD(/E)EF motif which involves in GTP binding and serves as an active site of the protein. This family of proteins is thought to be linked with external environmental signalling and work based on various environmental clues. Several scientific reports revealed the coexistence of GGDEF protein fused with various environmental sensing domains such as PAS, GAF, REC, HTH, etc (**Watnick et al 2001**).

Many bacterial species report multiple proteins with GGDEF domains, for example, *V. cholerae* encodes 51 different proteins for GGDEF and EAL domain (showing in Table 5), *E. coli* has 31 proteins and *Shewanella oneidensis* contains 57 proteins. The multiplicity of this protein in microbial genomes indicates that different signals can be integrated at the same time and diverse processes regulated or controlled in parallel mode (Jenal and Malone 2006, Opoku-Temeng et al 2016).

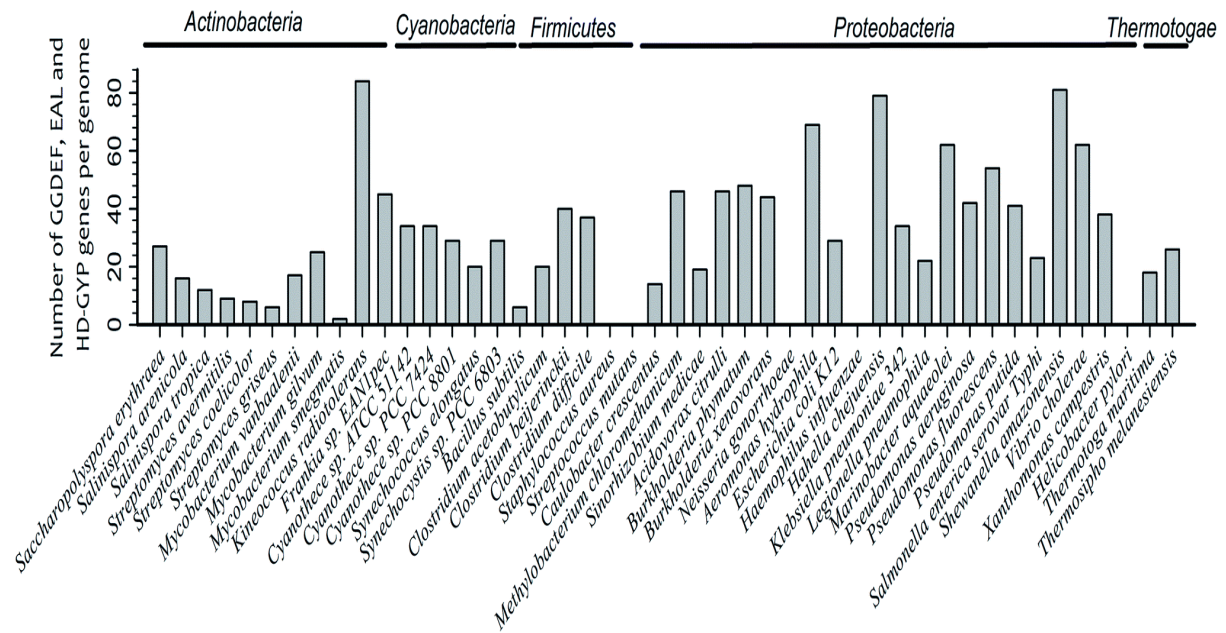


Figure 1.12: GGDEF and EAL domain-containing protein in five major bacterial phyla. Source Zhao-Xun L. 2015.

Table 1.5 Showing various GGDEF domain-containing proteins in *V. cholerae*.

	Gene	Transmembrane part	Other sensory domain	EAL
Chromosomes I				
1	VC0395_0636	YES	PAS, PAC, HAMP	---
2	VC0395_0160	YES	HAMP	EAL
3	VC0395_0493	YES	---	---
4	VC0395_1013	YES	---	---
5	VC0395_0279	YES	CHASE	---
6	VC0395_0065	YES	---	---

7	VC0395_0489	YES	---	---
8	VC0395_0273	YES	---	---
9	VC0395_0300	---	PAS and PAC	---
10	VC0395_0283	---	---	---
11	VC0395_0059	---	---	EAL
12	VC0395_0086	---	---	---
13	VC0395_0389	---	---	---
14	VC0395_0726	---	---	EAL
15	VC0395_1112	---	---	---

Chromosomes II

1	VC0395_A0983	YES	HAMP	---
2	VC0395_A0967	YES	---	---
3	VC0395_A1949	YES	PAC	---
4	VC0395_A0622	YES	---	---
5	VC0395_A2031	YES	HAMP	---
6	VC0395_A0233	YES	HAMP	YES
7	mshH	YES	---	YES
8	VC0395_A0991	YES	CHASE	---
9	VC0395_A0806	YES	---	---
10	VC0395_A1874	YES	---	---
11	VC0395_A2442	YES	PAS	YES
12	VC0395_A1523	YES	---	YES
13	VC0395_A1817	YES	---	---
14	VC0395_A0985	YES	---	---
15	VC0395_A1195	YES	---	---
16	VC0395_A2322	---	HAMP	YES
17	VC0395_A0585	YES	---	---
18	VC0395_A0979	---	---	---

19	VC0395_A0841	---	---	---
20	VC0395_A0188	---	---	YES
21	VC0395_A0184	---	---	YES
22	VC0395_A0549	---	---	---
23	VC0395_A0422	---	---	---
24	VC0395_A2269	---	---	---
25	VC0395_A1204	---	---	---

1.8 Gaps in existing research

Based on available research data about GGDEF domain protein we found following gaps in existing research:

- The GGD(/E)EF domain, though ubiquitous in bacteria but it is still a relatively novel domain with very little information about its functional sites (Active site and Inhibitory site) and folding status available.
- With respect to *V. cholerae*, this domain has been found in both the chromosome of *V. cholerae* GGDEF domain protein. Nobody has ever attempted to mutate any of the signature amino acids in the domain and check for the consequences. The mutation in signature amino acids of GGD(/E)EF domain can surely alter the bacterial morphology and physiology.
- No one has tried to crystallize this novel protein to find accurate protein structure, its folding status, and arrangement of signature amino acids in GGD(/E)EF domain. In the absence of crystal structure prediction of activity by bioinformatics method is also not feasible.
- In the absence of crystal structure of this novel protein information regarding the binding of substrate molecule GTP to the active site and binding of c-di-GMP as a regulatory molecule to this domain is still not available.

1.9 Objectives of the proposed research:

The *VC0395_0300* is one of the putative GGD(/E)EF protein-coding genes in the chromosome I of *V. cholerae*. GGD(/E)EF domain-containing proteins are now well known for diguanylate cyclase activity, this protein utilizes two molecules of GTP as a substrate and converts them to one molecule of the c-di-GMP molecule. These domains can recognize first messengers (from environmental changes or signals) such as light in certain wavelength regions, oxygen concentration, and phosphorylation etc. Several processes such as exopolysaccharide synthesis, biofilm formation, motility and cell differentiation are thus regulated by this molecule

I will try to find out the importance of putative protein *VC0395_0300* from *V. cholerae*, functional characterizations of its GGEEF domain. It would be interesting for us to know how these GGD(/E)EF protein control modules are integrated with global regulatory circuits that can control bacterial stress responses, development, environmental or social behavior etc. In other words, we will have to know the biology of c-di-GMP signaling mediated by GGD(/E)EF domain proteins.

Therefore, the goal of this research for my doctoral thesis is to fulfil the existing gaps in research about the GGDEF domain protein, the following research objectives are proposed for this study:

- Cloning of mutants of *VC0395_0300* gene in *E. coli*.
- Expression and purification of mutant proteins.
- Biophysical characterization of *VC0395_0300* mutant proteins.
- Structure elucidation of *VC0395_0300* mutant proteins.

1.10 References

- Ahmad I, Lamprokostopoulou A, Le Guyon S, Streck E, Peters V, Barthel M, Hardt W-D, Römling U.** 2011. Complex c-di-GMP signaling networks mediate the transition between virulence properties and biofilm formation in *Salmonella enterica* serovar Typhimurium. *PLoS One*. **6**: 28351.
- Aldridge P, Jenal U.** 1999. Cell cycle-dependent degradation of a flagellar motor component requires a novel-type response regulator. *Mol. Microbiol.* **32**: 379–391.
- Amikam D, Steinberger O, Shkolnik T, Ben-Ishai Z.** 1995. The novel cyclic dinucleotide 3'-5'-cyclic diguanylic acid binds to p21ras and enhances DNA synthesis but not cell replication in the Molt 4 cell line. *Biochem. J.* **311**: 921–927.
- Aschner M, Hestrin S.** 1946. Fibrillar structure of cellulose of bacterial and animal origin. *Nature*. **157**: 659.
- Ausmees N, Jonsson H, Höglund S, Ljunggren H, Lindberg M.** 1999. Structural and putative regulatory genes involved in cellulose synthesis in *Rhizobium leguminosarum* bv. trifolii. *Microbiology* **145**: 1253–1262.
- Ausmees N, Mayer R, Weinhouse H, Volman G, Amikam D, Benziman M, Lindberg M.** 2001. Genetic data indicate that proteins containing the GGDEF domain possess diguanylate cyclase activity. *FEMS Microbiol. Lett.* **204**: 163–167.
- Amikam D, Galperin MY.** 2006. PilZ domain is part of the bacterial c-di-GMP binding protein. *Bioinformatics*. **22**: 3–6.
- Barends TR, Hartmann E, Griese JJ, Beitlich T, Kirienko NV, Ryjenkov DA, Reinstein J, Shoeman RI, Gomelsky M, Schlichting I.** 2009. Structure and mechanism of a bacterial light-regulated cyclic nucleotide phosphodiesterase. *Nature* **459**: 1015–1018.
- Beyhan S, Bilecen K, Salama SR, Casper-Lindley C, Yildiz FH.** 2007. Regulation of rugosity and biofilm formation in *Vibrio cholerae*: comparison of VpsT and VpsR regulons and epistasis analysis of *vpsT*, *vpsR*, and *hapR*. *J. Bacteriol.* **189**: 388–402.
- Benach J, Swaminathan SS, Tamayo R, Handelman SK, Folta Stogniew E, Ramos JE, Forouhar F, Neely H, Seetharaman J, Camilli A, Hunt JF.** 2007. The structural basis of cyclic diguanylate signal transduction by PilZ domains. *EMBO J.* **26**: 5153–5166.
- Bharati BK, Sharma IM, Kasetty S, Kumar M, Mukherjee R, Chatterji D.** 2012. A full length bifunctional protein involved in c-di-GMP turnover is required for long term survival under nutrient starvation in *Mycobacterium smegmatis*. *Microbiology* **158**: 1415–1427.
- Boehm A, Kaiser M, Li H, Spangler C, Kasper CA, Ackermann M, Kaefer V, Jenal U.** 2010. Second messenger-mediated adjustment of bacterial swimming velocity. *Cell* **141**: 107–116.
- Bobrov AG, Kirillina O, Perry RD.** 2005. The phosphodiesterase activity of the HmsP EAL domain is required for negative regulation of biofilm formation in *Yersinia pestis*. *FEMS Microbiol. Lett.* **247**: 123–130.

- Boles BR, McCarter LL.** 2002. *Vibrio parahaemolyticus* *scrABC*, a novel operon affecting swarming and capsular polysaccharide regulation. *J. Bacteriol.* **184**: 5946 – 5954.
- Boyd CD, O’Toole GA.** 2012. Second messenger regulation of biofilm formation: breakthroughs in understanding c-di-GMP effector systems. *Annu Rev Cell Dev Biol.* **28**: 439–62.
- Carla L, Martina E, Parisa N, Shuyang S, Diane Mc D.** 2013. Environmental reservoirs and mechanisms of persistence of *Vibrio cholerae*. *Frontier in microbio.* **4**: 375.
- Chang AL, Tuckerman JR, Gonzalez G, Mayer R, Weinhouse H, Volman G, Amikam D, Benziman M, Gilles-Gonzalez MA.** 2001. Phosphodiesterase A1, a regulator of cellulose synthesis in *Acetobacter xylinum*, is a heme-based sensor. *Biochemistry* **40**: 3420 –3426.
- Chan C, Paul R, Samoray D, Amiot NC, Giese B, Jenal U, Schirmer T.** 2004. Structural basis of activity and allosteric control of diguanylate cyclase. *Proc. Natl. Acad. Sci. U. S. A.* **101**: 17084 –17089.
- Charles, RC, Ryan ET.** 2011. Cholera in the 21st century. *Curr. Opin. Infect. Dis.* **24**: 472–477.
- Christen B, Christen M, Paul R, Schmid F, Folcher M, Jenoe P, Meuwly M, Jenal U.** 2006. Allosteric control of cyclic di-GMP signaling. *J. Biol. Chem.* **281**: 32015–32024.
- Christen M, Christen B, Allan MG, Folcher M, Jenoe P, Grzesiek S, Jenal U.** 2007. DgrA is a member of a new family of cyclic diguanosine monophosphate receptors and controls flagellar motor function in *Caulobacter crescentus*. *Proc. Natl. Acad. Sci. U. S. A.* **104**: 4112– 4117.
- Christen M, Christen B, Folcher M, Schauerte A, Jenal U.** 2005. Identification and characterization of a cyclic di-GMP-specific phosphodiesterase and its allosteric control by GTP. *J. Biol. Chem.* **280**: 30829–30837.
- Colwell RR, Huq A.** 1994. Environmental reservoir of *Vibrio cholerae*. The causative agent of cholera. *Ann. NY Acad. Sci.* **740**: 44-54.
- Chou SH, Galperin MY.** 2016 Diversity of cyclic di-GMP binding proteins and mechanisms. *J. Bacteriol.* **198**: 32–46.
- Claret L, Miquel S, Vieille N, Ryjenkov DA, Gomelsky M, Darfeuille Michaud A.** 2007. The flagellar sigma factor FliA regulates adhesion and invasion of Crohn’s disease-associated *Escherichia coli* via a c-di-GMP dependent pathway. *J. Biol. Chem.* **282**: 33275–33283.
- D’Argenio DA, Miller SI.** 2004. Cyclic di-GMP as a bacterial second messenger. *Microbiology.* **150**: 2497–502.
- Dahlstrom KM, Giglio KM, Collins AJ, Sondermann H, O’toole GA.** 2015. Contribution of physical interactions to signaling specificity between a diguanylate cyclase and its effector. *MolBio* **6**: 01978-15.
- Drescher K, Jörn D, Carey DN, Sven van T, Ivan G, Ned SW, Howard AS, Bonnie LB.** 2016. Architectural transitions in *Vibrio cholerae* biofilms at single-cell resolution. *Proceedings of the National Academy of Sciences* **113**: E2066-E2072.

Ebensen T, Schulze K, Riese P, Morr M, Guzman CA. 2007. The bacterial second messenger c-di-GMP exhibits promising activity as a mucosal adjuvant. *Clin. Vaccine Immunol.* **14**: 952–958.

Ferreira RB, Antunes LC, Greenberg EP, McCarter LL. 2008. *Vibrio parahaemolyticus* ScrC modulates cyclic dimeric GMP regulation of gene expression relevant to growth on surfaces. *J. Bacteriol.* **190**: 851–860.

Fang X, Gomelsky M. 2010. A post-translational, c-di-GMP-dependent mechanism regulating flagellar motility. *Mol. Microbiol.* **76**: 1295–1305.

Galperin MY, Natale DA, Aravind L, Koonin EV. 1999. A specialized version of the HD hydrolase domain implicated in signal transduction. *J. Mol. Microbiol. Biotechnol.* **1**: 303–305.

Galperin MY, Nikolskaya AN, Koonin EV. 2001. Novel domains of the prokaryotic two-component signal transduction systems. *FEMS Microbiol. Lett.* **203**: 11–21.

Galperin MY. 2005. A census of membrane-bound and intracellular signal transduction proteins in bacteria: bacterial IQ, extroverts and introverts. *BMC Microbiol.* **5**: 35.

Glass RI, Becker S, Huq MI, Stoll BJ, Khan MU, Merson MH, Lee JV, Black RE. 1982 Endemic cholera in rural Bangladesh, 1966 to 1980. *Am. J. Epidemiol.* **116**: 959–970.

Gerard CL Wong. 2016. Three-dimensional architecture of *Vibrio cholerae* biofilms. *PNAS* **113**: 3711–3713.

Gjermansen M, Ragas P, Tolker-Nielsen T. 2006. Proteins with GGDEF and EAL domains regulate *Pseudomonas putida* biofilm formation and dispersal. *FEMS Microbiol. Lett.* **265**: 215–224.

Hammer BK, Bassler BL. 2003. Quorum sensing controls biofilm formation in *Vibrio cholerae*. *Mol. Microbiol.* **50**: 101–104.

Hammer BK, Bassler BL. 2009. Distinct sensory pathways in *Vibrio cholerae* El Tor and classical biotypes modulate cyclic dimeric GMP levels to control biofilm formation. *J. Bacteriol.* **91**: 169–177.

Hay AJ, Zhu J. 2015. Host intestinal signal-promoted biofilm dispersal induces *Vibrio cholerae* colonization. *Infect. Immun.* **83**: 317–323.

Heithoff DM, Mahan MJ. 2004. *Vibrio cholerae* Biofilms: Stuck between a Rock and a Hard Place. *J. bacteriol.* **15**: 4835–4837.

Hengge R. 2016 Trigger phosphodiesterases as a novel class of c-di-GMP effector proteins. *Phil. Trans. R. Soc. B* **371**: 20150498.

Hengge R. 2009. Principles of c-di-GMP signaling in bacteria. *Nat. Rev. Microbiol.* **7**: 263–273.

Hestrin S, Aschner M, Mager J. 1947. Synthesis of cellulose by resting cells of *Acetobacter xylinum*. *Nature* **159**: 64–65.

Hecht GB, Newton A. 1995. Identification of a novel response regulator required for the swarmer-to-stalked-cell transition in *Caulobacter crescentus*. *J. Bacteriol.* **177**: 6223–6229.

Hdelberg JF, Venter C. et al. 2000. DNA sequence of both chromosomes of the cholera pathogen *Vibrio cholerae*. *Nature review* **406**: 477-484.

Jenal U. 2004. Cyclic di-guanosine-monophosphate comes of age: a novel secondary messenger involved in modulating cell surface structures in bacteria? *Curr. Opin. Microbiol.* **7**: 185-191.

Jenal U, Malone J. 2006. Mechanisms of cyclic-di-GMP signaling in bacteria. *Annu. Rev. Genet.* **40**: 385- 407.

Jonas K, Edwards AN, Simm R, Romeo T, Römling U, Melefors O. 2008. The RNA binding protein CsrA controls cyclic di-GMP metabolism by directly regulating the expression of GGDEF proteins. *Mol. Microbiol.* **70**: 236 -257.

Jonas K, Edwards AN, Ahmad I, Romeo T, Römling U, Melefors O. 2010. Complex regulatory network encompassing the Csr, c-di-GMP and motility systems of *Salmonella Typhimurium*. *Environ. Microbiol.* **12**: 524 -540.

Joachim R, Karl EK. 2002. *Vibrio cholerae* and cholera: out of the water and into the host. *FEMS microbial review.* **26**: 125-139.

Johnson JG, Murphy CN, Sippy J, Johnson TJ, Clegg S. 2011. Type 3 fimbriae and biofilm formation are regulated by the transcriptional regulators MrkHI in *Klebsiella pneumoniae*. *J. Bacteriol.* **193**: 3453-3460.

Karaolis DK, Means TK, Yang D, Takahashi M, Yoshimura T, Muraille E, Philpott D, Schroeder JT, Hyodo M, Hayakawa Y, Talbot BG, Brouillette E, Malouin F. 2007. Bacterial c-di-GMP is an immunostimulatory molecule. *J. Immunol.* **178**: 2171-2181.

Karaolis DK, Newstead MW, Zeng X, Hyodo M, Hayakawa Y, Bhan U, Liang H, Standiford TJ. 2007. Cyclic di-GMP stimulates protective innate immunity in bacterial pneumonia. *Infect. Immun.* **75**: 4942- 4950.

Karaolis DK, Rashid MH, Chythanya R, Luo W, Hyodo M, Hayakawa Y. 2005. c-di-GMP (3-5-cyclic diguanylic acid) inhibits *Staphylococcus aureus* cell-cell interactions and biofilm formation. *Antimicrob. Agents Chemother.* **49**: 1029-1038.

Karatan E, Watnick P. 2009. Signals, regulatory networks, and materials that build and break bacterial biofilms. *Microbiol. Mol. Biol. Rev.* **73**: 310-347.

Kim YK, McCarter LL. 2007. ScrG, a GGDEF-EAL protein, participates in regulating swarming and sticking in *Vibrio parahaemolyticus*. *J. Bacteriol.* **189**: 4094-4107.

Kirillina O, Fetherston JD, Bobrov AG, Abney J, Perry RD. 2004. HmsP, a putative phosphodiesterase, and HmsT, a putative diguanylate cyclase, control Hms-dependent biofilm formation in *Yersinia pestis*. *Mol. Microbiol.* **54**: 75- 88.

Krasteva PV, Giglio KM, Sondermann H. 2012. Sensing the messenger: the diverse ways that bacteria signal through c-di-GMP. *Protein Sci.* **21**: 929-948.

Kumagai Y, Matsuo J, Hayakawa Y, Rikihisa Y. 2010. Cyclic di-GMP signaling regulates invasion by *Ehrlichia chaffeensis* of human monocytes. *J. Bacteriol.* **192**: 4122- 4133.

- Kuchma SL, Delalez NJ, Filkins LM, Snaveley EA, Armitage JP, O'Toole GA.** 2015. Cyclic di-GMP-mediated repression of swarming motility by *Pseudomonas aeruginosa* PA14 Requires the MotAB stator. *J. Bacteriol.* **197**: 420–430.
- Kulshina N, Baird NJ, Ferre-D'Amare AR.** 2009. Recognition of the bacterial second messenger cyclic diguanylate by its cognate riboswitch. *Nat. Struct. Mol. Biol.* **16**: 1212–1217.
- Kulesekara H, Lee V, Brencic A, Liberati N, Urbach J, Miyata S, Lee DG, Neely AN, Hyodo M, Hayakawa Y, Ausubel FM, Lory S.** 2006. Analysis of *Pseudomonas aeruginosa* diguanylate cyclases and phosphodiesterases reveals a role for bis-(3-5)-cyclic-GMP in virulence. *Proc. Natl. Acad. Sci. U.S.A.* **103**: 2839 –2844.
- Lai TH, Kumagai Y, Hyodo M, Hayakawa Y, Rikihisa Y.** 2008. *Anaplasma phagocytophilum* PleC histidine kinase and PleD diguanylate cyclase two-component system and role of cyclic di-GMP in host-cell infection. *J. Bacteriol.* **191**: 693–700.
- Lee HS, Gu F, Ching SM, Lam Y, Chua KL.** 2010. CdpA is a *Burkholderia pseudomallei* cyclic di-GMP phosphodiesterase involved in autoaggregation, flagellum synthesis, motility, biofilm formation, cell invasion, and cytotoxicity. *Infect. Immun.* **78**: 1832–1840.
- Lee ER, Baker JL, Weinberg Z, Sudarsan N, Breaker RR.** 2010. An allosteric self-splicing ribozyme triggered by a bacterial second messenger. *Science* **329**: 845– 848.
- Levi A, Folcher M, Jenal U, Shuman HA.** 2011. Cyclic diguanylate signaling proteins control the intracellular growth of *Legionella pneumophila*. *Mol. Bio.* **2**: 00316–10.
- Lim B, Beyhan S, Yildiz FH.** 2007. Regulation of *Vibrio* polysaccharide synthesis and virulence factor production by CdgC, a GGDEF-EAL domain protein, in *Vibrio cholerae*. *J. Bacteriol.* **189**: 717–729.
- Lim B, Beyhan S, Meir J, Yildiz FH.** 2006. Cyclic-diGMP signal transduction systems in *Vibrio cholerae*: modulation of rugosity and biofilm formation. *Mol. Microbiol.* **60**: 331–348.
- Linder JU.** 2006. Class III adenylyl cyclases: molecular mechanisms of catalysis and regulation. *Cell. Mol. Life Sci.* **63**: 1736 –1751.
- Liu N, Pak T, Boon EM.** 2010. Characterization of a diguanylate cyclase from *Shewanella woodyi* with cyclase and phosphodiesterase activities. *Mol. Biosyst.* **6**: 1561–1564.
- Minasov G, Padavattan S, Shuvalova L, Brunzelle JS, Miller DJ, Basle A, Massa C, Collart FR, Schirmer T, Anderson WF.** 2009. Crystal structures of YkuI and its complex with second messenger cyclic di-GMP suggest a catalytic mechanism of phosphodiester bond cleavage by EAL domains. *J. Biol. Chem.* **284**: 13174 –13184.
- Merkel TJ, Barros C, Stibitz S.** 1998. Characterization of the *bvgR* locus of *Bordetella pertussis*. *J. Bacteriol.* **180**: 1682–1690.
- Nelson EJ, Harris JB, Morris Jr JG, Calderwood SB, Camilli A.** 2009. Cholera transmission: the host, pathogen and bacteriophage dynamic. *Nature microbio review.* **7**: 693-702.

Opoku-Temeng C, Zhou A, Zheng Y, Jianmei S, Sintim HO. 2016. Cyclic dinucleotide (c-di-GMP, c-di-AMP, and cGAMP) signalings have come of age to be inhibited by small molecules. *Chem. Commun.* **52**: 9327-9342.

Ogunniyi AD, Paton JC, Kirby AC, McCullers JA, Cook J, Hyodo M, Hayakawa Y, Karaolis DK. 2008. c-di-GMP is an effective immunomodulator and vaccine adjuvant against pneumococcal infection. *Vaccine* **26**: 4676-4685.

Paul R, Weiser S, Amiot NC, Chan C, Schirmer T, Giese B, Jenal U. 2004. Cell cycle-dependent dynamic localization of a bacterial response regulator with a novel diguanylate cyclase output domain. *Genes Dev.* **18**: 715-727.

Paul K, Nieto V, Carlquist WC, Blair DF, Harshey RM. 2010. The c-di-GMP binding protein YcgR controls flagellar motor direction and speed to affect chemotaxis by a "backstop brake" mechanism. *Mol. Cell* **38**: 128 -139.

Pei J, Grishin NV. 2001. GGDEF domain is homologous to adenyl cyclase. *Proteins* **42**: 210 -216.

Petersen E, Chaudhuri P, Gourley C, Harms J, Splitter G. 2011. *Brucella melitensis* cyclic di-GMP phosphodiesterase BpdA controls expression of flagellar genes. *J. Bacteriol.* **193**: 5683-5691.

Rodney MD. 2002. Biofilms: Microbial Life on Surfaces. *Emerging Infectious Diseases.* **8**: 881-890.

Ross P, Weinhouse H, Aloni Y, Michaeli D, Weinberger-Ohana P, Mayer R, Braun S, de Vroom E, van der Marel GA, van Boom JH, Benziman M. 1987. Regulation of cellulose synthesis in *Acetobacter xylinum* by cyclic diguanylic acid. *Nature* **325**: 279 - 281.

Römling, U, Galperin, MY, Gomelsky M. 2013. Cyclic di-GMP: the first 25 years of a universal bacterial second messenger. *Microbiol. Mol. Biol. Rev.* **77**: 1-52.

Römling U, Rohde M, Olsen A, Normark S, Reinköster J. 2000. AgfD, the checkpoint of multicellular and aggregative behavior in *Salmonella typhimurium* regulates at least two independent pathways. *Mol. Microbiol.* **36**: 10 -23.

Ryan RP, Fouhy Y, Lucey JF, Jiang BL, He YQ, Feng JX, Tang JL, Dow JM. 2007. Cyclic di-GMP signaling in the virulence and environmental adaptation of *Xanthomonas campestris*. *Mol. Microbiol.* **63**: 429-442.

Ryan RP, McCarthy Y, Andrade M, Farah CS, Armitage JP, Dow JM. 2010. Cell-cell signaldependent dynamic interactions between HD-GYP and GGDEF domain proteins mediate virulence in *Xanthomonas campestris*. *Proc. Natl Acad. Sci. USA* **107**: 5989-5994.

Ryan RP, Fouhy Y, Lucey JF, Dow JM. 2006. Cyclic di-GMP signaling in bacteria: recent advances and new puzzles. *J Bacteriol.* **188**: 8327-34.

Ryjenkov DA, Tarutina M, Moskvin OV, Gomelsky M. 2005. Cyclic diguanylate is a ubiquitous signaling molecule in bacteria: insights into biochemistry of the GGDEF protein domain. *J. Bacteriol.* **187**:1792-1798.

Ryjenkov DA, Simm R, Römling U, Gomelsky M. 2006. The PilZ domain is a receptor for the second messenger c-di-GMP. The PilZ domain protein YcgR controls motility in enterobacteria. *J. Biol. Chem.* **281**: 30310-30314.

- Schmidt AJ, Ryjenkov DA, Gomelsky M.** 2005. The ubiquitous protein domain EAL is a cyclic diguanylate-specific phosphodiesterase: enzymatically active and inactive EAL domains. *J. Bacteriol.* **187**: 4774–4781.
- Simm R, Fetherston JD, Kader A, Römling U, Perry RD.** 2005. Phenotypic convergence mediated by GGDEF-domain-containing proteins. *J. Bacteriol.* **187**: 6816–6823.
- Simm R, Morr M, Kader A, Nimtz M, Römling U.** 2004. GGDEF and EAL domains inversely regulate cyclic di-GMP levels and transition from sessility to motility. *Mol. Microbiol.* **53**: 1123–1134.
- Sisti F, Ha DG, O'Toole GA, Hozbor D, Fernández J.** 2013. Cyclic-di-GMP signalling regulates motility and biofilm formation in *Bordetella bronchiseptica*. *Microbiology* **159**: 869–879.
- Slater H, Alvarez-Morales A, Barber CE, Daniels MJ, Dow JM.** 2000. A two-component system involving an HD-GYP domain protein links cell-cell signaling to pathogenicity gene expression in *Xanthomonas campestris*. *Mol. Microbiol.* **38**: 986 – 1003.
- Srivastava D, Hsieh ML, Khataokar A, Neiditch MB, Waters CM.** 2013. Cyclic di-GMP inhibits *Vibrio cholerae* motility by repressing induction of transcription and inducing extracellular polysaccharide production. *Mol. Microbiol.* **90**: 1262–1276.
- Stefan S, Anne LB, Camilli A.** 2008. Ins and Outs of *Vibrio cholerae*. *Microbe.* **3**: 131–136.
- Sudarsan N, Lee ER, Weinberg Z, Moy RH, Kim JN, Link KH, Breaker RR.** 2008. Riboswitches in eubacteria sense the second messenger cyclic di-GMP. *Science* **321**: 411– 413.
- Tamayo R, Tischler AD, Camilli A.** 2005. The EAL domain protein VieA is a cyclic diguanylate phosphodiesterase. *J. Biol. Chem.* **280**: 33324–33330.
- Tamayo R, Pratt JT, Camilli A.** 2007. Roles of cyclic diguanylate in the regulation of bacterial pathogenesis. *Annu. Rev. Microbiol.* **61**: 131–148.
- Tal R, Wong HC, Calhoon R, Gelfand DH, Fear AL, Volman G, Mayer R, Ross P, Amikam D, Weinhouse H, Cohen A, Sapir S, Ohana P, Benziman M.** 1998. Three *cdg* operons control cellular turnover of cyclic di-GMP in *Acetobacter xylinum*: genetic organization and occurrence of conserved domains in isoenzymes. *J. Bacteriol.* **180**: 4416–4425.
- Tarutina M, Ryjenkov DA, Gomelsky M.** 2006. An unorthodox bacteriophytochrome from *Rhodobacter sphaeroides* involved in the turnover of the second messenger c-di-GMP. *J. Biol. Chem.* **281**: 34751–34758.
- Tatusov RL, Galperin MY, Natale DA, Koonin EV.** 2000. The COG database: a tool for genome-scale analysis of protein functions and evolution. *Nucleic Acids Res.* **28**: 33–36.
- Tchigvintsev A, Xu X, Singer A, Chang C, Brown G, Proudfoot M, Cui H, Flick R, Anderson WF, Joachimiak A, Galperin MY, Savchenko A, Yakunin AF.** 2010. Structural insight into the mechanism of c-di-GMP hydrolysis by EAL domain phosphodiesterases. *J. Mol. Biol.* **402**: 524–538.

- Teschler JK, Zamorano-Sánchez D, Andrew SU, Christopher JA, Gerard CL, Roger GL, Fitnat H. Yildiz.** 2015. Living in the matrix: assembly and control of *Vibrio cholerae* biofilms. *Nature microbio review*. **13**: 255-268.
- Tischler AD, Camilli A.** 2004. Cyclic diguanylate (c-di-GMP) regulates *Vibrio cholerae* biofilm formation. *Mol. Microbiol.* **53**: 857– 869.
- Tischler AD, Camilli A.** 2005. Cyclic diguanylate regulates *Vibrio cholerae* virulence gene expression. *Infect. Immun.* **73**: 5873–5882.
- Trimble MJ, McCarter LL.** 2011. Bis-(3-5)-cyclic dimeric GMP-linked quorum sensing controls swarming in *Vibrio parahaemolyticus*. *Proc. Natl. Acad. Sci. U. S. A.* **108**: 18079–18084.
- Trucksis M, Michalski J, Deng YK, Kaper JB.** (1998). The *Vibrio cholerae* genome contains two unique circular chromosomes. *Proc. Natl Acad. Sci. USA* **95**: 14464-14469.
- Urs J, Jacob M.** 2006. Mechanisms of Cyclic-di-GMP Signaling in Bacteria. *Annu. Rev. Genet.* **40**: 385–407.
- Waters CM, Lu W, Rabinowitz JD, Bassler BL.** 2008. Quorum sensing controls biofilm formation in *Vibrio cholerae* through modulation of cyclic di-GMP levels and repression of *vpsT*. *J. Bacteriol.* **190**: 2527–2536.
- Watnick PI, Kolter R.** 1999. Steps in the development of a *Vibrio cholerae* El Tor biofilm. *Mol. Microbiol.* **34**: 586–595.
- Watnick PI, Kolter R.** 2000. Biofilm, city of microbes. *J. Bacteriol.* **182**: 2675–2679.
- Watnick PI, Lauriano CM, Klose KE, Croal L, Kolter R.** 2001. The absence of a flagellum leads to altered colony morphology, biofilm development and virulence in *Vibrio cholerae* O139. *Mol. Microbiol.* **39**: 223–235.
- Weber H, Pesavento C, Possling A, Tischendorf G, Hengge R.** 2006. Cyclic-di-GMP-mediated signaling within the sigma network of *Escherichia coli*. *Mol. Microbiol.* **62**: 1014–1034.
- Zhao-Xun L.** 2015. The expanding roles of c-di-GMP in the biosynthesis of exopolysaccharides and secondary metabolites. *Nat. Prod. Rep.* **32**: 663-683.
- Zogaj X, Wyatt GC, Klose KE.** 2012. Cyclic di-GMP stimulates biofilm formation and inhibits virulence of *Francisella novicida*. *Infect. Immun.* **80**: 4239–4247.

2.1 Introduction

V. cholerae, the causative agent of cholera disease, possesses two circular chromosomes which have 41 putative GGDEF domain-containing proteins, speculated to be involved in several signaling pathways and in the regulation of the pathogen's life cycle. The sequence similarities for these GGDEF-domain proteins are very low, but the overall secondary or tertiary structure may throw up some interesting similarities. Most of the GGDEF proteins also possess some other sensory domains such as PAS, CHASE, PAC, and EAL (**Jenal et al 2004**). These extra domains are involved in other regulatory functions as follows:

PAS: Respond and relay external environmental signal using an associated cofactor.

PAC: Associated at C-terminal of PAS domain, contribute to proper folding of PAS domain.

CHASE: Extracellular receptor-like protein, which involves in ligand binding reactions.

EAL: Known for diguanylate phosphodiesterase activity.

HAMP: Linker domain which is always associated with other sensory or receptor domains and involves in chemotaxis reaction.

There are several reports available now that reveal that the signature motif of this domain (for the five conserved amino acids GGD(/E)EF) serve as an active site for substrate binding. Though GGDEF domain-containing proteins are universally found in all groups of eubacteria, we still don't know the complete reaction mechanisms for activation of these proteins. Which external environmental signal responsible for trigger the function of these proteins and how they transfer the signal to another target are enigmas that need further disclosure.

In this study, we therefore, tried to find out the biochemical reaction mechanisms for a GGDEF protein. We selected a putative GGDEF protein encoded by the *vc0395_0300* gene from chromosome 1 of the *V. cholerae* classical strain O395, serotype O1. The VC0395_0300 protein shows the presence of PAS and PAC domain in the N-terminal

region and the C-terminal region mostly represents a GGEEF domain – an overall count of 321 amino acids present in this protein. We attempted to mutate the signature GGEEF motif and replaced each individual amino acid by site-directed mutagenesis. Biophysical characterization of all mutant proteins and comparisons with wild-type protein would be attempted to find out the actual role of each single amino acid individually in the light of protein functions.

2.2 Materials and methods

2.2.1 Genomic DNA isolation

Genomic DNA was isolated from *V. cholerae* classical strain O395 after 16-hour growth at 37 °C according to the methods of Hammer and Bassler (2009). In this method, harvested cell were lysed by 10% SDS in a 10 mM Tris buffer (pH 8) containing 1 mM EDTA and lysozyme. Lysed cells were treated with Proteinase K (100 µg/ml in 1% SDS). After incubation at 37 °C for 1 hour, RNAase was added to remove RNA and incubated again at 37°C for 30 minutes. The cell suspension was centrifuged at 14000 rpm for 30 minutes, and the clear suspension was followed by phenol-chloroform extraction. DNA was allowed to precipitate using isopropanol. Excess salt in precipitated DNA was removed by washing using 70% ethanol. Air-dried DNA pellet was resuspended in sterile distilled water and stored at -20 °C for further use.

2.2.2 Site-directed mutagenesis

Site-Directed Mutagenesis (SDM) in the GGEEF protein-coding gene (*vc0395_0300*) from *V. cholerae* was performed using two-step PCR megaprimer method (Tyagi et al 2004). Polymerase chain reactions were performed in an Applied Biosystems Veriti Thermal Cycler. All primers used for SDM, viz. internal primers, forward and reverse primers were purchased from New England Biolabs. In the first step, half of the gene was amplified using internal mutation containing forward primer and reverse primer (Table 2.1). Low-fidelity Dream Taq polymerase and dNTP mix from Fermentas were used for first PCR amplification reaction. For gene amplification, the PCR reactions were set up according to tables 2.2 and 2.3. After the first PCR reaction, product was purified using Qiaquick kit from Qiagen according to manufacturer's protocol. Purified product of first PCR reaction was used as a reverse primer

in the second round of PCR. In second step, the PCR reaction was set up similarly as the first PCR, except for annealing temperature. The second PCR reaction was done at a little higher temperature to assure specificity of megaprimer (**Zhen-Hua and Xiao-Jun 2009**). The product of second PCR reaction was purified using the same protocol as mentioned for the first PCR.

Table 2.1. Components for PCR reactions.

Components	Volume	Final concentrations
Taq buffer	5 μ l	1 X
Forward primer	2.0 μ l	20 pmol
Reverse primer	2.0 μ l	20 pmol
dNTP mix	1.2 μ l	200 μ M each
Template DNA	2.5 μ l	500 ng
Water	36.8 μ l	
Taq polymerase	0.5 μ l	1 U

Table 2.2. PCR program for amplification

PCR Step	Temperature	Time	Cycles
Initial denaturation	95 °C	5 min	1
Denaturation	95 °C	1 min	35
Annealing	58 °C	1 min	
Extensions	72 °C	1 min	
Final extensions	72 °C	10 min	1
Hold	6 °C	infinite	

Table 2.3. List of primers used for amplification of *vc0395_0300* gene. The restriction enzyme recognition sites in primer sequence are indicated as underlined. The site of the mutation has been shown in red color and italics in the above primers.

	Primer Sequence	Restriction enzyme
	<i>Forward Primer</i>	
Primer for full length of VC0395_0300	5'ATAATACT <u>GGATCC</u> ATGAAAAATTGGCTGTGTCAGGCAGT 3'	BamH1
	<i>Reverse Primer</i>	
	5'ATAATACT <u>CTCGAG</u> TTATTCTGTGGATTGGCGATAGATAC3'	Xho1
	<i>VC0395_0300(G237R)</i>	
	5' GATGATGAACTCTTCAC <u>G</u> TCCCACACG 3'	
	<i>VC0395_0300(E238K)</i>	
Internal Mutation containing forward primer	5' GATGATGAACTCTT <u>T</u> ACCTCCCACACG 3'	
	<i>VC0395_0300(E239K)</i>	
	5' GATGATGAACT <u>T</u> TTACCTCCCACACG 3'	
	<i>VC0395_0300(F240I)</i>	
	5' GATGATGA <u>T</u> CTCTTCACCTCCCACACG 3'	

2.2.3 Agarose gel electrophoresis

The PCR product was visualized by agarose gel electrophoresis. 1% agarose gel was prepared in TAE buffer supplemented with 0.5 µg/ml ethidium bromide. DNA samples were a mix of 6X DNA loading dye and loaded onto agarose gel after solidification and allowed to run at constant voltage (70-80 V). For the comparisons of size, DNA ladder (100 bp) was also loaded onto the gel. The gel was analyzed in UV light and sizes of products were estimated by comparison with DNA ladder.

2.2.4 Restriction digestion

Purified PCR products were further double digested with appropriate restriction enzymes to generate compatible sticky ends for directional cloning. The reorganization site in PCR product for the corresponding enzyme was inserted using primer design during PCR reactions. For digestion reaction, 5-10 µg of DNA was mixed with appropriate enzymes and buffer and incubated at 37 °C (Table 2.4). After 4 hours of incubation, digested DNA fragments were run on 0.8% agarose gel. The desired DNA fragments were excised from the gel and purified using Qiaquick gel extraction kit from Qiagen according to manufacturer's protocol.

Table 2.4. Components for restriction digestion mixture.

S. No.	Component	amount
1	DNA sample	1 µg
2	10X restriction buffer	2 µl
3	Xho1	1 µl
4	BamH1	1 µl
5	Nuclease-free distilled water	Up to 20 µl

2.2.5 Vector DNA preparation

For the cloning of *vc0395_0300* gene, GST tag containing vector pGEX- 6P1 was used. Plasmid pGEX-6P1 containing strain was grown overnight at 37°C with continuous shaking. After 16 hours incubation, plasmid was purified using GeneJet Plasmid extraction kit according to manufacturer's method. Purified plasmid was further subjected to double digestion with same restriction enzymes as PCR product and cut plasmid was purified by Qiaquick gel extraction kit.

2.2.6 Ligation

A 6 fold molar excess of restriction digested insert (PCR product) was added to 50-80 ng of restriction digested plasmid. The concentrations of DNA insert and cut plasmids were determined by spectrophometric method. The amount of insert DNA needed for ligation was calculated using the formula:

$$\text{ng of insert DNA required} = \frac{(\text{ng of Vector}) \times (\text{insert length in bp})}{\text{Vector length in bp}} \times \text{Molar ratio of } \frac{\text{insert}}{\text{vector}}$$

Before setting the ligation reaction restriction, digested vector DNA and insert DNA were mixed in a 1.5 ml tube and incubated at 65 °C for 10 min. Heating before setting the ligation reaction disrupt self-ligated vectors or insert-insert cohesive-end interactions which give false results for cloning and reduce ligation efficiency. The complete reaction mixture for ligation was prepared as mentioned in table 2.5 and incubated at 16 °C for overnight. Ligation reactions were stopped by incubating the reactions at 65 °C for 10 minutes.

Table 2.5. Components for ligation reaction mixture

S. No.	Component	Amount
1	Insert DNA (PCR product)	250-300 ng
2	Vector DNA	50-100 ng
3	10X T4 Ligase buffer	2 µl
4	T4 DNA Ligase	1 µl
5	Nuclease-free distilled water	Up to 20 µl

2.2.7 Preparation of competent *E. coli* cells

To prepare competent cells, single colony of DH5α *E. coli* was inoculated in 5 ml of LB liquid medium and allowed to grow at 37 °C overnight. 1% of saturated overnight culture was further inoculated into fresh LB medium and subjected to growth at 37 °C with shaking until absorbance A₆₀₀ reached 0.5. The cells were kept on ice for 15 minutes and harvested at 4000

rpm for 10 minutes at 4 °C. The harvested cells were washed with 75 mM ice cold CaCl₂ to remove residual culture medium. After washing, cells were resuspended in 75 mM ice cold CaCl₂ and incubated on ice for 30 minutes. Cells were again subjected to harvesting at 4 °C, and harvested cells resuspended in ice-cold 75 mM CaCl₂ and incubated for 16-18 hours.

2.2.8 Transformation

For transformation, 100 ng of plasmid DNA and ligation reaction mixture was mixed with 50 µl of CaCl₂ competent cells and incubated on ice for 10 minutes. The mixture was further given a heat shock at 42 °C for 90 seconds in a water bath and immediately transferred to ice for 15 minutes. 1 ml of liquid LB medium was added to cells and incubated at 37 °C for 1 hour with constant agitation for revival. After revival, cells were spread on LB agar plates containing 100 µg/ml of ampicillin antibiotic. The positive colonies which contained appropriate plasmid were further grown in liquid LB medium, glycerol stock was prepared using sterile glycerol and stored in -80 °C.

2.2.9 Plasmid isolation

Plasmid DNA was isolated according to modified alkaline lysis method. This method was initially developed by Brinboim and Doly (1979). According to this method, overnight saturated bacterial cells were harvested from LB medium by centrifugation. The bacterial pellets were resuspended in resuspension buffer and incubate on ice for 5 minutes. This bacterial cells suspension was allowed to lysis for 3-5 minutes on the ice after adding freshly prepared lysis solution. Bacterial lysate was neutralized by chilled neutralization solution. Bacterial cell debris and insoluble material separated from the suspension by high-speed centrifugation for 20 minutes. The supernatant was gently mixed with one volume of isopropanol and mixture was kept at room temperature to precipitated plasmid DNA. After high-speed centrifuge pellet was washed twice with 70% ethanol for removal of excess salt content. Ethanol was removed completely by centrifugation and pellet of plasmid DNA was redissolved in sterile double distilled water. The purity of plasmid DNA was checked by agarose electrophoresis and quantified using spectrophometric method or Nanodrop. To verify the mutation at A - site in *vc0395_0300* gene, all purified plasmids send for sequencing.

2.3 Results and discussions

The *V. cholerae* gene *vc0395_0300* codes for a protein which belongs to GGEEF family. This family of proteins is well-known for their diguanylate cyclase activity, which can synthesize a bacterial secondary messenger molecule c-di-GMP using two molecules of GTP (Ryjenkov et al. 2005, Waters et al. 2008). This signaling molecule c-di-GMP has been reported in all prokaryotic as well as some lower eukaryotic organisms (D'Argenio and Miller 2004, Jenal et al 2004, 2006, Ryjenkov et al. 2005, Römling 2013). Bacterial c-di-GMP has been reported as a regulatory molecule which plays very important role in various cellular functions such as cell morphology, motility, virulence, antibiotic production, cell-cell communications and many more functions (Ryjenkov et al. 2005, Ryan et al. 2006, Lim et al. 2007). The product of *vc0395_0300* gene has 321 amino acids with three distinct predicted domains, viz., PAS, PAC and GGEEF domain (figure 2.1). PAS domain is well distributed in bacteria and also found in some eukaryotes. This has its role in sensing environmental signals like light, oxygen level, voltage, etc. to regulate cellular responses. PAC domain is always linked to the PAS domain and found in its C-terminal, with a proposed role in proper folding of PAS domain.

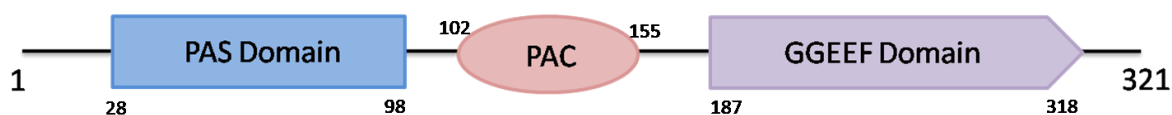
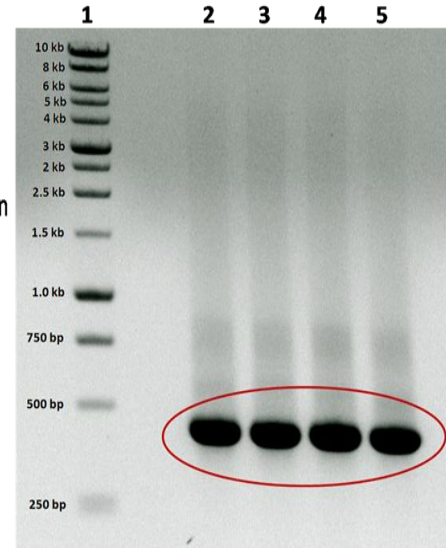
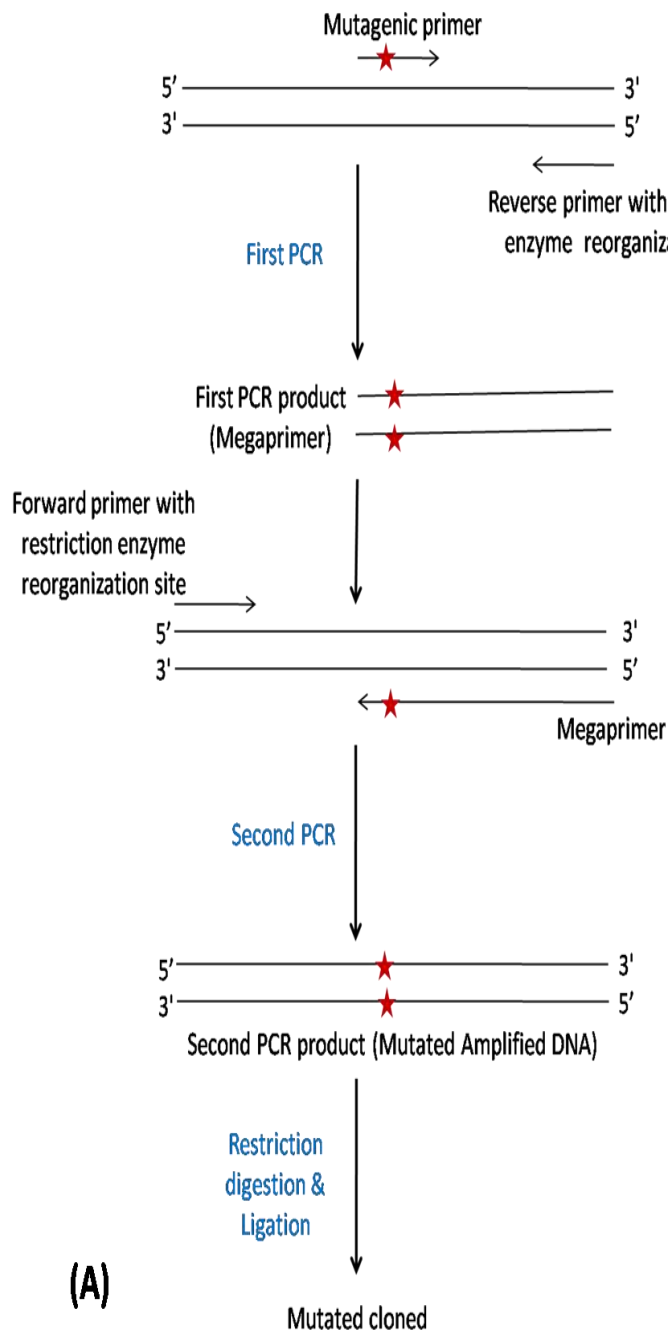


Figure 2.1: Domain structure of VC0395_0300 protein with the position of amino acid in the polypeptide chain.

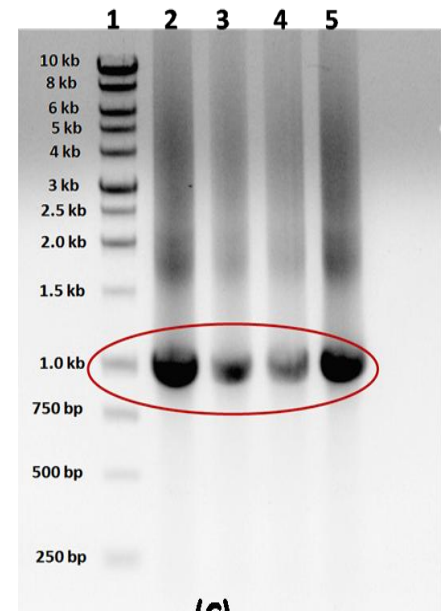
2.3.1 Site-Directed Mutagenesis

In VC0395_0300 protein GGD(E)EF domain consists of a conserved five amino acid (Gly-Gly-Asp/Glu-Glu-Phe) sequence. Mutations were introduced in this signature GGEEF domain by site-directed mutagenesis using two-step megaprimer PCR method (figure 2.2). All five signature amino acids of the active site were individually replaced by some other amino acids. In the initial PCR reactions, mutated flanking forward primer and reverse primer (with the restriction enzyme recognition site sequence) used to amplify the gene *vc0395_0300*. After the first PCR reactions, the 5' end of the gene was amplified with desired mutations in DNA sequence. The mutated product of first PCR reaction (483 bp) was purified

by PCR purification kit. In the second step, PCR was done using one forward primer (with the restriction enzyme recognition site sequence) and purified product of first PCR as a reverse primer. The full-length amplified product of *vc0395_0300* gene (963 bp) with mutation site in it was purified after this second step PCR (Figure 2.2). All PCR products were purified using Qiaquick kit from Qiagen according to manufacturer's protocol and concentrations were measured by Nanodrop (Figure 2.3).



(B)



(C)

Figure 2.2: Site-Directed Mutagenesis. (A) Strategy for two-step PCR SDM method (Tayagi et al 2004). (B) Agarose gel showing first PCR Product. (C) Agarose gel showing second PCR product, where lane 1; DNA ladder, 2; VC0395_0300(G237R), 3; VC0395_0300(E238K), 4; VC0395_0300(E239K) and 5; VC0395_0300(F240I).

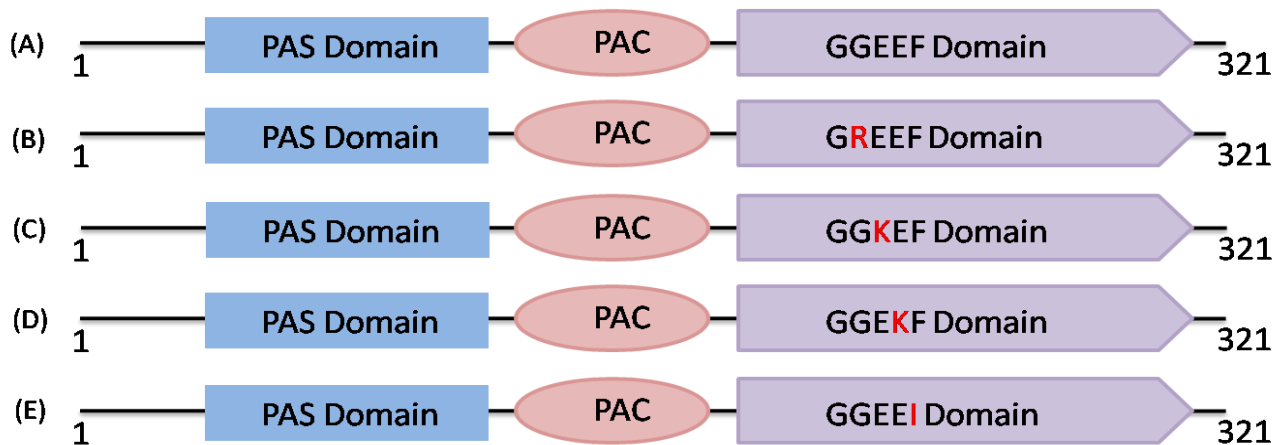


Figure 2.3: Wild type VC0395_0300 and all mutated protein constructs. Site of mutation are showed in red colour. (A) VC0395_0300 (WT); (B) VC0395_0300(G237R); (C) VC0395_0300(E238K); (D) VC0395_0300(E239K) and (E) VC0395_0300(F240I).

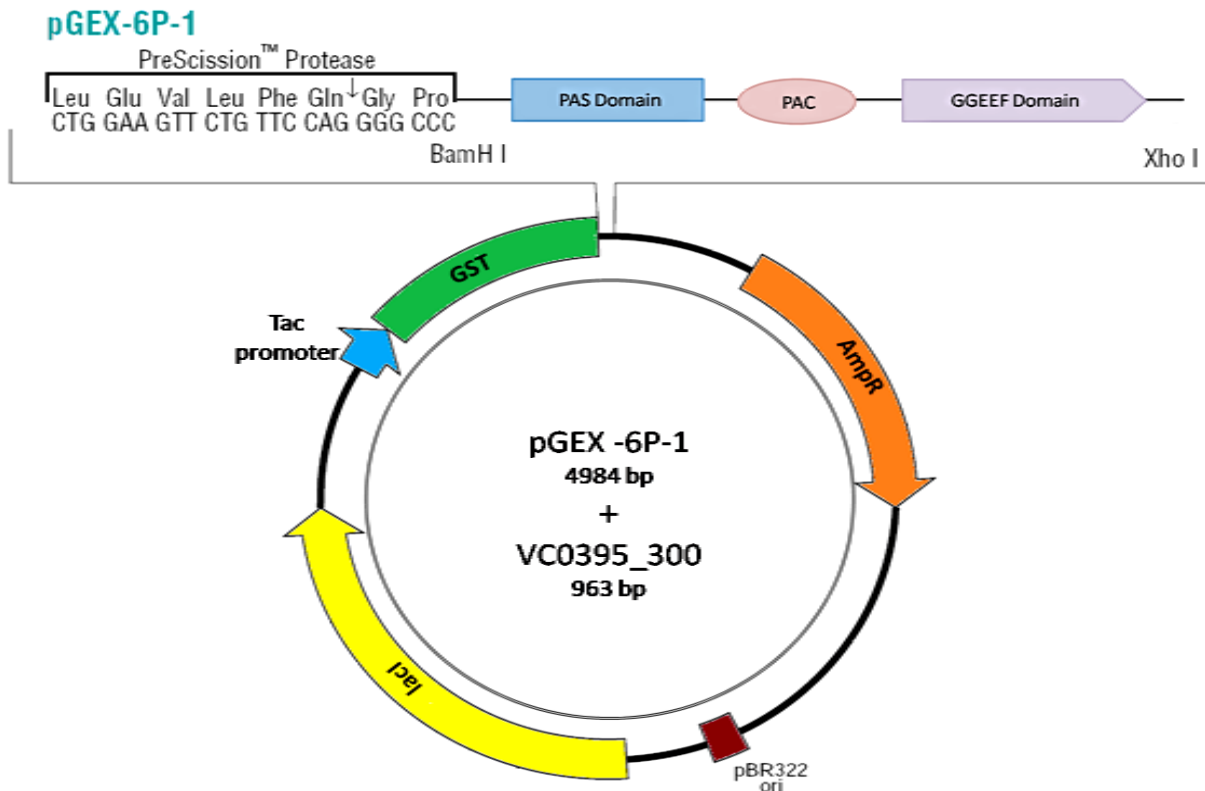


Figure 2.4: representation of recombinant plasmid of gene *vc0395_0300* with pGEX-6P1 vector DNA.

2.3.2 Cloning of recombinant plasmid DNA

All mutated PCR products of *vc0395_0300* gene and vector plasmid pGEX-6P1 were double digested by same restriction enzyme (BamH1 and Xho1). Digested DNA was run on an agarose gel and purified by the kit method. Purified mutated DNA insert individually ligated with digested vector DNA which had an appropriate sticky complementary site for ligation. Ligated plasmid DNA was transformed into competent DH5 α cells. Plasmid DNA isolated from all cloned colonies and circular vector DNA (without insert DNA) were run on the agarose gel, and the cloned plasmid DNA showed some retardation on an agarose gel as compared to the circular plasmid DNA (Figure 2.4). When all constructed plasmids with mutated insert DNA was digested with same restriction enzymes, they showed two distinct bands of vector and insert DNA on the agarose gel (Figure 2.5). To confirm positive clones, all constructs were sequenced. The site of mutation was carefully checked in DNA sequencing results for all constructed plasmids. Only positive bacterial clone (which has a mutation in plasmid) were maintained and further used for other experiments.

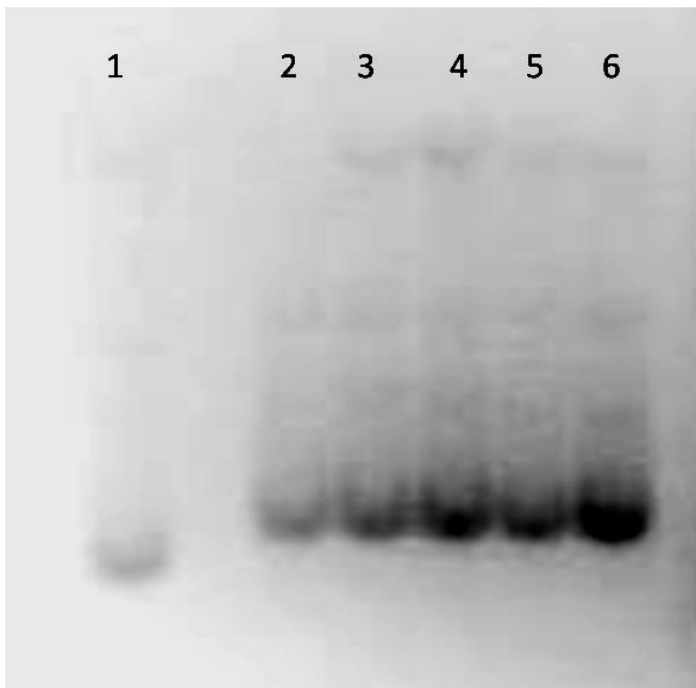


Figure 2.5: Agarose gel (1%) for cloned plasmid and vector. Where lane 1; vector DNA (pGEX-6P1), 2; pGEX-6P1+ VC0395_0300, 3; pGEX-6P1+ VC0395_0300(G237R), 4; pGEX-6P1+ VC0395_0300(E238K), 5; pGEX-6P1+ VC0395_0300(E239K) and 6; pGEX-6P1+ VC0395_0300(F240I).

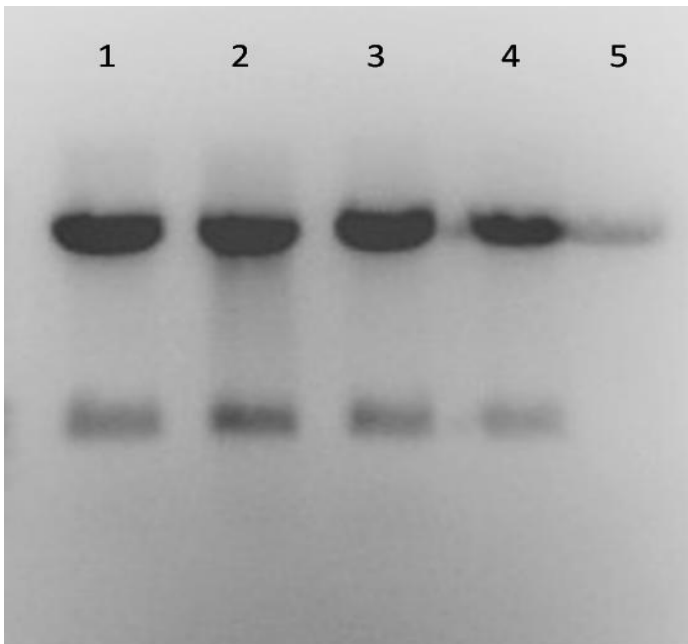


Figure 2.6: Agarose gel (1%) for restriction digested mutated constructed plasmid and vector DNA. Where lane 1; pGEX-6P1+ VC0395_0300(G237R), 2; pGEX-6P1+ VC0395_0300(E238K), 3; pGEX-6P1+ VC0395_0300(E239K), 4; pGEX-6P1+ VC0395_0300(F240I) and 5; vector DNA (pGEX-6P1).

2.4 Conclusions

V. cholerae serotype O1 classical strain O395 genome was used for amplification of putative *vc0395_0300* gene. The *vc0395_0300* gene located in chromosome 1 of the *V. cholerae* genome possesses a GGDEF domain along with PAS domain at amino terminal. GGDEF domain-containing proteins are very important for bacteria due to their role in various signaling pathways and for regulation of bacterial life cycle. The full length *vc0395_0300* gene contained 969 bases. A point mutation was introduced in the active site of GGDEF domain coding region, according to the following:

1. Four point mutations were individually made at the GGDEF active site of *vc0395_0300* gene using site-directed mutagenesis. In each of mutations, one amino acid at the GGDEF sequence was replaced by another amino acid.
2. Residue no. 237th Glycine was replaced with Arginine, 238th Glutamic acid by Lysine, 239th Glutamic acid by Lysine and 240th Phenylalanine replaced with Isoleucine.
3. All four mutated insert DNA were separately ligated with cut pGEX-6P1 vector DNA and four mutated plasmids were constructed.
4. Mutated plasmids were effectively transformed into cloning host *E. coli* strain DH5 α .
5. The site of mutation in all four mutated plasmids was confirmed by DNA sequencing.
6. Four different mutated clones of *vc0395_0300* gene having a mutation at active site were successfully prepared and transformed into expression host *E. coli* BL21 and used for further study.

2.5 References

- Bhuiyan NA, Nusrin S, Ansaruzzaman M, Islam A, Sultana M, Alam M, Islam MA, Cravioto A, Mukhopadhyay AK, Nair GB, Endtz HP.** 2012. Genetic characterization of *Vibrio cholerae* O1 strains isolated in Zambia during 1996–2004 possessing the unique VSP-II region of El Tor variant. *Epidemiol Infect.* **140**: 510–518.
- Birnboim HC, Doly J.** 1979. A rapid alkaline extraction procedure for screening recombinant plasmid DNA. *Nucleic Acids Research.* **7**: 1513-1523.
- Brons-Poulsen J, Petersen NE, Horder M, Kristiansen K.** 1998. An improved PCR-based method for site directed mutagenesis using megaprimers. *Molecular and Cellular Probes* **12**: 345–348.
- D’Argenio DA, Miller SI.** 2004. Cyclic di-GMP as a bacterial second messenger. *Microbiology.* **150**: 2497–502.
- Erik T, Aune V, Aachmann FL.** 2010. Methodologies to increase the transformation efficiencies and the range of bacteria that can be transformed. *Appl Microbiol Biotechnol.* **85**: 1301–1313.
- Hammer BK, Bassler BL.** 2009. Distinct sensory pathways in *Vibrio cholerae* El Tor and classical biotypes modulate cyclic dimeric GMP levels to control biofilm formation. *J. Bacteriol.* **91**: 169–177.
- Jenal U.** 2004. Cyclic di-guanosine-monophosphate comes of age: a novel secondary messenger involved in modulating cell surface structures in bacteria? *Curr. Opin. Microbiol.* **7**: 185–191.
- Jenal U, Malone J.** 2006. Mechanisms of cyclic-di-GMP signaling in bacteria. *Annu. Rev. Genet.* **40**: 385– 407.
- Korbie DJ, Mattick JS.** 2008. Touchdown PCR for increased specificity and sensitivity in PCR amplification. *Nature protocol.* **3**: 1452-1456.
- Lim B, Beyhan S, Yildiz FH.** 2007. Regulation of *Vibrio* polysaccharide synthesis and virulence factor production by CdgC, a GGDEF-EAL domain protein, in *Vibrio cholerae*. *J. Bacteriol.* **189**: 717–729.
- Liang Q, Chen L, Fulco AJ.** 1995. An efficient and optimized PCR method with high fidelity for site-directed mutagenesis. *Genome Res* **4**: 269-274.
- Lund AH, Duch M, Pedersen S.** 1996. Increased cloning efficiency by temperature-cycle Ligation. *Nucleic Acids Research.* **24**: 800–801
- Moore E, Arnscheidt A, Kruger A, Strompl C, Mau M.** 2004. Simplified protocols for the preparation of genomic DNA from bacterial cultures. *Molecular Microbial Ecology.* **2**: 1-18.
- Römling, U, Galperin, MY, Gomelsky M.** 2013. Cyclic di-GMP: the first 25 years of a universal bacterial second messenger. *Microbiol. Mol. Biol. Rev.* **77**: 1–52.
- Ryan RP, Fouhy Y, Lucey JF, Dow JM.** 2006. Cyclic di-GMP signaling in bacteria: recent advances and new puzzles. *J Bacteriol.* **188**: 8327–34.

Ryjenkov DA, Tarutina M, Moskvin OV, Gomelsky M. 2005. Cyclic diguanylate is a ubiquitous signaling molecule in bacteria: insights into biochemistry of the GGDEF protein domain. *J. Bacteriol.* **187**: 1792–1798.

Sambrook J, Fritsch EF, Maniatis T. 1989. *Molecular Cloning: A Laboratory Manual*. Second edition. Cold Spring Harbor Laboratory Press, Cold Spring Harbor.

Tyagi R, Lai R, Duggleby RG. 2004. A new approach to 'megaprimer' polymerase chain reaction mutagenesis without an intermediate gel purification step. *BMC Biotechnol BioMed central.* **4**: 1-6.

Waters CM, Lu W, Rabinowitz JD, Bassler BL. 2008. Quorum sensing controls biofilm formation in *Vibrio cholerae* through modulation of cyclic di-GMP levels and repression of *vpsT*. *J. Bacteriol.* **190**: 2527–2536.

Weiner MP, Costa GL. 1994. Rapid PCR site-directed mutagenesis. *Genome Res.* **4**: S131-S136.

Zhen-Hua X, Xiao-Jun S. 2009. Fast and almost 100% efficiency site directed mutagenesis by the megaprimer PCR method. *Biochem and Biophysics.* **36**: 1490-1494.

Zheng L, Baumann U, Reymond JL. 2004. An efficient one-step site-directed and site-saturation mutagenesis protocol. *Nucleic Acids Research.* **32**: 1-5.

3.1 Introduction

The genic sequence for VC0395_0300 and all its mutants were cloned into the expression vector pGEX-6P1. The pGEX series of vectors was designed by a gene from *Schistosoma japonicum*, whose product, the Glutathione S-transferase (GST) serves as a tag for the desired protein (**Smith and Johnson 1988, Parker et al 1990**). GST has high binding affinity to glutathione ligands; for example, to a glutathione-Sepharose matrix. The pGEX vector also contains the *lacI Q* gene, which codes for a repressor protein that binds to the operator region and prevents expression of fusion protein before IPTG induction. The recombinant protein is designed by introducing a desired gene into the multiple cloning sites of the pGEX vector. The pGEX vectors allow expression of desired protein after isopropyl β -D thiogalactoside (IPTG) induction under the control of the *tac* promoter.

Recombinant proteins contain a large GST (26 kD) tag at the amino-terminal end, and a PreScission protease cleavage site in between the protein and the GST tag (**Smith and Johnson 1988, Parker et al 1990**). This protein can be purified by affinity chromatography from the bacterial lysate. GST fusion proteins are trapped by immobilized glutathione columns which possess high affinity for a GST tag, and can be further eluted using reduced glutathione. Recombinant protein possesses a recognition sequence for a specific protease, which can be used for GST tag cleavage, either in-column or outside the column (**Hakes DJ, Dixon 1992, Harper and Speicher 2011**). The following steps were used for the purification of GST tag fusion recombinant protein:

- 1) GST affinity chromatography
- 2) Tag cleavage
- 3) Separation of GST tag and
- 4) Size-exclusion chromatography.

All purification steps were performed at 4 °C, the protein was continuously monitored by checking its concentration at all steps and continuously analyzed by SDS-PAGE. The detailed description for individual protein purification steps is given in the following sections.

3.2 Materials and methods

3.2.1 Culture condition

All recombinant *E. coli* strains were grown for 12-16 hours at 37 °C with continuous shaking in autoclaved liquid LB medium (LB-Luria Bertani medium, 1% Tryptone, 0.5% Yeast Extract, and 1% NaCl at pH 7) supplemented with 100 µg/ml ampicillin. All *E. coli* strains were preserved in glycerol stocks at -80 °C for long-term storage. Glycerol stocks were prepared by adding sterile glycerol final concentration up to 25% in overnight liquid *E. coli* culture.

3.2.2 Protein over expression and solubility test

A single colony of *E. coli* strain BL21 (DE3) containing a recombinant plasmid (VC0395_0300 + pGEX-6P1, or its mutants) was individually grown overnight in 10 ml of LB medium supplemented with 100 µg/ml of ampicillin. This overnight bacterial culture was diluted 100 times in sterile LB medium and grown under constant shaking until absorption reached an OD₆₀₀ of 0.6 to 0.8. This culture was induced with isopropyl β-D-1-thiogalactopyranoside (IPTG) for another 16 hours for protein over expression. The culture was harvested by centrifugation at 6000 rpm for 10 min at 4 °C. The bacterial cell pellet was resuspended in lysis buffer (20 ml resuspension buffer per pellet from 1 liter bacterial culture). Resuspended bacterial cells were lysed by sonification with low amplitude 30-second pulses and 5 minutes resting time in ice for each of duration. Sonification was followed by high-speed centrifugation to separate soluble and insoluble fractions. All fractions were mixed with 5X SDS sample buffer boiled at 90 °C for 5 minutes and subjected to SDS-PAGE analysis. For maximum protein over expression, conditions were optimized by changing induction temperature, the time duration for growth after induction and IPTG concentrations.

3.2.3 SDS-PAGE

The mixture of proteins was separated by Sodium Dodecyl Sulfate-Polyacrylamide Gel Electrophoresis (SDS-PAGE), and the presence of desired protein band in a sample and/or purity of proteins were determined. 12-15% SDS-polyacrylamide gels were prepared (based on protein size) according to standard gel preparation protocols

(Laemmli 1970). Protein samples were mixed in an SDS sample buffer and boiled at 90 °C for 5 minutes prior to applying on the SDS-PAGE gel. The loaded gel was allowed to be electrophoresced in presence of 1X SDS running buffer until the dye bromophenol blue reached the bottom of the gel. To determine the size of desired protein band in gel, protein molecular weight standard markers were used. After electrophoresis, the gel was removed from glass plates and stained with Coomassie brilliant blue solution R-250 for 30 minutes, followed by destaining for 1 hour or overnight in destaining solution.

3.2.4 Protein constructs

Different protein constructs of varied protein length were prepared based on the secondary structure of VC0395_0300 protein. The secondary structure of VC0395_0300 protein was predicted by various prediction tools such as psipred, jpred, predict protein (Jones 1990, Buchan et al 2013, Cuff et al 1999). The protein constructs of different lengths were prepared by PCR amplification using following primers.

Table 3.1. List of plasmids used to produce different protein constructs of VC0395_0300 gene.

Vector	Protein	length	Mutation
PGEX- 6P1	VC0395_0300	1---321	Wild Type
PGEX- 6P1	VC0395_0300	1---321	Δ 237 (Amino acid G replaced by R)
PGEX- 6P1	VC0395_0300	1---321	Δ 238 (Amino acid E replaced by K)
PGEX- 6P1	VC0395_0300	1---321	Δ 239 (Amino acid E replaced by K)
PGEX- 6P1	VC0395_0300	1---321	Δ 240 (Amino acid F replaced by I)
PGEX- 6P1	VC0395_0300	161---321	Wild Type
PGEX- 6P1	VC0395_0300	161---321	Δ 237 (Amino acid G replaced by R)
PGEX- 6P1	VC0395_0300	161---321	Δ 238 (Amino acid E replaced by K)
PGEX- 6P1	VC0395_0300	161---321	Δ 239 (Amino acid E replaced by K)
PGEX- 6P1	VC0395_0300	161---321	Δ 240 (Amino acid F replaced by I)
pET28a	VC0395_0300	161---321	Wild Type

Table 3.2 List of primers used to make different protein constructs of VC0395_0300 gene. The restriction enzyme recognition sites in primer sequence are indicated as underlined.

S. No	Primer Sequences	Length of products
1	Forward Primer 5' ATAATACT <u>GGATCC</u> ATGAAAAATTGGCTGTGTCAGGCAGTG 3' Reverse Primer 5'ATAATACT <u>CTCGAG</u> TTATTCTGTGGATTGGCGATAGATACA 3'	VC0395_0300 1---321
2	Forward Primer 5' ATAATACT <u>GGATCC</u> ATGCGTCTCTCGGTTGTACATGAAGAA 3' Reverse Primer 5'ATAATACT <u>CTCGAG</u> TTATTCTGTGGATTGGCGATAGATACA 3'	VC0395_0300 102---321
3	Forward Primer 5' ATAATACT <u>GGATCCA</u> TGTTAAGACAGCCGTTAAGTTGCATC 3' Reverse Primer 5'ATAATACT <u>CTCGAG</u> TTATTCTGTGGATTGGCGATAGATACA 3'	VC0395_0300 187---321
4	Forward Primer 5' ATACGC <u>GGATCC</u> ATGTCTTTAACTCAGCTGTGT 3' Reverse Primer 5'ATAATACT <u>CTCGAG</u> TTATTCTGTGGATTGGCGATAGATACA 3'	VC0395_0300 161---321
5	Forward Primer 5' ATACCG <u>CTCGAG</u> ATGTCTTTAACTCAGCTGTGT 3' Reverse Primer 5' ATACGC <u>GGATCC</u> TTATTCTGTGGATTGGCGATA 3'	VC0395_0300 161---321

3.2.5 Large scale protein purification

Bacterial strains which show positive results for soluble protein over expression were further used for large-scale protein productions. Respective *E. coli* BL21 (DE3) strains were inoculated 1:100 into 10-12 liter LB medium supplemented with 100 µg/ml ampicillin. The culture was incubated at 37 °C with continuous shaking at 120 rpm and grown to an OD₆₀₀ of 0.6 - 0.8. Bacterial culture was allowed to grow at 18 °C, and, then induced by adding IPTG of 50 µM concentrations. The culture flask was further incubated at 18 °C for 16 hours with continuous shaking at 120 rpm. After incubation,

bacterial cells were centrifuged at 6000 rpm for 10 minutes and the cell pellet was kept in -80 °C until further use.

3.2.6 Cell lysis

The bacterial cell pellet was thawed in ice for 20-30 minutes and resuspended in lysis buffer (according to the calculation of 3 ml per 1 gram of cell pellet). Lysis buffer contained DNase (1mg/100 ml), Complete Mini-EDTA free protease inhibitor (one tablet per 100 ml) and lysozyme. The cell pellet was dissolved by vortexing, and then the bacterial suspension was homogenized by stirring at 4 °C for 15 minutes. Cells were lysed by passing three times through a microfluidizer at 20000 psi. Bacterial lysate was centrifuged at 22000 rpm for 45 minutes at 4 °C to separate insoluble materials. After centrifugation, soluble fraction or clear supernatant was passed through a 0.2 µm membrane filter and further used for protein purification.

3.2.7 GST affinity chromatography and Tag cleavage

All recombinant proteins contain an N-terminal GST tag, followed by target protein. The GST tag has an affinity to immobilized glutathione sepharose column, which facilitates its purification. The cell lysate, after high-speed centrifugation and filtration was used to purify the soluble protein. GSTrap FF column (GE Healthcare and Life sciences) was equilibrated with 5 column volumes of lysis buffer, and then the pre-equilibrated column was used for binding of GST fusion protein. For binding of protein, filtered supernatant was passed three times (3 ml/minutes) through 5 ml GSTrap FF column. After the binding of protein, the column was washed 2 times with equilibration buffer and followed by 5 times with wash buffer (containing 1 mM MgCl₂ and 1 mM ATP). This step helps to eliminate non-specific binding of other proteins on the column. MgCl₂ and ATP in wash buffer make easy to remove co-purifications of bacterial chaperones (**Rial et al 2002**). N-terminal GST tag was allowed to be cleaved on a column or in solution by Precession protease (1:300 protease and fusion protein ratio). For on-column cleavage, Precession protease was mixed with four columns volume cleavage buffer and applied to the column at a constant, and slow flow rate of 1.5-2 ml/minutes) for overnight in circulation. Next day or after 16 hours, desired protein (without tag) was collected from flow through and column washed with two column volumes of equilibration buffer. For in-solution tag cleavage, Precession protease was mixed with the protein solution (1:300 protease and

fusion protein ratio) after elution from GST column for 16 hours at cold room or 6 °C. Protein was subsequently dialyzed in the equilibration buffer and the dialyzed protein was used for further protein purification steps. All protein purification steps (chromatography, dialysis and tag cleavage) were carried out at 4-6 °C.

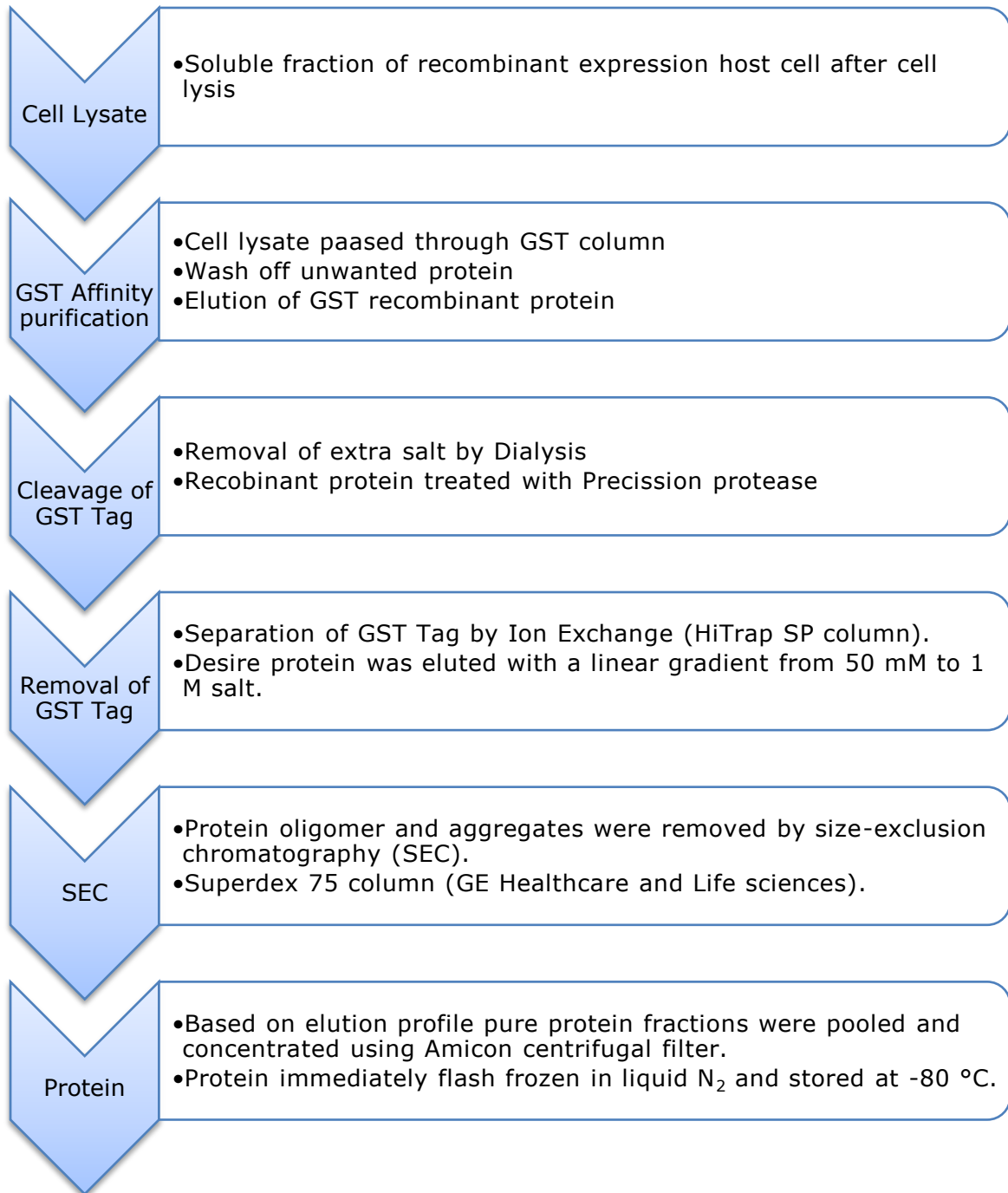


Figure 3.1: Protein purification steps used for all proteins.

3.2.8 Cation exchange chromatography

After GST affinity purification, tag cleavage and dialysis, the protein still contained some other proteins and nucleic acid as impurities. These were further removed by cation exchange chromatography. At this step of protein purification, a 5 ml HiTrap SP column (GE Healthcare and Life sciences) was used to separate all impurities from desired protein. The protein was dialyzed in cation exchange buffer (composition) for 2 hours before application to the pre-equilibrated column. The dialyzed buffer containing low salt and pH was deliberately kept at a lower pH than the desired protein's pI to make sure that the protein was positively charged. This positive charge on the protein allow stronger binding on the sulfopropyl cation exchange resin while other neutral or positive charged proteins and negatively charged nucleic acids do not bind to the column and get washed away. For binding of protein on the column, the protein was passed two times (3 ml/minutes) through 5 ml HiTrap SP column. After binding the protein to column, protein was eluted with a linear gradient from 50 mM to 1 M salt. Protein elution was continuously observed by Äkta Prime FPLC purification where the absorption was measured at 280 nm. The protein fractions were run on the SDS PAGE gel, were pooled and used for further purification steps.

3.2.9 Size-exclusion chromatography (SEC)

After cation exchange chromatography, eluted protein still contained protein in aggregates and higher oligomeric form of the protein. Protein aggregates and higher oligomeric species were removed by size-exclusion chromatography. All fractions from cation exchange chromatography were pooled, volume was reduced to 2 ml and concentrated protein solution was centrifuged at higher speed (14000 rpm) for 2 minutes to remove all possible precipitates. The concentrated protein was injected into the pre-equilibrated Superdex 75 column (16/60 or 26/60 based on the amount of protein column was used) (GE Healthcare and Life sciences) which has optimal separation range of 3-70 kDa. The protein was eluted at a slow flow rate (0.8 ml/minute) and elution was observed by measuring the absorption at 280 nm. All fractions containing protein were run on SDS PAGE gel and purity of the protein was observed by the visible band on SDS PAGE gel. The protein peak fractions which contained desired protein were pooled and concentrated to approximately 8-10 mg/ml.

3.2.10 Concentration of protein and protein storage

All peak fractions after size exclusion chromatography containing pure protein were pooled together and concentrated using Amicon centrifugal filter devices (Merck Millipore) with a molecular weight cut off of 5 kDa. The protein solution was allowed to be centrifuged at 4000 rpm for 15 minutes at 4 °C. The concentrations of protein were continuously measured in the supernatant and flowthrough. When the desirable concentration was achieved for purified protein, the protein was divided into small volume of 50 or 100 µl aliquots. All aliquoted protein was immediately flash frozen in liquid N₂ and stored at -80 °C.

3.2.11 Protein concentration determination

Protein concentration was carefully measured and recorded at all steps of protein purification. The concentration was determined using UV-Vis Spectrophotometer (Thermo Scientific) which is based on Beer's law. The absorbance at 280nm for protein was measured by UV-Vis Spectrophotometer and molar extinction coefficient for desired protein was calculated with ProtParam tool in ExPASy.

$$C_{\text{(Protein)}} = \frac{A_{(280)}}{\epsilon_{(280)} \cdot d}$$

$C_{\text{(protein)}}$	protein concentration (M)
$A_{(280)}$	Absorbance at 280 nm
$\epsilon_{(280)}$	molar extinction coefficient at 280 nm in (M ⁻¹ cm ⁻¹)
d	path length in (cm)

3.3 Results and discussions

3.3.1 Pilot scale protein expression

All proteins from *vc0395_0300* gene (mutants and different protein constructs) were cloned into the expression vector pGEX-6P1 vector DNA and recombinant plasmids were transformed into BL21 DE3 expression host. The product from the recombinant plasmid was a fusion protein which has additional an N-terminal GST tag with PreScission Protease cleavage site in between protein and GST tag. The choice of pGEX-6P1 vector become more advantageous because it improves protein solubility and PreScission protease is a more specific protease with a longer recognition sequence and cleavage can actively work at 4 °C (**Harper and Speicher 2011**). The expression of the recombinant fusion protein was checked in a small volume (50 ml culture) first before growing in large-scale culture. The conditions for maximum protein expression in soluble form were optimized by changing various parameters such as induction temperature (16 °C, 22 °C, 30 °C and 37 °C), induction time (4, 8, 12 and 16 hours) and IPTG concentration (1.0, 0.5, 0.1 and 0.05 mM). The bacterial cells were grown in multiple conditions (mentioned above) and after cell lysis, soluble and insoluble fractions were analyzed by SDS PAGE for maximum production of soluble fusion proteins. Most of the proteins showed good expression in soluble form at 16 °C. The maximum over expression of all full-length mutants proteins were observed at 16 °C, at 16 hours induction with 0.1 mM IPTG concentrations (Figure 3.2). At these conditions, a clear distinguished protein band of 63.2 kDa (GST fusion full-length protein) was visible in soluble fractions for all protein constructs. All these optimized conditions were used for larger scale protein production for all proteins.

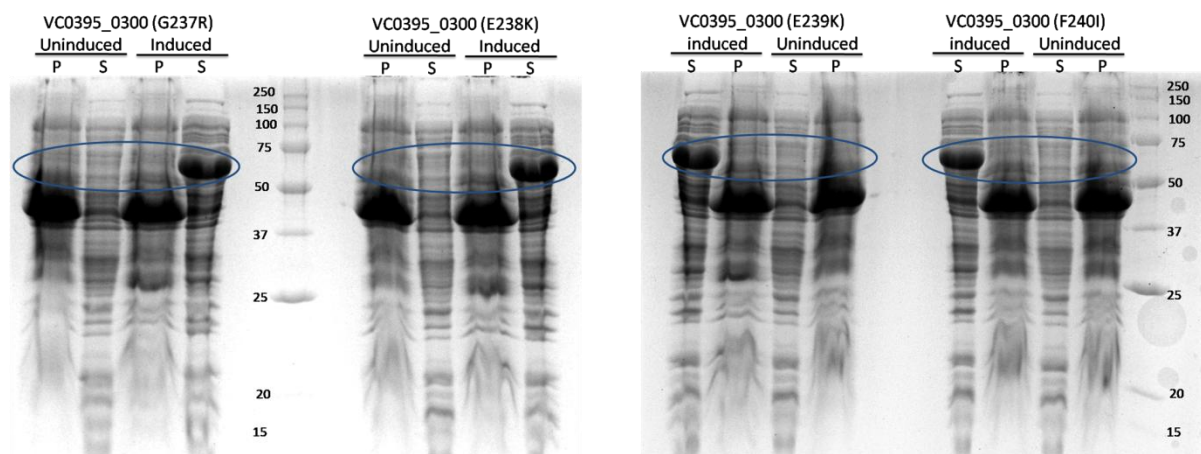


Figure 3.2: showing over expression of all mutant proteins at best-optimized conditions. Here “P” indicates cell pellet or insoluble fraction after cell lysis and “S” indicates soluble fractions or supernatants after cell lysis.

3.3.2 Bulk protein production

All optimized conditions were used for expression or productions of large-scale of all mutated proteins. For production of protein bacterial cells were grown in 10-12 liter culture medium and soluble fractions of proteins were purified within two days in four different steps of purifications. In the first step of protein purification, GST tagged fusion proteins were purified by affinity chromatography. After first GST affinity chromatography run, the yields of full-length protein for all mutants were around 0.4 to 0.8 mg per litre. N-terminal GST tag was cleaved from all the proteins by Precession Protease after incubation at 6 °C for 16 hours. Tagless protein was dialyzed for two hours at lower salt concentrations (50 mM) and lower pH than the pI of the protein to keep a positive charge on the protein for consequent binding to the negatively charged column. Followed by cleavage and dialysis, GST tag and other impurities were separated from protein by cation exchange chromatography. In this step of purification, the protein was eluted by increasing the salt concentration gradually (100 mM to 1000 mM). The next step size-exclusion chromatography was used to separate any remaining protein aggregates and higher oligomeric species to get pure homogeneous protein. As an example, all the purification steps for one mutated protein VC0395_0300(G237R) are shown here in figure 3.3.

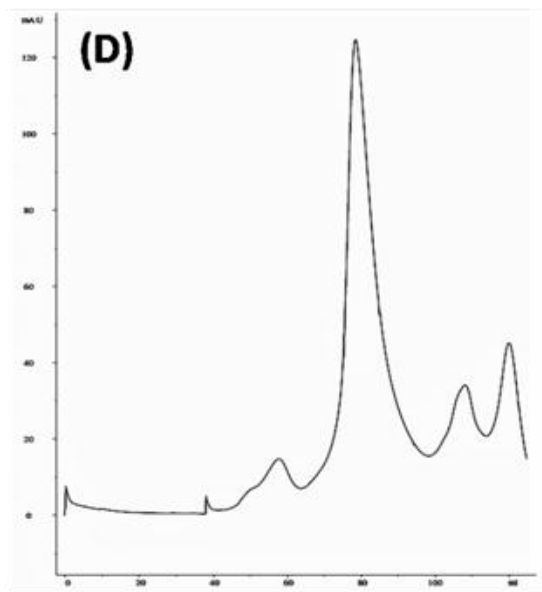
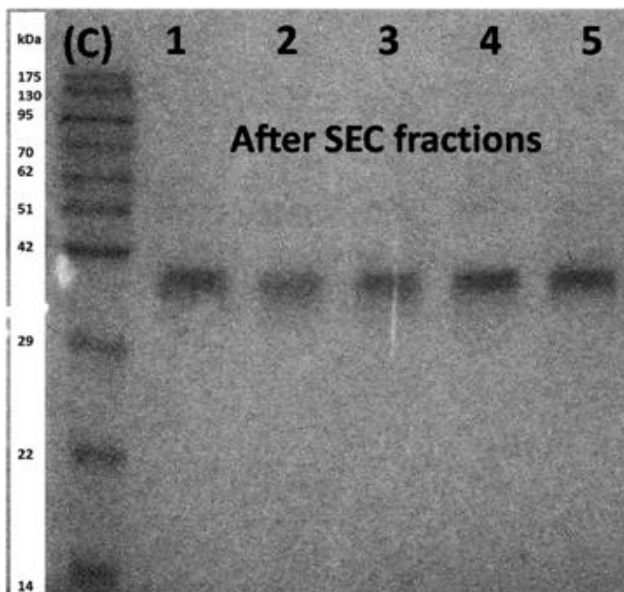
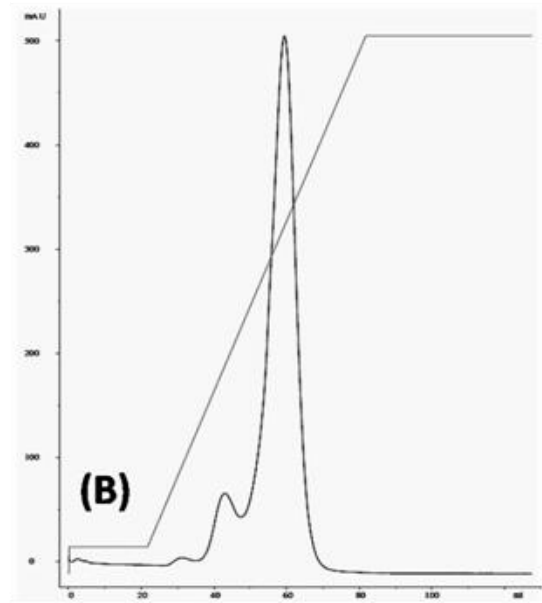
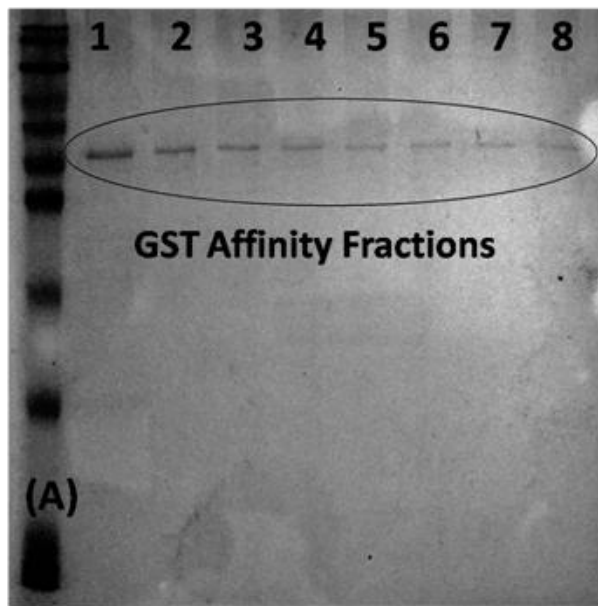


Figure 3.3: Overall protein purification steps for full length VC0395_0300(G237R) protein. (A) 15% SDS - PAGE gel showing elution fractions after GST affinity chromatography. (B) Showing cation exchange chromatograph with a linear gradient of salt concentration (from 100 mM to 1 M). GST tag and other protein remain in flow-through while elution fractions mainly contain protein. (C) 15% SDS - PAGE gel showing sample after elution fractions after Size-exclusion chromatography. (D) Showing size-exclusion chromatography.

size exclusion chromatography) similar to the full length mutated protein. The results of all the purification steps are shown here in figures 3.4, 3.5 and 3.6.

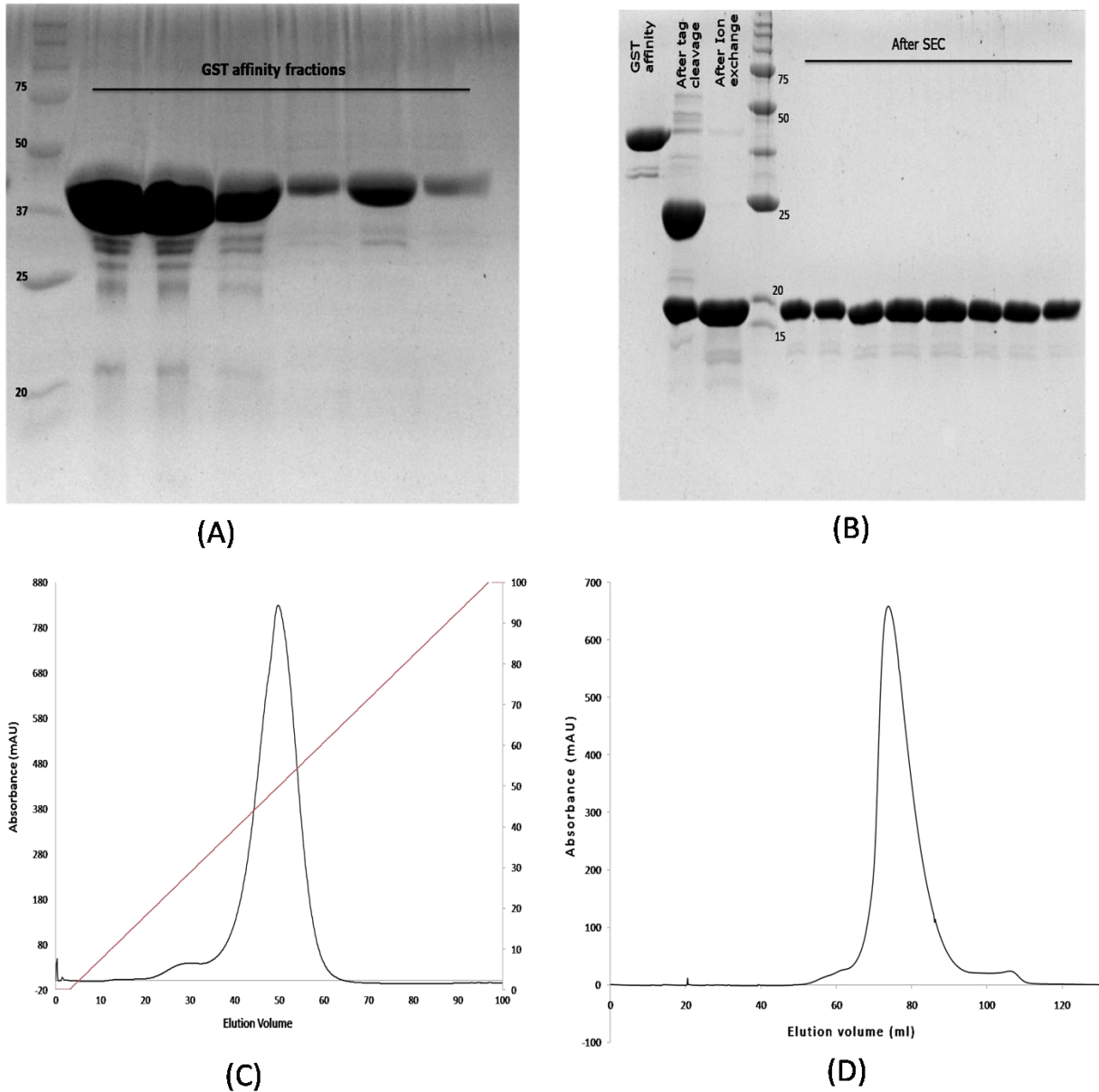


Figure 3.5: Overall protein purification steps for VC0395_0300(G237R)₁₆₁₋₃₂₁. (A) 15% SDS - PAGE gel showing elution fractions after GST affinity chromatography. (B) Showing cation exchange chromatograph with a linear gradient of salt concentration (from 50 mM to 1 M). GST tag and other protein remain in flow-through while elution fractions mainly contain protein. (C) 15% SDS - PAGE gel showing sample after tag cleavage, cation exchange chromatography and elution fractions after Size-exclusion chromatography. (D) Showing size-exclusion chromatograph.

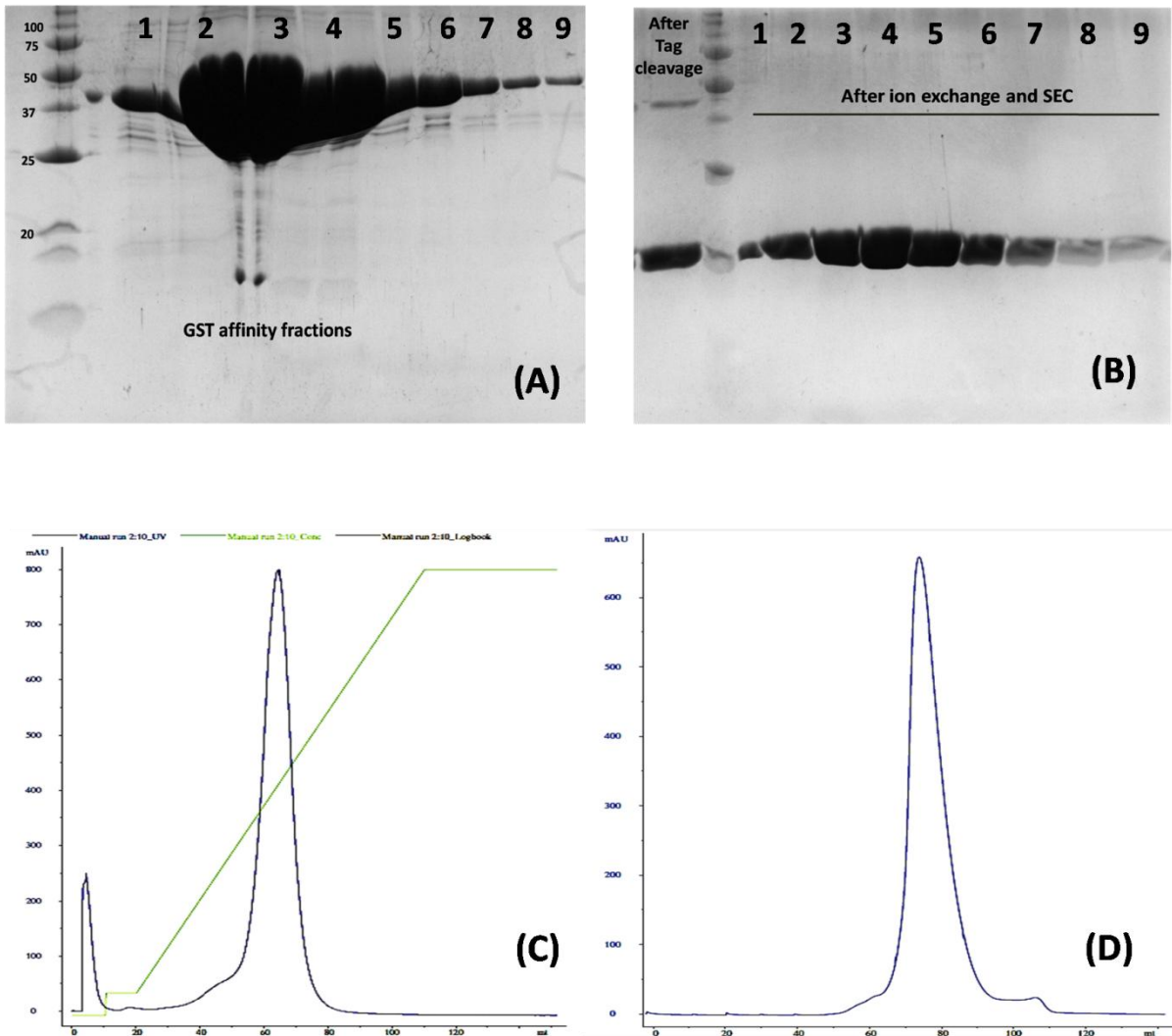


Figure 3.6: Protein purification steps VC0395_0300(E238K)₁₆₁₋₃₂₁. (A) 15% SDS - PAGE gel showing elution fractions after GST affinity chromatography. (B) 15% SDS - PAGE gel showing sample after tag cleavage, cation exchange chromatography and elution fractions after Size-exclusion chromatography. (C) Showing cation exchange chromatograph with a linear gradient of salt concentration (from 50 mM to 1 M). GST tag and other protein remain in flow-through while elution fractions mainly contain protein. (D) Showing size-exclusion chromatograph.

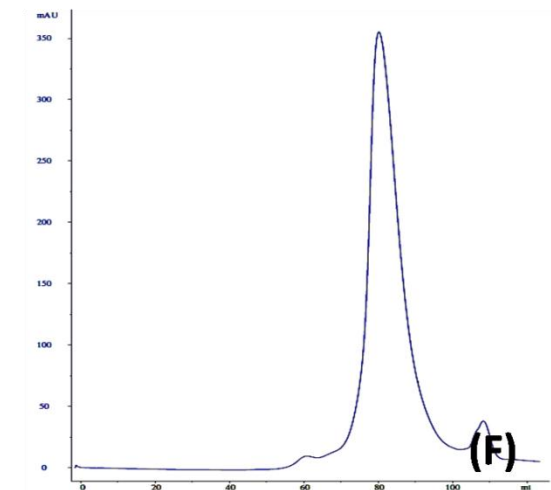
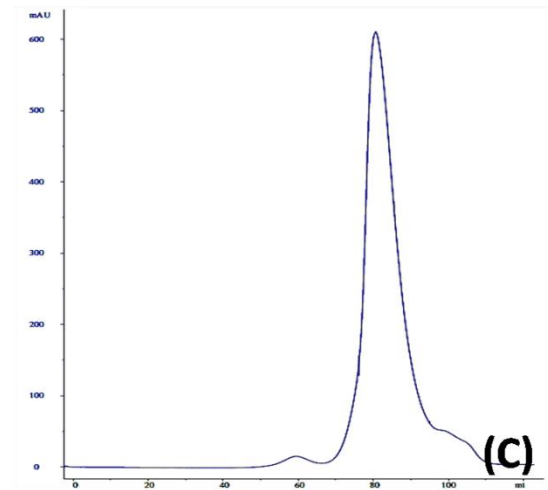
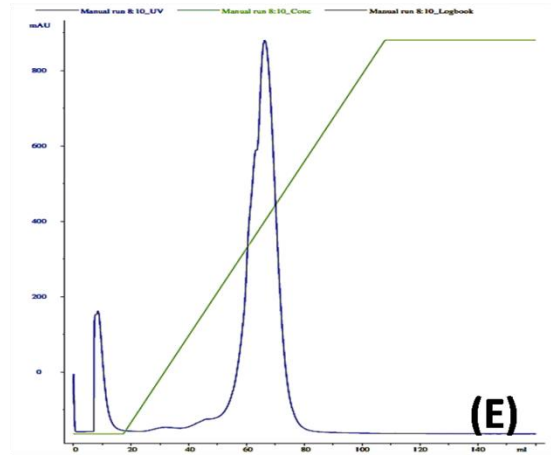
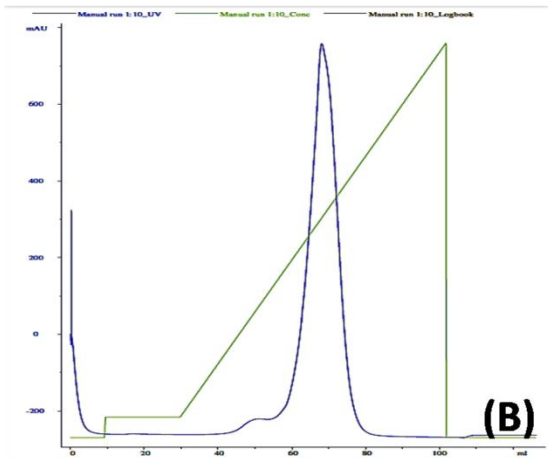
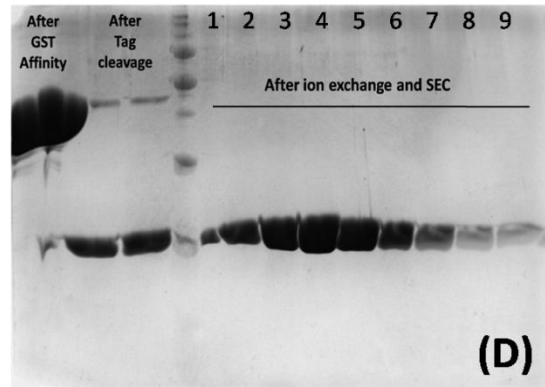
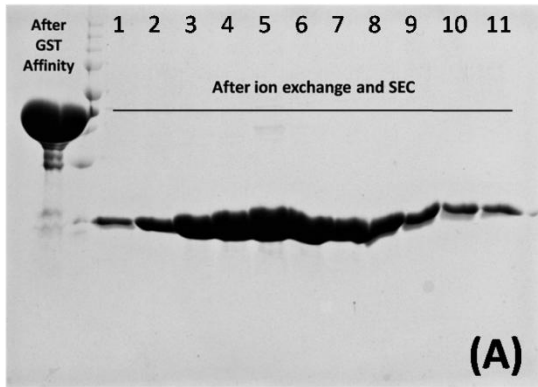


Figure 3.7: Protein purification steps VC0395_0300 (E239K)₁₆₁₋₃₂₁ (figure A,B and C). (A) 15% SDS - PAGE gel showing elution fractions after SEC chromatography with first lane of GST affinity fraction. (B) Showing cation exchange chromatograph with a linear gradient of salt concentration (C) Showing size-exclusion chromatograph. Figure D, E, and F for VC0395_0300 (F240I)₁₆₁₋₃₂₁.

Table 3.3. Different protein constructs for VC0395_0300 and their protein expressions properties.

Vector	Protein Constructs	Expression / solubility	Protein yield (mg / ltr)	Comments
PGEX- 6P1	1---321 Wild Type	Yes / Yes	0.2 - 0.4	
PGEX- 6P1	1---321 Δ237 (G replaced by R)	Yes / Yes	0.2 - 0.4	Protein is unstable and continuously degraded during purification steps. Protein start precipitated after 6 mg/ml concentration.
PGEX- 6P1	1---321 Δ238 (E replaced by K)	Yes / Yes	0.2 - 0.4	
PGEX- 6P1	1---321 Δ239 (E replaced by K)	Yes / Yes	0.2 - 0.4	
PGEX- 6P1	1---321 Δ240 (F replaced by I)	Yes / Yes	0.2 - 0.4	
PGEX- 6P1	161---321 Wild Type	Yes / Yes	1.0 - 1.4	
PGEX- 6P1	161---321 Δ237 (G replaced by R)	Yes / Yes	1.0 - 1.4	Protein behaves quite stable during purification steps. Protein can be concentrated up to 10 mg/ml.
PGEX- 6P1	161---321 Δ238 (E replaced by K)	Yes / Yes	1.0 - 1.4	
PGEX- 6P1	161---321 Δ239 (E replaced by K)	Yes / Yes	1.0 - 1.4	
PGEX- 6P1	161---321 Δ240 (F replaced by I)	Yes / Yes	1.0 - 1.4	
pET28a	161---321 Wild Type	No / No	-----	-----

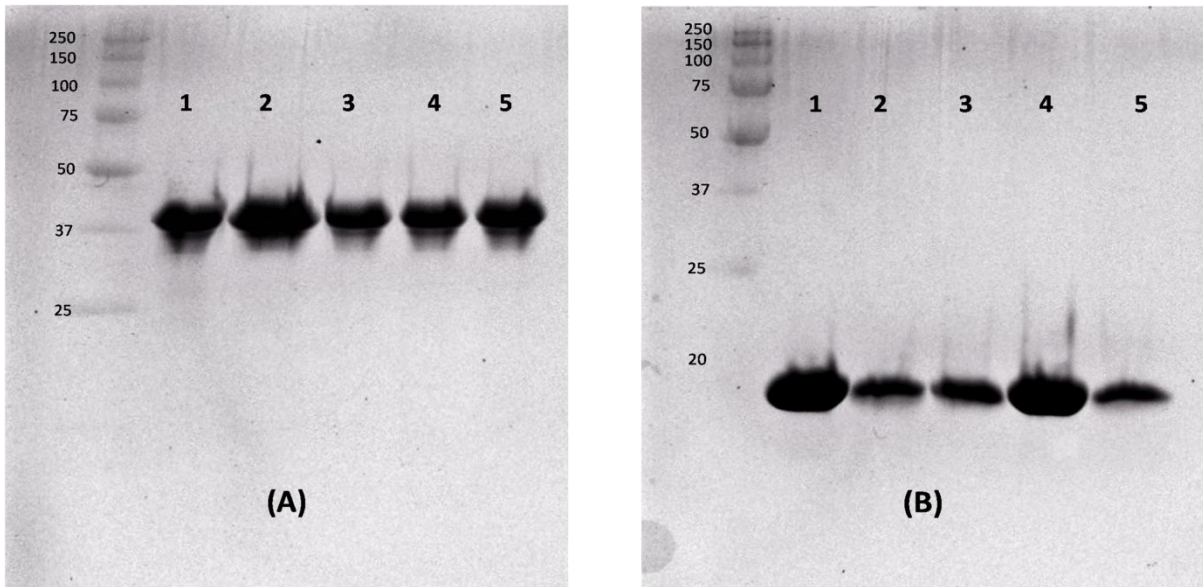


Figure 3.8: 15% SDS - PAGE gel showing full-length protein and N-terminal truncates of VC0395_0300 protein which were used for various experiments. (A) Gel showing final step purified protein after Size-exclusion chromatography where the first lane is protein standard ladder and (1) VC0395_0300 (WT); (2) VC0395_0300(G237R); (3) VC0395_0300(E238K); (4) VC0395_0300(E239K) and (5) VC0395_0300(F240I). (B) N-terminal truncated purified protein after Size-exclusion chromatography where the first lane is Protein standard ladder and (1) VC0395_0300 (WT)₁₆₁₋₃₂₁; (2) VC0395_0300(G237R)₁₆₁₋₃₂₁; (3) VC0395_0300(E238K)₁₆₁₋₃₂₁; (4) VC0395_0300(E239K)₁₆₁₋₃₂₁ and (5) VC0395_0300(F240I)₁₆₁₋₃₂₁.

3.4 Conclusions

vc0395_0300 gene from *V. cholerae* O395 successfully cloned into cloning (DH5) and expression (BL21) host. It was observed that *vc0395_0300* gene is not able to express as a soluble protein with pET 28a (His-Tag containing) vector (Table 3.3), but with pGEX-6P1 it produced soluble protein for full length and truncated gene. In pGEX-6P1, the protein is produced with large GST tag which enables dimerized and increased solubility (**Mitchell et al 1993, Harper and Speicher 2011**). After removal of GST tag from protein, it becomes a monomer observed by size exclusion chromatography (**Bandekar et al 2017**). The wild type full length VC0395_0300 protein expression and purification was performed and optimized earlier in our ViStA lab (**Bandekar et al 2017**), hence, only the conditions for the mutated full length proteins and their N-terminal truncated constructs have been described in this chapter.

1. In small scale protein overexpression test soluble protein was observed for GST tag containing all clone.
2. Best conditions were optimized for maximum overexpression of soluble VC0395_0300 protein and all mutants.
3. Various protein constructs for VC0395_0300 protein were prepared based on secondary structure predictions and conditions for maximum soluble protein overexpression were optimized.
4. The conditions were also optimized for all purified proteins stability in buffer using several buffer parameters.
5. All proteins (full-length wild-type and mutants, constructs of wild type and mutants) were successfully purified and concentrated up to 5-7 mg/ml.

3.5 References

Bandekar D, Chouhan OP, Mohapatra S, Hazra M, Hazra S, Biswas S. 2017. Putative protein VC0395_0300 from *Vibrio cholerae* is a diguanylate cyclase with a role in biofilm formation. *Microbiol. Res.* **202**: 61–70.

Buchan DWA, Minneci F, Nugent TCO, Bryson K, Jones DT. 2013. Scalable web services for the PSIPRED Protein Analysis Workbench. *Nucleic Acids Research.* **41**: W340-W348.

Christine A. White-Ziegler, Suzin U, Natalie MP, Abby LB, Amy JM, Sarah Y. 2008. Low temperature (23 °C) increases expression of biofilm, cold-shock and RpoS dependent genes in *Escherichia coli* K-12. *Microbiology.* **154**: 148–166.

Chatterjee S, Schoepe J, Lohmer S, Schomburg D. 2005. High level expression and single-step purification of hexahistidine-tagged l-2-hydroxyisocaproate dehydrogenase making use of a versatile expression vector set. *Protein Expr. Purif.* **39**: 137–143.

Cuff JA, Clamp ME, Siddiqui AS, Finlay M, Barton GJ. 1998. JPred: a consensus secondary structure prediction server. *Bioinformatics (Oxford, England).* **14(10)**: 892-893.

Fairlie WD, Uboldi AD, De Souza DP, Hemmings GJ, Nicola NA, Baca M. 2002. A fusion protein system for the recombinant production of short disulfide-containing peptides, *Protein Expr. Purif.* **26**: 171–178.

Garcia B, Latasa C, Solano C, Garcia-del Portillo F, Gamazo C, Lasa I. (2004). Role of the GGDEF protein family in *Salmonella* cellulose biosynthesis and biofilm formation. *Mol Microbiol* **54**: 264–277.

Gupta JC, Jisani M, Pandey G, Mukherjee KJ. 1999. Enhancing recombinant protein yields in *Escherichia coli* using the T7 system under the control of heat inducible λ PL promoter. *J. Biotechnol.* **68**: 125–134.

Hage DS. 1999. Affinity chromatography: a review of clinical applications, *Clin. Chem.* **45**: 593–615.

Hannig G, Makrides S. 1998. Strategies for optimizing heterologous protein expression in *Escherichia coli*. *Trends Biotechnol.* **16**: 54–60.

Hakes DJ, Dixon JE. 1992. New vectors for high level expression of recombinant proteins in bacteria. *Anal Biochem.* **202**: 293–298.

Harper S, Speicher DW. 2011. Purification of proteins fused to glutathione S-transferase. *Methods Mol Biol.* **681**: 259–280.

Higgins DA, Pomianek ME, Kraml CM, Taylor RK, Semmelhack MF, Bassler BL. 2007. The major *Vibrio cholerae* autoinducer and its role in virulence factor production. *Nature* **450**: 883–886.

Hunt I. 2005. From gene to protein: a review of new and enabling technologies for multi-parallel protein expression, *Protein Expr. Purif.* **40**: 1–22.

Jones DT. 1999. Protein secondary structure prediction based on position-specific scoring matrices. *J. Mol. Biol.* **292**: 195–202.

José A, Lauritzen C, Petersen GE, Pedersen J. 2006. Current strategies for the use of aYnity tags and tag removal for the purification of recombinant proteins. *Protein Expression and Purification.* **48**: 1–13.

Korf U, Kohl T, van der Zandt H, Zahn R, Schlegler S, Ueberle B, Wandschneider S, Bechtel S, Schnolzer M, Oettleben H, Wiemann S, Poustka A. 2005. Large-scale protein expression for proteome research, *Proteomics* **5**: 3571–3580.

Laemmli UK. 1970. Cleavage of structural protein during the assembly of the head of bacteriophage T4. *Nature* **227**: 680–685.

Lichty JJ, Malecki JL, Agnew HD, Michelson DJ, Tan S. 2005. Comparison of affinity tags for protein purification. *Protein Expr. Purif.* **41**: 98–105.

Lim B, Beyhan S, Yildiz FH. 2007. Regulation of *Vibrio* polysaccharide synthesis and virulence factor production by CdgC, a GGDEF-EAL domain protein, in *Vibrio cholerae*. *J. Bacteriol.* **189**: 717–729.

Mitchell DA, Marshall TK, Deschenes RJ. 1993. Vectors for the inducible over expression of glutathione S-transferase fusion proteins in yeast. *Yeast.* **9**: 715–722.

Nallamsetty S, Waugh DS. 2007. A generic protocol for the expression and purification of recombinant proteins in *Escherichia coli* using a combinatorial His6-maltose binding protein fusion tag. *Nature Protocols.* **2**: 383–391.

Parker MW, Bello ML, Federici G. 1990. Crystallization of glutathione S-transferase from human placenta. *Journal of molecular biology.* **213(2)**: 221–222.

Palomares LA, Estrada-Mondaca S, Octavio TR. 2004. Production of Recombinant Proteins. *Methods in Molecular Biology,* **267**: 15–51.

Rais-Beghdadi C, Roggero MA, Fasel N, Reymond CD. 1998. Purification of recombinant proteins by chemical removal of the aYnity tag, *Appl. Biochem. Biotechnol.* **74**: 95–103.

Ryjenkov DA, Tarutina M, Moskvina OV, Gomelsky M. 2005. Cyclic diguanylate is a ubiquitous signaling molecule in bacteria: insights into biochemistry of the GGDEF protein domain. *J. Bacteriol.* **187**:1792–1798.

Smith DB, Johnson KS. 1988. Single-Step Purification of Polypeptides Expressed in *Escherichia coli* as Fusions with Glutathione S-Transferase. *Gene.* **67**: 31-40.

Sivashanmugam A, Murray V, Chunxian C, Zhang Y, Wang J, Qianqian L. 2009. Practical protocols for production of very high yields of recombinant proteins using *Escherichia coli*. *Protein Science.* **18**: 936–948.

Terpe K. 2003. Overview of tag protein fusions: from molecular and biochemical fundamentals to commercial systems, *Appl. Microbiol. Biotechnol.* **60**: 523–533.

Tischler AD, Camilli A. 2004. Cyclic diguanylate (c-di-GMP) regulates *Vibrio cholerae* biofilm formation. *Mol. Microbiol.* **53**: 857– 869.

Tischler AD, Camilli A. 2005. Cyclic diguanylate regulates *Vibrio cholerae* virulence gene expression. *Infect. Immun.* **73**: 5873–5882.

Turner P, Holst O, Karlsson EN. 2005. Optimized expression of soluble cyclomalto-dextrinase of thermophilic origin in *Escherichia coli* by using a soluble fusion-tag and by tuning of inducer concentration. *Protein Expr. Purif.* **39**: 54–60.

Waugh DS. 2005. Making the most of affinity tags, *Trends Biotechnol.* **23**: 316–320.

4.1 Introduction

It has been reported that the Gram-negative flagellate *V. cholerae* possesses 41 different putative GGD(/E)EF domain-containing proteins, which are directly or indirectly involved in life changing strategies through c-di-GMP signalling pathways (**D'Argenio and Miller 2004, Tischler and Camilli 2004, Ryan et al. 2006, Yan and Chen 2010, Hengge 2013**). These proteins are involved in the regulation of intracellular concentration of the c-di-GMP molecule (**Lim et al 2007, Waters et al 2008**). During higher concentration of c-di-GMP, bacteria have been known to switch their lifestyle from motile to sessile and begin secretion of an external exopolysaccharide matrix to form a biofilm, which provide extra defence mechanisms against external adverse conditions (**Ryjenkov et al 2005, Hammer and Bassler 2009, Karatan and Watnick 2009**).

Although bacteria contain multiple copies of such GGEEF domain proteins in their whole genome, it is also observed that a mutation in a single protein can result in disruption of morphology for the bacterium (**Tamayo et al 2007**). Why all this multiple coding systems has been sustained in bacteria and why all morphological changes occur due to a single mutation, have also been subjects of intense debate. The putative GGD(/E)EF protein VC0395_0300 from the chromosome I of *V. cholerae* classical strain O395 shows the presence of a GGD(/E)EF domain. This protein was over expressed as a recombinant system in *E. coli* and purified. The protein did have a distinct role in biofilm formation as well. Several biophysical analyses were performed to characterize this protein to get information about structural features.

4.2 Materials and methods

4.2.1 Diguanylate cyclase activity

Diguanylate cyclases convert two molecules of GTP to one molecule of the c-di-GMP. *In vitro*, purified VC0395_0300 and all mutated protein samples were tested for diguanylate cyclase activity using High-Pressure Liquid Chromatography (HPLC). In this method, a reaction mixture of 5 μ M protein, 50 mM Tris-HCl (pH 8.0), and 10 mM MgCl₂ was pre-warmed at 37 °C for 10 minutes before initiating the reaction. 50 μ M of Guanosine-5'-Triphosphate (GTP) was used as a substrate and added to the prewarmed reaction mixture and incubated at 37 °C for another 45 minutes. The reaction was terminated by addition of one-fourth volume of 0.5 M EDTA and followed by boiling the entire reaction mixture for 5 minutes (**Ryjenkov et al 2005 and 2006**). After termination of the reaction, the entire reaction mixture was centrifuged at high speed (12000 rpm) for 20 minutes to remove any traces of the residual protein, any precipitated or suspended particle in the final solution.

Subsequently, the separation of the reaction product was achieved in a reverse phase HPLC C-18 column (Waters Xterra-3.5 μ m \times 4.6 \times 250 mm) connected to an Agilent Infinity 1260 system. 20 μ l of the sample was separated using a gradient of mobile phase consisting of solvent A with 100% methanol and solvent B with 10 mM tributylamine and 15 mM acetic acid in water: methanol (97:3) (**Ruiz et al 2012**). The sample was injected into the column, maintained at a slow flow rate of 0.4 ml/min and the following the gradient was used:

0% to 10% solvent B in 15 mins,
10–20% solvent B from 15–20 mins,
20–30% solvent B from 20–25 mins,
30–50% solvent B from 25–30 mins,
50–90% solvent B from 30–35 mins,
90–95% solvent B from 35–40 mins and
95–0% solvent B from 40–45 mins.

Commercially available GTP and c-di-GMP (Sigma Aldrich) were used to calibrate the reverse phase HPLC C-18 column. The retention time for these commercially

synthesized GTP and c-di-GMP were also determined using same solvent and same HPLC method to compare with the reaction product.

4.2.2 Scanning electron microscopy

Scanning electron microscopy (SEM) is one of the most effective methods for analysis of microbial biofilm morphology. By using this technique we can effectively analyze the adequate depth of biofilm, and high-resolution images can be captured for observing the morphology of microbial biofilm **(Walmsley et al 2016)**. For SEM analysis, 5 to 7 days old cultures of all the mutated clones were used. Bacteria were first allowed to grow in LB medium at 37 °C for 24 hours with continuous shaking at 120 rpm. After sufficient growth, a sterile glass coverslip (20 mm X 20 mm) was introduced to culture tube at the air-liquid interface, and culture tubes were transferred to static conditions (without any disturbance) and incubated for 5 days at 37 °C. Bacterial strains grown on the solid surface of glass coverslips were gently removed after 5 days of growth. Glass coverslips with microbial biofilm were gently washed with 1X PBS (pH 7.2), to ensure the removal of any unattached or loosely attached bacterial cells to coverslips. Microbial biofilm was fixed on these coverslips by treating with 2.5% glutaraldehyde for 30 minutes, and fixed biofilms on the coverslips were washed three times by 1X PBS. After fixation, biofilms were treated with 1% osmium tetroxide for 1 hour which was followed by gradual dehydration in graded acetone series with 20 to 100 % (for 15 minutes each) concentration at room temperature. Dehydrated microbial biofilm containing coverslips were subjected to complete drying by liquid carbon dioxide in Critical Point Dryer, CPD (EMITECH, K850). In CPD chamber, coverslips were cooled to 15 °C during 20 cycles of CO₂ exchange and then, further heated up to 35 °C. At 35 °C, all CO₂ was allowed to vent out from the chamber, thus enabling a controlled drop of pressure at the end of the critical drying process. All dried microbial biofilm-containing coverslips were mounted on stubs or SEM chucks and subjected to sputter coating with gold-palladium in vacuum. Sputter coating with gold-palladium masking of biofilm makes it more conductive and helpful for SEM visualization **(Lamed et al 1987, Hassan et al 2003, Allan-Wojtas et al 2008)**.

Followed by the above mentioned treatments, microbial biofilms were imaged using Field Emission Scanning Electron Microscope (FE-SEM QUANTA 200 FEG,

Netherlands). All treated biofilm samples were observed by the secondary electron scanning mode at high vacuum conditions with 5, 10 and 15 kV of accelerating voltage and all images were captured at a magnification range of 10000X, 15000X and 30000X.

4.2.3 Quantification of microbial biofilm

For the quantification of biofilm formation capacity in all mutated strains, crystal violet assay was performed (**Boyd and O'Toole 2012**). In this method, after all strains were grown overnight in 5 ml LB medium, 1% of overnight grown culture was transferred to glass tubes (18 X 150 mm) containing fresh 10 ml LB medium with 100 µg/ml ampicillin and 0.05 mM IPTG, and then incubated at 37 °C for 12 hours with continuous shaking at 120 rpm. After overnight growth in shaking condition, all the tubes were transferred to static culture conditions for 5 to 7 days incubation at 37 °C. After 5 days of growth, a thin slimy layer was visible in all culture-containing tubes at the air-liquid interface. The liquid media were gently removed or drained off from all the glass test tubes. After the removal of medium, bacterial biofilm still clings to the walls of the glass tubes, which were then stained with 0.2% crystal violet for 5 min at room temperature. Unbound bacterial cells or excess of crystal violet was removed by washing the glass tube with distilled water. Tubes were air dried at room temperature and photographed. For the quantification, crystal violet bound biofilms were dissolved in 4 ml of 75 % v/v ethanol for 10 minutes and absorbance were taken at 570 nm using Shimadzu UV-VIS spectrophotometer (UV-VIS 2450, Japan).

4.2.4 Bacterial motility assays

Bacterial motility can be examined by several techniques such as microscopy using a hanging drop, movement on solid or semi-solid culture agar medium, in culture tube or culture plate method. Here in this study, bacterial movement was observed by two different manners.

1. TTC assay
2. Soft agar plate method

4.2.4.1 TTC assay

In TTC assay bacterial motility was assessed by the ability to utilize the colour conversion of triphenyl tetrazolium chloride (TTC) as described in previous reports **(Ball and Sellers 1966, An et al 2010)**. TTC is a water-soluble colourless compound in its oxidized form and when it is reduced, forms a red coloured pigment known as formazan. To check bacterial movement, LB agar tubes were prepared with 8 to 10 ml medium in glass tubes (18 X 150 mm). Sterile TTC (1 mg/ml) solution was mixed in LB agar medium in sterile conditions prior to solidification. Bacterial culture was deep stabbed into such an LB agar tube, using a sterile needle and incubated at 37 °C till visible bacterial growth. Bacterial growth is indicated by the appearance of a red colour formed due to the production of formazan, radiating away from the inoculation stab line.

4.2.4.2 Soft agar plate method

Surface bacterial motility was also observed in petri plates containing soft agar culture medium. Plates were prepared by LB medium containing 0.05 mM IPTG and 0.3 % agar as a solidifying agent. 5 µl of overnight grown liquid bacterial culture was introduced as a single spot on the semisolid surface. All culture plates were incubated at 37 °C for 24 hours, and thereafter size of bacterial colony (which indicates the migration of bacteria from the spot of inoculation) was measured.

4.2.5 Circular dichroism (CD) spectroscopy

The secondary structure or folding status of VC0395_0300 and the mutants were analyzed by Circular dichroism (CD) spectroscopy **(Greenfield N 2006)**. CD is an important analytical technique for protein secondary structure prediction. By using this technique we can get a predictive evaluation of the fraction of amino acids involved in α -helices, β -strands or random coils. To analyze the secondary structure, all protein samples were dialyzed for overnight against CD buffer containing 50 mM Sodium phosphate buffer and 150 mM sodium fluoride. The measurements for all diluted protein samples (0.1 mg/ml) were carried out in a 1.0 mm quartz cuvette at 20 °C on a Chirascan spectropolarimeter (Applied Photophysics, London, UK). All measurements were performed in triplicate and CD spectra recorded in the range of 190 nm to 260 nm

at a resolution of 0.5 nm. The averaged data of protein samples were corrected against buffer spectrum and secondary structure prediction was analyzed using the Dichroweb online server.

4.2.6 Fluorescence spectroscopy

The folding and/or unfolding behavior of the protein was studied by fluorescence spectroscopy. The aromatic amino acid (tryptophan, tyrosine, and phenylalanine) are known to contribute to intrinsic fluorescence. Tryptophan is preferably used to observe intrinsic fluorescence since it gives maximum fluorescence intensity, because of its highest quantum yield amongst the three amino acids. Fluorescence signal spectrum was measured for all protein samples using JASCO FP8200 spectrofluorometer. For measurement of intrinsic fluorescence, tryptophans were selectively excited at 295 nm wavelength and the emission spectrum was observed between 310 to 400 nm (**Ghisaidoobe and Chung 2014**). Both the excitation and emission band passes were kept at 5 nm.

4.2.6.1 Thermal denaturation

To check the effect of temperature on protein folding, the fluorescence spectrum was observed for all protein samples. For this experiment, the spectrofluorometer was connected to a ESCY IC201 temperature controller fitted water bath, used to increase or decrease the ambient temperature of the sample via a jacket. Protein denaturation was carried out by gradually increasing the temperature over a range of 20 to 80 °C. The emission spectrum was observed between 310 to 400 nm for excited tryptophan after incubating the protein samples for 10 minutes at a set temperature in cuvettes surrounded by constant temperature water jacket.

4.2.6.2 Chemical denaturation

The protein samples were denatured by gradually increasing concentration (0.5 to 5 M) of guanidine hydrochloride (GdnHCl). 10 µM of purified protein samples were individually incubated at 25 °C with different concentrations of GdnHCl in Tris buffer pH 7.4. The mixture of an equal volume of the Tris buffer and the same volume of GdnHCl was used as blank, whereas, pure protein sample in Tris buffer without GdnHCl has used a positive control. All fluorescence spectra were blank corrected and emission spectra observed between 310 to 400 nm for excited tryptophan residue.

4.2.6.3 Fluorescence quenching

All protein samples were preincubated with three different quencher molecules, *viz.*, acrylamide (neutral quencher), potassium chloride, KI (negative quencher) and cesium chloride, CsCl (positive quencher). Aliquots of 5 M quencher stock solution was added to reaction mixture containing a final concentration of 10 μ M of purified protein. The final volume was adjusted by the addition of Tris buffer. The reaction mixture was incubated at 25 °C for 4 hours and emission spectrum was collected for excited tryptophan residues following a method similar as above. All results were analyzed according to the Stern-Volmer equation:

$$F_0/F = 1 + K_{sv} [Q]$$

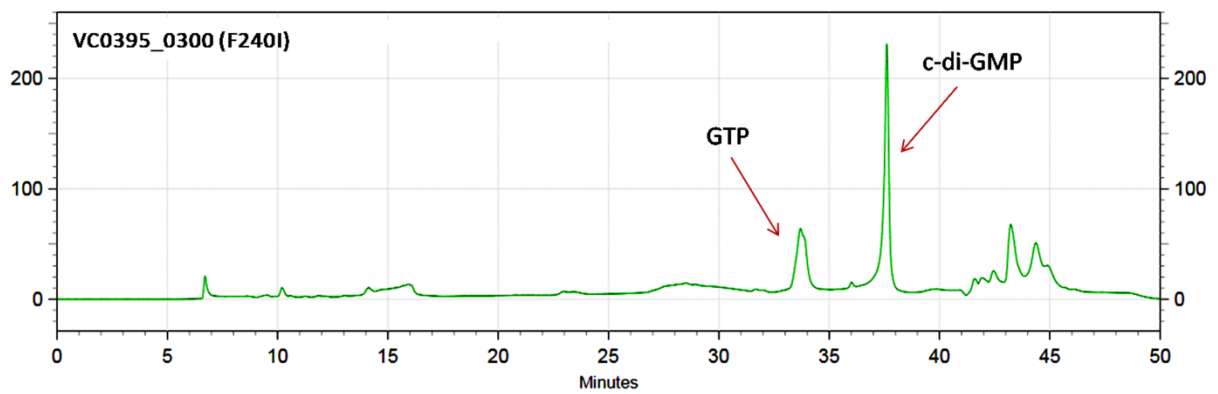
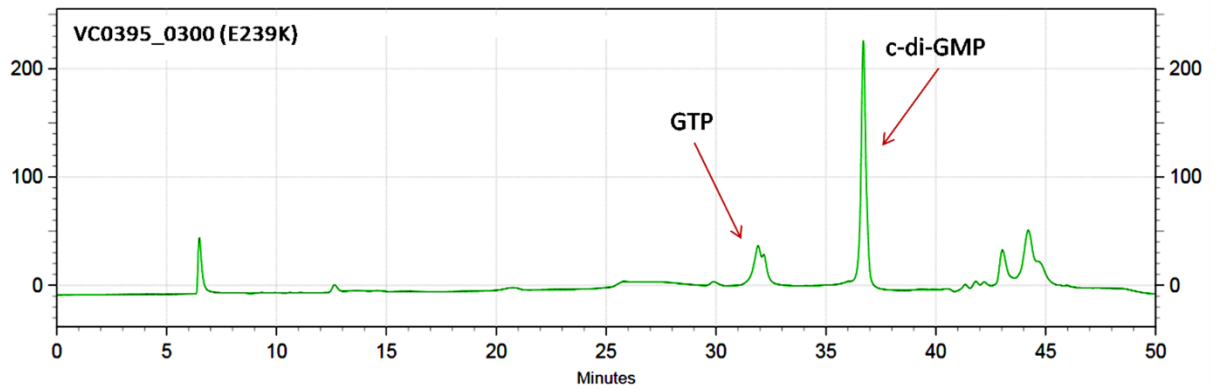
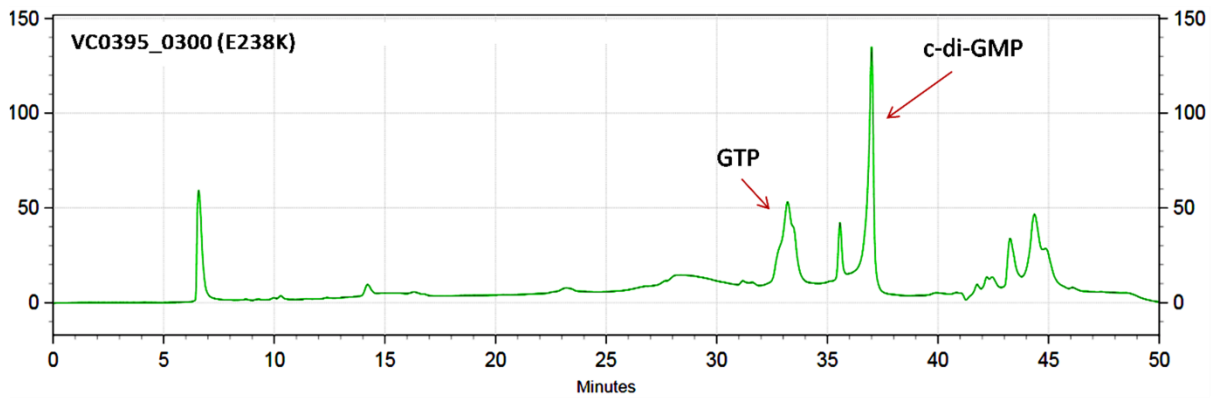
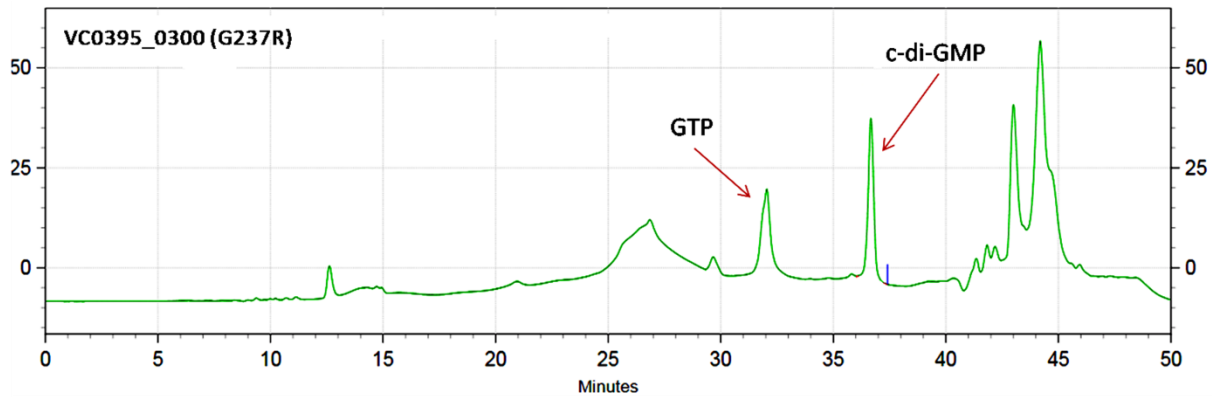
where F_0 and F represent fluorescence intensities for the protein in the absence of quencher and presence of quencher respectively, K_{sv} represents Stern-Volmer equation constant and Q is a concentration of quencher molecule used in the reaction.

4.3 Results and discussions

4.3.1. Diguanylate cyclase activity of mutants

To determine the enzymatic activity of the VC0395_0300 protein, the purified protein was incubated *in vitro* with the substrate (GTP) and checked for synthesized products. The methodology followed was more-or-less similar to our earlier protocol (**Christen et al 2005**), except for the addition of a divalent cation, which has been now established to be crucial for the activity of most diguanylate cyclases (**Stelitano et al 2013**). We tried with both Mg^{2+} and Mn^{2+} , but the magnesium salt yielded results alone, indicating that Mg^{2+} ions are indeed needed for the activity of VC0395_0300 protein. The reaction product was cross-checked by comparing the retention time with commercially available c-di-GMP which was run as a control using same HPLC method. It was observed that 5 μ M VC0395_0300 was able to convert GTP to c-di-GMP, as evident from the HPLC peak profile of the products (Figure 4.1). The ability of an enzyme to convert GTP to c-di-GMP is a testimony to its activity as a diguanylate cyclase.

The intensity of a peak in the HPLC graph is directly proportional to available amount or concentration of the compound in the reaction mixture. The comparative study for all mutants with wild type protein revealed that the ability of product (c-di-GMP) formation is less for VC0395_0300(G237R) and VC0395_0300(E238K) respectively, while strains VC0395_0300(E239K) and VC0395_0300(F240I) show results almost similar to the wild-type strain. These results showed that mutations in the active site amino acid residues 237 (Gly at second position GGEEF), and residue 238 (Glu at third position GGEEF) alter the potential GTP-binding and c-di-GMP formation abilities of the protein, which results in the non-conversion of all the available substrate into product c-di-GMP.



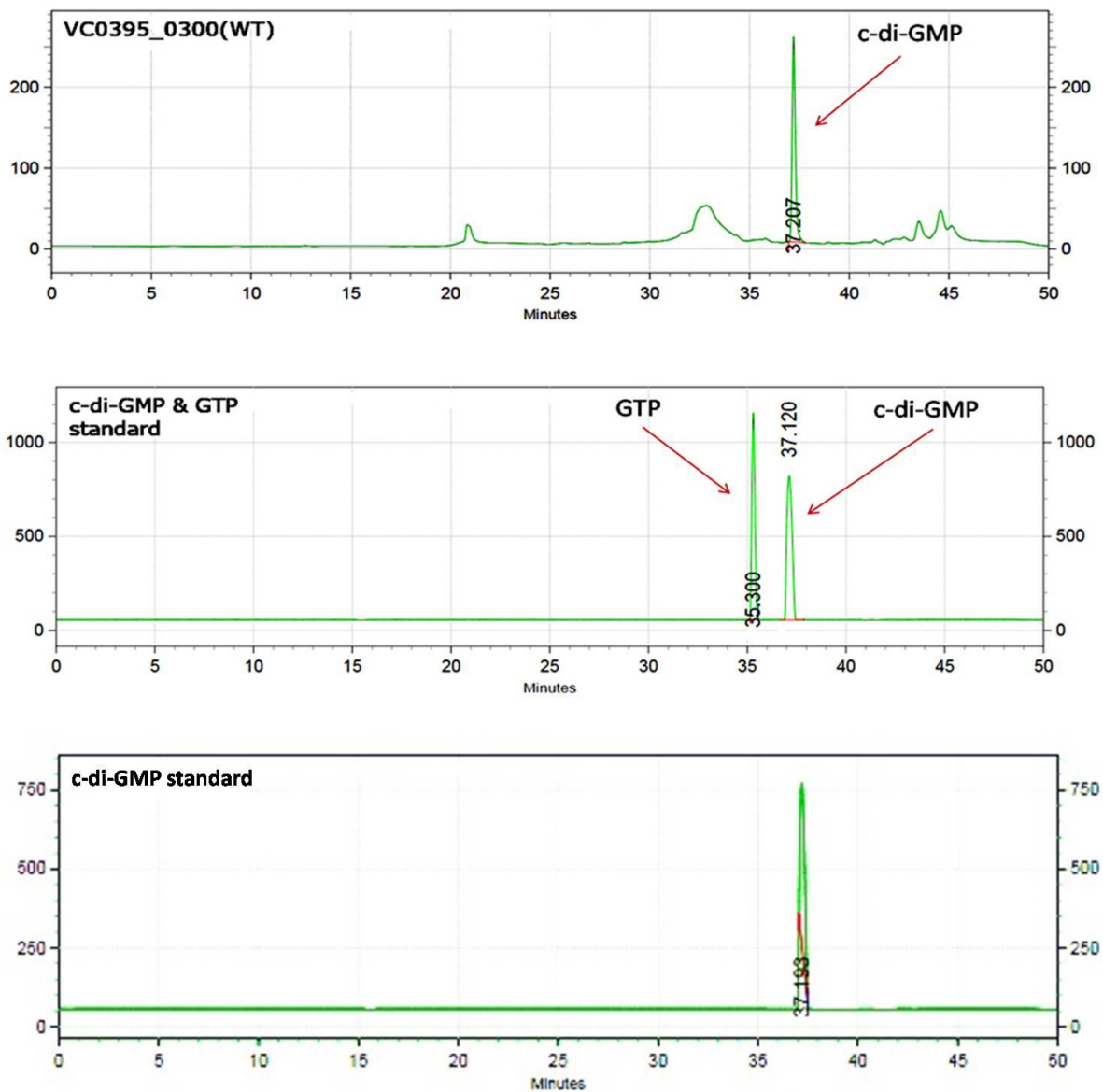


Figure 4.1: HPLC assay for diguanylate cyclase activity of mutant proteins at best-optimized conditions. Reaction mixtures were incubated for 45 minutes and after termination of the reaction mixture were analyzed by HPLC C-18 RP column. In graph substrate, GTP and product c-di-GMP peak are highlighted separately.

4.3.2 Structures of biofilms

Biofilm formation is a most common way of survival for the microorganism in surface-associated communities. It creates a severe problem for public health and makes bacteria resistant to most other external factors including chlorine and other reagents. Bacterial biofilm is a community of microbial life with three-dimensional (3D) structures, in which bacteria grow together on a solid surface enclosed in an exopolysaccharide matrix. These multi-cellular bacterial communities are favourite places for interspecies or intra-species gene transfer (**Molin 2003**), quorum sensing, development for antibacterial resistance etc (**Molin et al 2003, Lewis et al 2005, Nadell et al 2008**). Bacteria growing in surface-attached biofilm possess some extra morphological features such as cell surface appendage, pili, curli flagella, extra-cellular polymers which are essential for attachment on solid surfaces and mature biofilm development (**Busscher et al 2008, Rodrigues and Elimelech 2009**). There are many advanced techniques available now for the study of bacterial biofilm, but Scanning Electron Microscopy (SEM) has been proved an extremely powerful and appropriate tool for revealing the fine structure of microbial biofilm formation (**Eighmy et al 1983**). SEM uses a fine electron beam to study biofilm specimen and generates a high-quality image with higher resolution. It can also quantify the surface topographical three-dimensional features for a bacterial biofilm. For visualization of biofilm for all mutants, strains were grown in liquid medium and transferred to glass coverslips. After the maturation of biofilm on coverslips, it was fixed with glutaraldehyde and gradually dehydrated with acetone to minimize the water content which is not suitable for electron beam in vacuum. To avoid charge build-up through electron beam in vacuum, the chemically fixed biofilm was coated with a conductive material (gold-palladium), followed by imaging in vacuum (**Lamed et al 1987, Hassan et al 2003, Allan-Wojtas et al 2008**).

SEM images revealed differential biofilm formation in the wild type strains versus the mutants. Biofilm formation was not completely disrupted and all strains produced some extracellular matrix on glass coverslips. In the wild type, microbial biofilm was distributed as a layer with different morphological shapes and sizes of bacterial cells (Figure 4.2). The same was not true for the two mutants, VC0395_0300(G237R) and

VC0395_0300(E238K), but again showed appreciable biofilm formation in VC0395_0300(E239K).

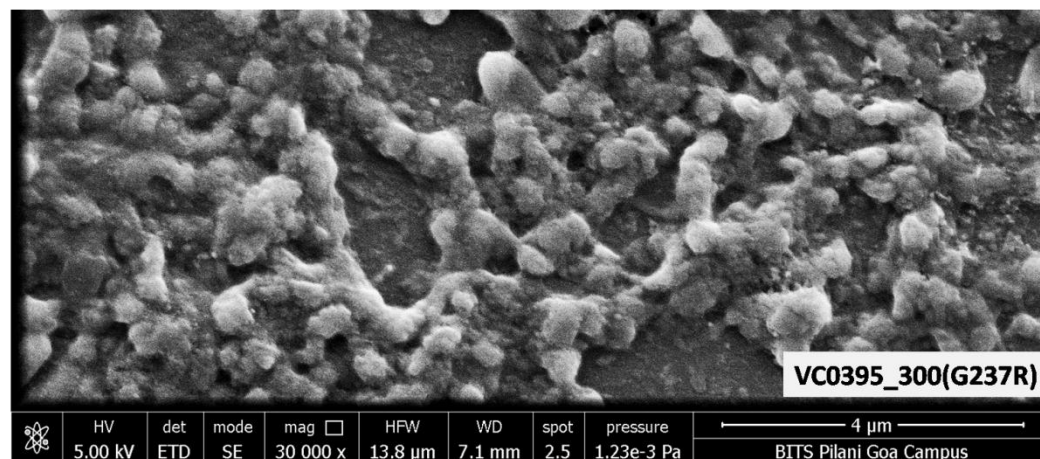
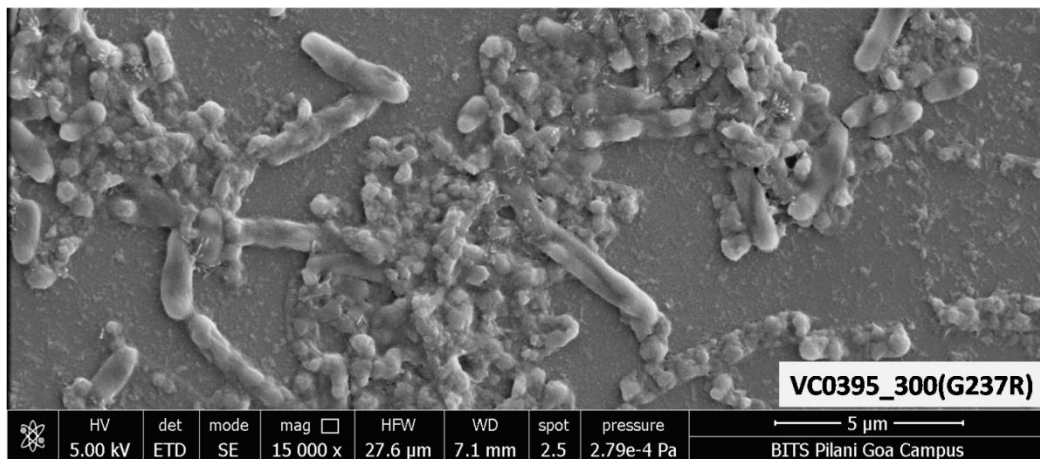
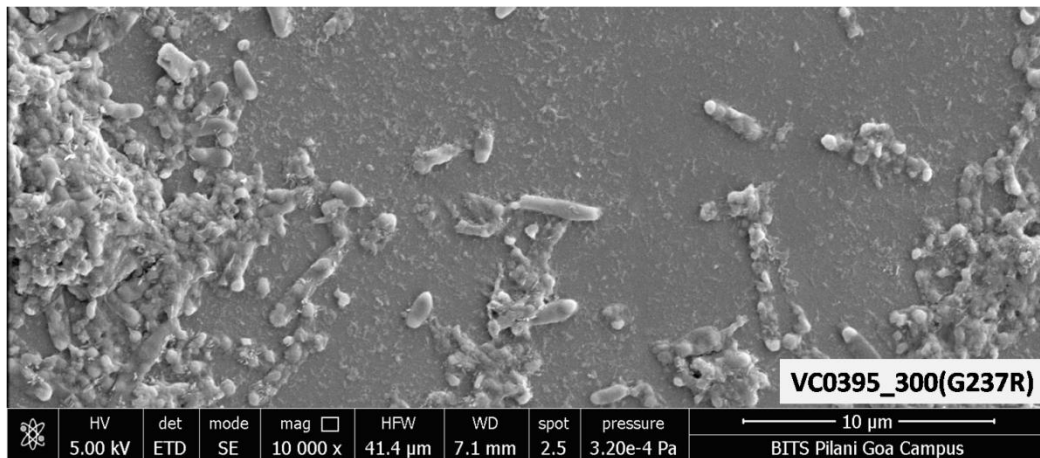


Figure 4.2: Scanning Electron microscopy images for biofilm of VC0395_0300(G237R) under high vacuum conditions at 10000, 15000 and 30000X zoom.

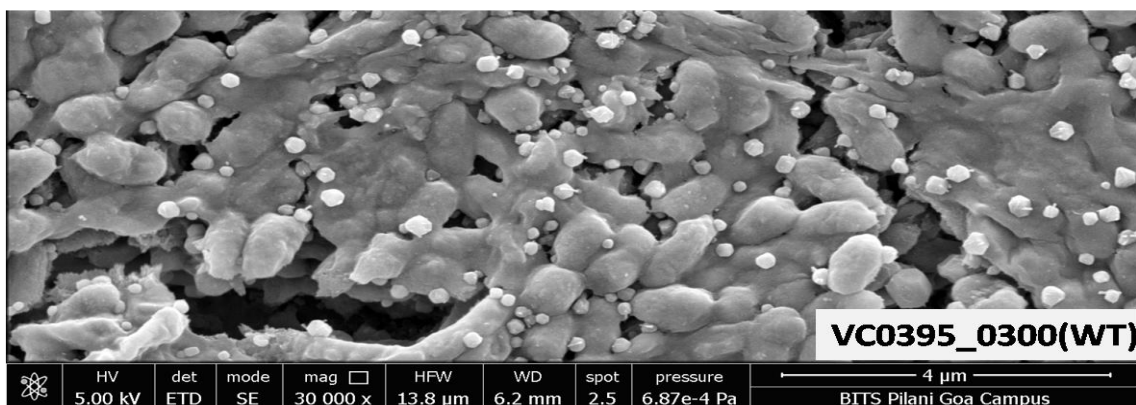
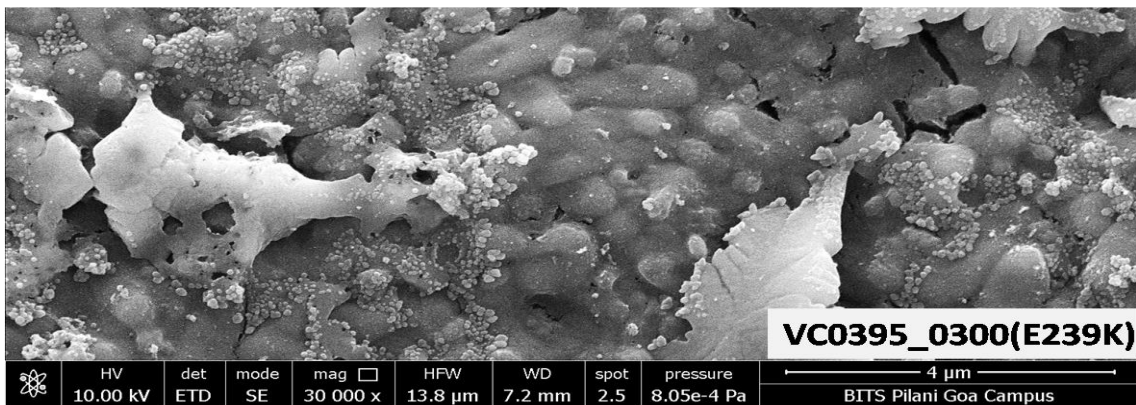
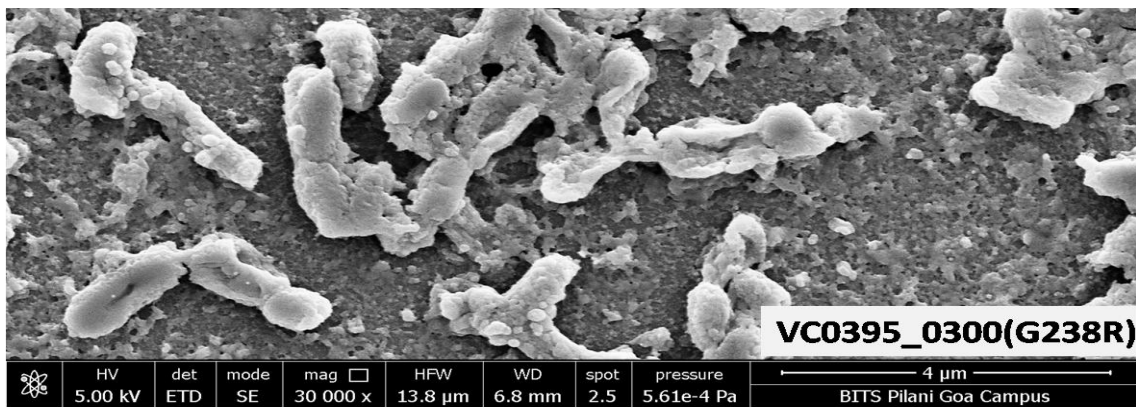
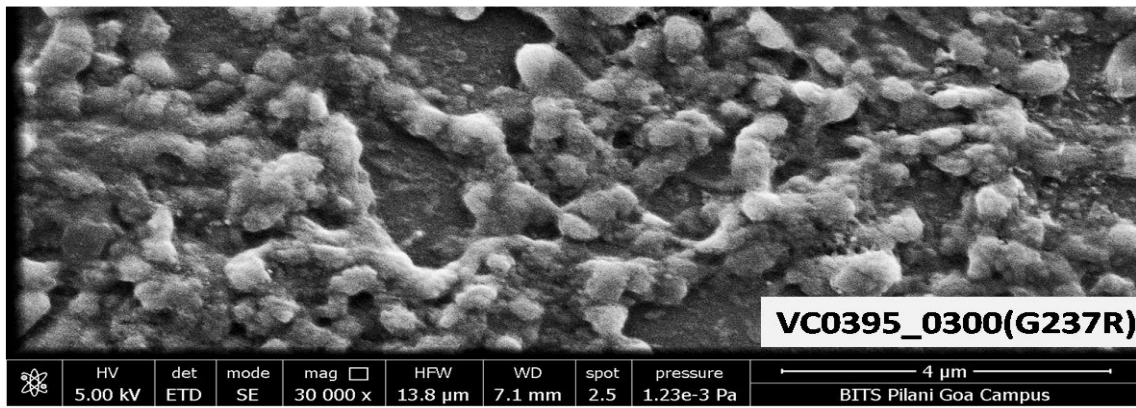


Figure 4.3: Scanning Electron microscopy images for all mutant strains and the wild-type strain. All treated biofilm samples were observed under high vacuum conditions at 30000X zoom.

4.3.3 Quantification of biofilm and bacterial motility

The biofilm is advantageous not only for the survival of stress conditions, it is also very important for disease transmission in *V. cholerae*. In a biofilm, bacteria grow as a multicellular entity where different kinds of morphological or physiological bacterial cells live together. The nonculturable but viable cell of *V. cholerae* are typically observed in biofilm only; these types of cell are thought to be very important for increasing the survivability of *V. cholerae* in harsh conditions and important for spreading cholera disease. Secondary messenger molecule c-di-GMP is a strong regulator of biofilm formation in bacteria – it regulates biofilm formation by regulation of extracellular matrix or polysaccharide synthesis, which is the main component of bacterial biofilm.

To visualize the effect of the mutation on A-site GGEEF amino acids, the multicellular behavior (or ability of biofilm formation) of recombinant strains were investigated. Typical biofilm- like behaviour such as clumping, adherence to solid surfaces, pellicle formation on liquid-air interface, etc. was individually examined for all strains. Bacteria were allowed to grow in liquid culture medium for 12-16 hours initially and then transferred to static conditions for observation of biofilm formation. Studies were undertaken for separate sets at 4 and 7 days intervals. After both 4 and 7 days, it was observed that the biofilm formation (adherence to the tube and pellicle formation at the air-liquid interface) was significantly lower or down-regulated for the mutants VC0395_0300(G237R), VC0395_0300(E238K), VC0395_0300(E239K) and VC0395_0300(F240I) when compared to the wild-type VC0395_0300 strain. Visual inspection of tubes after 7 days showed wild-type strain has thicker biofilm pellicle as compared to all other mutant strains. Also mutant strains have more planktonic bacterial cells in the liquid culture medium as compared to VC0395_0300 strain. Spectrophotometric analysis showed biofilms decreased almost by two to three folds in VC0395_0300(G237R), VC0395_0300(E238K), but, VC0395_0300(E239K) and VC0395_0300(F240I) showed more-or-less similar biofilm formation as wild-type strain (Figure 4.4).

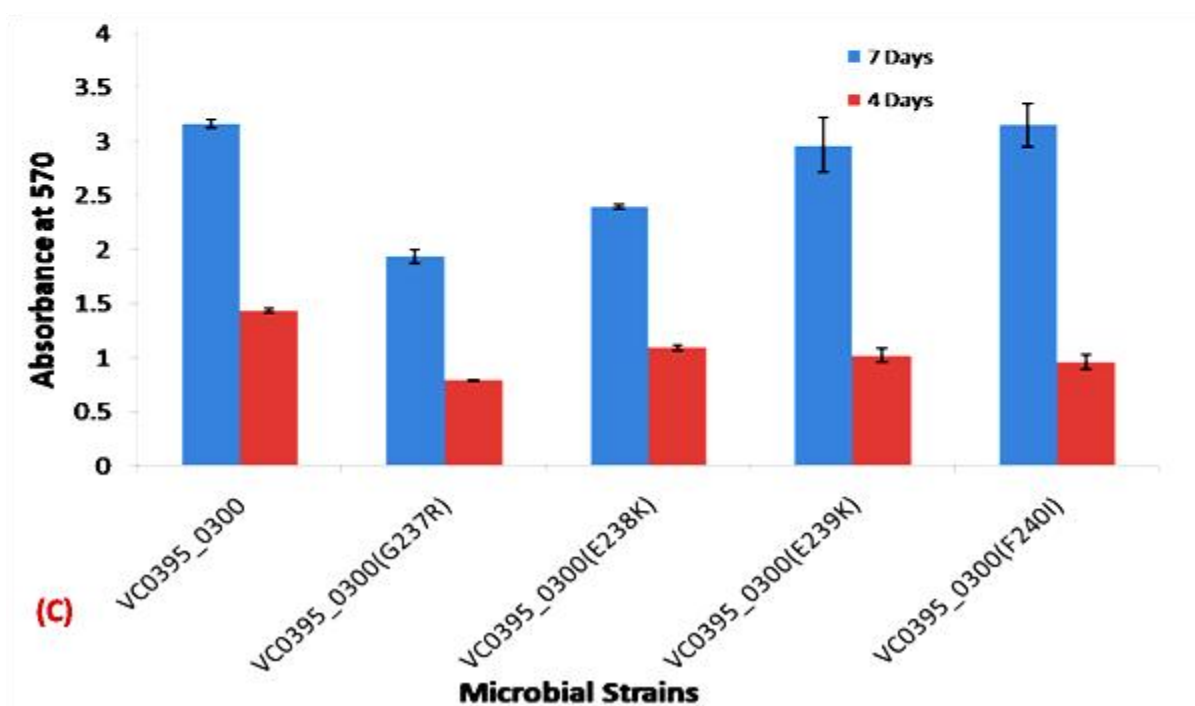
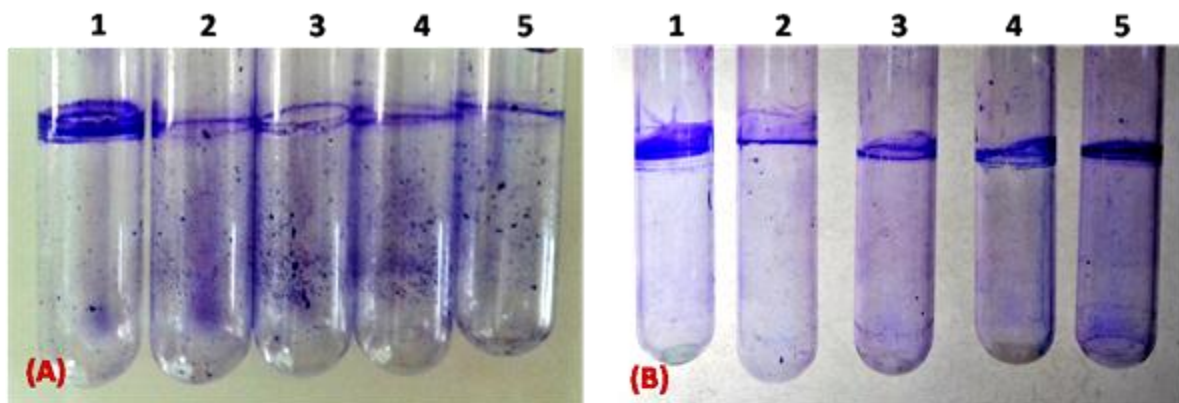


Figure 4.4: Crystal violet staining and quantification of bacterial biofilm. (A) Biofilm formation after four days of growth. (B) Biofilm formation after seven days of growth. (C) Quantification of biofilm by spectrophotometric method at 570 nm with STDEV. Where 1 = VC0395_0300, 2 = VC0395_0300 (G237R), 3 = VC0395_0300 (E238K), 4 = VC0395_0300 (E239K), and 5 = VC0395_0300 (F240I).

V. cholerae can spread themselves or colonize through movement. *V. cholerae* have single polar flagella (a thread-like extending appendage from interior plasma membrane) which facilitates movement of the bacteria. By using flagella, the bacteria can move from unfavourable to the favourable environment as a response to chemicals (chemotaxis), or for survival in stress conditions. Nonmotile or motile bacteria can be distinguished on the basis of their growth pattern in culture medium and bacterial

growth is indicated by the appearance of a red color formed due to the production of formazan by the reduction from triphenyl tetrazolium chloride (TTC) in the TTC assay. TTC is a colorless and water-soluble compound which, when present in culture medium, acts as an artificial electron acceptor molecule used in the electron transport chain reaction. In this reaction, TTC is reduced by an electron donor (such as cytochrome b or c) and turn into a red-coloured compound known as formazan. So when bacteria grow in TTC containing culture medium they utilize it and reduced it to red-coloured formazan. The presence of this formazan is a good indicator of the presence of bacteria. In case of motile bacteria, the red color is visible as radiating away from the inoculation stab line because bacteria grow along the stab line and also move out, away from the inoculated stab line. Non-motile bacteria which cannot swim or move grow only along the stab line where they are introduced in the soft agar culture medium.

In our experiments, after inoculation in the stab culture, all test tubes were allowed to incubate at 37 °C for 2 days without shaking. For the wild-type strain VC0395_0300, there was very less or near to no migration from the initial inoculation stab line and no expansions of the red colour were visible. However, for the mutant strains, there was the visible spread of the red formazan zone away from the site of inoculation of the initial stab (Figure 4.5). All mutated strains VC0395_0300(G237R), VC0395_0300(E238K), VC0395_0300(E239K), except VC0395_0300(F240I) showed a more-or-less comparable zone of motility, VC0395_0300(F240I) showed no migration or movement from stab line, confirming our initial observations about the loss of biofilm formation ability in the three mutants. The mutant strain VC0395_0300(F240I) showed similar migration zone as wild-type VC0395_0300 strain. Similar results are observed in motility soft agar plates test. In plate test, all mutant strains except VC0395_0300(F240I) showed larger migration zone as compared to the wild-type strain.

Motility test (TTC test tube assay and soft agar plate method) results indicate that GGEEF domain was functionally active in all strains, but with varying levels. Wild-type strain VC0395_0300 and one mutant strain VC0395_0300(F240I) showed similar growth pattern in culture tube and grow near stab or inoculation line. Mutations in signature amino acids of GGDEF domain cause alteration in c-di-GMP synthesis reaction (as compared to wild-type), and there was less production of the intracellular c-

di-GMP molecule which ultimately makes bacteria more motile as shown in tube and plate for VC0395_0300 (G237R), VC0395_0300 (E238K), and VC0395_0300 (E239K). This gain of motility is associated with reduced biofilm formation.

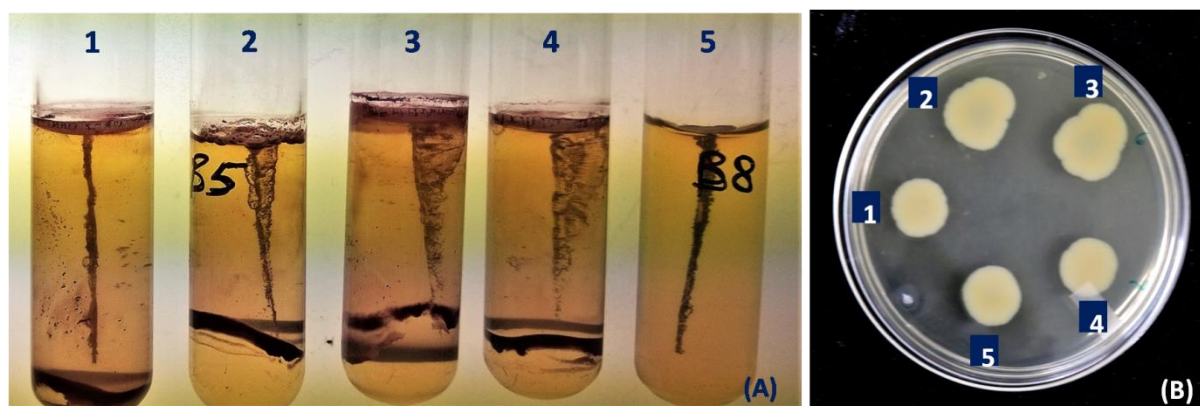


Figure 4.5: Bacterial motility test at best-optimized conditions (A) Bacterial motility test in TTC dye containing LB agar medium. (B) Bacterial motility test on soft agar LB medium plate. Where 1 = VC0395_0300, 2 = VC0395_0300 (G237R), 3 = VC0395_0300 (E238K), 4 = VC0395_0300 (E239K), and 5 = VC0395_0300 (F240I).

4.3.4 Effect of mutation on secondary and tertiary structure of protein

The proper or accurate folding of a protein molecule is important in terms of its biological activity; any alteration in protein folding can lead to nonspecific function or loss-of-function. The secondary structural composition of a protein (whether α helices or β strands) can be analyzed by Circular Dichroism (CD) spectroscopy, while the structure of an active tertiary protein can be studied using fluorescence spectroscopy.

4.3.4.1 Fluorescence spectroscopy

In fluorescence spectroscopy, the high sensitivity and non-invasiveness makes it a useful experimental technique for the study of protein folding mechanisms and conformational transitions. After absorption of a particular wavelength of light (λ_{ex}), a fluorophore (usually an aromatic compound) reaches a higher energy state for a short time and re-emits the light at a longer and specific wavelength (λ_{em}), wherein, the light signal can be measured by a spectrofluorimeter. The emitted light signals are highly

sensitive to the immediate environment, with drastic changes are possible according to the conformation and folding state of the protein.

Of the 20 different amino acids, only phenylalanine (Phe), tyrosine (Tyr) and tryptophan (Trp) have intrinsic fluorescence properties. Of these three, tyrosine and tryptophan are favorable for fluorescence study due to their higher quantum yields which give a better signal in fluorescence spectroscopy. The absorption capability of phenylalanine is very low which produce negligible fluorescence signal with minimum quantum yield. Though the quantum yield is similar for tyrosine and tryptophan and both amino acids produce a similar signal after excitation at 280 nm, most experiments involve excitation of the molecule at the λ_{max} of tryptophan. The preference is given to Trp over Tyr because Tyr emission is generally quenched by nearby peptide chain interaction. The emission fluorescence spectrum for Trp residue in a protein varies from 305 to 360 nm according to its position in the protein chain. When Trp residues are present in the hydrophobic environment (fully buried inside), they generally emit in the range of 305 to 310 nm; for partially buried Trp or those present in hydrophobic interfaces between two protein domains, signal is typically produced from 335 to 340 nm. Upon disruption of protein 3D structure or for fully exposed Trp residues, signal is produced typically in the 355 to 360 nm range (**Royer 2006**).

Table 4.1: Fluorescence properties of aromatic amino acids.

Residues	Life time (ns)	Absorption		Fluorescence	
		λ (nm)	Absorptivity (ϵ)	λ (nm)	Quantum Yield
Tryptophan	3.2	280 and 295	5600	348	0.2
Tyrosine	3.6	280 and 274	1400	303	0.14
Phenylalanine	6.4	257	200	282	0.04

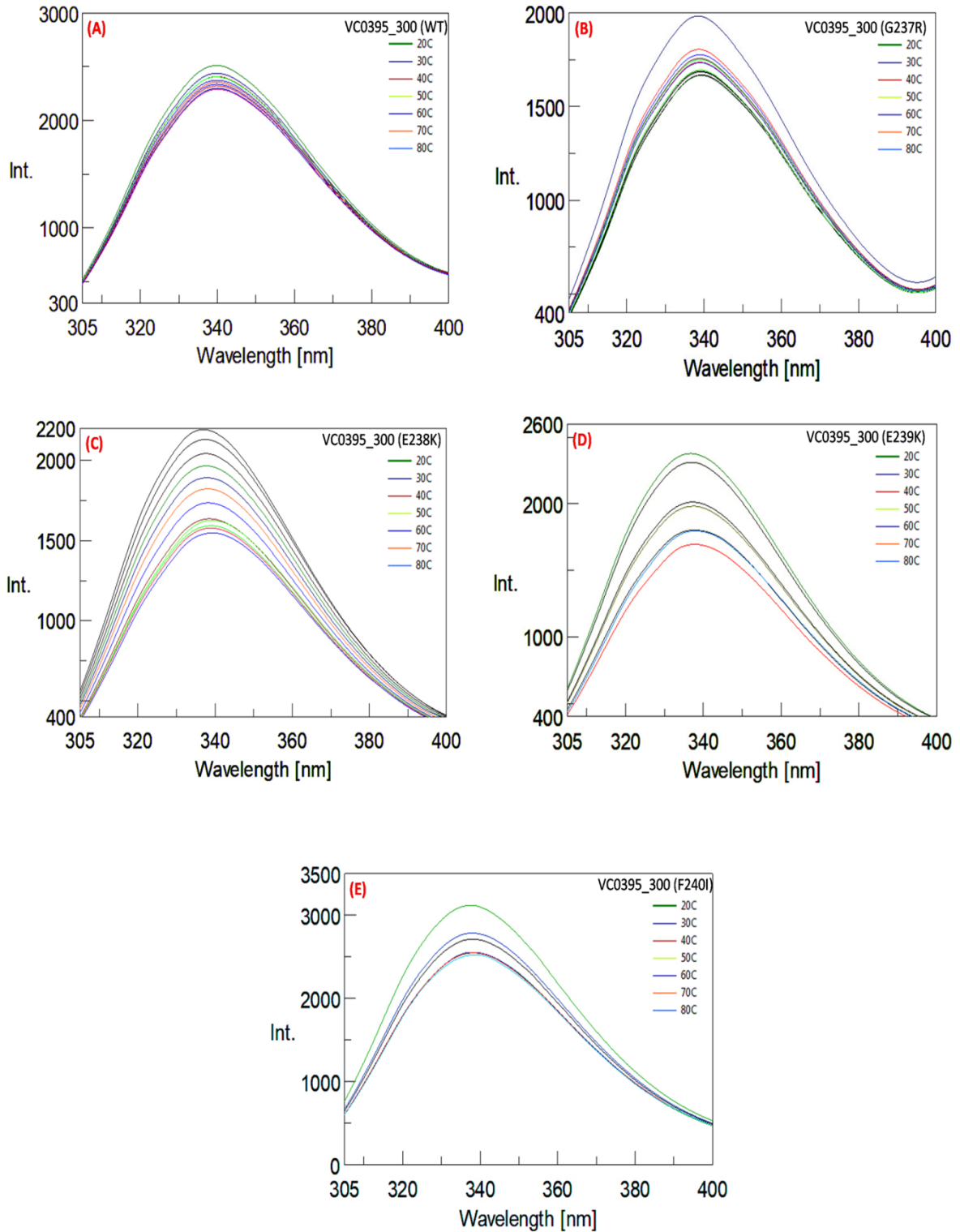


Figure 4.6: Fluorescence emission spectra after excitation of Trp residue at 295 nm. Emission spectra were taken after thermal denaturation at range of 20 to 80 °C. Results indicated Trp residue present in the stable domain which not unfold after thermal treatment. Where A = VC0395_0300 (WT), B = VC0395_0300 (G237R), C = VC0395_0300 (E238K), D = VC0395_0300 (E239K), and E = VC0395_0300 (F240I).

The primary amino acid sequence for VC0395_0300 protein shows two Trp residues to be present in the polypeptide chain. To analyze the position of the Trp residue in VC0395_0300 mutants, all protein were treated with increasing temperature range (20 - 80 °C) which leads to thermal denaturation or unfolding of the protein molecule. Increasing temperature leads to denaturation or unfolding of the protein by disruption of weak interactions such as hydrogen bonds, electrostatic bonds, polar and hydrophobic attractions. For all VC0395_0300 mutants, protein emission spectra were recorded for 305 nm to 400 nm after excitation of Trp residue at 295 nm. The λ_{max} in emission spectra for all protein samples was observed at 338 to 339 nm which shows Trp residue is present at hydrophobic interfaces between two subdomains or it can be in partially buried positions. There were not much changes in λ_{max} in emission spectra after thermal denaturation and while at 70 °C, protein started to precipitate. Results indicated that the Trp residue was present in the stable domain which does not unfold after thermal treatment (figure 4.6).

Guanidinium chloride (GdnHCl) is a charged molecule with strong chaotropic ability and can be used for protein unfolding. When GdnHCl is mixed with protein solution, it generates dipole moment which leads to protein unfolding due to ionic interactions between GdnHCl and charged residues of the protein. VC0395_0300 protein mutants show lower fluorescence signal at $\lambda_{\text{max}} = 338$ in its native state, indicating partially buried position of the Trp residues in a hydrophobic environment. In presence of GdnHCl, the protein solution shows an increase in fluorescence intensity and increased value for λ_{max} . The increasing λ_{max} values indicate unfolding of protein and exposure of Trp residue for the solvent molecule. The hydrophobic environment of Trp residue in the native protein is continuously changed with increasing concentration of GdnHCl in solution. At 4 M of GdnHCl the protein is fully unfolded showing maximum intensity of fluorescence signal and $\lambda_{\text{max}} = 355$ to 360 nm for all mutant proteins. The difference in λ_{max} value of Trp residue in native protein and unfolded protein indicates that lower fluorescence signal in the native state may be due to one partially buried Trp, while gradually increasing λ_{max} value with increasing concentration of GdnHCl may lead to the gradual exposure of fully buried second Trp residue in protein (Figure 4.7).

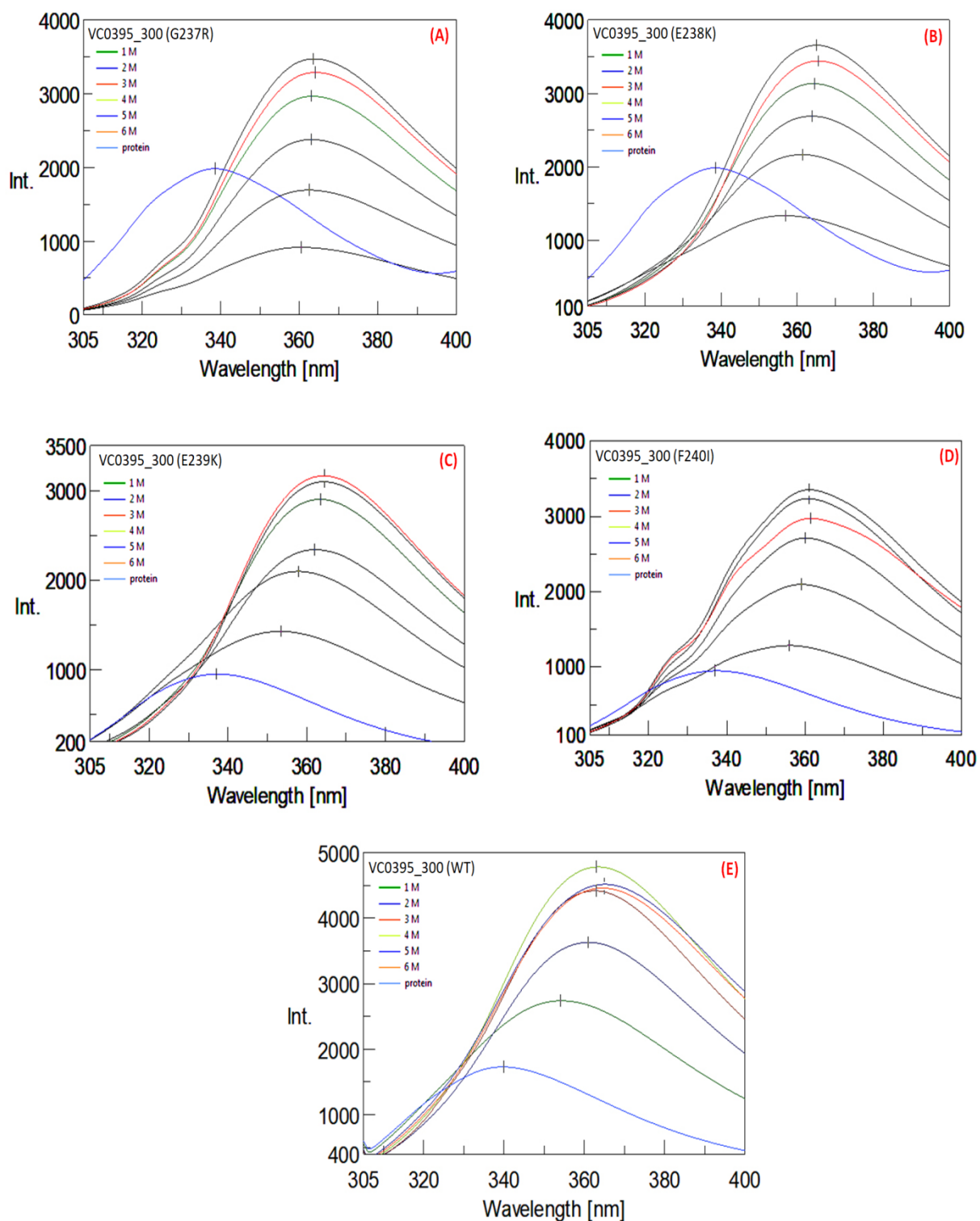


Figure 4.7: Fluorescence emission signal of GdnHCl denatured protein after excitation of Trp residue at 295 nm. Changes in λ max in emission spectra were recorded after denaturation by GdnHCL. A = VC0395_0300 (WT), B = VC0395_0300 (G237R), C = VC0395_0300 (E238K), D = VC0395_0300 (E239K), and E = VC0395_0300 (F240I).

Quenching of Trp fluorescence was also performed to find out the nature of local surrounding residues using the neutral quencher acrylamide, the negative quencher potassium iodide, and the positive quencher cesium chloride. As per expectations, acrylamide showed maximum quenching activity for all proteins because acrylamide is a small neutral compound which can easily access to the buried Trp residue and quench maximum fluorescence signal (Figure 4.8). The other quencher potassium iodide (KI bigger in size and negatively charged) also showed quenching for fluorescence signal, indicating that the Trp residue might be present in a positively charged local surrounding. The quenching by the bigger sized iodide molecule also gave a useful hint that one of the Trp residues may be present as partially buried or near to surface which is available to access for iodide molecule. The positive quencher cesium chloride was unable to quench fluorescence signal suggesting the position of Trp residue in the positively charged pocket.

The high values for Stern-Volmer constant (K_{SV} = indicates comparison between the rate of quenching and the rate for first excited state formation) for acrylamide and potassium iodide (Table 4.2) also support the presence of at least one Trp residue at accessible position while caesium chloride has minimum Stern-Volmer constant (K_{SV}) value indicating the inability to access the Trp placed in the positively charged environment. Overall, the quenching results showed that one of the Trp residues might be present near the surface in a positively charged pocket, which is accessible to the negatively charged molecule and other Trp residue might be present in the hydrophobic core of the protein.

Table 4.2: Stern - Volmer constant (K_{SV}) values for all mutated protein in presence with different concentration of quencher.

Name of Quencher	Concentration of Quencher	VC0395_0300	VC0395_0300	VC0395_0300	VC0395_0300
		(G237R) K_{SV}	(E238K) K_{SV}	(E239K) K_{SV}	(F240I) K_{SV}
Acrylamide	0.2 M	0.0252	0.096	0.718	0.076
	0.4 M	0.0838	0.215	1.503	0.296
	0.6 M	0.2034	0.998	2.293	0.968
	0.8 M	0.3258	2.292	2.842	1.556
	1.0 M	-----	3.068	3.921	3.387
Cesium chloride	0.2 M	0.0098	0.008	0.036	0.004
	0.4 M	0.0228	0.015	0.070	0.004
	0.6 M	0.0358	0.007	0.105	-0.017
	0.8 M	0.0497	0.074	0.121	0.067
	1.0 M	-----	0.031	0.101	0.038
Potassium iodide	0.2 M	0.0348	-0.001	0.065	0.040
	0.4 M	0.0795	0.051	0.242	0.146
	0.6 M	0.1662	0.188	0.401	0.248
	0.8 M	0.2669	0.311	0.723	0.446
	1.0 M	-----	0.839	1.380	0.732

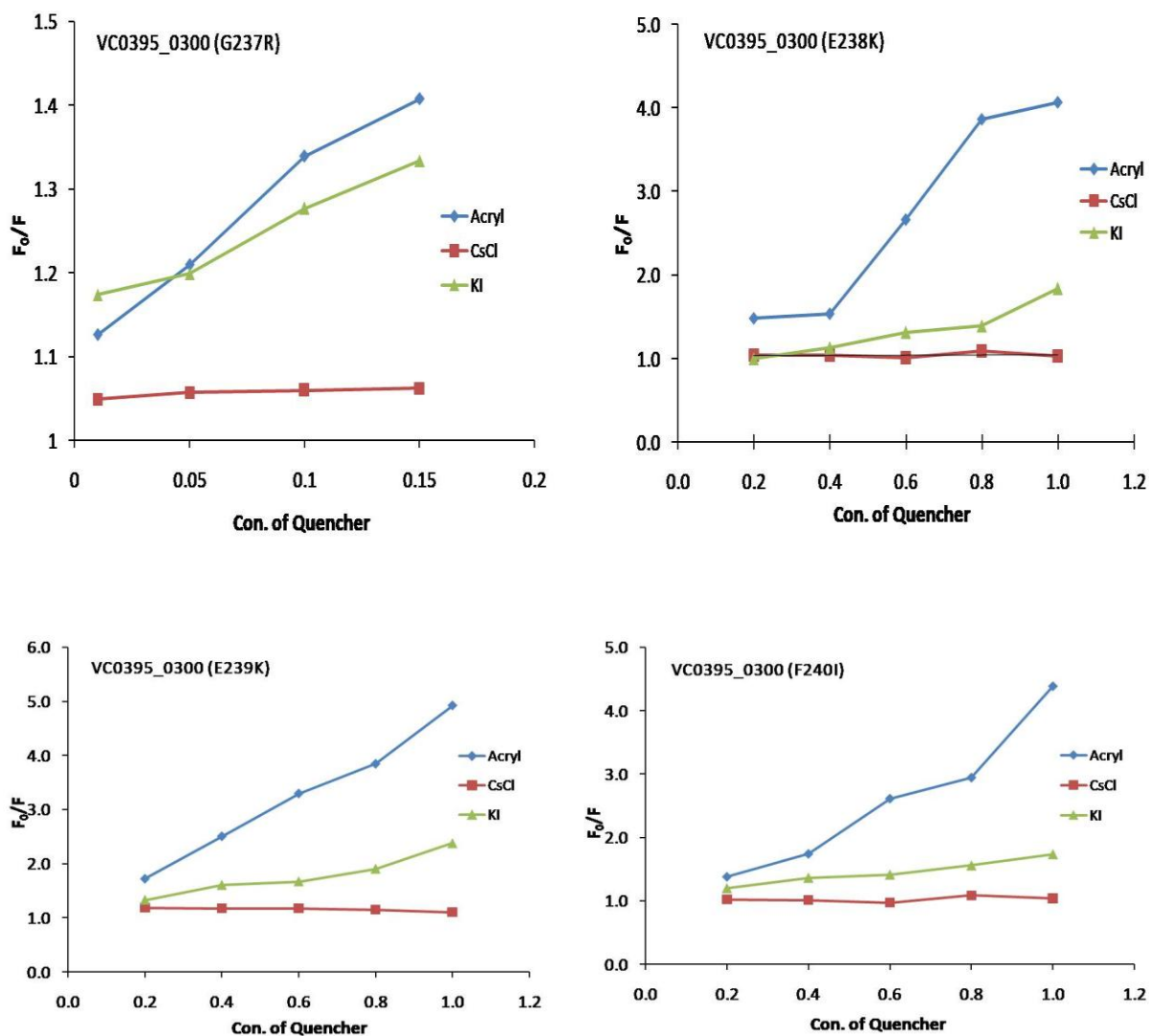


Figure 4.8: Stern-Volmer curves for fluorescence signal after quenching of Trp residues in protein. Fluorescence signal quenching was done by incubation of protein samples with acrylamide, potassium iodide, and cesium chloride.

4.3.4.2 Analysis of secondary structural composition of protein by CD

The secondary structure of VC0395_0300 and all protein mutants were analyzed by CD spectroscopy. CD spectroscopy measures the differential absorption of the left circular polarized light and the right circular polarized lights by the protein. Asymmetrical conformations of peptide bonds in the protein chain generate the differential absorption pattern for left- and right-handed circularly polarized light. The differential absorption data can be deconvoluted to the secondary structural conformation present in the protein chain.

In a typical polypeptide chain, the aromatic amino acids (absorption at 260 to 320 nm), the disulfide bonds (absorption at 260 nm) and the peptide bond (absorption at 190 to 240 nm) show absorptions in particular wavelengths, which can be used for protein secondary structure predictions. The amide in the peptide bond mainly absorbs light at the far-UV region ranging from 240 to 190 nm (absorption near 240 due to $n \rightarrow \pi^*$ transition and a stronger absorption near 190 nm due to $\pi \rightarrow \pi^*$ transition). A negative weak signal at 222 nm is generally attributed to the $n \rightarrow \pi^*$ transition characteristic of the α -helix, and the weak signal at 216 – 218 nm represents β -sheet in the spectrum. The strong positive signal near 190 nm due to $\pi \rightarrow \pi^*$ transition and a negative band at 208 shows the presence of α -helix. In CD spectroscopy, the signal for α -helix is stronger as compared to the β -sheet signal. Denatured protein or when the protein in the unfolded state shows CD signal close to zero in the region 210-220 nm for a typical peptide bond.

The CD spectra of all VC0395_0300 protein mutants showed a typical positive peak at 198 nm indicating a well folded β -sheet in the secondary structure. The presence of two negative peaks at 224 nm (due to $n \rightarrow \pi^*$ transition) and 208 nm in all protein showed occurrences of α -helix as well. CDSSTR algorithm for secondary structure prediction estimate presence of 49.2% of α -helix, 18.6% of β -sheet and remaining 31.4% as random coils in the overall secondary structure. Comparative study of all the mutated proteins with the wild-type protein revealed that a single point mutation in the active site of GGEEF domain does not significantly alter the overall secondary structure of the proteins.

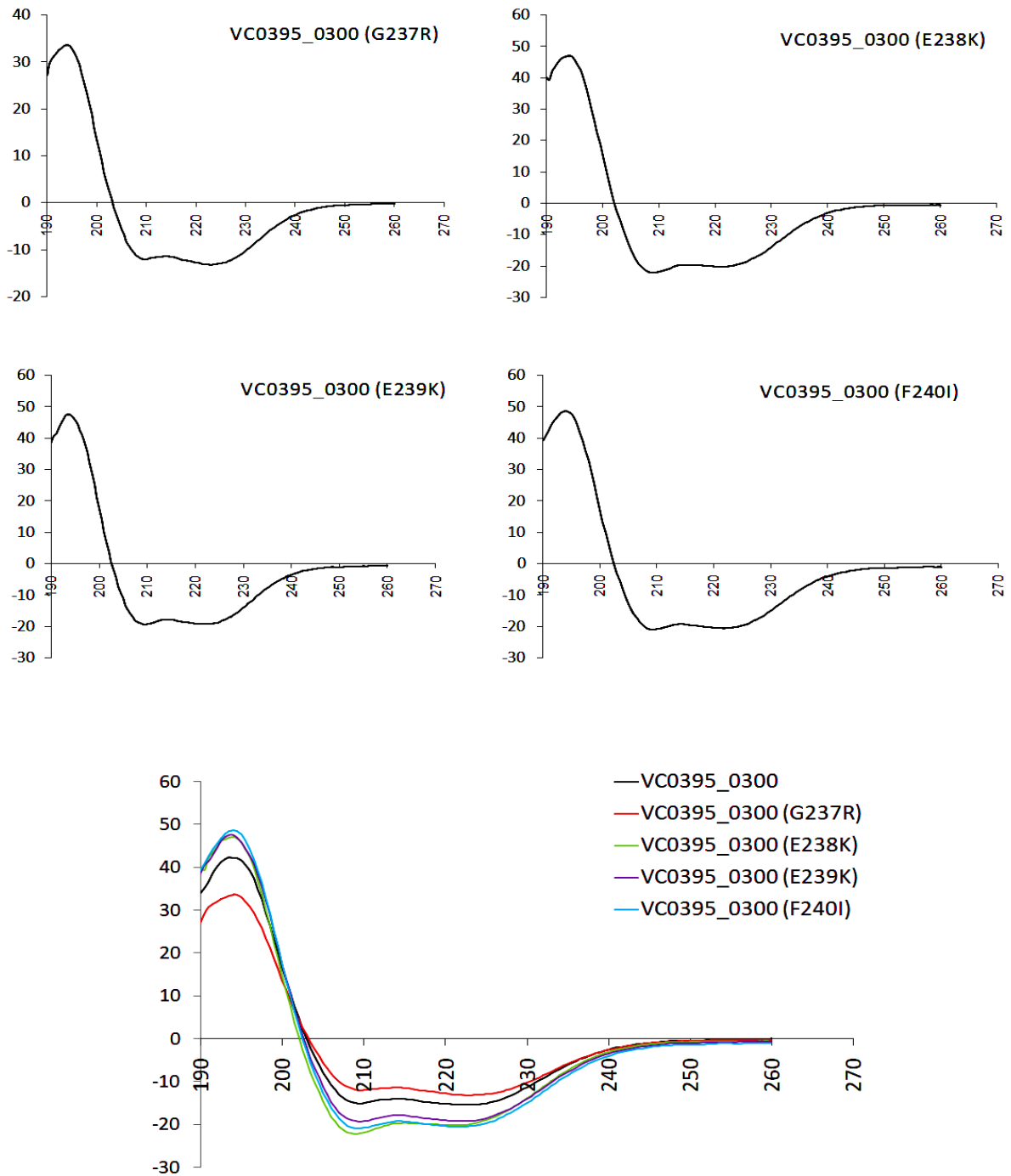


Figure 4.9: Circular dichroism spectroscopy analysis of VC0395_0300 and all protein mutants. For a comparative study, curves for all mutated proteins overlapped with wild-type protein.

4.4 Conclusions

VC0395_0300 and its mutated proteins (mutation at the active site or GGEEF signature sequence) were chosen for physicochemical characterization. For functional characterizations, all mutated strains along with wild type were analyzed for biofilm formation ability, bacterial motility and c-di-GMP formation capacity. The surface topography of biofilm was also checked by scanning electron microscopy. To analyze the effect of mutations on the protein, secondary and tertiary structural conformations of all mutated proteins and wild type were studied through fluorescence spectroscopy and CD spectroscopy. Mutations in the active site (GGEEF signature amino acids) does not alter overall protein fold (secondary structure) and 3D structure but the functional determination of activity revealed that mutations in the signature amino acids did induce alteration of biofilm formation ability and bacterial motility. From these analyses, the results can be summarized as below:

1. Digunylate cyclase activity by HPLC assay results indicate mutation in active site amino acids (replaced by other amino acid) affects product formation, but does not abolish it completely. All mutated proteins were able to produce c-di-GMP, but with a much reduced intensity of the product peak. This was indicative of a partial loss-of-function for the protein. However, the mutation in VC0395_0300 (F240I) did not have significant reduction of diguanylate cyclase activity.
2. SEM analysis for biofilms revealed that biofilm formation differed in some strains. While the wild type and the VC0395_0300 (E239K) showed considerable biofilm formation (a thick layer of extracellular polysaccharides is clearly visible), the other mutants showed reduced biofilm forming ability. VC0395_0300 (F240I) strains could not be plated in coverslips and hence, data for the same was not available.

3. The assays for quantification of biofilm formation showed that mutations in the active site significantly decreased biofilm formation in mutants, predominantly in VC0395_0300 (G237R) and VC0395_0300 (E238K).
4. For motility, TTC tube and soft agar plate assay also showed that after mutation in the central amino acids of the active site, bacteria become more motile as compared to the wild type strain.
5. Secondary and tertiary structure of VC0395_0300 protein does not alter significantly after mutation in the active site as seen from similar structure features in fluorescence spectroscopy and CD spectroscopy.
6. Thermal denaturation and GdnHCl denaturation results from fluorescence spectroscopy revealed the position of Trp residues as one partially buried, and one fully buried, but did not reveal differences in the mutants.
7. The partially buried Trp was also confirmed after quenching by neutral or negative quencher with high Stern - Volmer constant.
8. The similar fluorescence signals after mutation indicates Trp residues does not contribute to any secondary structure near the near active site and do not participate to make binding pocket for substrate molecule.

4.5 References

- Allan-Wojtas P, Hansen LT, Paulson AT.** 2008. Microstructural studies of probiotic bacteria loaded alginate microcapsules using standard electron microscopy techniques and anhydrous fixation. *LWT-Food Science and Technology*. **1**; 101–108.
- An S, Wu J, Zhang LH.** 2010. Modulation of *Pseudomonas aeruginosa* biofilm dispersal by a cyclic-di-GMP phosphodiesterase with a putative hypoxiasensing domain. *Appl Environ Microbiol*. **76**; 8160–8173.
- Ball RJ, Sellers W.** 1966. Improved motility medium. *Appl Microbiol*. **14**; 670–673.
- Basak S, Chattopadhyay K.** 2014. Studies of protein folding and dynamics using single molecule fluorescence spectroscopy. *Physical Chemistry Chemical Physics*. **16**; 11139–11149.
- Bhuyan AK.** 2002. Protein stabilization by urea and guanidine hydrochloride. *Biochemistry*. **41**; 13386–13394.
- Boyd CD, O'Toole GA.** 2012. Second messenger regulation of biofilm formation: breakthroughs in understanding c-di-GMP effector systems. *Annu Rev Cell Dev Biol*. **28**: 439–62.
- Busscher HJ, van de Belt-Gritter B, Dijkstra RJ, Norde W. van der Mei HC.** 2008. *Streptococcus mutans* and *Streptococcus intermedius* adhesion to fibronectin films are oppositely influenced by ionic strength. *Langmuir*, **24**; 10968–10973.
- Camargo PA, Pizzolitto AC, Pizzolitto EL.** (2005). Biofilm formation on catheters used after cesarean section as observed by scanning electron microscopy. *International Journal of Gynecology and Obstetrics*. **90**; 148–149.
- Camilloni C, Rocco AG, Eberini I, Gianazza E, Broglia RA, Tiana G.** 2008. Urea and guanidinium chloride denature protein L in different ways in molecular dynamics simulations. *Biophysical journal*. **94**; 4654–4661.
- Carpentier B, Cerf O.** 1993. Biofilms and their consequences, with particular reference to hygiene in the food industry. *Journal of Applied Bacteriology*. **75**; 499–511.
- Christen M, Christen B, Folcher M, Schauerte A, Jenal U.** 2005. Identification and characterization of a cyclic di-GMP-specific phosphodiesterase and its allosteric control by GTP. *Journal of Biological Chemistry*. **280**; 30829–30837.
- D'Argenio DA, Miller SI.** 2004. Cyclic di-GMP as a bacterial second messenger. *Microbiology*. **150**: 2497–2502.
- Eighmy TT, Maratea D, Bishop PL.** 1983. Electron microscopic examination of wastewater biofilm formation and structural components. *Applied and environmental microbiology*. **45**; 1921–1931.
- Ganderton L, Chawla J, Winters C, Wimpenny J, Stickler D.** 1992. Scanning electron microscopy of bacterial biofilms on indwelling bladder catheters. *European Journal Of clinical Microbiololgy Infection Diseases*, **11**; 789–796.

Ghisaidoobe AB, Chung SJ. 2014. Intrinsic tryptophan fluorescence in the detection and analysis of proteins: a focus on Förster resonance energy transfer techniques. *International journal of molecular sciences*, **15**; 22518-22538.

Greenfield NJ. 2006. Using circular dichroism spectra to estimate protein secondary structure *Nature Protocols*. **6**; 2876–2890.

Greenfield NJ. 2006. The use of circular dichroism to study the kinetics of protein folding and unfolding. *Nature Protocols* 1: 2891–2899.

Hassan AN, Frank JF, Elsoda M. 2003. Observation of bacterial exopolysaccharide in dairy products using cryo-scanning electron microscopy. *International Dairy Journal*. 9; 755–762.

Hammer BK, Bassler BL. 2003. Quorum sensing controls biofilm formation in *Vibrio cholerae*. *Mol. Microbiol.* **50**: 101–104.

Hammer BK, Bassler BL. 2009. Distinct sensory pathways in *Vibrio cholerae* El Tor and classical biotypes modulate cyclic dimeric GMP levels to control biofilm formation. *J. Bacteriol.* **91**: 169–177.

Johnson WC. 1990. Protein secondary structure and circular dichroism: a practical guide. *Proteins*. **7**; 205–214.

Karatan E, Watnick P. 2009. Signals, regulatory networks, and materials that build and break bacterial biofilms. *Microbiol. Mol. Biol. Rev.* **73**: 310–347.

Lamed R, Naimark J, Morgenstern E, Bayer EA. 1987. Scanning electron microscopic delineation of bacterial surface topology using cationized ferritin. *Journal Microbiological. Methods*. **7**; 233–240.

Lewis K. 2005. Persister cells and the riddle of biofilm survival. *Biochemistry (Moscow)*. **70**; 267-274.

Lim B, Beyhan S, Yildiz FH. 2007. Regulation of *Vibrio* polysaccharide synthesis and virulence factor production by CdgC, a GGDEF-EAL domain protein, in *Vibrio cholerae*. *J. Bacteriol.* **189**: 717–729.

Molin S. 2003. Gene transfer occurs with enhanced efficiency in biofilms and induces enhanced stabilisation of the biofilm structure. *Current Opinion in Biotechnology*. **14**; 255-261.

Nadell CD, Xavier JB, Levin SA, Foster KR. 2008. The evolution of quorum sensing in bacterial biofilms. *PLoS biology*. **6**; p.e14.

Rodrigues DF, Elimelech M. 2009. Role of type 1 fimbriae and mannose in the development of *Escherichia coli* K12 biofilm: from initial cell adhesion to biofilm formation. *Biofouling*, **25**; 401-411.

Royer CA. 2006. Probing protein folding and conformational transitions with fluorescence. *Chemical reviews*, **106**; 1769-1784.

Ryjenkov DA, Tarutina M, Moskvina OV, Gomelsky M. 2005. Cyclic diguanylate is a ubiquitous signaling molecule in bacteria: insights into biochemistry of the GGDEF protein domain. *J. Bacteriol.* **187**:1792–1798.

Ryjenkov DA, Simm R, Römling U, Gomelsky M. 2006. The PilZ domain is a receptor for the second messenger c-di-GMP. The PilZ domain protein YcgR controls motility in enterobacteria. *J. Biol. Chem.* **281**: 30310–30314.

Ruiz LM, Castro M, Barriga A, Jerez CA, Guilianani N. 2012. The extremophile *Acidithiobacillus ferrooxidans* possesses a c-di-GMP signalling pathway that could play a significant role during bioleaching of minerals. *Lett. Appl. Microbiol.* **54**; 133–139.

Ryan RP, Fouhy Y, Lucey JF, Dow JM. 2006. Cyclic di-GMP signaling in bacteria: recent advances and new puzzles. *J Bacteriol.* **188**: 8327–8334.

Tamayo R, Pratt JT, Camilli A. 2007. Roles of cyclic diguanylate in the regulation of bacterial pathogenesis. *Annu. Rev. Microbiol.* **61**: 131–148.

Tischler AD, Camilli A. 2004. Cyclic diguanylate (c-di-GMP) regulates *Vibrio cholerae* biofilm formation. *Mol. Microbiol.* **53**: 857–869.

Vyas N, Sammons RL, Addison O, Dehghani H, Walmsley AD. 2016. A quantitative method to measure biofilm removal efficiency from complex biomaterial surfaces using SEM and image analysis. *Nature Scientific Reports* **6**: 32694-32704.

Waters CM, Lu W, Rabinowitz JD, Bassler BL. 2008. Quorum sensing controls biofilm formation in *Vibrio cholerae* through modulation of cyclic di-GMP levels and repression of *vpsT*. *J. Bacteriol.* **190**: 2527–2536.

Yan H, Chen W. 2010. 3, 5'-Cyclic diguanylic acid: a small nucleotide that makes big impacts. *Chem Soc Rev.* **39**: 2914–2924.

Yu H, Tan Y, Cunningham BT. 2014. Smartphone fluorescence spectroscopy. *Analytical Chemistry.* **86**; 8805–8813.

5.1 Introduction

Biofilm formation in bacteria has generally been associated with the formation of an external polysaccharide matrix (**Colwell 2004, Sikora 2013, Hengge 2013**). Evidence gathered over the last two decades from *Yersinia pestis*, *Salmonella typhimurium*, *Pseudomonas aeruginosa* and almost all eubacterial species (**D'Argenio and Miller 2004, Simm et al 2005, Rao et al 2008, Wang et al 2010, Giardina et al 2013**) has confirmed the regulation of this exopolysaccharide to be under the control of a class of enzymes known as diguanylatecyclases. Diguanylatecyclases typically possess a GGDEF signature domain which is responsible for the synthesis of the bacterial secondary messenger, c-di-GMP from two molecules of GTP (**Yildiz and Visick 2009, Yan and Chen 2010, Massie et al 2012, Srivastava and Waters 2012, Romling et al 2013**).

There have been some reports of structures of GGDEF domain proteins (**Chan et al 2004, Lim et al 2007, Navarro et al 2009, Marmont et al 2012, Vorobiev et al 2012, Tarnawski et al 2015**) from different mesophilic and extremophilic bacteria, but there has not been a single report either of structures of GGDEF domain proteins or diguanylatecyclases from *V. cholerae* (**Bandekar et al 2017**). The putative protein VC0395_0300 from the *V. cholerae* genome is labeled as a putative GGDEF domain encoding protein. The protein has been predicted to be a diguanylatecyclase by Pfam with a high degree of certainty. The protein has been characterized as a diguanylatecyclase involved in the biofilm formation of the bacteria (**Chouhan et al 2016, Bandekar et al 2017**). VC0395_0300 possesses affinity for binding GTP and can convert it into c-di-GMP.

However, the presence of a flexible domain in the N-terminal end of the protein led to issues with its stability. As a result, the first 160 residues of the whole protein were systematically truncated to generate an active diguanylatecyclase, labeled as VC0395_0300₍₁₆₁₋₃₂₁₎. Here in this chapter, we report the bulk production, purification, crystallization and preliminary X-ray diffraction analysis of the truncated VC0395_0300 from *V. cholerae* as well as the mutant proteins.

5.2 Materials and methods

5.2.1 Protein production in bulk scale

The genomic DNA for the desired protein construct was isolated from *V. cholerae* classical strain O395 and the construct was obtained as has been explained in previous chapters. Expression of the recombinant GST-tagged protein was induced at 16 °C after addition of 0.05 mM isopropyl β -D-1-thiogalactopyranoside (IPTG) to *E. coli* BL21 (DE3) in 2x LB medium. Cells were harvested after 16 h and resuspended in lysis buffer (50 mM Tris pH7.4, 200 mM NaCl, 1 mM MgCl₂). Resuspended cells were lysed by passing through a microfluidizer (Microfluidics USA) at a pressure of 2000 psi, followed by centrifugation of the lysate. The cell-free supernatant was used for GST affinity chromatography as previously described (**Bandekar et al 2017**). Post-purification, the GST tag was cleaved by incubation with GST-tagged PreScission protease (1:300 ratio of protease to protein, 12h, 4 °C). The GST tag and PreScission protease were separated by cation exchange HiTrap SP Sepharose FF column (GE Healthcare), using 25mM MES buffer pH 6.0 with 1 mM MgCl₂. The protein was further purified by size-exclusion chromatography (Superdex 75 column (GE Healthcare)) to yield a highly purified fraction. Purified protein fractions were pooled and concentrated to 8 mg/ml and stored at -80 °C.

5.2.2 Crystallization

Protein crystallization experiments were setup by a Gryphon crystallization robot (Art Robbins Instruments, Sunnyvale, CA) in a 96-well plate using the sitting-drop vapour diffusion method. Concentrated protein solution (8 mg/ml) was mixed with an equal volume (200 nl) of mother liquor and equilibrated against the same solution in the reservoir well. Crystallization plates were incubated at 4 °C, until protein crystals grew and reached maximum size. Initially, small crystals were visible after 6 days (in 2M ammonium sulphate and 0.1M sodium acetate pH 5.0 buffer). These small crystals were further fine-screened by varying the concentration of precipitant as well as the pH of the sodium acetate buffer. After the screening, crystals were visible in 6-8 days and grew to their maximum size in 18-20 days. The best protein crystals were observed in a crystallization condition where the

precipitant was 0.5M ammonium sulphate with 0.1 M sodium acetate at pH 5.2. Prior to diffraction, crystals were soaked in 20% ethylene glycol in same reservoir solution for 3-5 seconds and stored by mounting in a cryo-loop and flash-frozen in liquid nitrogen. All crystallization data are summarized in Table 5.1.

Table 5.1. Method of crystallization set up for VC0395_0300₍₁₆₁₋₃₂₁₎ protein.

Crystallization set up	
Method	Sitting-drop
Plate type	Greiner, 96-well plate
Temperature (K)	277
Protein concentration (mg/ml)	8
Buffer composition of protein solution	50mM Tris (pH7), 150mM NaCl, and 1mM MgCl ₂
Composition of reservoir solution	0.5M (NH ₄) ₂ SO ₄ + 0.1M sodium acetate (pH 5.2)
Volume and ratio of drop	0.4 µl (1:1)
Volume of reservoir (µl)	80

5.2.3 Crystallization of mutant proteins

Mutated VC0395_0300 proteins constructs were also purified with same purification steps as wild type protein and tried for crystallization setup. Only two mutated protein constructs VC0395_0300_(G237R) and VC0395_0300_(E238K) were crystallized successfully. Mutated proteins' purified solution were concentrated up to 7-9 mg/ml and initial crystallization trials were setup using different conditions present in commercially available screens (Jena Biosciences and Qiagen). All crystallization setup were tried at two different temperatures, 4 °C and 20 °C, to incubate the protein crystal drops. The variations in crystallization drop conditions were tried (same as wild type VC0395_0300 protein and several other conditions were also used) to optimize the growth and shape of crystals.

Table 5.2. Method of crystallization set up for mutant protein constructs.

Crystallization for	VC0395_0300(G237R) ₍₁₆₁₋₃₂₁₎	VC0395_0300(E238K) ₍₁₆₁₋₃₂₁₎
Method	Sitting-drop	Sitting-drop
Plate type	Greiner, 96-well plate	Greiner, 96-well plate
Temperature (K)	277	277
Protein concentration (mg/ml)	8	8
Buffer composition of protein solution	50 mM Tris (pH7), 150 mM NaCl, and 1 mM MgCl ₂	50 mM Tris (pH7), 150 mM NaCl, and 1 mM MgCl ₂
Composition of reservoir solution	0.7M (NH ₄) ₂ SO ₄ 0.1M sodium acetate (pH 5.2)	0.5M (NH ₄) ₂ SO ₄ 0.1M sodium acetate (pH 5.4)
Volume and ratio of drop	0.4 µl (1:1)	0.4 µl (1:1)
Volume of reservoir (µl)	80	80

5.2.4 Data collection and processing

The best protein crystals were screened according to their size and used for X-ray diffraction. The crystals were kept in liquid nitrogen, and diffraction data was collected at beam line BL14.1 at the BESSY II, electron-storage ring, Berlin-Adlershof, Germany operated by the joint Berlin MX-Laboratory. Crystals were soaked in 20% ethylene glycol in same reservoir solution (cryo-protectant) for sometime before mounting. The best crystal diffracted to a resolution of 1.9 Å in a flow of continuous liquid nitrogen stream. After X-ray exposure, all images were indexed and scaled by the graphical user interface XDSAPP (Krug et al 2012, Sparta et al 2016).

5.3 Results and discussions

5.3.1 Protein productions for crystallization setup

The full-length VC0395_0300 protein in solution proved to be difficult to stabilize owing to the presence of a flexible N-terminal region (**Chouhan et al 2016**). Several protein constructs were prepared by truncation of flexible N terminal amino acid residues based on secondary structure predictions (secondary structure prediction figures has been mentioned in chapter 3 as figure 3.3). All constructs were tested for soluble protein expression and initial crystallization setups were checked in different conditions. All previously optimized conditions were used for soluble protein production. The solubility of N-terminal truncated proteins was vastly improved, as was evident from the percentage yield of the recombinant protein in the supernatant fraction (detailed results are provided in chapter 3 in section 3.3, Figure 3.8). The detailed description for purification steps for VC0395_0300 and its constructs have been shown in chapter 3 (Section 3.2).

Table 5.3. Deign of VC0395_0300 protein constructs and trial for crystallization.

S. No.	Construct Name	Molecular Weight (KDa)	Domain construct	Soluble Protein Expression	DGC Activity assay	Protein Crystallization
1	VC0395_0300	37	PAS, PAC GGEEF	Yes	Yes	No
2	VC0395_0300 ₍₁₀₂₋₃₂₁₎	26	PAC GGEEF	Yes	Yes	No
3	VC0395_0300 ₍₁₆₁₋₃₂₁₎	18	GGEEF	Yes	Yes	Yes
4	VC0395_0300 ₍₁₈₇₋₃₂₁₎	16	GGEEF	No	No	No

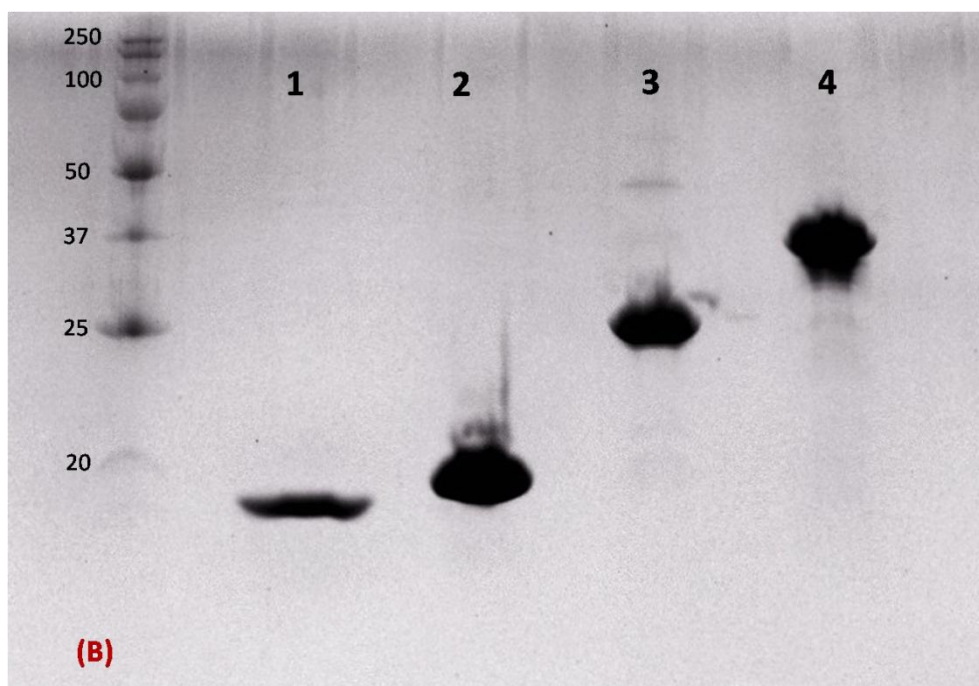
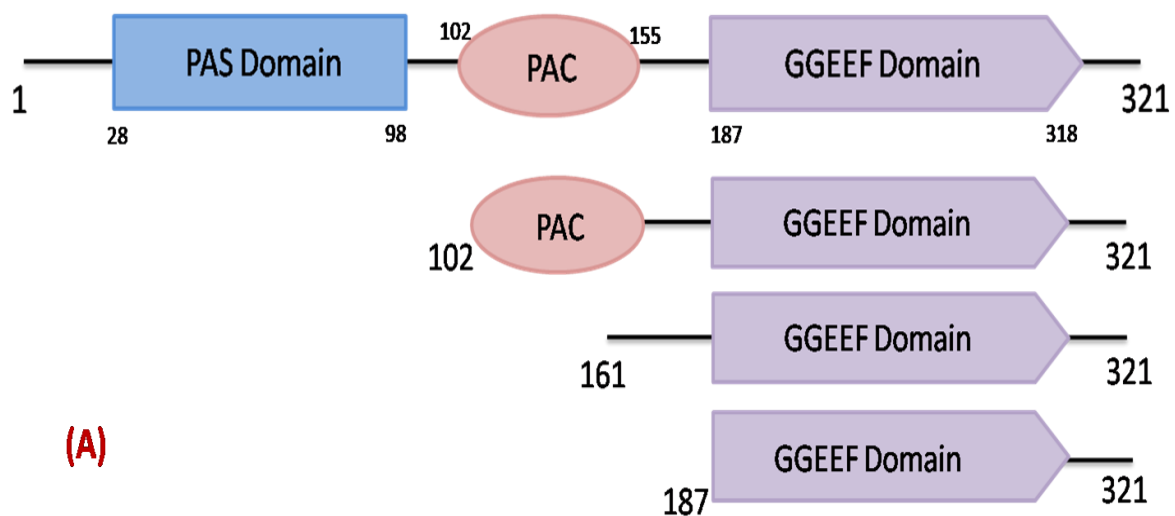


Figure 5.1: Various protein constructs used for protein crystallization experiments. (A) All proteins with truncations of N terminal amino acids. (B) Finally purified proteins sample after size exclusion chromatography on 15% SDS – PAGE. 1. VC0395_0300₍₁₈₇₋₃₂₁₎ ; 2. VC0395_0300₍₁₆₁₋₃₂₁₎ ; 3. VC0395_0300₍₁₀₂₋₃₂₁₎ ; 4. VC0395_0300₍₁₋₃₂₁₎.

All purified protein solutions were concentrated and initial crystallization trials were setup using 768 different conditions present in commercially available screens as Qiagen (Classic suite, ComPAS suite, pH clear suite I, pH clear suite II, PACT suite) and Jena Biosciences (Bascis HTS, PEG salt I and PEG/salt HTS). Two different temperatures, 4 °C and 20 °C, were used to incubate the protein crystallizations drops. The variations in drop conditions were with respect to divalent ions, PEG, and different other precipitants (all chemical compositions of crystallization screens are given in appendix,). Initial hits were however obtained for VC0395_0300₍₁₆₁₋₃₂₁₎ protein at 4 °C in presence of salts such as lithium chloride, sodium chloride and ammonium sulphate at different pH buffer solutions (Figure 5.2). VC0395_0300 full length protein and other construct were not shown any positive results for crystallizations. Further optimization of initial crystallizations conditions for the VC0395_0300₍₁₆₁₋₃₂₁₎ protein through fine screens (Ammonium sulfate 0.5 to 2.0 M, and sodium acetate buffer pH 4 to 6) led to the best crystal being obtained in 0.5 M (NH₄)₂SO₄ and 0.1 M sodium acetate pH 5.2.

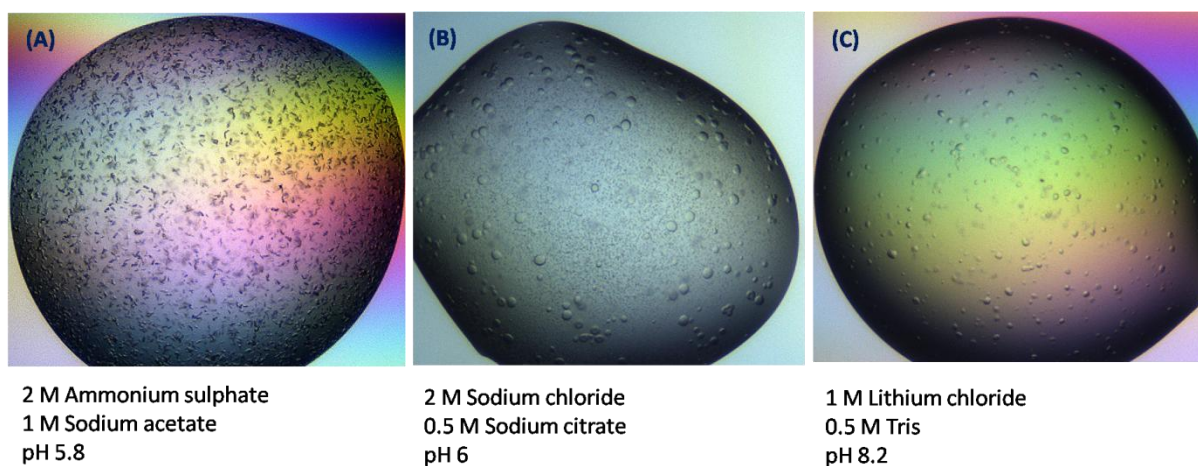
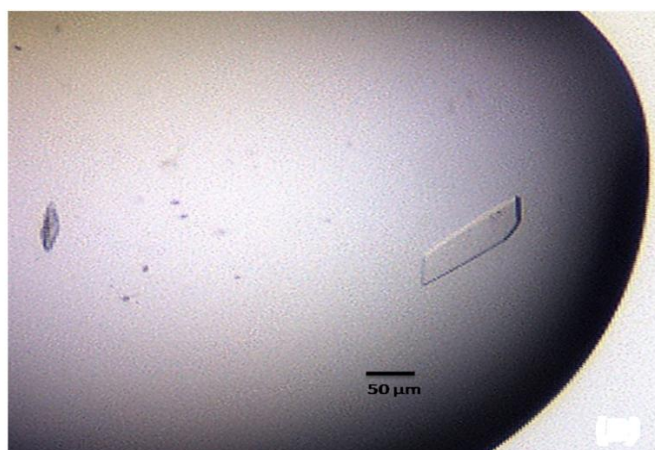


Figure 5.2: Crystallization drop pictures showing initial positive crystals formation in various conditions in primary screening. (A) Small sized protein crystal in presence of Ammonium sulphate salt and sodium acetate buffer. (B) Spheroids-like protein structure in presence of sodium chloride and sodium acetate buffer (C) protein nucleation in drop in presence of lithium chloride and tris buffer.



0.5 M $(\text{NH}_4)_2\text{SO}_4$
0.1 M sodium acetate
pH 5.2

Figure 5.3: Best protein crystal for VC0395_0300₍₁₆₁₋₃₂₁₎ protein after fine screen and all conditions optimized.

5.3.2 Structure of VC0395_0300₍₁₆₁₋₃₂₁₎

The best protein crystal of VC0395_0300₍₁₆₁₋₃₂₁₎ protein after optimizations of all crystallization conditions was collected with Hampton crystallization loop in a suitable cryoprotectant, which was diffracted to the best resolution of 1.9 Å at BESSY, Berlin. The crystal was found to belong to the $P2_1(4)$ space group, with unit cell parameters $a = 65.90 \text{ Å}$, $b = 80.27 \text{ Å}$, $c = 71.70 \text{ Å}$, $\beta = 97.59$. The asymmetric unit contained four protein molecules. Molecular replacement, phasing, model building and structure refinement was performed with Phenix, (**Adams et al 2012**). This was combined with manual structure building in Coot (**Emsley and Cowtan 2004, Emsley et al 2010**) and the final structure of the VC0395_0300₍₁₆₁₋₃₂₁₎ has been determined by CCP4 (**Winn et al 2011**). Crystallographic and refinement statistics are summarized in Table 5.4.

The electron density from the diffraction was interpretable for 160 amino acid residues out of the total 161. In the crystal structure, four protein chains were present in one asymmetric unit (ASU) of the lattice. The VC0395_0300₍₁₆₁₋₃₂₁₎ structure assumes the typical domain architecture as has been displayed in other GGDEF domain homologues from other bacteria. The GGDEF domain in VC0395_0300₍₁₆₁₋₃₂₁₎ contains seven β strands in which four (β_6 - β_1 - β_3 - β_2) are centrally located in an antiparallel manner, surrounded by six α helices. The remaining three β strands (β_4 , β_5 and β_7) are located in the periphery. The topology

displayed in other GGDEF domain proteins shows a similar arrangement of sheet and helices in their active sites, *viz.*, α 1- α 2- β 1- α 3- α 4 - β 2- β 3- α 5- β 4- β 5- β 6- α 6- β 7. This signature secondary structural motif (constituting the Active site or A-site), reported to bind GTP in all other GGDEF domain proteins is also conserved in VC0395_0300₍₁₆₁₋₃₂₁₎.

The structure of the GGEEF domain of VC0395_0300₍₁₆₁₋₃₂₁₎ showed topological similarity with respect to PleD, WspR and A1U3W3. Superimposition of VC0395_0300₍₁₆₁₋₃₂₁₎ with the three previous structures showed the similarity in their folds (rmsd from PleD being 1.56 over 154 residues, rmsd of 1.45 over 156 residues for WspR, and rmsd of 1.3 for A1U3W3 over 154 residues). This is in conjunction with our hypothesis that this protein has DGC activity which leads to binding GTP and form c-di-GMP as a product. The signature GGEEF (amino acids 236 to 240) sequence in VC0395_0300₍₁₆₁₋₃₂₁₎ is present as an extended loop located on the outer turn placed between the β 2 and β 3 strands. Electrostatic surface potential also revealed that the active site of the conserved motif is located in a positively charged pocket of the VC0395_0300₍₁₆₁₋₃₂₁₎ protein. Similar positively charged pockets also exist for PleD and WspR which serve as GTP binding site. Several amino acids residue which are conserved in diguanylatecyclases and important for GTP/Mg²⁺ binding are also present in this charged pocket.

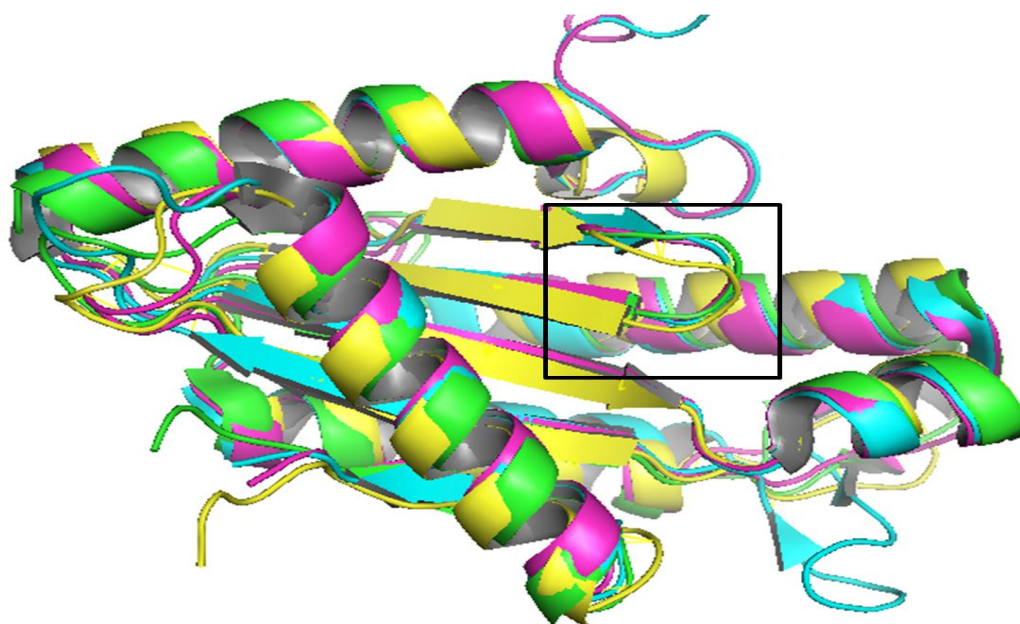


Figure 5.4. VC0395_0300₍₁₆₁₋₃₂₁₎ protein structure alignment with PleD, WspR and 3IGN. Alignment of conserved signature GGEEF motif or A-site are shown in box. This image was generated by PyMol alignment tool, rmsd value are mentioned in text.

Table 5.4. X-ray diffraction Crystallographic data and Refinement Statistics. Inner shell statistics are given in brackets, overall statistics are Unbracketed.

Data collection and processing	
Diffraction source	14.1 Beamline BESSY (Berlin)
Wavelength (Å)	0.91841
Temperature (K)	100 K
Detector	PILATUS 6M
Crystal-to-detector distance (mm)	239.07
Rotation range per image (°)	0.3
Total rotation range (°)	120
Exposure time per image (s)	2
Space group	P 1 21 1
<i>a, b, c</i> (Å)	65.90, 80.27, 71.70
α, β, γ (°)	90.00, 97.59, 90.00
Mosaicity (°)	0.135
Resolution range (Å)	43.41-1.94 (2.06-1.94)
Total no. of reflections	123623
Completeness (%)	96.3 (95.9)
Multiplicity	2.34
$I/\sigma(I)$	7.82 (1.26)
R_{meas} (%)	12.2 (98.2)
Overall <i>B</i> factor from Wilson plot (Å ²)	32.69

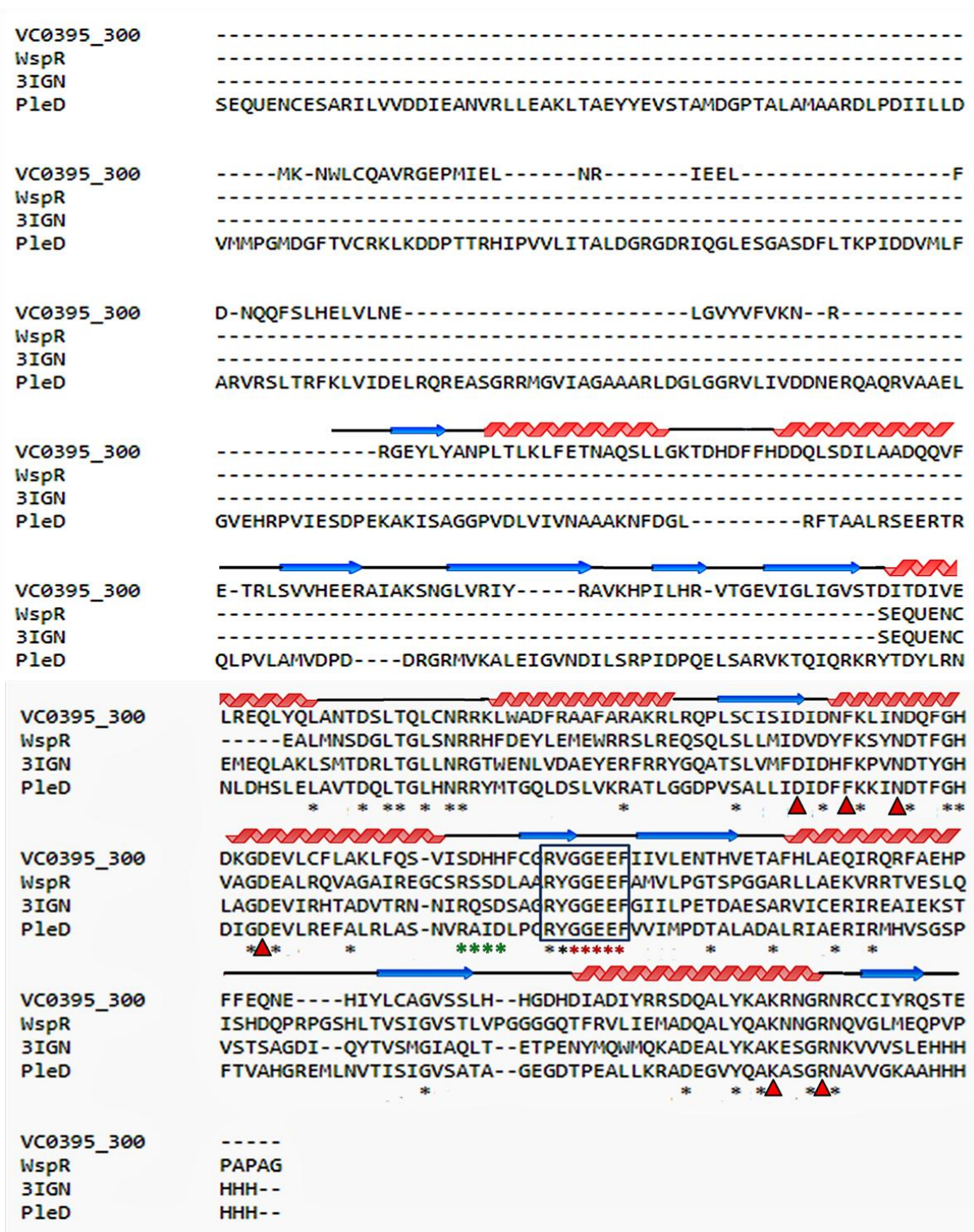


Figure 5.5. (A) VC0395_0300 protein sequence alignment with DGC protein in PleD from *Caulobacter crescentus*, 3IGN from *Marinobacter aquaeolei* and WspR from *Pseudomonas aeruginosa* by ClustalW. In box residues are conserved signature GGEEF motif. * showing for conserved residues in all four protein. The primary inhibitory site are shown by * sign (absent in VC0395_0300 protein). ▲ Showing conserved amino acids residues which are reported for involving in substrate GTP and Mg²⁺ binding. The secondary structure found in crystal structure of VC0395_0300₍₁₆₁₋₃₂₁₎ which are shown above the sequence alignment.

The crystal structure of VC0395_0300₍₁₆₁₋₃₂₁₎ apparently displays the presence of a tetramer, but the inter subunit distances reveals more of monomers. The thing to note here was the presence of VC0395_0300₍₁₆₁₋₃₂₁₎ mostly as a monomer in the other experiments performed till now. However the previously solved crystal structures (**Navarro et al 2009, Marmont et al 2012, Vorobiev et 2012**) envisage that the active site of the diguanylate cyclase is generally formed by the coming together of two monomers in a reverse orientation. This is because the active site of one monomer can conventionally bind one molecule of GTP, while two such active sites would be needed to bring together two molecules of GTP needed for the synthesis of c-di-GMP.

From the crystal structure, four VC0395_0300₍₁₆₁₋₃₂₁₎ molecules are found in the asymmetric unit. Two local dimers are seen to be formed by a crystallographic two-fold rotation axis along the $\alpha 4$ helix of both the monomers. The dimeric interface is found between chains B, C and chains A, D of the tetramer with an interface area of 1038 Å² and 972 Å², respectively (**Figure 5.6B**). The resulting interface corresponds to about 11% of the total accessible solvent area of a single monomer which ranges between 8700-9000 Å². Based on the determined size of the interface by the PISA server, it could be assumed that a relevant GGDEF dimer is formed, but the PISA server itself classifies this interface as not significant.

An interesting observation from the structure of the VC0395_0300₍₁₆₁₋₃₂₁₎ protein is the absence of a primary I site (RXXD), which is generally associated with the binding to the product of GTP cyclization, the c-di-GMP. In PleD or WspR, the I site is generally located five amino acids upstream from the active site (**Yang et al 2011, Vorobiev et al 2012, Robert-Paganin et al 2012**), where it allosterically inhibits further binding of GTP to the active site. The absence of an I site points to a different mechanism of c-di-GMP binding and release in this GGDEF domain protein from *V. cholerae*.

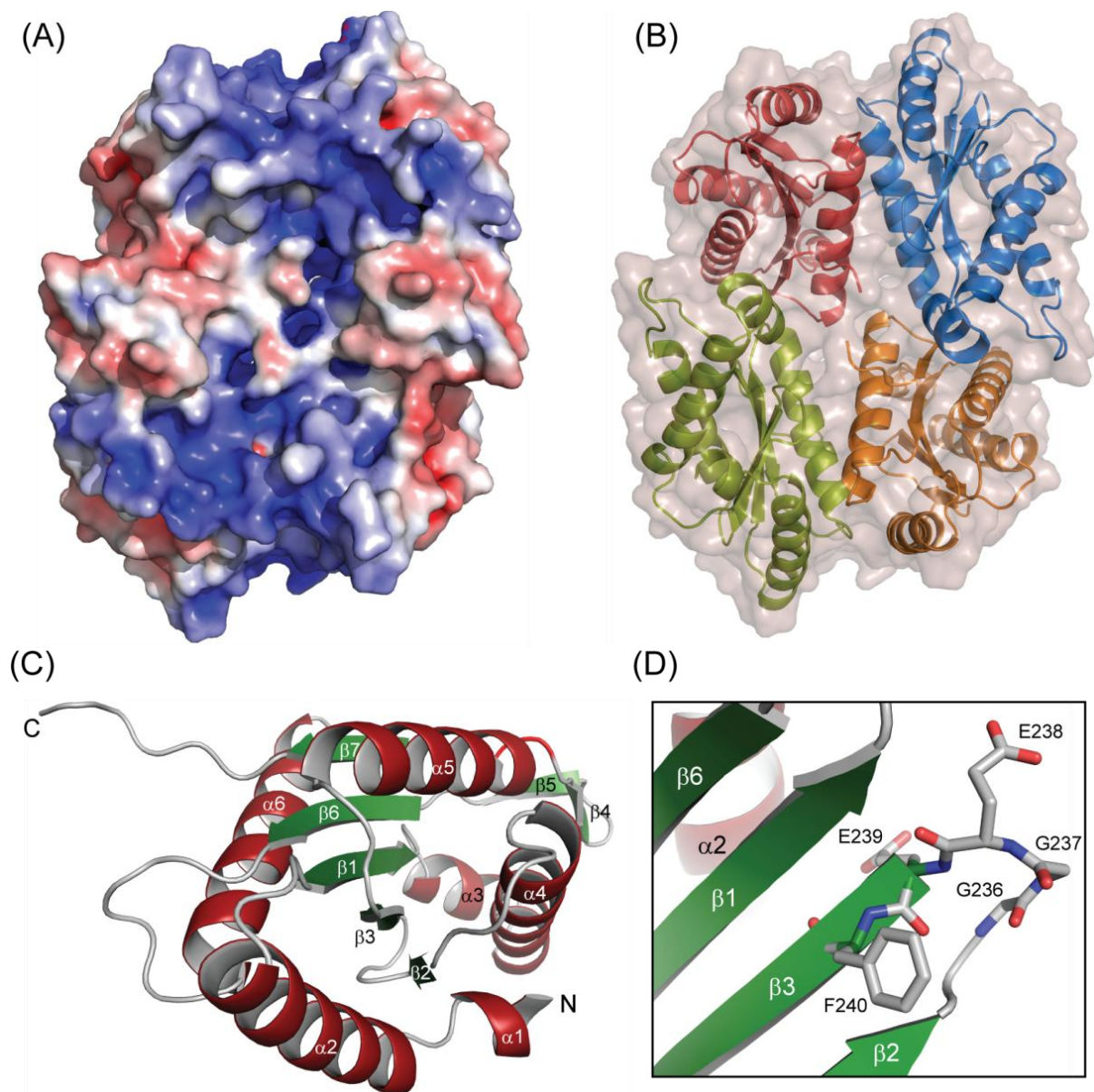


Figure 5.6. (A) Electrostatic surfacepotential on VC0395_0300₍₁₆₁₋₃₂₁₎ protein. Red colour and blue colour representing negative and positive respectively with ± 5 kT potentials at an ionic strength of 0.2 M. (B) Representation of single asymmetric unit cell for VC0395_0300₍₁₆₁₋₃₂₁₎. (C) The complete crystal structure of VC0395_0300₍₁₆₁₋₃₂₁₎ protein. The β -sheets are representing in green coloured, the α -helices are in red coloured, and the loops are gray coloured. (D) Representation of signature GGEEF residues for A-site.

5.3.3 Structure of mutants of VC0395_0300

Initial positive hits were obtained for both the proteins VC0395_0300_(G237R) and VC0395_0300_(E238K) at 4 °C in similar conditions as wild type protein (In presence of lithium chloride, sodium chloride and an ammonium sulphate salt at different pH buffer solutions). Further optimization by fine screens of initial crystallizations conditions for both the mutated protein led to the best crystal which was obtained in 0.7 M (NH₄)₂SO₄ and 0.1 M sodium acetate pH 5.2 for VC0395_0300_(G237R) and 0.5 M (NH₄)₂SO₄ and 0.1 M sodium acetate pH 5.4 for VC0395_0300_(E238K).

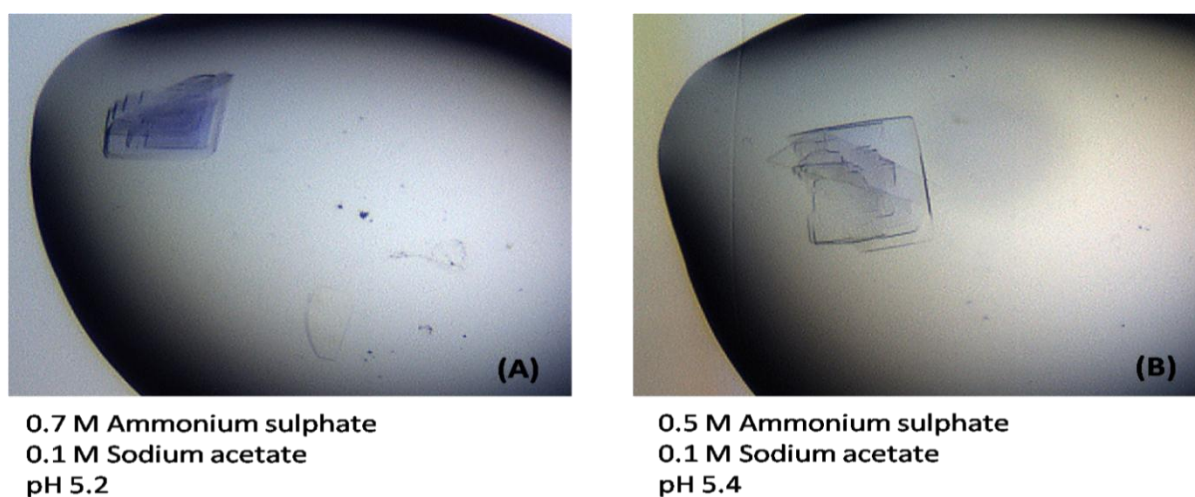


Figure 5.7. Best protein crystal after all conditions optimized for (A) Protein constructs VC0395_0300_(G237R) (B) Protein constructs VC0395_0300_(E238K).

The best protein crystal of VC0395_0300_(G237R) and VC0395_0300_(E238K) were collected with Hampton crystallization loops in a suitable cryoprotectant (20% ethylene glycol in same reservoir solution), and carried to synchrotron at BESSY, Berlin. Both the proteins crystals were diffracted at 1.7 Å and showed same space group {P2₁(4)} as wild type. All crystallographic statistics are summarized in Table 5.5. One asymmetric unit restricted four polypeptide chains in it as in wild type protein. Molecular replacement, phasing, model building and structure refinement were performed as for wild type protein with Phenix, (Adams et al 2012) and proteins structure were build in Coot (Emsley and Cowtan 2004, Emsley et al 2010).

Table 5.5. X-ray diffraction Crystallographic data and Refinement Statistics for mutant proteins. Inner shell statistics are given in brackets, overall statistics are Unbracketed.

Protein Name	VC0395_0300 (G237R)	VC0395_0300 (E238K)
Diffraction source	14.1 Beamline BESSY (Berlin)	
Wavelength (Å)	0.91841	0.91841
Temperature (K)	100 K	100 K
Detector	PILATUS 6M	PILATUS 6M
Crystal-to-detector distance (mm)	239.07	239.07
Rotation range per image (°)	0.3	0.3
Total rotation range (°)	120	120
Exposure time per image (s)	2	2
Space group	P 1 21 1	P 1 21 1
<i>a, b, c</i> (Å)	66.13 80.22 71.85	65.50 80.04 72.30
<i>α, β, γ</i> (°)	90.0 97.8 90.0	90.0 97.57 90.0
Mosaicity (°)	0.086	0.117
Resolution range (Å)	45.25-1.73 (1.83-1.73)	45.24-1.7 (1.80-1.70)
Total no. of reflections	276188	297016
Completeness (%)	99.0 (97.9)	98.7 (97.6)
Multiplicity	3.59	3.68
<i>I</i> / <i>σ</i> (<i>I</i>)	10.13 (1.13)	10.83 (1.08)
<i>R</i> _{meas} (%)	10.0 (130.6)	9.0 (140.1)
Overall <i>B</i> factor from Wilson plot (Å ²)	26.07	24.21

The electron density from the diffraction data was interpretable for 160 and 161 amino acids for VC0395_0300_(G237R) and VC0395_0300_(E238K) respectively. The GGEEF domain of the resultant structures had similar architecture as the wild type protein. For both the mutant proteins, it starts with a short helix α 1 and contains a central five stranded β -sheet, with strand β 1 to β 3 and β 6 running in antiparallel fashion, surrounded by helices α 1 to α 5. The remaining two β strands (β 4 and β 5) are located in the outer region. The A site for VC0395_0300_(G237R) protein expectedly showed the presence of a mutation at the 237th amino acid where instead of glycine, arginine was present, as incorporated by the site-directed mutation. The flexible long side chain of arginine imparts a difference in the two structures (compared to wild type). The comparison of the molecular surfaces of the two proteins reveals the presence of a shoulder-like hump in the mutant. The resolved structure also displays 0.5 occupancy with respect to the arginine side chain, due to the inherent flexibility in the amino acid.

In the VC0395_0300_(E238K) protein, the A site shows the presence of a lysine in the 238th position which was earlier a glutamate. Similar to the other mutant, this mutant also shows a probable steric hindrance in the active site for the entry of the GTP molecule. This is caused due to the extension of the side chain of the lysine from the A site, which creates a shoulder-like obstacle, otherwise absent in the wild type.

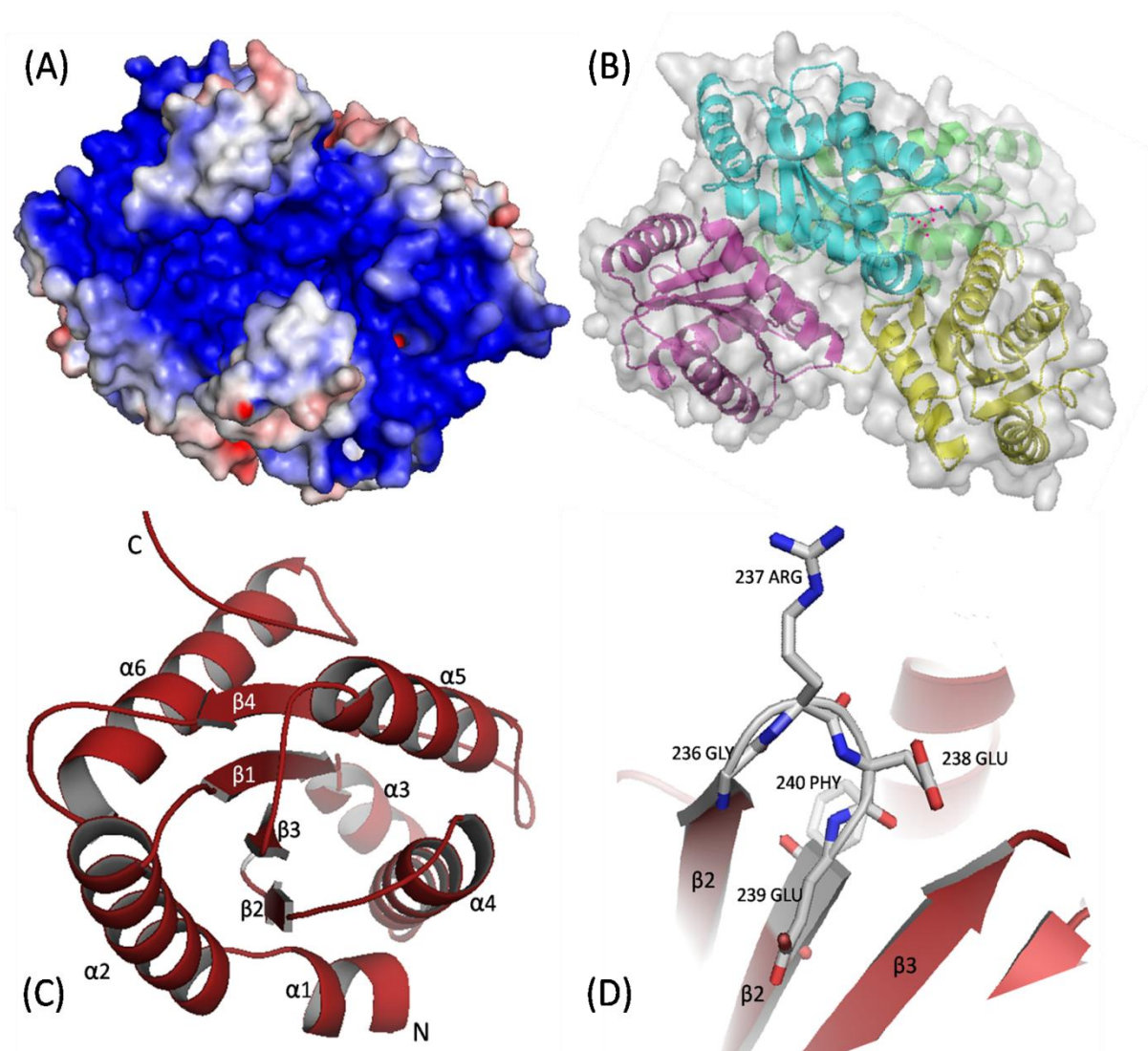


Figure 5.8. Crystal structure for protein constructs of VC0395_0300_(G237R) protein (A) Electrostatic surface potential. Red colour and blue colour representing negative and positive respectively with \pm kT potentials at an ionic strength of 0.2 M. (B) Representation of single asymmetric unit cell for VC0395_0300_(G237R). (C) The complete crystal structure of VC0395_0300_(G237R) protein. The centrally located β -sheets are surrounded by the α -helices. (D) Representation of signature GGEEF residues for A-site where 237th amino acid Glycine is replaced by Arginine.

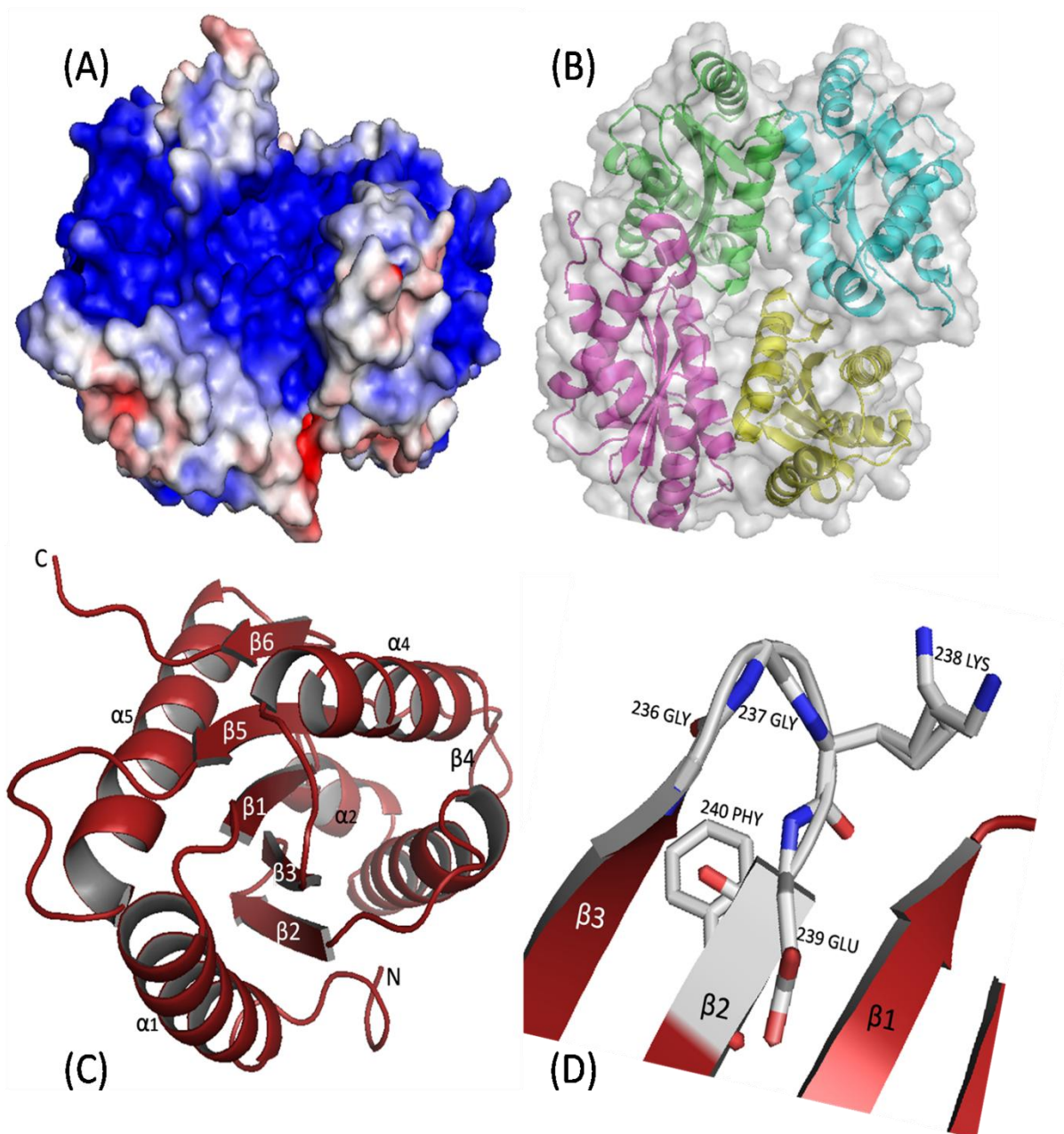


Figure 5.9. Crystal structure for protein constructs of VC0395_0300_(E238K) protein (A) Electrostatic surfacepotential. Red colour and blue colour representing negative and positive respectively with $\pm kT$ potentials at an ionic strength of 0.2 M. (B) Representation of single asymmetric unit cell for VC0395_0300_(E237K). (C) The complete crystal structure of VC0395_0300_(E237K) protein. The centrally located β -sheets are surrounded by the α -helices. (D) Representation of signature GGEEF residues for A-site where 238th amino acid Glutamate is replaced by Lysine.

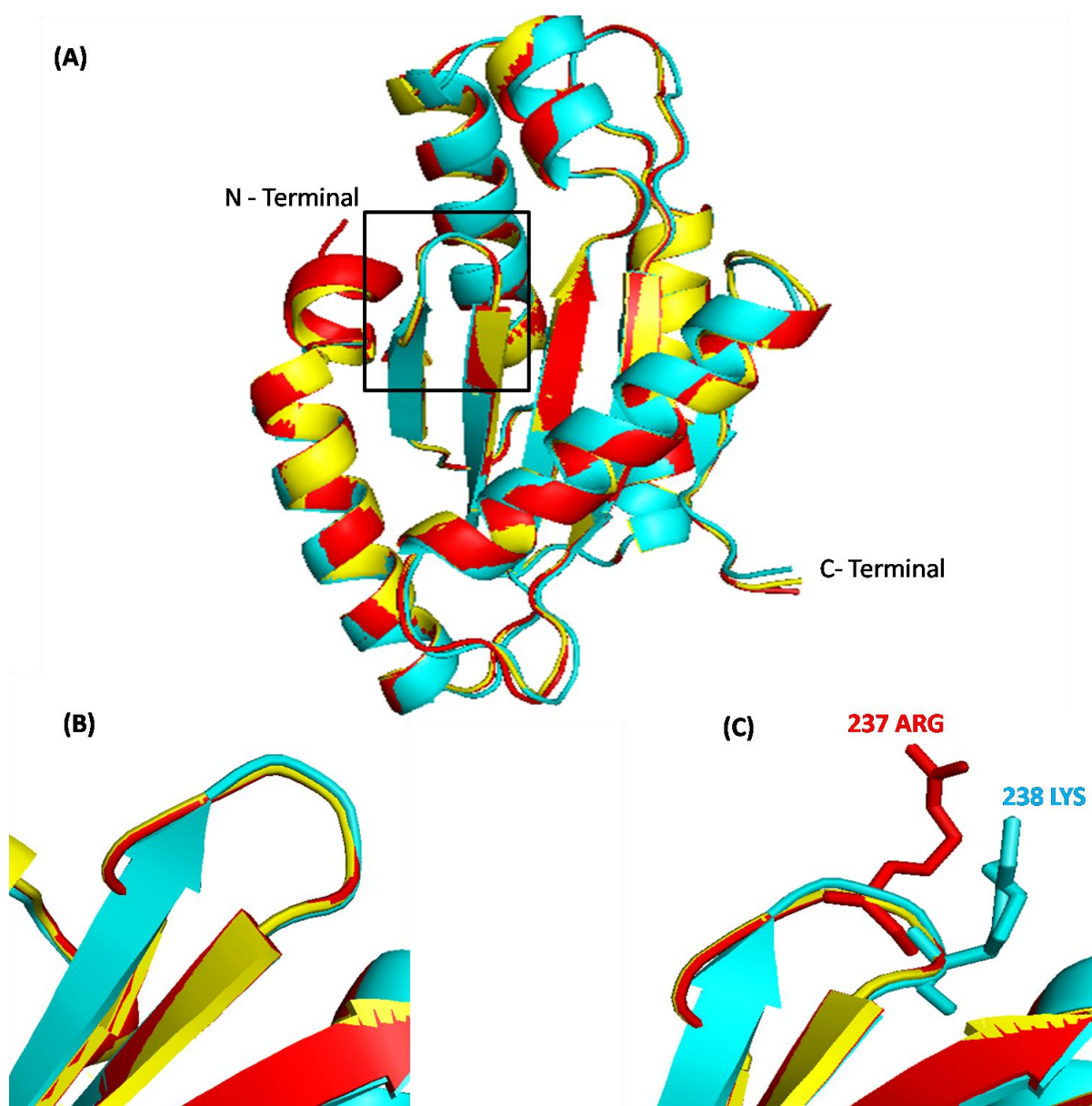


Figure 5.10. Alignment of mutant protein constructs with wild type VC0395_0300₍₁₆₁₋₃₂₁₎ protein. (A) Complete GGEEF domain alignment. (B) Alignment of conserved signature GGEEF motif or A-site. (C) Mutation site of VC0395_0300_(G237R) and VC0395_0300_(E238K) protein constructs align with VC0395_0300₍₁₆₁₋₃₂₁₎ wild type protein. Here Yellow coloured for VC0395_0300₍₁₆₁₋₃₂₁₎, Red coloured chain is VC0395_0300_(G237R) and Blue coloured chain is VC0395_0300_(E238K).

The overall structures of the GGEEF domain of both the mutant proteins construct (VC0395_0300_(G237R) and VC0395_0300_(E238K)) have topological similarity with wild type protein construct VC0395_0300₍₁₆₁₋₃₂₁₎. Superimposition of wild type protein VC0395_0300₍₁₆₁₋₃₂₁₎ with the mutated constructs showed higher similarity in their topological folds (rmsd value 1.36 from VC0395_0300_(G237R), and rmsd 1.34 for VC0395_0300_(E238K) over 160 residues), highlighting the conservation of the GGEEF fold in these structures. However, the effects of the mutations result in the deviation from the normal functions of the protein. The postulated path-of-entry of the GTP molecule is understandably free in the wild type protein due to the lack of bulky amino acids in the flexible loop of the GGEEF motif. The action is offset in the mutants due to the presence of a bulky side chain of either the arginine or the lysine, thereby blocking the entry of the GTP. This prevents the docking of the GTP on the modeled site of contact, and even inhibits the coordination with the magnesium, resulting in loss-of-function in the mutants.

5.4 Conclusions

The VC0395_0300 is an active diguanylate cyclase from *V. cholerae* which has been shown to play an important role in biofilm formation by the bacteria (**Bandekar et al 2017, Chouhan et al 2016**). While the C-terminal region of the protein houses the GGEEF domain, additional sensory domains like the PAS and PAC have been predicted in the N-terminal region as well (Figure 5.1). The full-length protein posed problems with its solubility and had an inherent propensity to form aggregates. This was attributed to the presence of a flexible region in the N-terminal end, as suggested from partial proteolysis and mass spectrometry methods. Attempts to generate truncates of the full-length protein were thus concentrated on shortening of the N-terminal part. The truncate with the best solubility and activity, VC0395_0300₍₁₆₁₋₃₂₁₎, was subsequently chosen for further structure determination studies.

The truncate was demonstrably similar in activity to the full-length protein and had comparable biofilm formation abilities. The utilization of Congo Red for the formation of biofilm was also indicative of the production of cellulosic components by the bacteria, for the extracellular matrix of the biofilm. Congo Red is known to bind β -glucans in cellulose, and the diminishing amount of residual Congo Red was suggestive of the formation of cellulose in the medium (**Romling et al 2013, Cowles et al 2016**). Diguanylate cyclase activity of the truncated protein and other assays (like the swarming motility assay) also ratified the presence of functional activity in the truncated protein. However, there was a distinct loss-of-activity for the mutated proteins.

The basic GGEEF domain architecture is omnipresent in all the three structures that we have solved. However, what really differs is the topology of the GTP binding site. If our previous modeled data (**Bandekar et al 2017, Chouhan et al 2016**) with respect to establishing contact with GTP and coordination of the Magnesium ion is true, the variation in the local environment because of the bulky side chains of VC0395_0300_(G237R) and VC0395_0300_(E238K) leaves huge pointers to the loss-of-activity in the mutants. As verified by the functional data presented in the previous chapters, it can be safely postulated that the bulky side chain of the arginine and lysine prevent the entry of the GTP molecule and do not allow for the binding to the active site, even when the divalent cation is present. This in turn,

disrupts the diguanylate cyclase activity in the mutants, even though the basic GGEEF motif is not hampered. All results for this chapter are summarized here:

1. The full-length VC0395_0300 protein proved unable to crystallize and have difficult to stabilize in solution due to the presence of a flexible N-terminal region.
2. Protein construct VC0395_0300₍₁₆₁₋₃₂₁₎ successfully crystallized after fine screen in presence of 0.5 M ammonium sulphate, 0.1 M sodium acetate at pH 5.2.
3. Best protein crystal of VC0395_0300₍₁₆₁₋₃₂₁₎ protein diffracted at 1.9 Å and belong to P 1 21 1 space group with four polypeptide chain in one asymmetric unit (which can be assume as four independent monomers as well).
4. A hypothetical dimeric interface is found between chains B, C and chains A, D with an interface area of 1038 Å² and 972Å², respectively but the dimeric contacts seem insignificant.
5. The structure of the GGEEF domain in VC0395_0300₍₁₆₁₋₃₂₁₎ showed similar architecture of (sheet and helices in their active sites, viz., α1- α2- β1- α3- α4 - β2- β3- α5- β4- β5- β6- α6- β7) as previously reported PleD, WspR and A1U3W3 protein.
6. The signature GGEEF amino acids for VC0395_0300₍₁₆₁₋₃₂₁₎ protein were present at 236 to 240 positioned in sequence as an extended loop located on the outer turn placed between the β2 and β3 strands.
7. Electrostatic surface potential showed that the A site of the GGEEF domain is located in a positively charged pocket of the VC0395_0300₍₁₆₁₋₃₂₁₎ protein, serve as a binding site for negatively charged GTP molecule.
8. Two mutants proteins VC0395_0300_(G237R) and VC0395_0300_(E238K) were diffracted at 1.73 and 1.7 Å respectively.
9. Both the mutant proteins have topological similarity with wild type protein construct VC0395_0300₍₁₆₁₋₃₂₁₎ with rmsd value 1.36 and rmsd 1.34 respectively for VC0395_0300_(G237R) and VC0395_0300_(E238K).
10. Both the mutant proteins show a steric obstruction due to the extension of the extra side chain in the active site for binding substrate GTP molecule which causes partial loss of functions.

5.5 References

- Adams PD, Afonine PV, Bunkoczi G, Chen VB, Davis IW, Echols N, Headd JJ, Hung LW, Kapral GJ, Grosse-Kunstleve RW et al.** 2010. PHENIX: a comprehensive Python-based system for macromolecular structure solution. *Acta Cryst D* **66**: 213-221.
- Afonine PV, Grosse-Kunstleve RW, Echols N, Headd JJ, Moriarty NW, Mustyakimov M, Terwilliger TC, Urzhumtsev A, Zwart PH, Adams PD.** 2012. Towards automated crystallographic structure refinement with phenix.refine. *Acta Crystallogr. Sect. D Biol. Crystallogr.* **68**: 352-367.
- Bandekar D, Chouhan OP, Mohapatra S, Hazra M, Hazra S., Biswas S.** 2017. Putative protein VC0395_0300 from *Vibrio cholerae* is a diguanylate cyclase with a role in biofilm formation. *Microbiol. Res.* **202**: 61-70.
- Beyhan S, Bilecen K, Salama SR, Casper-Lindley C., Yildiz FH.** 2007. Regulation of rugosity and biofilm formation in *Vibrio cholerae*: Comparison of VpsT and VpsR regulons and epistasis analysis of vpsT, vpsR, and hapR. *J. Bacteriol.* **189**: 388-402.
- Beyhan S, Odell LS, Yildiz FH.** 2008. Identification and characterization of cyclic diguanylate signaling systems controlling rugosity in *Vibrio cholerae*. *J. Bacteriol.* **190**: 7392-7405.
- Boyd CD, O'Toole G.** 2012. Second Messenger Regulation of Biofilm Formation: Breakthroughs in Understanding c-di-GMP Effector Systems. *Annu. Rev. Cell Dev. Biol.* **28**: 439-462.
- Castiglione N, Stelitano V, Rinaldo S, Giardina G, Caruso M, Cutruzzolà F.** 2011. Metabolism of cyclic-di-GMP in bacterial biofilms: From a general overview to biotechnological applications. *Indian J. Biotechnol.* **10**: 423-431.
- Chan C, Paul R, Samoray D, Amiot NC, Giese B, Jenal U., Schirmer T.** 2004. Structural basis of activity and allosteric control of diguanylate cyclase. *Proc. Natl. Acad. Sci. U. S. A.* **101**: 17084-17089.
- Chouhan OP, Bandekar D, Hazra M, Baghudana A, Hazra S, Biswas S.** 2016. Effect of site-directed mutagenesis at the GGEEF domain of the biofilm forming GGEEF protein from *Vibrio cholerae*. *AMB Express* **6**: 2.
- Colwell RR.** 2004. Infectious disease and environmental cholera as a paradigm for waterborne disease. *Int. Microbiol.* **7**: 285-289.
- D'Argenio D., Miller SI.** 2004. Cyclic di-GMP as a bacterial second messenger. *Microbiology* **150**: 2497-2502.
- Emsley P, Cowtan K.** 2004 Coot: Model-building tools for molecular graphics. *Acta Crystallogr. Sect. D Biol. Crystallogr.* **60**: 2126-2132.
- Emsley P, Lohkamp B, Scott WG, Cowtan K.** 2010. Features and development of Coot. *Acta Crystallogr. Sect. D Biol. Crystallogr.* **66**: 486-501.

Escobar LE, Ryan SJ, Stewart-Ibarra AM, Finkelstein JL, King CA, Qiao H & Polhemus ME. 2015. A global map of suitability for coastal *Vibrio cholerae* under current and future climate conditions. *Acta Trop.* **149**: 202–211.

Gao R, Stock AM. 2009. Catalytically Incompetent by Design. *Structure* **17**: 1038–1040.

Giardina G, Paiardini A, Fernicola S, Franceschini S, Rinaldo S, Stelitano V & Cutruzzolà F. 2013. Investigating the allosteric regulation of YfiN from *Pseudomonas aeruginosa*: Clues from the structure of the catalytic domain. *PLoS One* **8**: 1–15.

Ghose AC. 2011. Lessons from cholera & *Vibrio cholerae*. *Indian J. Med. Res.* **133**: 164–70.

Hammer BK, Bassler BL. 2009. Distinct sensory pathways in *Vibrio cholerae* El Tor and classical biotypes modulate cyclic dimeric GMP levels to control biofilm formation. *J. Bacteriol.* **91**: 169–177.

Hengge R. 2013. Novel tricks played by the second messenger c-di-GMP in bacterial biofilm formation. *EMBO J.* **32**: 322–3.

Hengge R. 2016. Trigger phosphodiesterases as a novel class of c-di-GMP effector proteins. *Philos. Trans. R. Soc. B Biol. Sci.* **371**: 20150498.

Jenal U, Malone J. 2006. Mechanisms of cyclic-di-GMP signaling in bacteria. *Annu. Rev. Genet.* **40**: 385–407.

Krug M, Weiss MS, Heinemann U, Mueller U. 2012. XDSAPP: A graphical user interface for the convenient processing of diffraction data using XDS. *J. Appl. Crystallogr.* **45**: 568–572.

Lim B, Beyhan S, Yildiz FH. 2007. Regulation of *Vibrio* polysaccharide synthesis and virulence factor production by CdgC, a GGDEF-EAL domain protein, in *Vibrio cholerae*. *J. Bacteriol.* **189**: 717–729.

Marmont LS, Whitney JC, Robinson H, Colvin KM, Parsek MR, Howell PL. 2012. Expression, purification, crystallization and preliminary X-ray analysis of *Pseudomonas aeruginosa* PelD. *Acta Crystallogr. Sect. F Struct. Biol. Cryst. Commun.* **68**: 181–184.

Massie JP, Reynolds EL, Koestler BJ, Cong J-P, Agostoni M, Waters CM. 2012. Quantification of high-specificity cyclic diguanylate signaling. *Proc. Natl. Acad. Sci.* **109**: 12746–12751.

Navarro MV a S, De N, Bae N, Wang Q, Sondermann H. 2009. Structural Analysis of the GGDEF-EAL Domain-Containing c-di-GMP Receptor FimX. *Structure* **17**: 1104–1116.

Nelson EJ, Harris JB, Morris JG, Calderwood SB, Camilli A. 2009. Cholera transmission: The host, pathogen and bacteriophage dynamic. *Nat. Rev. Microbiol.* **7**: 693–702.

Pesavento C, Hengge R. 2009. Bacterial nucleotide-based second messengers. *Curr. Opin. Microbiol.* **12**: 170–176.

- Rao F, Yang Y, Qi Y, Liang ZX.** 2008. Catalytic mechanism of cyclic di-GMP-specific phosphodiesterase: A study of the EAL domain-containing RocR from *Pseudomonas aeruginosa*. *J. Bacteriol.* **190**: 3622–3631.
- Reidi J, Kloese KE.** 2002. *Vibrio cholerae* and cholera: out of the water and into the host. *FEMS Microbiol. Rev.* **26**: 125–139.
- Robert-Paganin J, Nonin-Lecomte S, Réty S.** 2012. Crystal Structure of an EAL Domain in Complex with Reaction Product 5'-pGpG. *PLoS One* **7**: 1–13.
- Romling U, Galperin MY, Gomelsky M.** 2013. Cyclic di-GMP: the First 25 Years of a Universal Bacterial Second Messenger. *Microbiol. Mol. Biol. Rev.* **77**: 1–52.
- Simm R, Fetherston JD, Kader A, Römling U, Perry RD.** 2005. Phenotypic convergence mediated by GGDEF-domain-containing proteins. *J. Bacteriol.* **187**: 6816–6823.
- Sikora AE.** 2013 Proteins secreted via the type II secretion system: Smart strategies of *Vibrio cholerae* to maintain fitness in different ecological niches. *PLoS Pathog.* **9**: e1003126.
- Sparta KM, Krug M, Heinemann U, Mueller U, Weiss MS.** 2016. Xdsapp2.0. *J. Appl. Crystallogr.* **49**: 1085–1092.
- Srivastava D, Waters CM.** 2012. A tangled web: Regulatory connections between quorum sensing and cyclic Di-GMP. *J. Bacteriol.* **194**: 4485–4493.
- Tarnawski M, Barends TRM, Schlichting I.** 2015. Structural analysis of an oxygen-regulated diguanylate cyclase. *Acta Crystallogr. Sect. D Biol. Crystallogr.* **71**: 2158–2177.
- Vorobiev SM, Neely H, Yu B, Seetharaman J, Xiao R, Acton TB, Montelione GT, Hunt JF.** 2012. Crystal structure of a catalytically active GG(D/E)EF diguanylate cyclase domain from *Marinobacter aquaeolei* with bound c-di-GMP product. *J. Struct. Funct. Genomics* **13**: 177–183.
- Wang Y, Xu J, Chen A, Wang Y, Zhu J, Yu G, Xu L, Luo L.** 2010. GGDEF and EAL proteins play different roles in the control of *Sinorhizobium meliloti* growth, motility, exopolysaccharide production, and competitive nodulation on host alfalfa. *Acta Biochim. Biophys. Sin. (Shanghai).* **42**: 410–417.
- Waters CM, Lu W, Rabinowitz JD, Bassler BL.** 2008. Quorum sensing controls biofilm formation in *Vibrio cholerae* through modulation of cyclic Di-GMP levels and repression of *vpsT*. *J. Bacteriol.* **190**: 2527–2536.
- Winn MD, Ballard CC, Cowtan KD, Dodson EJ, Emsley P, Evans PR, Keegan RM, Krissinel EB, Leslie AGW, McCoy A, McNicholas SJ, Murshudov GN, Pannu NS, Potterton EA, Powell HR, Read RJ, Vagin A, Wilson KS.** 2011. Overview of the CCP4 suite and current developments. *Acta Crystallogr. Sect. D Biol. Crystallogr.* **67**: 235–242.
- Yan H, Chen W.** 2010. 3',5'-Cyclic diguanylic acid: a small nucleotide that makes big impacts. *Chem. Soc. Rev.* **39**: 2914–2924.

Yang CY, Chin KH, Chuah MLC, Liang ZX, Wang AHJ, Chou SH. 2011. The structure and inhibition of a GGDEF diguanylate cyclase complexed with (c-di-GMP) 2 at the active site. *Acta Crystallogr. Sect. D Biol. Crystallogr.* **67**: 997–1008.

Yildiz FH, Visick KL. 2009. Vibrio biofilms: so much the same yet so different. *Trends Microbiol.* **17**: 109–118.

6.1 Summary of the results

Bacterial infections always proved to be difficult to eradicate when they form a bacterial biofilm due to the protective nature, which gives an extra advantage to bacteria to survive in harsh conditions. Research on bacterial biofilm formation and motility has been gaining increasing medical attention because biofilms represent a mode of survival for numerous pathogenic bacteria like *V. cholerae*, *Salmonella typhimurium*, and *Staphylococcus aureus*. Consequently, biofilm infections are difficult to treat with conventional drugs. An additional motivation to study the molecular biology of signaling mechanism in biofilms is thus provided, because of the omnipresent need to develop novel strategies to treat persistent bacterial infections. The formation of the biofilm is associated with the secretion of an exopolysaccharide, which in turn, has been shown to be under the regulation of c-di-GMP levels in the cell (**Tischler and Camilli, 2005**). The c-di-GMP molecule is universally reported in all bacterial groups, synthesized by the diguanylate cyclase activity of GGD(E)EF domain proteins. Diguanylate cyclases have an important role to play in the lifestyle switching mechanisms of bacteria like *V. cholerae* by involving in the stimulation and maintenance of surface biofilms (**Beyhan et al 2007, Lim et al 2007, Pesavento and Hengge 2009, Camilli et al 2009**). The ability to produce c-di-GMP by the utilization of GTP makes this class of enzymes completely essential for the lifecycle of the bacteria. The universality of c-di-GMP as a key player in other signaling pathways in bacteria, and the mechanism of regulation of DGC activity have now been both strongly affirmed (**Hammer and Bassler 2009, Yang et al 2011, Robert-Paganin et al 2012**).

This prompted us to investigate the properties of the protein coded by the *vc0395_0300* gene, with a putative GGEEF domain, and a PAS domain signature as well. I proceeded with my research work using VC0395_0300 protein and its mutant clones in *E. coli*. These were subsequently analyzed for functional and structural features of the protein along with comparisons of mutant proteins. The conclusions of this study are summarized here:

Chapter1: Introduction and review of literature

In the first chapter, I described about *V. cholerae*, cholera disease history, route of transmission, its life cycle and why vaccination for cholera disease is difficult. Biofilm formation in *V. cholerae* was intensely described with all steps during bacterial biofilm formation. The intricate details about the c-di-GMP molecule, history, role in biofilm formation, the effect on bacterial virulence and effect on microbial physiology have been deliberated. The *V. cholerae* genome, with its multiplicity of GGEEF domains was also highlighted.

Chapter2: Site-directed mutagenesis of VC0395_0300 gene and cloning in *E. coli*.

In this chapter, I explained experiments about site-directed mutagenesis of *vc0395_0300* gene. Genomic DNA of *V. cholerae* serotype O1 classical strain O395 was isolated and served as a template DNA in PCR reaction. Four point mutations were individually made at the GGEEF active site of *VC0395_0300* gene using PCR based site-directed mutagenesis. In each of the mutations, one amino acid at the GGEEF sequence was replaced by another amino acid. All four mutated insert DNAs were separately ligated into cut pGEX-6P1 vector and four mutated clones were constructed. Mutated clones were effectively transformed into host *E. coli* strain DH5 α and expression host BL21 (DE3).

Chapter3: Expression and purification of mutant proteins

Here, I described experiments for protein expression methods, and small-scale overexpression of mutant proteins. The optimizations for overexpression of all proteins were achieved by checking at different IPTG concentrations and induction time. It was observed that the *VC0395_0300* gene was not able to express as a soluble protein with pET-28a (His-Tag containing) vector, but with pGEX-6P1, soluble protein could be obtained. Various protein constructs for *VC0395_0300* protein were also prepared by systematic truncations (based on secondary structure predictions) and conditions for maximum soluble protein overexpression was optimized.

Chapter4: Biophysical characterization of VC0395_0300 mutant proteins

This chapter deals with comparative studies of all mutant proteins versus the wild-type VC0395_0300 protein. For functional characterizations, all mutated strains along with wild-type were analyzed for biofilm formation ability and bacterial motility. All mutant strains showed significantly decreased biofilm formation and increase in bacterial motility (predominantly in VC0395_0300_(G237R) and VC0395_0300_(E238K)). Diguanylate cyclase activity results showed that mutations in active site amino acids do not abolish product formation completely, but reduce the activity significantly. All mutated proteins were therefore able to produce c-di-GMP, but with a much-reduced intensity of product peak. This was indicative of a partial loss-of-function for the protein. Secondary and tertiary structures of the VC0395_0300 mutant proteins do not alter significantly as seen from overall similar structural features in fluorescence spectroscopy and CD spectroscopy.

Chapter5: Structure elucidation of VC0395_0300 and its mutant proteins

In this chapter, I elucidated the protein structural features by X-ray crystallography. The full-length VC0395_0300 protein proved difficult to crystallize, due to the presence of a flexible region in the N-terminal end. So, I attempted to generate truncates of the full-length protein by shortening of the N-terminal flexible part and generate four different protein constructs of VC0395_0300 protein. The VC0395_0300₍₁₆₁₋₃₂₁₎ truncated protein was successfully crystallized, which showed the arrangement of α 1- α 2- β 1- α 3- α 4 - β 2- β 3- α 5- β 4- β 5- β 6- α 6- β 7 sheet and helices in their active sites, with 11% of the total accessible solvent area. One asymmetric unit of VC0395_0300₍₁₆₁₋₃₂₁₎ protein possesses four polypeptide chains in it. Two mutant proteins VC0395_0300_(G237R) and VC0395_0300_(E238K) were also crystallized with similar architecture, but showing the presence of arginine at 237th position and lysine in the 238th position in the A-site. Both the mutant proteins show a steric obstruction due to the extension of the extra side chain in the active site for binding the substrate GTP molecule.

The work from this thesis therefore, highlights the importance of the previously putative protein VC0395_0300 from *V. cholerae*. The central amino acids of the inherent GGEEF domain of this protein have an immense importance in the functional activity of this

protein. Mutations in the amino acids G (237) and E (238) seemed to have the maximum effect, resulting in a significant loss of diguanylate cyclase activity of this protein. Though the loss of activity was not associated with a complete structural rearrangement of the entire protein (as predicted by indirect structural methods like spectrofluorimetry and CD spectroscopy), the mutations appeared to have created some subtle changes which debilitated the protein. Since the protein does not have a I-site or inhibitory site to regulate c-di-GMP formation, the mystery was further deepened.

The answers came to light when the crystal structure of the wild type and mutant proteins were solved. The presence of an obstacle in the postulated path-of-entry of GTP to bind the GGEEF signature motif pointed to a mechanism for the loss of activity in the mutants. The steric hindrance may also inhibit the activity of the protein by not allowing a dimerization of two monomers of the protein. Dimerization is essential for the alignment of two GTP molecules to be cyclised into c-di-GMP. More about the mechanism could be elucidated if the attempted crystallizations with GTP were successful, but the crystals with GTP proved to be always elusive. Nevertheless, the work done in this thesis presents a novel finding of the function and structure of the VC0395_0300 protein from *V. cholerae*.

Future Scope of the work:

- Crystallization of the wild type and mutant proteins with the GTP and c-di-GMP in their respective sites.
- Design of diguanylate cyclase deficient *V. cholerae* and insertion of mutated *vc0395_0300* inserts.
- Examination of the roles of the PAS and PAC domains in the functional activity of the protein.
- Response of deletion mutants to environmental stimuli.

Appendix A

Reagents Used

Culture media

Medium	Chemical component
Luria-Bertani (LB)	5 g/l yeast extract 10 g/l Tryptone 5 g/l NaCl
LB Agar	1.6% (w/v) Agar in LB
SOB medium (For Transformation)	20 g/l Tryptone 5 g/l yeast extract 0.5 g/l NaCl 2.5 mM KCl
TB medium (4x) (Large scale protein production)	96 g/l yeast extract 48 g/l Tryptone 16% (w/v) glycerol
TB buffer	0.34 M KH_2PO_4 1.44 M K_2HPO_4

Plasmid DNA Isolation

Solution I (Resuspension buffer)	50 mM Glucose (Autoclave separately) 25 mM Tris pH 8 10 mM EDTA	
Solution II (Lysis buffer) (Freshly prepared)	0.2 N NaOH 1% SDS	
Solution III (Neutralizing buffer)	3 M potassium acetate, pH 4.8 pH adjusted by glacial acetic acid	
STET buffer (for boiling prep)	8% sucrose, 5% Triton X-100, 50 mM Tris pH 8.0, 50 mM EDTA pH 8.0 0.5 mg/ml lysozyme	
Other	Tris saturated phenol 70% ethanol Isopropanol Phenol : Chloroform : Isoamyl alcohol (25 : 24 : 1) (optional)	
Agarose Gel electrophoresis	50 X TAE stock buffer (1 ltr)	242 g Tris 57.1 mL Glacial Acetic Acid 10 mL 0.5 M EDTA
	1 X TAE Working concentration	40 mM Tris pH 8 1 mM EDTA
	TE buffer	10 mM Tris 1 mM EDTA
	EtBr	10 mg/ml Ethium bromide in distilled water
	DNA loading dye	20 mM Tris 30 % Glycerol 2 mM EDTA 0.25% (w/v) bromophenol blue 0.25% (w/v) xylene cyanol (optional)

Protein purification buffers

Buffer	Chemical components
General buffers	
1x PBS pH 7.4 (for small scale expression test)	137 mM NaCl 2.7 mM KCl 4.37 mM Na ₂ HP ₄ 1.47 mM KH ₂ PO ₄
Lysis buffer	1x PBS pH 7.4 300 mM NaCl 1 mM dithiothreitol (DTT) 2.5 mM β-ME 1 μg/ml DNase I 1 U/ml Benzoase 1 tablet EDTA-free Complete Protease Inhibitor/100 ml
GST Affinity Chromatography	
GST equilibration buffer	50 mM Tris pH 7.5 200 mM NaCl 1 mM DTT (or 2.5 mM β-ME) 1 mM MgCl ₂
GST wash buffer I	50 mM Tris pH 7.5 200 mM NaCl 1 mM DTT (or 2.5 mM β-ME) 1 mM MgCl ₂
GST wash buffer II	50 mM Tris pH 7.5 300 mM NaCl 1 mM DTT (or 2.5 mM β-ME) 1 mM MgCl ₂
GST elution buffer	50 mM Tris pH 7.5 200 mM NaCl 1 mM DTT (or 2.5 mM β-ME)

	1 mM MgCl ₂ 20 mM glutathione (reduced)
Dialysis buffer	50 mM Tris pH 7.5 150 mM NaCl 1 mM DTT (or 2.5 mM β-ME) 1 mM MgCl ₂
GST Tag cleavage buffer	50 mM Tris pH 7.0 150 mM NaCl 1 mM DTT (or 2.5 mM β-ME) 1 mM MgCl ₂
Cation exchange chromatography	
Column loading buffer	50 mM Tris pH 7.5 50 mM NaCl 1 mM DTT (or 2.5 mM β-ME) 1 mM MgCl ₂
Column Elution buffer	50 mM Tris pH 7.5 1 M NaCl 1 mM DTT (or 2.5 mM β-ME) 1 mM MgCl ₂
Size exclusion chromatography (SEC)	
SEC buffer	50 mM Tris pH 7.5 1 M NaCl 1 mM DTT (or 2.5 mM β-ME) 1 mM MgCl ₂

SDS-PAGE		
SDS-PAGE preparation	Solution I	29.2 % Acrylamide 0.8 % Bis- Acrylamide
	Solution II	1.5 M Tris pH 8.8 0.4 % SDS
	Solution III	0.5 M Tris pH 6.8 0.4 % SDS
	Other	TEMED 10 % Ammonium per sulphate
10X SDS running buffer	250 mM Tris 2.5 M Glycine 1% (w/v) SDS	
1X SDS running buffer	100 ml/l 10x SDS buffer 900 ml/l H ₂ O	
5X SDS sample buffer	50 mM Tris (pH 6.8) 100 mM DTT 5% β-ME 2% (w/v) SDS 0.25 % (w/v) Bromphenol blue 25% Glycerol	
staining solution	Staining solution I	50% (v/v) Ethanol 10% (v/v) acetic acid
	Staining solution II	5% (v/v) Ethanol 7.5% (v/v) acetic acid
	Staining solution III	0.25% Coomassie R-250 (w/v) in absolute Ethanol

Coomassie staining solution	0.25% (w/v) Coomassie brilliant blue R250 50% (v/v) Methanol 10% (v/v) acetic acid
Destaining solution	40% methanol 10% (v/v) acetic acid

SDS-PAGE preparation

Gel (%)	Stock I (ml)	Stock II (ml)	Stock III (ml)	Water (ml)	APS (μ l)	TEMED (μ l)
Resolving gel						
7.5	2.00	2	---	3.90	100	5
10	2.66	2	---	3.24	100	5
12.5	3.33	2	---	2.57	100	5
13.5	3.60	2	---	2.30	100	5
15	4.00	2	---	2.00	100	5
17.5	4.66	2	---	1.24	100	5
20	5.33	2	---	0.57	100	5
22	5.86	2	---	0.04	100	5
Stacking gel						
7.5	1.00	---	1	2.00	100	5

*Tables for Crystal screens are attached at the end of the thesis

Appendix B

Softwares and licences used

PyMOL

PyMOL is computer software, a molecular visualization system created by Warren Lyford DeLano. Open source software, release under the Python License.

Coot

Crystallographic Object-Oriented Toolkit (Coot) is for macromolecular model building, model completion and validation, particularly suitable for protein modelling using X-ray data.

CCP4

Integrated suite of programs that allows to determine macromolecular structures by X-ray crystallography, and other biophysical techniques.

Phenix

PHENIX is a software suite for the automated determination of molecular structures using X-ray crystallography and other methods.

Publications from PhD thesis

Subtle changes due to mutations in the GGDEF domain result in loss of biofilm forming activity in the VC0395_0300 protein from *Vibrio cholerae*, but no major change in the overall structure.

Protein Peptide Letter (2018), DOI: 10.2174/0929866525666180628162405

Om Prakash Chouhan, Sumit Biswas

Putative protein VC0395_0300 from *Vibrio cholerae* is a diguanylate cyclase with a role in biofilm formation.

Microbiological Research (2017), DOI: 10.1016/j.micres.2017.05.003

Divya Bandekar, **Om Prakash Chouhan**, Swati Mohapatra, Mousumi Hazra, Saugata Hazra, Sumit Biswas.

Effect of Site-Directed Mutagenesis at the GGEEF Domain of the Biofilm Forming GGEEF Protein from *Vibrio cholerae*.

AMB Express (2016), DOI: 10.1186/s13568-015-0168-6

Om Prakash Chouhan, Divya Bandekar, Mousumi Hazra, Ashish Baghudana, Saugata Hazra and Sumit Biswas

Structural studies of the active GGEEF domain of VC0395_0300 from *Vibrio cholerae*. **(In revision)**.

Om Prakash Chouhan, Divya Bandekar, Yvette Roske, Udo Heinemann, Sumit Biswas

Other Publications

Spectroscopic, electrochemical and DNA binding studies of some monomeric copper (II) complexes containing N2S(thiolate)Cu core and N4S(disulfide)Cu core.

Inorganica Chimica Acta (2017), DOI: 10.1016/j.ica.2016.10.045

Manjuri K. Koley, **Om Prakash Chouhan**, Sumit Biswas, Joseph Fernandes, Arnab Banerjee, Anjan Chattopadhyay, Babu Varghese, Aditya P. Koley.

DNA binding, cleavage and cytotoxicity studies of three mononuclear Cu(II) chloro-complexes containing N2S(thiolate)Cu core and N4S(disulfide)Cu core. **(In Process)**.

Sidhali U Parsekar, Joseph Fernandes, Arnab Banerjee, **Om Prakash Chouhan**, Sumit Biswas, Manjuri K Koley.

Effect of ions and inhibitors on the catalytic activity and the structural stability of *S. aureus* Enolase. **(In Process)**.

Vijay Hemmadi, Avijit Das, **Om Prakash Chouhan**, Sumit Biswas, Malabika Biswas.

Appendix D

Workshop and Conferences

INTERNATIONAL CONFERENCE on “Trends in Biochemical & Biomedical Research – Advances and Challenges (TBBR-2018) organized by Banaras Hindu University, Varanasi, INDIA in Feb 2018.

NATIONAL WORKSHOP on “DBT BIRAC Workshop Bio-Entrepreneurship – Grant Writing & Intellectual Property Management” organized by BITS Pilani KK Birla Goa Campus, INDIA in Feb 2016.

NATIONAL WORKSHOP on “An Introduction to Practical NMR Spectroscopy” organized by National Chemical laboratory (NCL) Venture Center, Pune, INDIA in Aug 2015.

NATIONAL CONFERENCE on “Gel-based Proteomics” organized by “PROTEOMICS SOCIETY, INDIA (PSI)” held at Indian Institute of Technology (IIT) Mumbai, INDIA in Dec 2014.

INTERNATIONAL CONFERENCE on “Biology of natural toxins”, annual conference of the toxinological society of India, organized by BITS Pilani KK Birla Goa Campus, INDIA in Dec 2013.

Appendix E

Brief Biography of the Candidate

Name	Om Prakash Chouhan
Education	M.Phil (Microbiology), MDS University, Ajmer, Rajasthan (2010) M.Sc. (Microbiology), MDS University, Ajmer, Rajasthan (2008)
Email	omprakashksg@gmail.com

Work Experience:

Om Prakash Chouhan joined BITS Pilani K K Birla Goa campus after qualifying the PhD examination as a PhD student or research scholar in the Department of Biological Sciences in the year of 2013. Before he joined PhD, he completed his Master degree in microbiology from MDS University Ajmer (Rajasthan) in the year 2008. After completing his master degree he finished his M.Phil from same department and joined one project as a junior research fellow funded by the ministry of environment and forest New Delhi. He has also cleared CSIR NET (2010), ICAR NET (2010) and GATE (2011) national level exam. Om Prakash was awarded DAAD fellowship in year of 2016. He has spent the 15 months in MDC, Berlin under a DAAD Scholarship program. He is also assisting the faculty for various labs as a teaching assistant. He has worked in protein structural biology and X-ray crystallography. He has successfully crystallized three difficult proteins and solved their protein structures. He has published three research articles in peer review journal.

Appendix F

Biography of the Supervisor

Dr. Sumit Biswas completed his Ph.D. in Bose Institute, Kolkata, under the supervision of Prof. Pinak Chakrabarti, as a CSIR fellow in 2008. His doctoral work elucidated the interfaces of protein-nucleic acid interactions, as well as the structure determination of two very important proteins. He went on to work as a DBT Research Associate in the DBT initiative, "Setting up of National Facility on Interactive Graphysics Computer System for Biomolecular Modelling, Molecular Dynamics & Structures" till 2009. Dr. Biswas joined BITS, Pilani, K K Birla Goa Campus as a faculty in 2009. He has since been involved as the Principal Investigator of four research projects funded by BRNS, DAE, DBT and DST, as well as the co-Investigator of a UGC project. His work in the institute involves the molecular mechanism and biology of the *Vibrio* life cycle, bioinformatics of non-coding RNA and protein-nucleic acid interactions, and therapeutic biology of natural products. Dr. Sumit Biswas has 16 publications in reputed journals and several conference publications to his name. He is also working on a book on Biophysics sanctioned by Prentice Hall of India.

Dr. Biswas has acted as the convenor for 4 meetings/symposia and workshops funded by DST, DBT, DSTE, Goa and BRNS. He is a life member of the Indian Crystallography Association, and a member of CholdInet (a WHO initiative for cholera research) and the Proteomics Society of India. He has received several awards and honours, the most recent being the prestigious EMBL Scholarship for presenting paper at EMBL Conference on Cancer Genomics, held at Heidelberg. Besides, he has delivered invited talks at different international conferences as well as institutes of repute like IIT, Kharagpur, IIT-BHU, etc. He has been actively involved as a reviewer of international journals from OUP, Elsevier, etc., as well as a question setter for DBT. Presently, he has three registered Ph.D. students under his tutelage and numerous thesis dissertation and project students working with him. He has also been the certified Radiological Safety Officer for the Institute, and is instrumental in setting up biosafety practices in BITS.

The Classics II Suite Composition Table

Number	Salt	Buffer	Precipitant	Cat. no. (Refill-Hit Solution, 4 x 12.5 ml tubes)
1		0.1 M Citric acid pH 3.5	2 M Ammonium sulfate	136101
2		0.1 M Sodium acetate pH 4.5	2 M Ammonium sulfate	136102
3		0.1 M Bis-Tris pH 5.5	2 M Ammonium sulfate	136103
4		0.1 M Bis-Tris pH 6.5	2 M Ammonium sulfate	136104
5		0.1 M HEPES pH 7.5	2 M Ammonium sulfate	136105
6		0.1 M Tris pH 8.5	2 M Ammonium sulfate	136106
7		0.1 M Citric acid pH 3.5	3 M Sodium chloride	136107
8		0.1 M Sodium acetate pH 4.5	3 M Sodium chloride	136108
9		0.1 M Bis-Tris pH 5.5	3 M Sodium chloride	136109
10		0.1 M Bis-Tris pH 6.5	3 M Sodium chloride	136110
11		0.1 M HEPES pH 7.5	3 M Sodium chloride	136111
12		0.1 M Tris pH 8.5	3 M Sodium chloride	136112
13	0.3 M Magnesium formate	0.1 M Bis-Tris pH 5.5		136113
14	0.5 M Magnesium formate	0.1 M Bis-Tris pH 6.5		136114
15	0.5 M Magnesium formate	0.1 M HEPES pH 7.5		136115
16	0.3 M Magnesium formate	0.1 M Tris pH 8.5		136116
17	1.26 M Sodium phosphate; 0.14 M Potassium phosphate			136117
18	0.49 M Sodium phosphate; 0.91 M Potassium phosphate			136118
19	0.056 M Sodium phosphate; 1.344 M Potassium phosphate			136119
20		0.1 M HEPES pH 7.5	1.4 M Sodium citrate	136120
21		1.8 M Ammonium citrate pH 7.0		136121
22		0.8 M Succinic acid pH 7.0		136122
23		2.1 M DL-Malic acid pH 7.0		136123
24		2.8 M Sodium acetate pH 7.0		136124
25		3.5 M Sodium formate pH 7.0		136125
26		1.1 M Ammonium tartrate pH 7.0		136126
27		2.4 M Sodium malonate pH 7.0		136127
28		0.56 M Sodium citrate pH 7.0		136128
29		0.96 M Sodium citrate pH 7.0		136129
30	0.1 M Sodium chloride	0.1 M Bis-Tris pH 6.5	1.5 M Ammonium sulfate	136130
31	0.8 M Sodium/Potassium tartrate	0.1 M Tris pH 8.5	0.5% (w/v) PEG 5000 MME	136131
32	1 M Ammonium sulfate	0.1 M Bis-Tris pH 5.5	1% (w/v) PEG 3350	136132
33	1.1 M Sodium malonate	0.1 M HEPES pH 7.0	0.5% (v/v) Jeffamine ED-2001	136133
34	1 M Succinic acid	0.1 M HEPES pH 7.0	1% (w/v) PEG 2000 MME	136134
35	1 M Ammonium sulfate	0.1 M HEPES pH 7.0	0.5% (w/v) PEG 8000	136135
36	0.191 M Sodium citrate pH 7.0	0.1 M HEPES pH 7.0	2% (w/v) PEG 3350	136136
37			25% (w/v) PEG 1500	136137
38		0.1 M HEPES pH 7.0	30% (v/v) Jeffamine M-600	136138
39		0.1 M HEPES pH 7.0	30% (v/v) Jeffamine ED-2001	136139
40		0.1 M Citric acid pH 3.5	25% (w/v) PEG 3350	136140
41		0.1 M Sodium acetate pH 4.5	25% (w/v) PEG 3350	136141
42		0.1 M Bis-Tris pH 5.5	25% (w/v) PEG 3350	136142
43		0.1 M Bis-Tris pH 6.5	25% (w/v) PEG 3350	136143
44		0.1 M HEPES pH 7.5	25% (w/v) PEG 3350	136144
45		0.1 M Tris pH 8.5	25% (w/v) PEG 3350	136145
46		0.1 M Bis-Tris pH 6.5	20% (w/v) PEG 5000 MME	136146
47		0.1 M Bis-Tris pH 6.5	28% (w/v) PEG 2000 MME	136147
48	0.2 M Calcium chloride	0.1 M Bis-Tris pH 5.5	45% (v/v) MPD	136148

The Classics II Suite Composition Table

Number	Salt	Buffer	Precipitant	Cat. no. (Refill-Hit Solution, 4 x 12.5 ml tubes)
49	0.2 M Calcium chloride	0.1 M Bis-Tris pH 6.5	45% (v/v) MPD	136149
50	0.2 M Ammonium acetate	0.1 M Bis-Tris pH 5.5	45% (v/v) MPD	136150
51	0.2 M Ammonium acetate	0.1 M Bis-Tris pH 6.5	45% (v/v) MPD	136151
52	0.2 M Ammonium acetate	0.1 M HEPES pH 7.5	45% (v/v) MPD	136152
53	0.2 M Ammonium acetate	0.1 M Tris pH 8.5	45% (v/v) MPD	136153
54	0.05 M Calcium chloride	0.1 M Bis-Tris pH 6.5	30% (v/v) PEG 550 MME	136154
55	0.05 M Magnesium chloride	0.1 M HEPES pH 7.5	30% (v/v) PEG 550 MME	136155
56	0.2 M Potassium chloride	0.05 M HEPES pH 7.5	35% (v/v) Pentaerythritol propoxylate	136156
57	0.05 M Ammonium sulfate	0.05 M Bis-Tris pH 6.5	30% (v/v) Pentaerythritol ethoxylate	136157
58		0.1 M Bis-Tris pH 6.5	45% (v/v) PEG P 400	136158
59	0.02 M Magnesium chloride	0.1 M HEPES pH 7.5	22% (w/v) Sodium Polyacrylate 5100	136159
60	0.01 M Cobalt (II) chloride	0.1 M Tris pH 8.5	20% (w/v) PVP K15	136160
61	0.2 M L-Proline	0.1 M HEPES pH 7.5	10% (w/v) PEG 3350	136161
62	0.2 M Trimethylamine N-oxide	0.1 M Tris pH 8.5	20% (w/v) PEG 2000 MME	136162
63	0.064 M Sodium citrate pH 7.0	0.1 M HEPES pH 7.0	10% (w/v) PEG 5000 MME	136163
64	0.005 M Magnesium chloride; 0.005 M Cobalt chloride; 0.005 M Nickel chloride; 0.005 M Cadmium chloride	0.1 M HEPES pH 7.5	12% (w/v) PEG 3350	136164
65	0.1 M Ammonium acetate	0.1 M Bis-Tris pH 5.5	17% (w/v) PEG 10000	136165
66	0.2 M Ammonium sulfate	0.1 M Bis-Tris pH 5.5	25% (w/v) PEG 3350	136166
67	0.2 M Ammonium sulfate	0.1 M Bis-Tris pH 6.5	25% (w/v) PEG 3350	136167
68	0.2 M Ammonium sulfate	0.1 M HEPES pH 7.5	25% (w/v) PEG 3350	136168
69	0.2 M Ammonium sulfate	0.1 M Tris pH 8.5	25% (w/v) PEG 3350	136169
70	0.2 M Sodium chloride	0.1 M Bis-Tris pH 5.5	25% (w/v) PEG 3350	136170
71	0.2 M Sodium chloride	0.1 M Bis-Tris pH 6.5	25% (w/v) PEG 3350	136171
72	0.2 M Sodium chloride	0.1 M HEPES pH 7.5	25% (w/v) PEG 3350	136172
73	0.2 M Sodium chloride	0.1 M Tris pH 8.5	25% (w/v) PEG 3350	136173
74	0.2 M Lithium sulfate	0.1 M Bis-Tris pH 5.5	25% (w/v) PEG 3350	136174
75	0.2 M Lithium sulfate	0.1 M Bis-Tris pH 6.5	25% (w/v) PEG 3350	136175
76	0.2 M Lithium sulfate	0.1 M HEPES pH 7.5	25% (w/v) PEG 3350	136176
77	0.2 M Lithium sulfate	0.1 M Tris pH 8.5	25% (w/v) PEG 3350	136177
78	0.2 M Ammonium acetate	0.1 M Bis-Tris pH 5.5	25% (w/v) PEG 3350	136178
79	0.2 M Ammonium acetate	0.1 M Bis-Tris pH 6.5	25% (w/v) PEG 3350	136179
80	0.2 M Ammonium acetate	0.1 M HEPES pH 7.5	25% (w/v) PEG 3350	136180
81	0.2 M Ammonium acetate	0.1 M Tris pH 8.5	25% (w/v) PEG 3350	136181
82	0.2 M Magnesium chloride	0.1 M Bis-Tris pH 5.5	25% (w/v) PEG 3350	136182
83	0.2 M Magnesium chloride	0.1 M Bis-Tris pH 6.5	25% (w/v) PEG 3350	136183
84	0.2 M Magnesium chloride	0.1 M HEPES pH 7.5	25% (w/v) PEG 3350	136184
85	0.2 M Magnesium chloride	0.1 M Tris pH 8.5	25% (w/v) PEG 3350	136185
86	0.2 M Potassium Sodium tartrate		20% (w/v) PEG 3350	136186
87		0.24 M Sodium malonate pH 7.0	20% (w/v) PEG 3350	136187
88		0.2 M Ammonium citrate pH 7.0	20% (w/v) PEG 3350	136188
89		0.1 M Succinic acid pH 7.0	15% (w/v) PEG 3350	136189
90	0.2 M Sodium formate		20% (w/v) PEG 3350	136190
91		0.15 M DL-Malic acid pH 7.0	20% (w/v) PEG 3350	136191
92	0.1 M Magnesium formate		15% (w/v) PEG 3350	136192
93	0.05 M Zinc acetate		20% (w/v) PEG 3350	136193
94	0.2 M Sodium citrate		20% (w/v) PEG 3350	136194
95	0.1 M Potassium thiocyanate		30% (w/v) PEG 2000 MME	136195
96	0.15 M Potassium bromide		30% (w/v) PEG 2000 MME	136196

The Classics Suite Composition Table

Number	Salt	Buffer	Precipitant	Cat. no. (Refill-Hit Solution, 4 x 12.5 ml tubes)
1	0.01 M Cobalt chloride	0.1 M Sodium acetate pH 4.6	1.0 M 1,6-Hexanediol	134001
2		0.1 M tri-Sodium citrate pH 5.6	2.5 M 1,6-Hexanediol	134002
3	0.2 M Magnesium chloride	0.1 M Tris pH 8.5	3.4 M 1,6-Hexanediol	134003
4			5% (v/v) Isopropanol; 2.0 M Ammonium sulfate	134004
5		0.1 M HEPES sodium salt pH 7.5	10% (v/v) Isopropanol; 20% (w/v) PEG 4000	134005
6	0.2 M Calcium chloride	0.1 M Sodium acetate pH 4.6	20% (v/v) Isopropanol	134006
7		0.1 M tri-Sodium citrate pH 5.6	20% (v/v) Isopropanol; 20% (w/v) PEG 4000	134007
8	0.2 M tri-Sodium citrate	0.1 M HEPES sodium salt pH 7.5	20% (v/v) Isopropanol	134008
9	0.2 M tri-Sodium citrate	0.1 M Sodium cacodylate pH 6.5	30% (v/v) Isopropanol	134009
10	0.2 M Magnesium chloride	0.1 M HEPES sodium salt pH 7.5	30% (v/v) Isopropanol	134010
11	0.2 M Ammonium acetate	0.1 M Tris-HCl pH 8.5	30% (v/v) Isopropanol	134011
12			10% (v/v) Ethanol; 1.5 M Sodium chloride	134012
13		0.1 M Tris pH 8.5	20% (v/v) Ethanol	134013
14			25% (v/v) Ethylene glycol	134014
15	0.02 M Calcium chloride	0.1 M Sodium acetate pH 4.6	30% (v/v) MPD	134015
16	0.2 M Sodium chloride	0.1 M Sodium acetate pH 4.6	30% (v/v) MPD	134016
17	0.2 M Ammonium acetate	0.1 M tri-Sodium citrate pH 5.6	30% (v/v) MPD	134017
18	0.2 M Magnesium acetate	0.1 M Sodium cacodylate pH 6.5	30% (v/v) MPD	134018
19	0.2 M tri-Sodium citrate	0.1 M HEPES sodium salt pH 7.5	30% (v/v) MPD	134019
20	0.5 M Ammonium sulfate	0.1 M HEPES pH 7.5	30% (v/v) MPD	134020
21	0.2 M Ammonium phosphate	0.1 M Tris pH 8.5	50% (v/v) MPD	134021
22		0.1 M HEPES pH 7.5	70% (v/v) MPD	134022
23		0.1 M Tris pH 8.5	25% (v/v) tert-Butanol	134023
24		0.1 M tri-Sodium citrate pH 5.6	35% (v/v) tert-Butanol	134024
25			0.4 M Ammonium phosphate	134025
26		0.1 M tri-Sodium citrate pH 5.6	1.0 M Ammonium phosphate	134026
27		0.1 M Tris-HCl pH 8.5	2.0 M Ammonium phosphate	134027
28		0.1 M HEPES pH 7.5	2.0 M Ammonium formate	134028
29		0.1 M Sodium acetate pH 4.6	2.0 M Ammonium sulfate	134029
30		0.1 M Tris-HCl pH 8.5	2.0 M Ammonium sulfate	134030
31			2.0 M Ammonium sulfate	134031
32	0.1 M Sodium chloride	0.1 M HEPES pH 7.5	1.6 M Ammonium sulfate	134032
33	0.01 M Cobalt chloride	0.1 M MES pH 6.5	1.8 M Ammonium sulfate	134033
34	0.2 M K/Na tartrate	0.1 M tri-Sodium citrate pH 5.6	2.0 M Ammonium sulfate	134034
35			1.0 M Imidazole pH 7.0	134035
36			0.4 M K/Na tartrate	134036
37		0.1 M HEPES sodium salt pH 7.5	0.8 M K/Na tartrate	134037
38		0.1 M Imidazole pH 6.5	1.0 M Sodium acetate	134038
39	0.05 M Cadmium sulfate	0.1 M HEPES pH 7.5	1.0 M Sodium acetate	134039
40		0.1 M Sodium cacodylate pH 6.5	1.4 M Sodium acetate	134040
41		0.1 M Sodium acetate pH 4.6	2.0 M Sodium chloride	134041
42	0.1 M Sodium phosphate; 0.1 M Potassium phosphate	0.1 M MES pH 6.5	2.0 M Sodium chloride	134042
43		0.1 M HEPES pH 7.5	4.3 M Sodium chloride	134043
44		0.1 M HEPES sodium salt pH 7.5	1.4 M tri-Sodium citrate	134044
45			1.6 M tri-Sodium citrate pH 6.5	134045
46		0.1 M HEPES sodium salt pH 7.5	0.8 M Sodium phosphate; 0.8 M Potassium phosphate	134046
47		0.1 M Sodium acetate pH 4.6	2.0 M Sodium formate	134047
48			4.0 M Sodium formate	134048

The Classics Suite Composition Table

Number	Salt	Buffer	Precipitant	Cat. no. (Refill-Hit Solution, 4 x 12.5 ml tubes)
49		0.1 M Bicine pH 9.0	2% (v/v) Dioxane; 10% (w/v) PEG 20000	134049
50		0.1 M MES pH 6.5	10% (v/v) Dioxane; 1.6 M Ammonium sulfate	134050
51			35% (v/v) Dioxane	134051
52	0.5 M Sodium chloride	0.1 M tri-Sodium citrate pH 5.6	2% (v/v) Ethylene imine polymer	134052
53		0.1 M Tris pH 8.5	12% (v/v) Glycerol; 1.5 M Ammonium sulfate	134053
54	0.5 M Sodium chloride; 0.01 M Magnesium chloride	0.01 M CTAB		134054
55	0.01 M Ferric chloride	0.1 M tri-Sodium citrate pH 5.6	10% (v/v) Jeffamine M-600	134055
56		0.1 M HEPES pH 7.5	20% (v/v) Jeffamine M-600	134056
57	0.5 M Ammonium sulfate	0.1 M tri-Sodium citrate pH 5.6	1.0 M Lithium sulfate	134057
58	0.01 M Nickel chloride	0.1 M Tris pH 8.5	1.0 M Lithium sulfate	134058
59		0.1 M HEPES sodium salt pH 7.5	1.5 M Lithium sulfate	134059
60		0.1 M Bicine pH 9.0	2.0 M Magnesium chloride	134060
61			0.2 M Magnesium formate	134061
62		0.1 M MES pH 6.5	1.6 M Magnesium sulfate	134062
63		0.1 M Tris-HCl pH 8.5	8% (w/v) PEG 8000	134063
64		0.1 M HEPES pH 7.5	10% (w/v) PEG 8000	134064
65	0.5 M Lithium sulfate		15% (w/v) PEG 8000	134065
66	0.2 M Zinc acetate	0.1 M Sodium cacodylate pH 6.5	18% (w/v) PEG 8000	134066
67	0.2 M Calcium acetate	0.1 M Sodium cacodylate pH 6.5	18% (w/v) PEG 8000	134067
68	0.2 M Magnesium acetate	0.1 M Sodium cacodylate pH 6.5	20% (w/v) PEG 8000	134068
69	0.05 M Potassium phosphate		20% (w/v) PEG 8000	134069
70	0.2 M Ammonium sulfate	0.1 M Sodium cacodylate pH 6.5	30% (w/v) PEG 8000	134070
71	0.2 M Sodium acetate	0.1 M Sodium cacodylate pH 6.5	30% (w/v) PEG 8000	134071
72	0.2 M Ammonium sulfate		30% (w/v) PEG 8000	134072
73		0.1 M HEPES sodium salt pH 7.5	2% (v/v) PEG 400; 2.0 M Ammonium sulfate	134073
74	0.2 M Calcium chloride	0.1 M HEPES sodium salt pH 7.5	28% (v/v) PEG 400	134074
75	0.1 M Cadmium chloride	0.1 M Sodium acetate pH 4.6	30% (v/v) PEG 400	134075
76	0.2 M Magnesium chloride	0.1 M HEPES sodium salt pH 7.5	30% (v/v) PEG 400	134076
77	0.2 M tri-Sodium citrate	0.1 M Tris-HCl pH 8.5	30% (v/v) PEG 400	134077
78	0.1 M Sodium chloride	0.1 M Bicine pH 9.0	20% (w/v) PEG 550 MME	134078
79	0.01 M Zinc sulfate	0.1 M MES pH 6.5	25% (w/v) PEG 550 MME	134079
80			10% (w/v) PEG 1000; 10% (w/v) PEG 8000	134080
81			30% (w/v) PEG 1500	134081
82	0.01 M Nickel chloride	0.1 M Tris pH 8.5	20% (w/v) PEG 2000 MME	134082
83	0.2 M Ammonium sulfate	0.1 M Sodium acetate pH 4.6	30% (w/v) PEG 2000 MME	134083
84		0.1 M Sodium acetate pH 4.6	8% (w/v) PEG 4000	134084
85	0.2 M Ammonium sulfate	0.1 M Sodium acetate pH 4.6	25% (w/v) PEG 4000	134085
86	0.2 M Ammonium acetate	0.1 M Sodium acetate pH 4.6	30% (w/v) PEG 4000	134086
87	0.2 M Ammonium acetate	0.1 M tri-Sodium citrate pH 5.6	30% (w/v) PEG 4000	134087
88	0.2 M Magnesium chloride	0.1 M Tris-HCl pH 8.5	30% (w/v) PEG 4000	134088
89	0.2 M Lithium sulfate	0.1 M Tris-HCl pH 8.5	30% (w/v) PEG 4000	134089
90	0.2 M Sodium acetate	0.1 M Tris-HCl pH 8.5	30% (w/v) PEG 4000	134090
91	0.2 M Ammonium sulfate		30% (w/v) PEG 4000	134091
92	0.2 M Ammonium sulfate	0.1 M MES pH 6.5	30% (w/v) PEG 5000 MME	134092
93		0.1 M HEPES pH 7.5	10% (w/v) PEG 6000; 5% (v/v) MPD	134093
94			10% (w/v) PEG 6000; 2.0 M Sodium chloride	134094
95		0.1 M HEPES pH 7.5	20% (w/v) PEG 10000; 8% (v/v) Ethylene glycol	134095
96		0.1 M MES pH 6.5	12% (w/v) PEG 20000	134096

The CompAS Suite Composition Table

Number	Salt	Buffer	Precipitant	Cat. no. (Refill-Hit Solution, 4 x 12.5 ml tubes)
1	0.1 M Potassium chloride		12% (w/v) PEG 8000; 5% (w/v) Glycerol	135601
2	0.5 M Potassium chloride		12% (w/v) PEG 8000; 10% (w/v) Glycerol	135602
3	0.2 M Ammonium sulfate		15% (w/v) PEG 8000	135603
4	0.5 M Lithium sulfate		15% (w/v) PEG 8000	135604
5	0.2 M Sodium acetate	0.1 M MES pH 6.5	15% (w/v) PEG 8000	135605
6	0.05 M Ammonium sulfate	0.1 M Sodium citrate	15% (w/v) PEG 8000	135606
7	0.2 M Calcium acetate	0.1 M HEPES pH 7.5	18% (w/v) PEG 8000	135607
8	0.1 M Sodium acetate	0.1 M HEPES pH 7.5	18% (w/v) PEG 8000; 2% (w/v) Isopropanol	135608
9	0.2 M Lithium sulfate	0.1 M Tris pH 8.5	18% (w/v) PEG 8000	135609
10		0.1 M HEPES pH 7.5	20% (w/v) PEG 8000	135610
11	0.2 M Magnesium acetate	0.1 M MES pH 6.5	20% (w/v) PEG 8000	135611
12		0.1 M CHES pH 9.5	20% (w/v) PEG 8000	135612
13	0.2 M Ammonium sulfate	0.1 M MES pH 6.5	22% (w/v) PEG 8000	135613
14	0.2 M Lithium chloride		25% (w/v) PEG 8000	135614
15	0.2 M Ammonium sulfate		30% (w/v) PEG 8000	135615
16		0.1 M Sodium acetate pH 4.6	8% (w/v) PEG 10000	135616
17		0.1 M Imidazole pH 8.0	14% (w/v) PEG 10000	135617
18		0.1 M Tris pH 8.5	16% (w/v) PEG 10000	135618
19	0.1 M Sodium chloride	0.1 M Tris pH 8.5	18% (w/v) PEG 10000; 20% (w/v) Glycerol	135619
20		0.1 M HEPES pH 7.5	20% (w/v) PEG 10000	135620
21		0.1 M Tris pH 8.5	30% (w/v) PEG 10000	135621
22		0.1 M MES pH 6.5	10% (w/v) PEG 20000	135622
23	0.1 M Magnesium chloride	0.1 M Tris pH 8.5	17% (w/v) PEG 20000	135623
24			20% (w/v) PEG 20000	135624
25	0.01 M Sodium acetate		50% (w/v) MPD; 15% (w/v) Ethanol	135625
26	0.05M Sodium chloride	0.05 M Sodium acetate	50% (w/v) MPD; 20% (w/v) Isopropanol	135626
27	0.1 M Ammonium phosphate	0.1 M Tris pH 8.5	50% (w/v) MPD	135627
28			55% (w/v) MPD	135628
29	0.01 M Calcium chloride	0.1 M Sodium acetate pH 4.6	60% (w/v) MPD	135629
30	0.02 M Sodium acetate		60% (w/v) MPD	135630
31		0.1 M MES pH 6.5	70% (w/v) MPD	135631
32		0.1 M Tris pH 8.5	70% (w/v) MPD	135632
33	0.01 M Calcium chloride	0.1 M Tris pH 8.5	20% (w/v) Methanol	135633
34		0.1 M Tris pH 8.5	2% (w/v) Ethanol	135634
35		0.1 M HEPES pH 7.5	5% (w/v) Ethanol; 5% (w/v) MPD	135635
36	0.2 M Sodium chloride	0.1 M Tris pH 8.5	5% (w/v) Ethanol; 5% (w/v) MPD	135636
37		0.1 M Tris pH 8.5	10% (w/v) Ethanol	135637
38		0.1 M Sodium acetate pH 4.6	12% (w/v) Ethanol; 4% (w/v) PEG 400	135638
39		0.1 M Tris pH 8.5	14% (w/v) Ethanol; 5% (w/v) Glycerol	135639
40		0.1 M Tris pH 8.5	18% (w/v) Ethanol	135640
41			20% (w/v) Ethanol	135641
42			20% (w/v) Ethanol; 10% (w/v) Glycerol	135642
43	0.1 M Sodium acetate		30% (w/v) Ethanol; 10% (w/v) PEG 6000	135643
44			45% (w/v) Ethanol	135644
45	0.01 M Sodium acetate		50% (w/v) Ethanol	135645
46	0.05 M Sodium acetate		60% (w/v) Ethanol; 1.5% (w/v) PEG 6000	135646
47	0.1 M Sodium chloride		60% (w/v) Ethanol	135647
48	0.01 M Magnesium sulfate	0.1 M Tris pH 8.5	2% (w/v) Isopropanol	135648

The CompAS Suite Composition Table

Number	Salt	Buffer	Precipitant	Cat. no. (Refill-Hit Solution, 4 x 12.5 ml tubes)
49		0.1 M HEPES pH 7.5	5% (w/v) Isopropanol	135649
50	0.2 M Calcium chloride	0.1 M Sodium acetate pH 4.6	10% (w/v) Isopropanol	135650
51	0.2 M Sodium citrate	0.1 M HEPES pH 7.5	10% (w/v) Isopropanol	135651
52	0.01 M Magnesium chloride	0.1 M Tris pH 8.5	10% (w/v) Isopropanol	135652
53	0.05 M Sodium chloride	0.1 M Tris pH 8.5	12% (w/v) Isopropanol	135653
54	0.2 M Sodium citrate	0.1 M MES pH 6.5	15% (w/v) Isopropanol	135654
55	0.2 M Sodium citrate	0.1 M HEPES pH 7.5	15% (w/v) Isopropanol	135655
56	0.2 M Magnesium chloride	0.1 M HEPES pH 7.5	15% (w/v) Isopropanol	135656
57	0.2 M Ammonium acetate	0.1 M Tris pH 8.5	15% (w/v) Isopropanol	135657
58	0.2 M Calcium chloride	0.1 M Sodium acetate pH 4.6	20% (w/v) Isopropanol	135658
59	0.2 M Sodium citrate	0.1 M HEPES pH 7.5	20% (w/v) Isopropanol	135659
60	0.1 M Magnesium chloride	0.1 M HEPES pH 7.5	25% (w/v) Isopropanol	135660
61	0.2 M Sodium citrate	0.1 M MES pH 6.5	30% (w/v) Isopropanol	135661
62	0.2 M Magnesium chloride	0.1 M HEPES pH 7.5	30% (w/v) Isopropanol	135662
63	0.2 M Ammonium acetate	0.1 M Tris pH 8.5	30% (w/v) Isopropanol	135663
64	0.1 M Calcium chloride	0.1 M Tris pH 8.5	25% (w/v) tert-Butanol	135664
65		0.1 M Sodium citrate pH 5.6	35% (w/v) tert-Butanol	135665
66			0.2 M Ammonium dihydrogen phosphate	135666
67			0.2 M Potassium/Sodium tartrate	135667
68			0.2 M Magnesium acetate	135668
69			0.4 M Ammonium dihydrogen phosphate	135669
70			0.4 M Potassium/Sodium tartrate	135670
71		0.1 M Tris pH 8.5	0.4 M Potassium/Sodium tartrate	135671
72	0.2 M Sodium citrate		0.5 M Ammonium dihydrogen phosphate	135672
73		0.1 M Imidazole pH 8.0	0.5 M Sodium acetate	135673
74		0.1 M HEPES pH 7.5	0.7 M Sodium citrate	135674
75		0.1 M Tris pH 8.5	0.7 M Lithium sulfate	135675
76		0.1 M HEPES pH 7.5	0.8 M Potassium/Sodium tartrate	135676
77		0.1 M Sodium citrate pH 5.6	1.0 M Ammonium dihydrogen phosphate	135677
78		0.1 M Tris pH 8.5	1.0 M Ammonium dihydrogen phosphate	135678
79	0.01 M Nickel chloride	0.1 M Tris pH 8.5	1.0 M Lithium sulfate	135679
80		0.1 M Imidazole pH 8.0	1.0 M Sodium acetate	135680
81		0.1 M Sodium acetate pH 4.6	1.0 M Sodium formate	135681
82		0.1 M MES pH 6.5	1.4 M Sodium acetate	135682
83		0.1 M HEPES pH 7.5	1.4 M Sodium citrate	135683
84		0.1 M Tris pH 8.5	1.5 M Lithium sulfate	135684
85		1 M Sodium citrate pH 6.5		135685
86		0.1 M MES pH 6.5	1.6 M Magnesium sulfate	135686
87		0.1 M MES pH 6.5	1.6 M Potassium/Sodium tartrate	135687
88		0.1 M MES pH 6.5	2.0 M Ammonium formate	135688
89		0.1 M Tris pH 8.5	2.0 M Ammonium dihydrogen phosphate	135689
90			2.0 M Sodium formate	135690
91		0.1 M Tris pH 8.5	2.0 M Magnesium chloride	135691
92	0.2 M Sodium acetate	0.1 M MES pH 6.5	2.0 M Sodium chloride	135692
93		0.1 M Sodium acetate pH 4.6	2.0 M Sodium formate	135693
94		0.1 M Tris pH 8.5	1.0 M Ammonium dihydrogen phosphate; 30% (w/v) Glycerol	135694
95		0.1 M HEPES pH 7.5	4.0 M Sodium chloride	135695
96			3.0 M Sodium formate	135696

The PEGs Suite Composition Table

Number	Salt	Buffer	Precipitant	Cat. no. (Refill-Hit Solution, 4 x 12.5 ml tubes)
1		0.1 M Sodium acetate pH 4.6	40% (v/v) PEG 200	134301
2		0.1 M Sodium acetate pH 4.6	30% (v/v) PEG 300	134302
3		0.1 M Sodium acetate pH 4.6	30% (v/v) PEG 400	134303
4		0.1 M Sodium acetate pH 4.6	25% (v/v) PEG 550 MME	134304
5		0.1 M Sodium acetate pH 4.6	25% (w/v) PEG 1000	134305
6		0.1 M Sodium acetate pH 4.6	25% (w/v) PEG 2000 MME	134306
7		0.1 M MES pH 6.5	40% (v/v) PEG 200	134307
8		0.1 M MES pH 6.5	30% (v/v) PEG 300	134308
9		0.1 M MES pH 6.5	30% (v/v) PEG 400	134309
10		0.1 M MES pH 6.5	25% (v/v) PEG 550 MME	134310
11		0.1 M MES pH 6.5	25% (w/v) PEG 1000	134311
12		0.1 M MES pH 6.5	25% (w/v) PEG 2000 MME	134312
13		0.1 M Sodium HEPES pH 7.5	40% (v/v) PEG 200	134313
14		0.1 M Sodium HEPES pH 7.5	30% (v/v) PEG 300	134314
15		0.1 M Sodium HEPES pH 7.5	30% (v/v) PEG 400	134315
16		0.1 M Sodium HEPES pH 7.5	25% (v/v) PEG 550 MME	134316
17		0.1 M Sodium HEPES pH 7.5	25% (w/v) PEG 1000	134317
18		0.1 M Sodium HEPES pH 7.5	25% (w/v) PEG 2000 MME	134318
19		0.1 M TRIS-HCl pH 8.5	40% (v/v) PEG 200	134319
20		0.1 M TRIS-HCl pH 8.5	30% (v/v) PEG 300	134320
21		0.1 M TRIS-HCl pH 8.5	30% (v/v) PEG 400	134321
22		0.1 M TRIS-HCl pH 8.5	25% (v/v) PEG 550 MME	134322
23		0.1 M TRIS-HCl pH 8.5	25% (w/v) PEG 1000	134323
24		0.1 M TRIS-HCl pH 8.5	25% (w/v) PEG 2000 MME	134324
25		0.1 M Sodium acetate pH 4.6	25% (w/v) PEG 3000	134325
26		0.1 M Sodium acetate pH 4.6	25% (w/v) PEG 4000	134326
27		0.1 M Sodium acetate pH 4.6	25% (w/v) PEG 6000	134327
28		0.1 M Sodium acetate pH 4.6	25% (w/v) PEG 8000	134328
29		0.1 M Sodium acetate pH 4.6	20% (w/v) PEG 10000	134329
30		0.1 M Sodium acetate pH 4.6	15% (w/v) PEG 20000	134330
31		0.1 M MES pH 6.5	25% (w/v) PEG 3000	134331
32		0.1 M MES pH 6.5	25% (w/v) PEG 4000	134332
33		0.1 M MES pH 6.5	25% (w/v) PEG 6000	134333
34		0.1 M MES pH 6.5	25% (w/v) PEG 8000	134334
35		0.1 M MES pH 6.5	20% (w/v) PEG 10000	134335
36		0.1 M MES pH 6.5	15% (w/v) PEG 20000	134336
37		0.1 M Sodium HEPES pH 7.5	25% (w/v) PEG 3000	134337
38		0.1 M Sodium HEPES pH 7.5	25% (w/v) PEG 4000	134338
39		0.1 M Sodium HEPES pH 7.5	25% (w/v) PEG 6000	134339
40		0.1 M Sodium HEPES pH 7.5	25% (w/v) PEG 8000	134340
41		0.1 M Sodium HEPES pH 7.5	20% (w/v) PEG 10000	134341
42		0.1 M Sodium HEPES pH 7.5	15% (w/v) PEG 20000	134342
43		0.1 M TRIS-HCl pH 8.5	25% (w/v) PEG 3000	134343
44		0.1 M TRIS-HCl pH 8.5	25% (w/v) PEG 4000	134344
45		0.1 M TRIS-HCl pH 8.5	25% (w/v) PEG 6000	134345
46		0.1 M TRIS-HCl pH 8.5	25% (w/v) PEG 8000	134346
47		0.1 M TRIS-HCl pH 8.5	20% (w/v) PEG 10000	134347
48		0.1 M TRIS-HCl pH 8.5	15% (w/v) PEG 20000	134348

The PEGs Suite Composition Table

Number	Salt	Buffer	Precipitant	Cat. no. (Refill-Hit Solution, 4 x 12.5 ml tubes)
49	0.2 M Sodium fluoride		20% (w/v) PEG 3350	134349
50	0.2 M Potassium fluoride		20% (w/v) PEG 3350	134350
51	0.2 M Ammonium fluoride		20% (w/v) PEG 3350	134351
52	0.2 M Lithium chloride		20% (w/v) PEG 3350	134352
53	0.2 M Magnesium chloride		20% (w/v) PEG 3350	134353
54	0.2 M Sodium chloride		20% (w/v) PEG 3350	134354
55	0.2 M Calcium chloride		20% (w/v) PEG 3350	134355
56	0.2 M Potassium chloride		20% (w/v) PEG 3350	134356
57	0.2 M Ammonium chloride		20% (w/v) PEG 3350	134357
58	0.2 M Sodium iodide		20% (w/v) PEG 3350	134358
59	0.2 M Potassium iodide		20% (w/v) PEG 3350	134359
60	0.2 M Ammonium iodide		20% (w/v) PEG 3350	134360
61	0.2 M Sodium thiocyanate		20% (w/v) PEG 3350	134361
62	0.2 M Potassium thiocyanate		20% (w/v) PEG 3350	134362
63	0.2 M Lithium nitrate		20% (w/v) PEG 3350	134363
64	0.2 M Magnesium nitrate		20% (w/v) PEG 3350	134364
65	0.2 M Sodium nitrate		20% (w/v) PEG 3350	134365
66	0.2 M Potassium nitrate		20% (w/v) PEG 3350	134366
67	0.2 M Ammonium nitrate		20% (w/v) PEG 3350	134367
68	0.2 M Magnesium formate		20% (w/v) PEG 3350	134368
69	0.2 M Sodium formate		20% (w/v) PEG 3350	134369
70	0.2 M Potassium formate		20% (w/v) PEG 3350	134370
71	0.2 M Ammonium formate		20% (w/v) PEG 3350	134371
72	0.2 M Lithium acetate		20% (w/v) PEG 3350	134372
73	0.2 M Magnesium acetate		20% (w/v) PEG 3350	134373
74	0.2 M Zinc acetate		20% (w/v) PEG 3350	134374
75	0.2 M Sodium acetate		20% (w/v) PEG 3350	134375
76	0.2 M Calcium acetate		20% (w/v) PEG 3350	134376
77	0.2 M Potassium acetate		20% (w/v) PEG 3350	134377
78	0.2 M Ammonium acetate		20% (w/v) PEG 3350	134378
79	0.2 M Lithium sulfate		20% (w/v) PEG 3350	134379
80	0.2 M Magnesium sulfate		20% (w/v) PEG 3350	134380
81	0.2 M Sodium sulfate		20% (w/v) PEG 3350	134381
82	0.2 M Potassium sulfate		20% (w/v) PEG 3350	134382
83	0.2 M Ammonium sulfate		20% (w/v) PEG 3350	134383
84	0.2 M di-Sodium tartrate		20% (w/v) PEG 3350	134384
85	0.2 M K/Na tartrate		20% (w/v) PEG 3350	134385
86	0.2 M di-Ammonium tartrate		20% (w/v) PEG 3350	134386
87	0.2 M Sodium phosphate		20% (w/v) PEG 3350	134387
88	0.2 M di-Sodium phosphate		20% (w/v) PEG 3350	134388
89	0.2 M Potassium phosphate		20% (w/v) PEG 3350	134389
90	0.2 M di-Potassium phosphate		20% (w/v) PEG 3350	134390
91	0.2 M Ammonium phosphate		20% (w/v) PEG 3350	134391
92	0.2 M di-Ammonium phosphate		20% (w/v) PEG 3350	134392
93	0.2 M tri-Lithium citrate		20% (w/v) PEG 3350	134393
94	0.2 M tri-Sodium citrate		20% (w/v) PEG 3350	134394
95	0.2 M tri-Potassium citrate		20% (w/v) PEG 3350	134395
96	0.18 M tri-Ammonium citrate		20% (w/v) PEG 3350	134396

The PEGs II Suite Composition Table

Number	Salt	Buffer	Precipitant	Cat. no. (Refill-Hit Solution, 4 x 12.5 ml tubes)
1	0.1 M Calcium chloride	0.1 M Sodium acetate pH 4.6	15% (w/v) PEG 400	135501
2		0.1 M MES pH 6.5	15% (w/v) PEG 400	135502
3	0.2 M Magnesium chloride	0.1 M HEPES pH 7.5	15% (w/v) PEG 400	135503
4	0.2 M tri-Sodium citrate	0.1 M Tris pH 8.5	15% (w/v) PEG 400	135504
5	0.1 M Magnesium chloride	0.1 M Sodium acetate pH 4.6	25% (w/v) PEG 400	135505
6	0.2 M Lithium sulfate	0.1 M Tris pH 8.5	25% (w/v) PEG 400	135506
7	0.2 M Calcium chloride	0.1 M HEPES pH 7.5	28% (w/v) PEG 400	135507
8	0.1 M Calcium chloride	0.1 M Sodium acetate pH 4.6	30% (w/v) PEG 400	135508
9	0.1 M Sodium acetate	0.1 M MES pH 6.5	30% (w/v) PEG 400	135509
10	0.1 M Magnesium chloride	0.1 M MES pH 6.5	30% (w/v) PEG 400	135510
11	0.2 M Magnesium chloride	0.1 M HEPES pH 7.5	30% (w/v) PEG 400	135511
12	0.2 M tri-Sodium citrate	0.1 M Tris pH 8.5	30% (w/v) PEG 400	135512
13	0.1 M Sodium chloride	0.1 M Bicine pH 9.0	30% (w/v) PEG 550 MME	135513
14	0.01 M Zinc sulfate	0.1 M MES pH 6.5	25% (w/v) PEG 550 MME	135514
15		0.1 M HEPES pH 7.5	25% (w/v) PEG 1000	135515
16		0.1 M Tris pH 8.5	30% (w/v) PEG 1000	135516
17			15% (w/v) PEG 1500	135517
18		0.1 M HEPES pH 7.5	20% (w/v) PEG 1500	135518
19			30% (w/v) PEG 1500	135519
20	0.01 M Nickel chloride	0.1 M Tris pH 8.5	20% (w/v) PEG 2000 MME	135520
21			25% (w/v) PEG 2000 MME	135521
22	0.1 M Sodium acetate	0.1 M MES pH 6.5	30% (w/v) PEG 2000 MME	135522
23	0.2 M Sodium acetate	0.1 M HEPES pH 7.5	20% (w/v) PEG 3000	135523
24	0.2 M Lithium sulfate	0.1 M Tris pH 8.5	30% (w/v) PEG 3000	135524
25		0.1 M Sodium acetate pH 4.6	4% (w/v) PEG 4000	135525
26			8% (w/v) PEG 4000	135526
27		0.1 M Sodium acetate pH 4.6	8% (w/v) PEG 4000	135527
28	0.2 M Magnesium chloride	0.1 M MES pH 6.5	10% (w/v) PEG 4000	135528
29	0.1 M Sodium acetate	0.1 M HEPES pH 7.5	12% (w/v) PEG 4000	135529
30		0.1 M Tris pH 8.5	12% (w/v) PEG 4000	135530
31	0.2 M Lithium sulfate	0.1 M Tris pH 8.5	16% (w/v) PEG 4000	135531
32	0.2 M Sodium acetate	0.1 M Tris pH 8.5	16% (w/v) PEG 4000	135532
33	0.2 M Magnesium chloride	0.1 M Tris pH 8.5	16% (w/v) PEG 4000	135533
34		0.1 M Sodium acetate pH 4.6	18% (w/v) PEG 4000	135534
35	0.2 M Lithium sulfate	0.1 M Tris pH 8.5	20% (w/v) PEG 4000	135535
36	0.2 M Calcium chloride	0.1 M Tris pH 8.5	20% (w/v) PEG 4000	135536
37	0.1 M Sodium acetate	0.1 M HEPES pH 7.5	22% (w/v) PEG 4000	135537
38		0.1 M Sodium acetate pH 4.6	25% (w/v) PEG 4000	135538
39	0.2 M Magnesium chloride	0.1 M MES pH 6.5	25% (w/v) PEG 4000	135539
40	0.2 M Calcium chloride	0.1 M Tris pH 8.5	25% (w/v) PEG 4000	135540
41			30% (w/v) PEG 4000	135541
42	0.1 M Magnesium chloride	0.1 M Sodium acetate pH 4.6	30% (w/v) PEG 4000	135542
43		0.1 M MES pH 6.5	30% (w/v) PEG 4000	135543
44	0.2 M Calcium chloride	0.1 M HEPES pH 7.5	30% (w/v) PEG 4000	135544
45	0.2 M Lithium sulfate	0.1 M Tris pH 8.5	30% (w/v) PEG 4000	135545
46	0.2 M Sodium acetate	0.1 M Tris pH 8.5	30% (w/v) PEG 4000	135546
47	0.2 M Magnesium chloride	0.1 M Tris pH 8.5	30% (w/v) PEG 4000	135547
48			35% (w/v) PEG 4000	135548

The PEGs II Suite Composition Table

Number	Salt	Buffer	Precipitant	Cat. no. (Refill-Hit Solution, 4 x 12.5 ml tubes)
49		0.1 M Tris pH 8.5	8% (w/v) PEG 4000; 0.8 M Lithium chloride	135549
50			10% (w/v) PEG 4000; 20% (w/v) Isopropanol	135550
51		0.1 M tri-Sodium citrate pH 5.6	10% (w/v) PEG 4000; 10% (w/v) Isopropanol	135551
52		0.1 M HEPES pH 7.5	10% (w/v) PEG 4000; 5% (w/v) Isopropanol	135552
53		0.1 M HEPES pH 7.5	10% (w/v) PEG 4000; 20% (w/v) Isopropanol	135553
54	0.2 M Ammonium sulfate	0.1 M Sodium acetate pH 4.6	12% (w/v) PEG 4000	135554
55	0.2 M Ammonium sulfate		15% (w/v) PEG 4000	135555
56	0.2 M Ammonium sulfate	0.1 M tri-Sodium citrate pH 5.6	15% (w/v) PEG 4000	135556
57	0.2 M Ammonium sulfate	0.1 M HEPES pH 7.5	16% (w/v) PEG 4000; 10% (w/v) Isopropanol	135557
58	0.2 M Ammonium sulfate		20% (w/v) PEG 4000	135558
59	0.2 M Magnesium sulfate		20% (w/v) PEG 4000; 10% (w/v) Glycerol	135559
60	0.1 M tri-Sodium citrate		20% (w/v) PEG 4000; 5% (w/v) Isopropanol	135560
61	0.1 M tri-Sodium citrate		20% (w/v) PEG 4000; 20% (w/v) Isopropanol	135561
62		0.1 M MES pH 6.5	20% (w/v) PEG 4000; 0.6 M Sodium chloride	135562
63		0.1 M HEPES pH 7.5	20% (w/v) PEG 4000; 10% (w/v) Isopropanol	135563
64	0.2 M Ammonium sulfate; 0.1 M Sodium acetate		22% (w/v) PEG 4000	135564
65	0.2 M Ammonium sulfate	0.1 M Sodium acetate pH 4.6	25% (w/v) PEG 4000	135565
66	0.2 M Ammonium sulfate	0.1 M tri-Sodium citrate pH 5.6	25% (w/v) PEG 4000	135566
67	0.1 M Sodium acetate; 0.2M Lithium sulfate	0.1 M HEPES pH 7.5	25% (w/v) PEG 4000	135567
68	0.1 M Sodium acetate		25% (w/v) PEG 4000; 8% (w/v) Isopropanol	135568
69	0.2 M Ammonium sulfate		30% (w/v) PEG 4000	135569
70	0.2 M Ammonium sulfate	0.1 M Sodium acetate pH 4.6	30% (w/v) PEG 4000	135570
71	0.2 M Ammonium sulfate	0.1 M Sodium acetate pH 5.6	30% (w/v) PEG 4000	135571
72		0.1 M Tris pH 8.5	32% (w/v) PEG 4000; 0.8 M Lithium chloride	135572
73	0.2 M Lithium sulfate	0.1 M Tris pH 8.5	25% (w/v) PEG 5000 MME	135573
74	0.2 M Ammonium sulfate	0.1 M MES pH 6.5	30% (w/v) PEG 5000 MME	135574
75	0.1 M Potassium chloride	0.1 M Tris pH 8.5	3% (w/v) PEG 6000	135575
76	0.01 M Magnesium chloride		10% (w/v) PEG 6000	135576
77	2.0 M Sodium chloride		12% (w/v) PEG 6000	135577
78			15% (w/v) PEG 6000; 5% (w/v) Glycerol	135578
79	0.05 M Potassium chloride; 0.01 M Magnesium chloride		15% (w/v) PEG 6000	135579
80	0.01 M tri-Sodium citrate		16% (w/v) PEG 6000	135580
81		0.05 M Imidazole pH 8.0	20% (w/v) PEG 6000	135581
82	0.1 M Lithium chloride	0.1 M HEPES pH 7.5	25% (w/v) PEG 6000	135582
83	0.5 M Lithium chloride	0.1 M Tris pH 8.5	28% (w/v) PEG 6000	135583
84	1.0 M Lithium chloride; 0.1 M Sodium acetate		30% (w/v) PEG 6000	135584
85	0.01 M tri-Sodium citrate		33% (w/v) PEG 6000	135585
86	0.5 M Lithium sulfate		2% (w/v) PEG 8000	135586
87	1.0 M Lithium sulfate		2% (w/v) PEG 8000	135587
88			4% (w/v) PEG 8000	135588
89	0.2 M Lithium chloride; 0.05 M Magnesium sulfate		8% (w/v) PEG 8000	135589
90		0.1 M Tris pH 8.5	8% (w/v) PEG 8000	135590
91	0.2 M Zinc acetate	0.1M Imidazole pH 6.5	10% (w/v) PEG 8000	135591
92	0.2 M Calcium acetate	0.1 M HEPES pH 7.5	10% (w/v) PEG 8000	135592
93	0.05 M Magnesium acetate; 0.1 M Sodium acetate		10% (w/v) PEG 8000	135593
94	0.2 M Magnesium acetate		10% (w/v) PEG 8000	135594
95		0.1 M HEPES pH 7.5	10% (w/v) PEG 8000; 10% (w/v) Ethylene Glycol	135595
96			10% (w/v) PEG 8000; 10% (w/v) PEG 1000	135596

The pHClear Suite Composition Table

Number	Buffer	Salt	pH	Cat. no. (Refill-Hit Solution, 4 x 12.5 ml tubes)
1	0.1 M Citric acid	1.0 M Sodium chloride	4.0	134801
2	0.1 M Citric acid	1.0 M Sodium chloride	5.0	134802
3	0.1 M MES	1.0 M Sodium chloride	6.0	134803
4	0.1 M HEPES	1.0 M Sodium chloride	7.0	134804
5	0.1 M Tris	1.0 M Sodium chloride	8.0	134805
6	0.1 M Bicine	1.0 M Sodium chloride	9.0	134806
7	0.1 M Citric acid	2.0 M Sodium chloride	4.0	134807
8	0.1 M Citric acid	2.0 M Sodium chloride	5.0	134808
9	0.1 M MES	2.0 M Sodium chloride	6.0	134809
10	0.1 M HEPES	2.0 M Sodium chloride	7.0	134810
11	0.1 M Tris	2.0 M Sodium chloride	8.0	134811
12	0.1 M Bicine	2.0 M Sodium chloride	9.0	134812
13	0.1 M Citric acid	3.0 M Sodium chloride	4.0	134813
14	0.1 M Citric acid	3.0 M Sodium chloride	5.0	134814
15	0.1 M MES	3.0 M Sodium chloride	6.0	134815
16	0.1 M HEPES	3.0 M Sodium chloride	7.0	134816
17	0.1 M Tris	3.0 M Sodium chloride	8.0	134817
18	0.1 M Bicine	3.0 M Sodium chloride	9.0	134818
19	0.1 M Citric acid	4.0 M Sodium chloride	4.0	134819
20	0.1 M Citric acid	4.0 M Sodium chloride	5.0	134820
21	0.1 M MES	4.0 M Sodium chloride	6.0	134821
22	0.1 M HEPES	4.0 M Sodium chloride	7.0	134822
23	0.1 M Tris	4.0 M Sodium chloride	8.0	134823
24	0.1 M Bicine	4.0 M Sodium chloride	9.0	134824
25	0.1 M Citric acid	5% (w/v) PEG 6000	4.0	134825
26	0.1 M Citric acid	5% (w/v) PEG 6000	5.0	134826
27	0.1 M MES	5% (w/v) PEG 6000	6.0	134827
28	0.1 M HEPES	5% (w/v) PEG 6000	7.0	134828
29	0.1 M Tris	5% (w/v) PEG 6000	8.0	134829
30	0.1 M Bicine	5% (w/v) PEG 6000	9.0	134830
31	0.1 M Citric acid	10% (w/v) PEG 6000	4.0	134831
32	0.1 M Citric acid	10% (w/v) PEG 6000	5.0	134832
33	0.1 M MES	10% (w/v) PEG 6000	6.0	134833
34	0.1 M HEPES	10% (w/v) PEG 6000	7.0	134834
35	0.1 M Tris	10% (w/v) PEG 6000	8.0	134835
36	0.1 M Bicine	10% (w/v) PEG 6000	9.0	134836
37	0.1 M Citric acid	20% (w/v) PEG 6000	4.0	134837
38	0.1 M Citric acid	20% (w/v) PEG 6000	5.0	134838
39	0.1 M MES	20% (w/v) PEG 6000	6.0	134839
40	0.1 M HEPES	20% (w/v) PEG 6000	7.0	134840
41	0.1 M Tris	20% (w/v) PEG 6000	8.0	134841
42	0.1 M Bicine	20% (w/v) PEG 6000	9.0	134842
43	0.1 M Citric acid	30% (w/v) PEG 6000	4.0	134843
44	0.1 M Citric acid	30% (w/v) PEG 6000	5.0	134844
45	0.1 M MES	30% (w/v) PEG 6000	6.0	134845
46	0.1 M HEPES	30% (w/v) PEG 6000	7.0	134846
47	0.1 M Tris	30% (w/v) PEG 6000	8.0	134847
48	0.1 M Bicine	30% (w/v) PEG 6000	9.0	134848

The pHClear Suite Composition Table

Number	Buffer	Salt	pH	Cat. no. (Refill-Hit Solution, 4 x 12.5 ml tubes)
49	0.1 M Citric acid	0.8 M Ammonium sulfate	4.0	134849
50	0.1 M Citric acid	0.8 M Ammonium sulfate	5.0	134850
51	0.1 M MES	0.8 M Ammonium sulfate	6.0	134851
52	0.1 M HEPES	0.8 M Ammonium sulfate	7.0	134852
53	0.1 M Tris	0.8 M Ammonium sulfate	8.0	134853
54	0.1 M Bicine	0.8 M Ammonium sulfate	9.0	134854
55	0.1 M Citric acid	1.6 M Ammonium sulfate	4.0	134855
56	0.1 M Citric acid	1.6 M Ammonium sulfate	5.0	134856
57	0.1 M MES	1.6 M Ammonium sulfate	6.0	134857
58	0.1 M HEPES	1.6 M Ammonium sulfate	7.0	134858
59	0.1 M Tris	1.6 M Ammonium sulfate	8.0	134859
60	0.1 M Bicine	1.6 M Ammonium sulfate	9.0	134860
61	0.1 M Citric acid	2.4 M Ammonium sulfate	4.0	134861
62	0.1 M Citric acid	2.4 M Ammonium sulfate	5.0	134862
63	0.1 M MES	2.4 M Ammonium sulfate	6.0	134863
64	0.1 M HEPES	2.4 M Ammonium sulfate	7.0	134864
65	0.1 M Tris	2.4 M Ammonium sulfate	8.0	134865
66	0.1 M Bicine	2.4 M Ammonium sulfate	9.0	134866
67	0.1 M Citric acid	3.2 M Ammonium sulfate	4.0	134867
68	0.1 M Citric acid	3.2 M Ammonium sulfate	5.0	134868
69	0.1 M MES	3.2 M Ammonium sulfate	6.0	134869
70	0.1 M HEPES	3.2 M Ammonium sulfate	7.0	134870
71	0.1 M Tris	3.2 M Ammonium sulfate	8.0	134871
72	0.1 M Bicine	3.2 M Ammonium sulfate	9.0	134872
73	0.1 M Citric acid	10% (v/v) MPD	4.0	134873
74	0.1 M Sodium acetate	10% (v/v) MPD	5.0	134874
75	0.1 M MES	10% (v/v) MPD	6.0	134875
76	0.1 M HEPES	10% (v/v) MPD	7.0	134876
77	0.1 M Tris	10% (v/v) MPD	8.0	134877
78	0.1 M Bicine	10% (v/v) MPD	9.0	134878
79	0.1 M Citric acid	20% (v/v) MPD	4.0	134879
80	0.1 M Sodium acetate	20% (v/v) MPD	5.0	134880
81	0.1 M MES	20% (v/v) MPD	6.0	134881
82	0.1 M HEPES	20% (v/v) MPD	7.0	134882
83	0.1 M Tris	20% (v/v) MPD	8.0	134883
84	0.1 M Bicine	20% (v/v) MPD	9.0	134884
85	0.1 M Citric acid	40% (v/v) MPD	4.0	134885
86	0.1 M Sodium acetate	40% (v/v) MPD	5.0	134886
87	0.1 M MES	40% (v/v) MPD	6.0	134887
88	0.1 M HEPES	40% (v/v) MPD	7.0	134888
89	0.1 M Tris	40% (v/v) MPD	8.0	134889
90	0.1 M Bicine	40% (v/v) MPD	9.0	134890
91	0.1 M Citric acid	65% (v/v) MPD	4.0	134891
92	0.1 M Sodium acetate	65% (v/v) MPD	5.0	134892
93	0.1 M MES	65% (v/v) MPD	6.0	134893
94	0.1 M HEPES	65% (v/v) MPD	7.0	134894
95	0.1 M Tris	65% (v/v) MPD	8.0	134895
96	0.1 M Bicine	65% (v/v) MPD	9.0	134896

The pHClear II Suite Composition Table

Number	Salt	Buffer	Precipitant	pH	Cat. no. (Refill-Hit Solution, 4 x 12.5 ml tubes)
1	1.0 M Lithium chloride	0.1 M Citric acid		4.0	134901
2	1.0 M Lithium chloride	0.1 M Citric acid		5.0	134902
3	1.0 M Lithium chloride	0.1 M MES		6.0	134903
4	1.0 M Lithium chloride	0.1 M HEPES		7.0	134904
5	1.0 M Lithium chloride	0.1 M Tris		8.0	134905
6	1.0 M Lithium chloride	0.1 M Bicine		9.0	134906
7	1.0 M Lithium chloride	0.1 M Citric acid	10% (w/v) PEG 6000	4.0	134907
8	1.0 M Lithium chloride	0.1 M Citric acid	10% (w/v) PEG 6000	5.0	134908
9	1.0 M Lithium chloride	0.1 M MES	10% (w/v) PEG 6000	6.0	134909
10	1.0 M Lithium chloride	0.1 M HEPES	10% (w/v) PEG 6000	7.0	134910
11	1.0 M Lithium chloride	0.1 M Tris	10% (w/v) PEG 6000	8.0	134911
12	1.0 M Lithium chloride	0.1 M Bicine	10% (w/v) PEG 6000	9.0	134912
13	1.0 M Lithium chloride	0.1 M Citric acid	20% (w/v) PEG 6000	4.0	134913
14	1.0 M Lithium chloride	0.1 M Citric acid	20% (w/v) PEG 6000	5.0	134914
15	1.0 M Lithium chloride	0.1 M MES	20% (w/v) PEG 6000	6.0	134915
16	1.0 M Lithium chloride	0.1 M HEPES	20% (w/v) PEG 6000	7.0	134916
17	1.0 M Lithium chloride	0.1 M Tris	20% (w/v) PEG 6000	8.0	134917
18	1.0 M Lithium chloride	0.1 M Bicine	20% (w/v) PEG 6000	9.0	134918
19	1.0 M Lithium chloride	0.1 M Citric acid	30% (w/v) PEG 6000	4.0	134919
20	1.0 M Lithium chloride	0.1 M Citric acid	30% (w/v) PEG 6000	5.0	134920
21	1.0 M Lithium chloride	0.1 M MES	30% (w/v) PEG 6000	6.0	134921
22	1.0 M Lithium chloride	0.1 M HEPES	30% (w/v) PEG 6000	7.0	134922
23	1.0 M Lithium chloride	0.1 M Tris	30% (w/v) PEG 6000	8.0	134923
24	1.0 M Lithium chloride	0.1 M Bicine	30% (w/v) PEG 6000	9.0	134924
25		0.1 M Citric acid	5% (v/v) Isopropanol	4.0	134925
26		0.1 M Citric acid	5% (v/v) Isopropanol	5.0	134926
27		0.1 M MES	5% (v/v) Isopropanol	6.0	134927
28		0.1 M HEPES	5% (v/v) Isopropanol	7.0	134928
29		0.1 M Tris	5% (v/v) Isopropanol	8.0	134929
30		0.1 M Bicine	5% (v/v) Isopropanol	9.0	134930
31		0.1 M Citric acid	10% (v/v) Isopropanol	4.0	134931
32		0.1 M Citric acid	10% (v/v) Isopropanol	5.0	134932
33		0.1 M MES	10% (v/v) Isopropanol	6.0	134933
34		0.1 M HEPES	10% (v/v) Isopropanol	7.0	134934
35		0.1 M Tris	10% (v/v) Isopropanol	8.0	134935
36		0.1 M Bicine	10% (v/v) Isopropanol	9.0	134936
37		0.1 M Citric acid	20% (v/v) Isopropanol	4.0	134937
38		0.1 M Citric acid	20% (v/v) Isopropanol	5.0	134938
39		0.1 M MES	20% (v/v) Isopropanol	6.0	134939
40		0.1 M HEPES	20% (v/v) Isopropanol	7.0	134940
41		0.1 M Tris	20% (v/v) Isopropanol	8.0	134941
42		0.1 M Bicine	20% (v/v) Isopropanol	9.0	134942
43		0.1 M Citric acid	30% (v/v) Isopropanol	4.0	134943
44		0.1 M Citric acid	30% (v/v) Isopropanol	5.0	134944
45		0.1 M MES	30% (v/v) Isopropanol	6.0	134945
46		0.1 M HEPES	30% (v/v) Isopropanol	7.0	134946
47		0.1 M Tris	30% (v/v) Isopropanol	8.0	134947
48		0.1 M Bicine	30% (v/v) Isopropanol	9.0	134948

The pHClear II Suite Composition Table

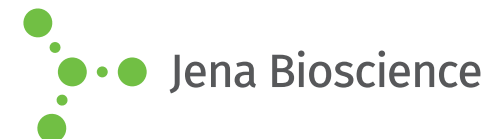
Number	Salt	Buffer	Precipitant	pH	Cat. no. (Refill-Hit Solution, 4 x 12.5 ml tubes)
49			0.8 M Na/K phosphate	5.0	134949
50			0.8 M Na/K phosphate	5.6	134950
51			0.8 M Na/K phosphate	6.3	134951
52			0.8 M Na/K phosphate	6.9	134952
53			0.8 M Na/K phosphate	7.5	134953
54			0.8 M Na/K phosphate	8.2	134954
55			1.0 M Na/K phosphate	5.0	134955
56			1.0 M Na/K phosphate	5.6	134956
57			1.0 M Na/K phosphate	6.3	134957
58			1.0 M Na/K phosphate	6.9	134958
59			1.0 M Na/K phosphate	7.5	134959
60			1.0 M Na/K phosphate	8.2	134960
61			1.4 M Na/K phosphate	5.0	134961
62			1.4 M Na/K phosphate	5.6	134962
63			1.4 M Na/K phosphate	6.3	134963
64			1.4 M Na/K phosphate	6.9	134964
65			1.4 M Na/K phosphate	7.5	134965
66			1.4 M Na/K phosphate	8.2	134966
67			1.8 M Na/K phosphate	5.0	134967
68			1.8 M Na/K phosphate	5.6	134968
69			1.8 M Na/K phosphate	6.3	134969
70			1.8 M Na/K phosphate	6.9	134970
71			1.8 M Na/K phosphate	7.5	134971
72			1.8 M Na/K phosphate	8.2	134972
73			1.0 M Sodium malonate	4.0	134973
74			1.5 M Sodium malonate	4.0	134974
75			1.9 M Sodium malonate	4.0	134975
76			2.4 M Sodium malonate	4.0	134976
77			2.9 M Sodium malonate	4.0	134977
78			3.4 M Sodium malonate	4.0	134978
79			1.0 M Sodium malonate	5.0	134979
80			1.5 M Sodium malonate	5.0	134980
81			1.9 M Sodium malonate	5.0	134981
82			2.4 M Sodium malonate	5.0	134982
83			2.9 M Sodium malonate	5.0	134983
84			3.4 M Sodium malonate	5.0	134984
85			1.0 M Sodium malonate	6.0	134985
86			1.5 M Sodium malonate	6.0	134986
87			1.9 M Sodium malonate	6.0	134987
88			2.4 M Sodium malonate	6.0	134988
89			2.9 M Sodium malonate	6.0	134989
90			3.4 M Sodium malonate	6.0	134990
91			1.0 M Sodium malonate	7.0	134991
92			1.5 M Sodium malonate	7.0	134992
93			1.9 M Sodium malonate	7.0	134993
94			2.4 M Sodium malonate	7.0	134994
95			2.9 M Sodium malonate	7.0	134995
96			3.4 M Sodium malonate	7.0	134996



JBScreen Basic HTS

Cat.-No.: CS-203L

SCREEN FORMULATION



No.	Precipitant 1	Precipitant 2	Buffer	Additive
A1	25 % v/v Ethylene glycol	none	none	none
A2	12 % v/v Glycerol	1.5 M Ammonium sulfate	100 mM TRIS; pH 8.5	none
A3	1 M 1,6-Hexanediol	none	100 mM Sodium acetate; pH 4.6	10 mM Cobalt (II) chloride
A4	2.5 M 1,6-Hexanediol	none	100 mM tri-Sodium citrate; pH 5.6	none
A5	3.4 M 1,6-Hexanediol	none	100 mM TRIS; pH 8.5	200 mM Magnesium chloride
A6	30 % v/v 2-Methyl-2,4-pentanediol	none	100 mM Sodium acetate; pH 4.6	200 mM Sodium chloride
A7	30 % v/v 2-Methyl-2,4-pentanediol	none	100 mM tri-Sodium citrate; pH 5.6	200 mM Ammonium acetate
A8	30 % v/v 2-Methyl-2,4-pentanediol	none	100 mM Sodium acetate; pH 4.6	20 mM Calcium chloride
A9	30 % v/v 2-Methyl-2,4-pentanediol	500 mM Ammonium sulfate	100 mM HEPES; pH 7.5	none
A10	30 % v/v 2-Methyl-2,4-pentanediol	none	100 mM HEPES; pH 7.5	200 mM tri-Sodium citrate
A11	50 % v/v 2-Methyl-2,4-pentanediol	none	100 mM TRIS; pH 8.5	200 mM Ammonium di-hydrogen phosphate
A12	70 % v/v 2-Methyl-2,4-pentanediol	none	100 mM HEPES; pH 7.5	none
B1	2 % w/v Ethylene imine polymer	none	100 mM tri-Sodium citrate; pH 5.6	500 mM Sodium chloride
B2	2 % v/v Polyethylene glycol 400	2 M Ammonium sulfate	100 mM HEPES; pH 7.5	none
B3	28 % v/v Polyethylene glycol 400	none	100 mM HEPES; pH 7.5	200 mM Calcium chloride
B4	30 % v/v Polyethylene glycol 400	none	100 mM TRIS; pH 8.5	200 mM tri-Sodium citrate
B5	30 % v/v Polyethylene glycol 400	none	100 mM HEPES; pH 7.5	200 mM Magnesium chloride
B6	30 % v/v Polyethylene glycol 400	none	100 mM Sodium acetate; pH 4.6	100 mM Calcium chloride
B7	20 % v/v Polyethylene glycol monomethyl ether 550	none	100 mM BICINE; pH 9.5	100 mM Sodium chloride
B8	25 % v/v Polyethylene glycol monomethyl ether 550	none	100 mM MES; pH 6.5	10 mM Zinc sulfate
B9	10 % w/v Polyethylene glycol 1,000	10 % w/v Polyethylene glycol 8,000	none	none
B10	30 % w/v Polyethylene glycol 1,500	none	none	none
B11	20 % w/v Polyethylene glycol monomethyl ether 2,000	none	100 mM TRIS; pH 8.5	10 mM Nickel (II) chloride
B12	30 % w/v Polyethylene glycol monomethyl ether 2,000	none	100 mM Sodium acetate; pH 4.6	200 mM Ammonium sulfate

*pH values indicated are those of the 1.0 M buffer stock solution prior to dilution with other components





JBScreen Basic HTS

Cat.-No.: CS-203L

SCREEN FORMULATION



No.	Precipitant 1	Precipitant 2	Buffer	Additive
C1	8 % w/v Polyethylene glycol 4,000	none	100 mM Sodium acetate; pH 4.6	none
C2	20 % w/v Polyethylene glycol 4,000	20 % v/v 2-Propanol	100 mM tri-Sodium citrate; pH 5.6	none
C3	20 % w/v Polyethylene glycol 4,000	10 % v/v 2-Propanol	100 mM HEPES; pH 7.5	none
C4	25 % w/v Polyethylene glycol 4,000	none	100 mM Sodium acetate; pH 4.6	200 mM Ammonium sulfate
C5	30 % w/v Polyethylene glycol 4,000	none	none	200 mM Ammonium sulfate
C6	30 % w/v Polyethylene glycol 4,000	none	100 mM Sodium acetate; pH 4.6	200 mM Ammonium acetate
C7	30 % w/v Polyethylene glycol 4,000	none	100 mM tri-Sodium citrate; pH 5.6	200 mM Ammonium acetate
C8	30 % w/v Polyethylene glycol 4,000	none	100 mM TRIS; pH 8.5	200 mM Sodium acetate
C9	30 % w/v Polyethylene glycol 4,000	none	100 mM TRIS; pH 8.5	200 mM Lithium sulfate
C10	30 % w/v Polyethylene glycol 4,000	none	100 mM TRIS; pH 8.5	200 mM Magnesium chloride
C11	30 % w/v Polyethylene glycol monomethyl ether 5,000	none	100 mM MES; pH 6.5	200 mM Ammonium sulfate
C12	10 % w/v Polyethylene glycol 6,000	2 M Sodium chloride	none	none
D1	10 % w/v Polyethylene glycol 6,000	5 % v/v 2-Methyl-2,4-pentanediol	100 mM HEPES; pH 7.5	none
D2	2 % w/v Polyethylene glycol 8,000	1 M Lithium sulfate	none	none
D3	8 % w/v Polyethylene glycol 8,000	none	100 mM TRIS; pH 8.5	none
D4	10 % w/v Polyethylene glycol 8,000	8 % v/v Ethylene glycol	100 mM HEPES; pH 7.5	none
D5	15 % w/v Polyethylene glycol 8,000	500 mM Lithium sulfate	none	none
D6	18 % w/v Polyethylene glycol 8,000	none	100 mM MES; pH 6.5	200 mM Calcium acetate
D7	18 % w/v Polyethylene glycol 8,000	none	100 mM MES; pH 6.5	200 mM Zinc acetate
D8	20 % w/v Polyethylene glycol 8,000	none	none	50 mM Potassium di-hydrogen phosphate
D9	20 % w/v Polyethylene glycol 8,000	none	100 mM MES; pH 6.5	200 mM Magnesium acetate
D10	30 % w/v Polyethylene glycol 8,000	none	100 mM MES; pH 6.5	200 mM Sodium acetate
D11	30 % w/v Polyethylene glycol 8,000	none	none	200 mM Ammonium sulfate
D12	30 % w/v Polyethylene glycol 8,000	none	100 mM MES; pH 6.5	200 mM Ammonium sulfate

*pH values indicated are those of the 1.0 M buffer stock solution prior to dilution with other components

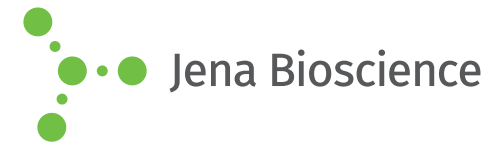




JBScreen Basic HTS

Cat.-No.: CS-203L

SCREEN FORMULATION



No.	Precipitant 1	Precipitant 2	Buffer	Additive
E1	10 % w/v Polyethylene glycol 10,000	2 % v/v 1,4-Dioxane	100 mM BICINE; pH 9.5	none
E2	20 % w/v Polyethylene glycol 10,000	none	100 mM HEPES; pH 7.5	none
E3	12 % w/v Polyethylene glycol 20,000	none	100 mM MES; pH 6.5	none
E4	5 % v/v 2-Propanol	2 M Ammonium sulfate	none	none
E5	20 % v/v 2-Propanol	none	100 mM HEPES; pH 7.5	200 mM tri-Sodium citrate
E6	20 % v/v 2-Propanol	none	100 mM Sodium acetate; pH 4.6	200 mM Calcium chloride
E7	30 % v/v 2-Propanol	none	100 mM HEPES; pH 7.5	200 mM Magnesium chloride
E8	30 % v/v 2-Propanol	none	100 mM TRIS; pH 8.5	200 mM Ammonium acetate
E9	10 % v/v 1,4-Dioxane	1.6 M Ammonium sulfate	100 mM MES; pH 6.5	none
E10	35 % v/v 1,4-Dioxane	none	none	none
E11	10 % v/v Ethanol	1.5 M Sodium chloride	none	none
E12	20 % v/v Ethanol	none	100 mM TRIS; pH 8.5	none
F1	25 % v/v 2-Methyl-2-propanol	none	100 mM TRIS; pH 8.5	none
F2	35 % v/v 2-Methyl-2-propanol	none	100 mM tri-Sodium citrate; pH 5.6	none
F3	1 M Imidazole; pH 7.0	none	none	none
F4	1 M Lithium sulfate	none	100 mM TRIS; pH 8.5	10 mM Nickel (II) chloride
F5	1.5 M Lithium sulfate	none	100 mM HEPES; pH 7.5	none
F6	400 mM Potassium Sodium tartrate	none	none	none
F7	800 mM Potassium Sodium tartrate	none	100 mM HEPES; pH 7.5	none
F8	1.4 M tri-Sodium citrate	none	100 mM HEPES; pH 7.5	none
F9	1.6 M tri-Sodium citrate; pH 6.5	none	none	none
F10	10 % v/v Jeffamine® M-600	none	100 mM tri-Sodium citrate; pH 5.6	10 mM Iron (III) chloride
F11	20 % v/v Jeffamine® M-600	none	100 mM HEPES; pH 7.5	none
F12	30 % v/v Jeffamine® M-600	none	100 mM MES; pH 6.5	50 mM Cesium chloride

*pH values indicated are those of the 1.0 M buffer stock solution prior to dilution with other components





JBScreen Basic HTS

Cat.-No.: CS-203L

SCREEN FORMULATION



No.	Precipitant 1	Precipitant 2	Buffer	Additive
G1	800 mM Potassium di-hydrogen phosphate	800 mM Sodium di-hydrogen phosphate	100 mM HEPES; pH 7.5	none
G2	400 mM Ammonium di-hydrogen phosphate	none	none	none
G3	1 M Ammonium di-hydrogen phosphate	none	100 mM tri-Sodium citrate; pH 5.6	none
G4	2 M Ammonium di-hydrogen phosphate	none	100 mM TRIS; pH 8.5	none
G5	2 M Ammonium formate	none	100 mM Sodium acetate; pH 4.6	none
G6	4 M Ammonium formate	none	100 mM HEPES; pH 7.5	none
G7	2 M Ammonium formate	none	none	none
G8	500 mM Ammonium sulfate	1 M Lithium sulfate	100 mM tri-Sodium citrate; pH 5.6	none
G9	1.6 M Ammonium sulfate	none	100 mM HEPES; pH 7.5	100 mM Sodium chloride
G10	1.8 M Ammonium sulfate	none	100 mM MES; pH 6.5	10 mM Cobalt (II) chloride
G11	2 M Ammonium sulfate	none	100 mM TRIS; pH 8.5	none
G12	2 M Ammonium sulfate	none	none	none
H1	2 M Ammonium sulfate	none	100 mM Sodium acetate; pH 4.6	none
H2	2 M Ammonium sulfate	none	100 mM tri-Sodium citrate; pH 5.6	200 mM Potassium Sodium tartrate
H3	200 mM Magnesium formate	none	none	none
H4	1.6 M Magnesium sulfate	none	100 mM MES; pH 6.5	none
H5	2 M Magnesium chloride	none	100 mM BICINE; pH 9.5	none
H6	1 M Sodium acetate	none	100 mM Imidazole; pH 6.5	none
H7	1 M Sodium acetate	none	100 mM HEPES; pH 7.5	50 mM Cadmium sulfate
H8	1.4 M Sodium acetate	none	100 mM MES; pH 6.5	none
H9	500 mM Sodium chloride	10 mM Magnesium chloride	none	10 mM Cetyltrimethylammonium bromide
H10	2 M Sodium chloride	none	100 mM Sodium acetate; pH 4.6	none
H11	2 M Sodium chloride	none	100 mM MES; pH 6.5	100 mM Sodium di-hydrogen phosphate, 100 mM Potassium di-hydrogen phosphate
H12	4.3 M Sodium chloride	none	100 mM HEPES; pH 7.5	none

*pH values indicated are those of the 1.0 M buffer stock solution prior to dilution with other components

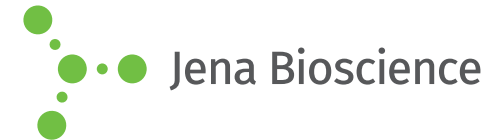




JBScreen PEG/Salt HTS

Cat.-No.: CS-205L

SCREEN FORMULATION



No.	Precipitant	Additive
A1	20 % w/v Polyethylene glycol 3,350	200 mM Ammonium acetate
A2	20 % w/v Polyethylene glycol 3,350	200 mM Ammonium chloride
A3	20 % w/v Polyethylene glycol 3,350	200 mM Ammonium fluoride
A4	20 % w/v Polyethylene glycol 3,350	200 mM Ammonium formate
A5	20 % w/v Polyethylene glycol 3,350	200 mM Ammonium iodide
A6	20 % w/v Polyethylene glycol 3,350	200 mM Ammonium nitrate
A7	20 % w/v Polyethylene glycol 3,350	200 mM Ammonium di-hydrogen phosphate
A8	20 % w/v Polyethylene glycol 3,350	200 mM di-Ammonium hydrogen phosphate
A9	20 % w/v Polyethylene glycol 3,350	200 mM Ammonium sulfate
A10	20 % w/v Polyethylene glycol 3,350	200 mM Ammonium sulfite
A11	20 % w/v Polyethylene glycol 3,350	200 mM Calcium acetate
A12	20 % w/v Polyethylene glycol 3,350	200 mM Calcium chloride
B1	20 % w/v Polyethylene glycol 3,350	200 mM di-Ammonium tartrate
B2	20 % w/v Polyethylene glycol 3,350	200 mM Potassium formate
B3	20 % w/v Polyethylene glycol 3,350	200 mM Lithium acetate
B4	20 % w/v Polyethylene glycol 3,350	200 mM Lithium chloride
B5	20 % w/v Polyethylene glycol 3,350	200 mM tri-Lithium citrate
B6	20 % w/v Polyethylene glycol 3,350	200 mM Lithium nitrate
B7	20 % w/v Polyethylene glycol 3,350	200 mM Lithium sulfate
B8	20 % w/v Polyethylene glycol 3,350	200 mM Magnesium acetate
B9	20 % w/v Polyethylene glycol 3,350	200 mM Magnesium chloride
B10	20 % w/v Polyethylene glycol 3,350	200 mM Magnesium formate
B11	20 % w/v Polyethylene glycol 3,350	200 mM Magnesium nitrate
B12	20 % w/v Polyethylene glycol 3,350	200 mM Magnesium sulfate

*pH values indicated are those of the 1.0 M buffer stock solution prior to dilution with other components

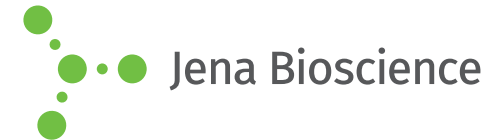




JBScreen PEG/Salt HTS

Cat.-No.: CS-205L

SCREEN FORMULATION



Jena Bioscience

No.	Precipitant	Additive
C1	20 % w/v Polyethylene glycol 3,350	200 mM Potassium acetate
C2	20 % w/v Polyethylene glycol 3,350	200 mM Potassium chloride
C3	20 % w/v Polyethylene glycol 3,350	200 mM Potassium fluoride
C4	20 % w/v Polyethylene glycol 3,350	200 mM Potassium iodide
C5	20 % w/v Polyethylene glycol 3,350	200 mM Potassium nitrate
C6	20 % w/v Polyethylene glycol 3,350	200 mM Potassium di-hydrogen phosphate
C7	20 % w/v Polyethylene glycol 3,350	200 mM di-Potassium hydrogen phosphate
C8	20 % w/v Polyethylene glycol 3,350	200 mM Potassium sulfate
C9	20 % w/v Polyethylene glycol 3,350	200 mM Potassium thiocyanate
C10	20 % w/v Polyethylene glycol 3,350	200 mM Potassium Sodium tartrate
C11	20 % w/v Polyethylene glycol 3,350	200 mM Sodium acetate
C12	20 % w/v Polyethylene glycol 3,350	200 mM Sodium chloride
D1	20 % w/v Polyethylene glycol 3,350	200 mM tri-Sodium citrate
D2	20 % w/v Polyethylene glycol 3,350	200 mM Sodium fluoride
D3	20 % w/v Polyethylene glycol 3,350	200 mM Sodium formate
D4	20 % w/v Polyethylene glycol 3,350	200 mM Sodium iodide
D5	20 % w/v Polyethylene glycol 3,350	200 mM Sodium thiocyanate
D6	20 % w/v Polyethylene glycol 3,350	200 mM Sodium nitrate
D7	20 % w/v Polyethylene glycol 3,350	200 mM Sodium di-hydrogen phosphate
D8	20 % w/v Polyethylene glycol 3,350	200 mM di-Sodium hydrogen phosphate
D9	20 % w/v Polyethylene glycol 3,350	200 mM Sodium sulfate
D10	20 % w/v Polyethylene glycol 3,350	200 mM di-Sodium tartrate
D11	20 % w/v Polyethylene glycol 3,350	200 mM tri-Potassium citrate
D12	20 % w/v Polyethylene glycol 3,350	200 mM Zinc acetate

*pH values indicated are those of the 1.0 M buffer stock solution prior to dilution with other components

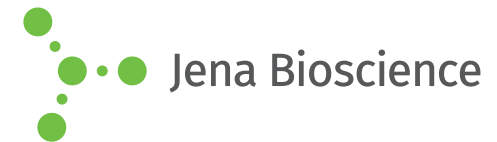




JBScreen PEG/Salt HTS

Cat.-No.: CS-205L

SCREEN FORMULATION



Jena Bioscience

No.	Precipitant	Additive
E1	20 % w/v Polyethylene glycol monomethyl ether 5,000	200 mM Ammonium acetate
E2	20 % w/v Polyethylene glycol monomethyl ether 5,000	200 mM Ammonium chloride
E3	20 % w/v Polyethylene glycol monomethyl ether 5,000	200 mM Ammonium fluoride
E4	20 % w/v Polyethylene glycol monomethyl ether 5,000	200 mM Ammonium formate
E5	20 % w/v Polyethylene glycol monomethyl ether 5,000	200 mM Ammonium iodide
E6	20 % w/v Polyethylene glycol monomethyl ether 5,000	200 mM Ammonium nitrate
E7	20 % w/v Polyethylene glycol monomethyl ether 5,000	200 mM Ammonium di-hydrogen phosphate
E8	20 % w/v Polyethylene glycol monomethyl ether 5,000	200 mM di-Ammonium hydrogen phosphate
E9	20 % w/v Polyethylene glycol monomethyl ether 5,000	200 mM Ammonium sulfate
E10	20 % w/v Polyethylene glycol monomethyl ether 5,000	200 mM Ammonium sulfite
E11	20 % w/v Polyethylene glycol monomethyl ether 5,000	200 mM Calcium acetate
E12	20 % w/v Polyethylene glycol monomethyl ether 5,000	200 mM Calcium chloride
F1	20 % w/v Polyethylene glycol monomethyl ether 5,000	200 mM di-Ammonium tartrate
F2	20 % w/v Polyethylene glycol monomethyl ether 5,000	200 mM Potassium formate
F3	20 % w/v Polyethylene glycol monomethyl ether 5,000	200 mM Lithium acetate
F4	20 % w/v Polyethylene glycol monomethyl ether 5,000	200 mM Lithium chloride
F5	20 % w/v Polyethylene glycol monomethyl ether 5,000	200 mM tri-Lithium citrate
F6	20 % w/v Polyethylene glycol monomethyl ether 5,000	200 mM Lithium nitrate
F7	20 % w/v Polyethylene glycol monomethyl ether 5,000	200 mM Lithium sulfate
F8	20 % w/v Polyethylene glycol monomethyl ether 5,000	200 mM Magnesium acetate
F9	20 % w/v Polyethylene glycol monomethyl ether 5,000	200 mM Magnesium chloride
F10	20 % w/v Polyethylene glycol monomethyl ether 5,000	200 mM Magnesium formate
F11	20 % w/v Polyethylene glycol monomethyl ether 5,000	200 mM Magnesium nitrate
F12	20 % w/v Polyethylene glycol monomethyl ether 5,000	200 mM Magnesium sulfate

*pH values indicated are those of the 1.0 M buffer stock solution prior to dilution with other components

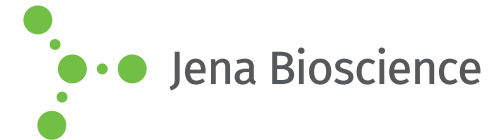




JBScreen PEG/Salt HTS

Cat.-No.: CS-205L

SCREEN FORMULATION



Jena Bioscience

No.	Precipitant	Additive
G1	20 % w/v Polyethylene glycol monomethyl ether 5,000	200 mM Potassium acetate
G2	20 % w/v Polyethylene glycol monomethyl ether 5,000	200 mM Potassium chloride
G3	20 % w/v Polyethylene glycol monomethyl ether 5,000	200 mM Potassium fluoride
G4	20 % w/v Polyethylene glycol monomethyl ether 5,000	200 mM Potassium iodide
G5	20 % w/v Polyethylene glycol monomethyl ether 5,000	200 mM Potassium nitrate
G6	20 % w/v Polyethylene glycol monomethyl ether 5,000	200 mM Potassium di-hydrogen phosphate
G7	20 % w/v Polyethylene glycol monomethyl ether 5,000	200 mM di-Potassium hydrogen phosphate
G8	20 % w/v Polyethylene glycol monomethyl ether 5,000	200 mM Potassium sulfate
G9	20 % w/v Polyethylene glycol monomethyl ether 5,000	200 mM Potassium thiocyanate
G10	20 % w/v Polyethylene glycol monomethyl ether 5,000	200 mM Potassium Sodium tartrate
G11	20 % w/v Polyethylene glycol monomethyl ether 5,000	200 mM Sodium acetate
G12	20 % w/v Polyethylene glycol monomethyl ether 5,000	200 mM Sodium chloride
H1	20 % w/v Polyethylene glycol monomethyl ether 5,000	200 mM tri-Sodium citrate
H2	20 % w/v Polyethylene glycol monomethyl ether 5,000	200 mM Sodium fluoride
H3	20 % w/v Polyethylene glycol monomethyl ether 5,000	200 mM Sodium formate
H4	20 % w/v Polyethylene glycol monomethyl ether 5,000	200 mM Sodium iodide
H5	20 % w/v Polyethylene glycol monomethyl ether 5,000	200 mM Sodium thiocyanate
H6	20 % w/v Polyethylene glycol monomethyl ether 5,000	200 mM Sodium nitrate
H7	20 % w/v Polyethylene glycol monomethyl ether 5,000	200 mM Sodium di-hydrogen phosphate
H8	20 % w/v Polyethylene glycol monomethyl ether 5,000	200 mM di-Sodium hydrogen phosphate
H9	20 % w/v Polyethylene glycol monomethyl ether 5,000	200 mM Sodium sulfate
H10	20 % w/v Polyethylene glycol monomethyl ether 5,000	200 mM di-Sodium tartrate
H11	20 % w/v Polyethylene glycol monomethyl ether 5,000	200 mM tri-Potassium citrate
H12	20 % w/v Polyethylene glycol monomethyl ether 5,000	200 mM Zinc acetate

*pH values indicated are those of the 1.0 M buffer stock solution prior to dilution with other components

